NISTIR 6872

Evaluation of Fire Models for Nuclear Power Plant Applications: Cable Tray Fires

International Panel Report

Compiled by Monideep K. Dey

NIST

National Institute of Standards and Technology
Technology Administration, U.S. Department of Commerce

Evaluation of Fire Models for Nuclear Power Plant Applications: Cable Tray Fires

International Panel Report

Compiled by Monideep K. Dey, Guest Researcher
Fire Research Division
Building and Fire Research Laboratory

June 2002

Abstract

This technical reference document was developed in the International Collaborative Project to Evaluate Fire Models for Nuclear Power Plant Applications. This volume reports on the results of the first task in the international collaborative project. The objective of the first task was to evaluate the capability of fire models to analyze cable tray fires of redundant safety systems in nuclear power plants. The evaluation of the capability of fire models to analyze these scenarios was conducted through an international benchmark exercise. Consideration of appropriate input parameters and assumptions, interpretation of the results, and determination of the adequacy of the physical sub-models established useful technical information regarding the capabilities and limitations of the fire models. The participants in the benchmark exercise determined that results indicate that the models provide a comprehensive treatment of most physical phenomena of interest in the scenarios analyzed. The predicted trends from the models were found to be similar and reasonable for their intended use. These fire models can provide useful results for nuclear power plant fire safety analysis for the types of scenarios analyzed.

Table of Contents

List of Figures

List of Tables

Executive Summary

Objective

This technical reference document was developed in the International Collaborative Project to Evaluate Fire Models for Nuclear Power Plant Applications. The objective of the collaborative project is to share the knowledge and resources of various organizations to evaluate and improve the state of the art of fire models for use in nuclear power plant fire safety and fire hazard analysis. The project is divided into two phases. The objective of the first phase is to evaluate the capabilities of current fire models for fire safety analysis in nuclear power plants. The second phase will implement beneficial improvements to current fire models that are identified in the first phase, and extend the validation database of those models. Currently, twenty-two organizations from six countries are represented in the collaborative project.

Problem

The first task of the international collaborative project was to evaluate the capability of various fire models to analyze cable tray fires of redundant safety systems in nuclear power plants. The evaluation of the capability of fire models to analyze these scenarios was conducted through an international benchmark exercise. The benchmark exercise was intended to simulate a basic scenario defined in sufficient detail to allow evaluation of the physics modeled in the fire computer codes. An assessment of appropriate input parameters and assumptions, interpretation of results, and determination of the adequacy of the physical sub-models in the codes for specific scenarios will establish useful technical information regarding the capabilities and limitations of the fire computer codes. Uncertainties in the predictions based on validations of each code will provide a basis for the confidence on the set of results developed in the exercise. Three zone, three Computational Fluid Dynamic (CFD), and two lumped-parameter models were used by eight organizations in the exercise.

A representative emergency switchgear room for a Pressurized Water Reactor (PWR) was selected for the benchmark exercise. There were two parts to the exercise. The objective of Part I was to determine the maximum horizontal distance between a specified transient (trash bag) fire and a cable tray that results in the ignition of the cable tray. Part II examined whether a target cable tray will be damaged by a fire of a cable tray stack that is separated by a horizontal distance, d. The effects of a fire door position (open & closed) and mechanical ventilation system are examined in both parts of the benchmark exercise.

Results

For Part I, none of the analyses conducted for the benchmark exercise predicted the ignition of the target cable (specified at 643 K) by the postulated trash bag fire for

varying ventilation conditions in the room. The predicted temperature rise for all the cases in Part I were similar. Given the dimensions of the room and the heat release rate of the trash bag, the maximum surface temperature of the target outside the fire plume region for all the cases analyzed is less than 350 K. This temperature is much less than 643 K, which is specified for target damage. The target cable may ignite only if it is in the plume region of the fire. The temperature of the target cable is predicted to significantly increase when the distance between the trash bag and cable is between 0.4 m and 0. 5 m, and the target is exposed to the high plume gas temperature. The predicted maximum surface temperature of the target in this region is predicted to be 550 K. Although the maximum predicted heat flux from the plume incident on the target is predicted to be $\approx$ 14 kW/m^2, the duration of the exposure is not long enough to increase the surface of the cable to the ignition temperature. A fire of similar intensity sustained over a longer period could ignite the cable. Based on this, one could establish a minimum horizontal safe separation distance[1] of 1.0 m between the trash bag and the target cable.

The predicted maximum temperatures of the target cable, using a lower oxygen limit of 12 %, were below 400 K for all the cases analyzed in Part II. The cable tray fire was limited between 10 min and 15 min by the depletion of oxygen near the cable tray. Given the elevation of the fire source and the predicted extinction of the fire, cable damage is unlikely for the scenarios examined. The analysis of an elevated fire source is key to the accuracy of the predicted result.

Input Parameters

The process for defining the input parameters for the fire models resulted in three main issues: (1) specification of the fire source; (2) modeling of the target; and (3) value for the lower oxygen limit (LOL). The specification of the fire source is fundamental to the input for fire models, and can significantly affect the predicted thermal environment. The specification of the above three parameters could lead to "user effects," and are the largest sources of uncertainty in the predicted results from the input parameter specification process for the types of scenarios examined in the benchmark exercise.

Verification and Validation

Verification is defined here as the process of determining that a model implementation accurately represents the developer's conceptual description of the model and the solution to the model. Validation is defined as the process of determining the degree to which a model is an accurate representation of the real world from the perspective of the intended uses of the model.

---

[1]The concept of safe separation distance is not directly applicable in all countries.

Verification

The results of the analyses indicate that the trends predicted by the sub-models are reasonable for the intended use of the models for analyzing the specified scenarios. The constitutive equations for mass and energy balances in the fire models provide a reasonable prediction of the hot gas layer development and temperatures in the compartment. The fire models generally provide an adequate method to balance and estimate the concentration of oxygen. Mass flows that result from the pressurization of the compartment, or natural and mechanical ventilation are reasonably predicted by the zone, CFD, and lumped-parameter models. Convective and radiative heat fluxes to the boundaries and target are comprehensively treated in the models but utilize different approaches. The thermal response of the target is coupled to the thermal environment created by the fire and would benefit from further investigation.

The analyses of the scenarios also demonstrate the complexity in modeling an elevated fire source which can be affected by a limited oxygen environment. The extinction sub-models utilized in the computer codes are approximations of the interaction of the complex combustion process with a limited oxygen environment. Therefore, the results from the extinction sub-models represent an approximation of the conditions expected for the fire scenarios. The assumption for the LOL will affect the predicted peak target temperature. Therefore, conservative assumptions are warranted due to the uncertainty in the extinction models used in the computer codes. Also, the target sub-model in some of the computer codes requires the specification of target orientation by the user. This may result in a non-conservative result and a "user effect" since the orientation of the target will determine the heat flux incident on it. This limitation may be overcome by establishing procedures for the use of the models to obtain conservative and consistent results. In some cases it may be difficult to define conservatism, therefore, the development of best-estimate methods may be desirable.

The inclusion of emission/absorption due to soot, water vapor, and carbon dioxide may play a significant role both in the radiation heat transfer to the target cable and also in the general thermodynamics inside the compartment. The latter will influence various matters including heat loss to the compartment boundaries and the mass flow rates through the opening(s). Radiation from the flaming region will be important in determining damage to cables close to the fire source.

Validation

Most of the fire models used in the benchmark exercise have been compared with test data for fires ranging from 100 kW to 2.5 MW in compartments with volumes ranging from 10 m^3 to 1300 m^3 . The comparisons are generally satisfactory, with different accuracies reported for the range of data sets. Tests conducted in a compartment with a similar volume and fire source indicated that the relative variation of pressure, temperature, and oxygen concentration predicted with test data was within 20 %. The comparison of cable surface temperature evolution was less successful due to the

vertical temperature gradient in the test data for the compartment and the vertical position of the target in the hot gas layer. The validations of the fire models conducted to date indicates that they generally provide a reasonably accurate representation of physical phenomena for the types of scenarios in the benchmark exercise.

Although the exercise reported here did not include comparisons of model results with test data, the analyses reported did include the comparison of the magnitudes of the parameters predicted by different fire models. Generally, the predictions were similar. Models developed independently, if based on the same fundamental laws, are expected to produce similar results. Codes that produce similar results in a benchmark exercise should accurately represent the physical phenomena modeled if the input parameters are representative (in particular for the fire source), and at least one of the codes has been validated for the studied configurations.

A distinction is made here between the variability of results due to differences in input parameters and to differences in the physics of the model. As indicated earlier, different assumptions of fire source power can significantly affect the results from the models. Other important input data are the thermophysical parameters, e.g., the convective heat transfer coefficient. It is judged that differences in model results due to the uncertainty of the models is less than differences caused by variations in input data and assumptions.

Conclusions

The international panel determined that the analysis of the results of the benchmark exercise demonstrates that current zone, CFD, and lumped-parameter fire models provide a comprehensive treatment of most physical phenomena of interest in the scenarios analyzed. The results indicate that the trends predicted by the sub-models are reasonable for the intended use of the models for analyzing the specified scenarios. The results obtained from these fire models can provide useful insights for nuclear power plant fire safety analysis for the types of scenarios analyzed.

There are benefits to extending the current validation database, especially for target response calculations. The continued validation of current models in international blind exercises will add confidence for the widespread use of these models in nuclear power plant fire safety analysis.

Most of the insights gained and conclusions drawn on the capabilities and limitations of fire models from this benchmark exercise is applicable to a broad range of fire scenarios expected in nuclear power plants. However, further benchmark and validation exercises are necessary for some specific configurations such as large compartments (like the turbine building) with large pool fires, multi compartments with horizontal and vertical vent connections, and control room configurations. Insights on some further specific modeling issues are likely to be developed from such exercises.

Foreword

This technical reference document was developed in the International Collaborative Project to Evaluate Fire Models for Nuclear Power Plant Applications. The objective of the collaborative project is to share the knowledge and resources of various organizations to evaluate and improve the state of the art of fire models for use in nuclear power plant fire safety and fire hazard analysis. The project is divided into two phases. The objective of the first phase is to evaluate the capabilities of current fire models for fire safety analysis in nuclear power plants. The second phase will extend the validation database of those models, and implement beneficial improvements to the models that are identified in the first phase. Currently, twenty-two organizations from six countries are represented in the collaborative project.

This volume reports on the results of the first task in the international collaborative project. The objective of the first task was to evaluate the capability of fire models to analyze cable tray fires of redundant safety systems in nuclear power plants. The evaluation of the capability of fire models to analyze these scenarios was conducted through an international benchmark exercise. Three zone, three computational fluid dynamic (CFD), and two lumped-parameter fire models were used by eight organizations in the exercise. The benchmark exercise simulated a basic scenario defined in sufficient detail to allow the evaluation of the physics modeled in the fire computer codes. Consideration of appropriate input parameters and assumptions, and the interpretation of the results to evaluate the adequacy of the physical sub-models established useful technical information regarding the capabilities and limitations of the fire models. This technical information is presented in this volume which is the first of a series of technical reference documents for fire model users. The objective of the exercise was not to compare the capabilities and strengths of specific models, address issues specific to a model, nor to recommend specific models over others. Future volumes of this series will report on the findings of other benchmark and validation exercises that are planned for this project.

This document is not intended to provide guidance to users of fire models. Guidance on the use of fire models is currently being developed by several national and international standards organizations, industry groups, and utilities. This document is intended to be a source and reference for technical information and insights gained through the exercises conducted, and provided by the experts participating in this project. This information may be beneficial to users of fire models and developers of guidance documents or standards for the use of fire models in nuclear power plant applications.

Acronyms and Initialisms

BFS	Bundesamt fur Strahlenschutz
BRE	Building Research Establishment
CIB	International Council for Research and Innovation in Building and Construction
CFAST	Consolidated Model for Fire and Smoke Transport
CFD	Computational Fluid Dynamics
CL	centerline
COCOSYS	Containment Code System
EdF	Electricite de France
EPRI	Electric Power Research Institute
FDS	Fire Dynamics Simulator
GRS	Gesellschaft fuer Anlagen-und Reaktorsicherheit
HGL	hot gas layer
HRR	Heat Release Rate
iBMB	Institut fuer Baustoffe, Massivbau und Brandschutz
IPSN	Institute for Protection and Nuclear Safety
JASMINE	Analysis of Smoke Movement in Enclosures
LL	Lower layer
LOL	Lower Oxygen Limit
NII	H. M. Nuclear Installations Inspectorate
NIST	National Institute of Standards and Technology
NPP	Nuclear Power Plant
NRC	Nuclear Regulatory Commission
PRA	Probabilistic Risk Analysis
PWR	Pressurized Water Reactor
TUV	Technical University of Vienna
UL	upper layer
VTT	Valtion Teknillinen Tutkimuskeskus
WPI	Worcester Polytechnic Institute

1 Introduction

The 1st planning meeting of the International Collaborative Project to Evaluate Fire Models for Nuclear Power Plant Applications was held at the University of Maryland at College Park, USA, on October 25-26, 1999. Attendees at the meeting agreed to share their knowledge and resources to evaluate and improve the state of the art of fire models for use in nuclear power plant (NPP) safety. It was decided that the project would be divided into two phases. The objective of the first phase would be to evaluate the capabilities of current fire models (zone, CFD, and lumped-parameter) for fire safety analysis in NPPs. The second phase will implement beneficial improvements to current fire models that are identified in the first phase, and extend the validation database of those models. The summary of the 1st meeting and the details of the objectives established for the project, including the goals for the benchmark exercise reported in this document may be found in NRC (2000). The benchmark exercise was defined at the 2nd project meeting at the Institute for Protection and Nuclear Safety (IPSN), Fontenay-aux-Roses, France, on June 19 and 20, 2000. The summary of the 2nd meeting is reported in NRC (2001).

The definition of the benchmark exercise is presented in Chapter 2. Chapter 3 provides a summary of the main issues that arose in the consideration of input parameters and assumptions for the scenarios in the exercise, and how participants decided to address the issues. Chapter 4 presents a summary of the main results that were sought in the definition of the benchmark exercise presented in Chapter 2. Chapter 5 finally provides a discussion of the general conclusions and issues derived from the benchmark exercise. Appendices A through I include the detailed results of the analyses for the benchmark exercise conducted by participants using different fire models.

This international panel report was developed by the following members that contributed either through the performance of analysis in the benchmark exercise, and/or by providing peer comments at various stages of the exercise:

ALVAREZ, Alberto, IPSN, France
BARNETT, Jonathan, WPI, USA
BERG, Heinz-Peter, BFS, Germany
BERTRAND, Remy, IPSN, France
BOUTON, Eric, IPSN, France
BRANDES, Doug, Duke Power Co., USA
CASSELMAN, Chantal, IPSN, France
COUTTS, Alan, Westinghouse, USA
DEY, Monideep, NRC/NIST, USA
ELICSON, Tom, Fauske & Assoc., USA
GAUTIER, Bernard, EDF, France
HEITSCH, Matthias, GRS, Germany
IQBAL, Naeem, NRC, USA

1

JOGLAR, Francisco, SAIC/EPRI, USA
JONES, Geoffrey, NII, UK
JONES, Walter, NIST, USA
JOYEUX, Daniel, CTICM, France
KAERCHER, Maurice, EDF, France
KASSAWARA, Bob, EPRI, USA
KESKI-RAHKONEN, Olavi, VTT, Finland
KLEIN-HESSLING, Walter, GRS, Germany
KLOOS, Martina, GRS, Germany
KRUPPA, Joel, CTICM, France
LACOUE, Jocelyne, IPSN, France
LEBEDA, Christian, TUV, Austria
MCGRATTAN, Kevin, NIST, USA
MILES, Stewart, BRE, UK
NAJAFI, Bijan, SAIC/EPRI, USA
PAGES, Olivier, EDF, France
PLYS, Marty, Fauske & Assoc., USA
REW, Peter, W S Atkins, UK
RIESE, Olaf, iBMB
ROEWEKAMP, Marina, GRS, Germany
ROY, Jean-Francois, EdF, France
SCHWINGES, Bernd, GRS, Germany
SUCH, Jean-Marc, IPSN, France
WILL, Juergen, iBMB, of Braunschweig Tech. Univ., Germany

The following organizations sponsored or collaborated with the organizations represented at the meeting:

- Industry Management Committee, UK
- National Institute of Standards and Technology, USA

The main report of this document is a result of the collective efforts of the individuals and organizations listed above. It is based on the separate reports included in the appendices and discussions at project meetings on the task. The separate reports in the appendices are authored by the analyst(s) identified in the title pages. It is not possible to provide all the results and insights gained from the analyses presented in the appendices in the main text. The reader is encouraged to review the discussions in the appendices to obtain a more comprehensive understanding of the results of the benchmark exercise reported here.

2 Definition of the Benchmark Exercise

2.1 Background

The benchmark exercise was developed to evaluate the capability of fire modeling analyses to provide results for a probabilistic risk analysis (PRA). In a PRA study, fire models are used to estimate the conditional probability of safe-shutdown equipment damage given a postulated fire. The main fire protection features that effect the development of a fire are:

- Automatic or manual isolation of the fire rooms by the closure of fire doors and dampers.
- Automatic fire detection (detection by operators is also important).
- Fire suppression (automatic and manual) with gaseous suppression systems (Halon or CO_2), and nongaseous water-based suppression (sprinkler) systems.

In a PRA study, the target damage time is compared with the duration of a specific fire scenario identified in an event tree. The conditional probability of damage to the safe shutdown equipment is equal to the probability of that fire scenario if the damage time is less than the duration of the fire scenario.

Given the state of the art of fire modeling, the adequacy of fire detection and suppression is normally not included in fire modeling analyses to support a PRA. Therefore, the benchmark exercise did not include the evaluation of these systems or events.

The benchmark exercise is for a basic fire scenario for an NPP defined in sufficient detail to allow the evaluation of the physics modeled in the fire computer codes. This approach is similar to that adopted by the CIB W14 effort (Keski-Rahkonen, 1998) for fire code assessment. An assessment of appropriate input parameters and assumptions, interpretation of results, and determination of the adequacy of the physical models in the codes for specific scenarios will establish useful technical information regarding the capabilities and limitations of the codes. Generic insights regarding the capabilities of the models will also be developed in this process.

The comparisons between fire codes can be used to understand the physics in them, i.e., if all the codes produce similar results over a range of fire scenarios then the physics modeled in the codes is probably adequate for the proposed scenario. However, the compounding effects of different phenomena will also need to be evaluated. Some uncertainty in the results may be acceptable depending on how the results will be used. Uncertainties in the predictions of the fire models based on validations of each fire code can provide a basis for the confidence on the set of results developed in the benchmark exercise.

2.2 Procedure

The following procedure was adopted for the benchmark exercise:

- Analysts should discuss and agree on the input data for the various fire codes that will be used in the benchmark exercise. The goal is to analyze the same problem and minimize the variation of results due to different input parameters. "User effects" will be examined at a later stage.
- The form of the results to be compared should be agreed upon by participants prior to the commencement of the exercise.
- Developers of the fire codes, and those not involved in the development of the codes, can conduct the code analyses for the benchmark exercise.
- Blind simulations will be conducted, i.e., each analyst will independently conduct his or her analyses. The results will be shared between participants when all the analyses by participants have been completed and the results are available. The results will be simultaneously posted on the collaborative project web portal prior to a meeting of the participants.
- If desired, the same code (e.g., CFAST) can be used by different organizations since this will provide useful information on whether the results vary with different users. However, the same version of the code should be used (for CFAST, use Version 3.1.6).
- A series of benchmark exercises will be defined and conducted in this project. This will allow the evaluation of the full spectrum of fire model features and applications, and facilitate the formulation of a comprehensive technical reference for users on the capabilities and limitations of the current fire models.

2.3 Fire Codes Used in the Exercise

The following fire models[2] were used in the benchmark exercise by the organizations listed:

Organization	Codes
1. IPSN	FLAMME-S (zone)
2. NRC/NIST	CFAST (zone), FDS (CFD)
3. GRS	COCOSYS (lumped parameter), CFX (CFD)
4. EdF	MAGIC (zone)
5. BRE/NII	CFAST, JASMINE (CFD)
6. iBMB/GRS	CFAST
7. CTICM	MAGIC

---

[2]The identification of any commercial software or trade name does not imply endorsement or recommendation by the National Institute of Standards and Technology.

A description of these models with references is presented in the Appendices that document the results of analyses using the models.

2.4 Room Size and Conditions

A representative pressurized water reactor emergency switchgear room is selected for this benchmark exercise. A simplified schematic of the room, illustrating critical cable tray locations, is shown in Figure 1. The room is 15.2 m (50 ft) deep, 9.1 m (30 ft) wide, and 4.6 m (15 ft) high. The room contains the power and instrumentation cables for the pumps and valves associated with redundant safe-shutdown equipment. The walls, floor and ceiling are composed of concrete and 152 mm thick. The power and instrument cable trays run the entire depth of the room, and are separated horizontally by a distance, D. The value of D, the safe separation distance, is varied and examined in this problem. The cable trays are 0.6 m (≈24 in) wide and 0.08 m (≈3 in) deep.

The postulated fire scenario is the possibility of the initial ignition of the cable tray labeled as "A," located at 0.9 m (≈3 ft) from the right wall of the room at an elevation of 2.3 m (7.5 ft) above the floor, by a trash bag fire on the floor. Cables for the redundant train are contained in another tray, labeled "B," the target. A horizontal distance, D, as shown in Figure 1, separates tray B from tray A. The room has a door, 2.4 m x 2.4 m (8 ft x 8 ft), located at the midpoint of the front wall, assumed to lead to the outside. The room has a mechanical ventilation system with a flowrate of 5 volume changes per hour into and out of the room. A constant flowrate of the mechanical ventilation system was assumed. The midpoint of the vertical vents for the supply and exhaust air are located at an elevation of 2.4 m and have area of 0.5 m² each. The vents were assumed to be square and located at the center of the side walls (parallel to the cable trays). The air was assumed to be supplied from the outside through the right wall, and exhausted to the outside from the left wall. The effects of the fire door being open or closed, and the mechanical ventilation on and off were examined.

It was also assumed that other cable trays (C1 and C2) containing critical and non-critical cables are located directly above tray A, and no combustible material is found between trays A and B.

2.5 Objectives of Exercise

There are two parts to the benchmark exercise. The objective of Part I is to determine the maximum horizontal distance between the trash bag fire and the target, tray A, that results in the ignition of tray A. This information is of use in a fire PRA to calculate the area reduction factor for the transient source fire frequency, which are derived to be applicable to the total area of the rooms. Analyses of this part of the problem will also provide insights regarding the capabilities of the models to predict simpler fire scenarios for risk analyses than those associated with fires of redundant cable trays.

The goal of the analyses for Part II was to determine the time to damage of the target cable tray B for several heat release rates of the cable tray stack (A, C2, and C1), and horizontal distance, D. The effects of target elevation and ventilation were also examined.

2.6 Properties and Ambient Conditions

2.6.1 Properties

The following are properties used in Part I and/or II of the exercise. Table 1 presents the thermophysical data for the concrete walls, floor, and ceiling, and Table 2 lists the thermophysical data for the electrical cables.

Table 1 Thermophysical Data for Walls, Floor, and Ceiling (Concrete)

Specific Heat	1000 J/(kg.K)
Thermal Conductivity	1.75 W/(m.K)
Density	2200 kg/m^3
Emissivity	0.94

Table 2 Thermophysical Data for Cables

Heat of combustion of cable insulation	16 MJ/kg
Fraction of flame heat released as radiation	0.48
Density	1710 kg/m^3
Specific Heat	1040 J/(kg.K)
Thermal Conductivity	0.092 W/(m.K)
Emissivity	0.8

The chemical properties of cables are obtained from Tewarson (1995). The cable insulation was assumed to be polyvinyl chloride (PVC) with a chemical formula of C_2H_3Cl, and oxygen-fuel mass ratio of 1.408. The yields (mass of species/mass of fuel) of PVC are listed in the following Table 3 from Tewarson, 1995.

Table 3 Yields for PVC

Species	Yield
CO_2	0.46
CO	0.063
HCl	0.5

Soot	0.172

The smoke potential of PVC is 1.7 ob.m^3/g, where the smoke potential is defined as the optical density (db/m or ob) x Volume of the compartment (m^3)/mass of the fuel pyrolyzed (g).

The following are details of the construction and properties of the fire door[2] that could be used in models that allow the incorporation of such features. The fire door is a metal-clad door with a wood core, and insulating panels between the wood core and the metal clad (on both sides of the wood core). The thickness of the metal clad, wood core, and insulating panels are 0.6 mm, 40 mm, and 3 mm respectively. The properties of the fire door are listed in Table 4.

Table 4 Properties of Fire Door

	Thermal Conductivity (W/(m.K))	Density (kg/m^3)	Specific Heat (kJ/(kg.K))
Metal Clad - Carbon Steel	43	7801	0.473
Wood Core - Yellow Pine	0.147	640	2.8
Fiber, insulating panel	0.048	240	

2.6.2 Ambient Conditions and Other Constants

Table 5 lists the internal and external ambient conditions, and Table 6 lists other constants and indices used in the exercise.

Table 5 Ambient Conditions

Temperature	300 K
Relative Humidity	50 %
Pressure	101300 Pa
Elevation	0
Wind Speed	0

---

[2]Derived from information in NFPA 80 and SFPE Handbook.

Table 6 Other Constants and Indices

Constriction coefficient for flow through door	0.68
Convective heat transfer coefficient (assumed the same for all surfaces)	15 $Wm^{-2}K^{-1}$
Lower Oxygen Limit	12 %[*]

*The fire source should pyrolyze at a rate corresponding to the specified heat release rate in Part II if oxygen depletion terminates combustion, i.e., the mass loss rate of the fuel is fixed rather than the "true" heat release rate associated with the oxidation process.

2.7 Heat Release Rates and Target Model

The following are the heat release rate data used for the two parts of the exercise.

2.7.1 Part I

The heat release rate for a 0.121-m^3 (2-gallon) trash bag fire (Lee, 1985, & Van Volkinburg, 1978) that was used for Part I of the exercise is characterized in Table 7. A linear growth between the data points was assumed for the calculation.

Table 7 32 Gallon Trash Bag Fire

Fire Growth Time (minutes)	Heat Release Rate (kW)
1	200
2	350
3	340
4	200
5	150
6	100
7	100
8	80
9	75
10	100

The trash bag consists of: (1) straw and grass cuttings (1.55 kg); (2) eucalyptus duffs (2.47 kg); and (3) a polyethylene bag (0.04 kg). The contents were thoroughly mixed, and then placed in the bag in a loose manner before ignition. The trash bag was approximated as a cylinder with a diameter of 0.49 m, and height of 0.62 m. A fraction of 0.3 for heat released as radiation was assumed, and the heat of combustion of the trash bag material is 24.1 MJ/kg.

The trash bag and the target (representing the tray A) were assumed to be at the center of the cable tray lengths. In order to conduct a simplified and conservative analysis, a single power cable with a diameter of 50 mm at the bottom left corner of the cable tray A was assumed as the target. For models in which the target is represented as a rectangular slab, the slab was assumed to be oriented horizontally with a thickness of 50 mm. The cable was assumed to ignite when the centerline of the cable reaches 643 K.

2.7.2 Part II

Predicting the heat release rate of a burning cable tray stack is extremely complex, and current models are not capable of realistically predicting such phenomena. Therefore, the mass loss rate of the burning cable tray stack was defined as input in the exercise. The consecutive ignition and burning of all 3 cable trays (trays A, C2, and C1) were modeled as one fire. The analyses were conducted assuming a peak heat release rate for the whole cable tray stack[3] between 1 MW – 3 MW. A t-squared fire growth with t_0 = 10 min, and Q_0 = 1 MW was assumed[4], where:

$$Q = Q_0 \, (t/t_0)^2$$

The cable fire was assumed to last for 60 minutes at the peak heat release rate, and decay in a t-squared manner with similar constants as for growth.

For point source calculations, the heat source (trays A, C2, and C1) was assumed to be at the center of the cable tray length and width and at the same elevation as the bottom of tray C2. For 3-D calculations, the fire source was assumed to be the entire length of tray C2 (15.2 m), width (0.6 m), and height of 0.24 m (0.08 x 3). The target (representing tray B) was assumed to be at the center of the cable tray length. In order to conduct a simplified and conservative analysis, the target was assumed to be a single power or instrumentation cable, without an electrical conductor inside the cable, and with a diameter of 50 mm or 15 mm respectively at the bottom right corner of cable tray B. For models in which the target is represented as a rectangular slab, the slab was assumed to be horizontally oriented with a thickness of 50 mm or 15 mm. The cable was assumed to be damaged when the centerline of the cable reached 473 K.

---

[3] The 1 MW to 3 MW range was chosen as bounding values for a stack of 3 cable trays. Considering a heat of combustion of 25 MJ/Kg and a surface controlled specific mass loss rate of about 3 g/m²-sec for cables that pass the IEEE tests, a cable tray 15 m long and 0.6 m wide will have an effective heat release rate of 0.9 MW. An earlier study (NUREG/CR-4230), and fire tests reported in EPRI NP-2660 and EPRI NP-2751 also concluded that the peak heat release rate for a cable tray is limited from 0.8 MW to 2 MW for a well ventilated room.
[4] EdF CNPP tests (1997)

2.8 Cases for Exercise

The following defines the cases for Part I and II of the exercise.

2.8.1 Part I

For the base case, the distance between the midpoints of the trash bag and tray A was 2.2 m (≈7 ft), the door was closed, and mechanical ventilation system was off. In order to facilitate comparisons of code results, simulations for horizontal distances between the trash bag and tray A of 0.3, 0.9, and 1.5 (≈1, ≈ 3, and ≈ 5 ft) were conducted (Cases 1–3). Simulations were also conducted with (a) the door open and mechanical system turned off; and (b) mechanical ventilation system on and the door closed (Cases 4-5). Table 8 provides a summary of the cases analyzed in Part I.

Table 8 Summary of Cases for Part I

Fire Scenario	Distance from Fire (m)	Door	Ventilation System
Base Case	2.2	Closed*	Off
Case 1	0.3+		
Case 2	0.9		
Case 3	1.5		
Case 4		Open	
Case 5			On

* For simulations with the door closed, a crack (2.4 m x 0.005 m) at the bottom of the doorway was assumed.
+A value in a cell indicates the parameter was varied from the base case.

The maximum horizontal distance between the trash bag and tray A, which results in the ignition of tray A, was to be determined by the extrapolation of results for the simulations with the door closed and mechanical ventilation system off (Base Case to Case 3).

The resulting centerline temperature (CL) of the cable was calculated for these simulations. In addition, the following parameters were reported:

- Upper layer temperature
- Lower layer temperature
- Depth of the hot gas layer
- Heat release rate
- Oxygen content[5] (upper and lower layer)
- Flow rates through the door and vents

---

[5]The oxygen present in the fuel was neglected in the calculation of the oxygen concentration in the compartment.

- Radiation flux on the target
- Target surface temperature
- Total heat loss to boundaries

For CFD and lumped-parameter models, the profiles at the midpoint of the room were presented. All results are presented in SI units.

2.8.2 Part II

For the base case, the heat release rate for the cable tray stack was 1 MW, reaching peak heat-release rate and decaying as specified above. The horizontal distance, D, was 6.1 m (20 ft). The door was closed and the ventilation system was off. The target was a power cable 1.1 m (3.5 ft) above tray A. The distance, D, was varied to 3.1 ($\approx$10 ft), and 4.6 m ($\approx$15 ft) for Cases 1 and 2. The peak heat release rate for the cable tray stack was varied at 2 MW, and 3 MW (reaching a peak heat-release rate and decaying as specified above) at a horizontal distance, D, of 3.1, 4.6, and 6.1 m (Cases 3-8). The door was closed and ventilation system operating initially; and the door opened, and ventilation system shut after 15 minutes in Case 9. The door and ventilation system was open throughout the simulation in Case 10. Two elevations for tray B were analyzed to examine the possible effects of the ceiling jet sublayer and the elevation of the target: (1) 2.0 m (6.5 ft) above tray A, (i.e., 0.3 m (1 ft) below the ceiling)in Case 11; and (2) at the same elevation as tray A in Case 12. An instrumentation cable with a diameter of 15 mm was used in Case 13.

The resulting centerline temperature of the target, and time to damage of the target, were to be calculated for these analyses. In addition, the following parameters were reported:

- Upper layer temperature
- Lower layer temperature
- Depth of the hot gas layer
- Heat release rate
- Oxygen content (upper and lower layer)
- Flow rates through the door and vents
- Radiation flux on the target
- Target surface temperature
- Total heat loss to boundaries
- Chemical species (CO, HCl, soot) in the upper layer
- Optical density of smoke (optional)

For CFD and lumped-parameter models, profiles at the midpoint of the room were reported. All results were presented in SI units.

Table 9 Summary of Cases for Part II

Fire Scenario	HRR (MW)	D (m)	Door Position	Mech. Vent. Sys.	Target	Target Elev. (m)
Base Case	1	6.1	Closed[*]	Off	Power Cable	1.1
Case 1		3.1[+]				
Case 2		4.6				
Case 3	2	3.1				
Case 4	2	4.6				
Case 5	2	6.1				
Case 6	3	3.1				
Case 7	3	4.6				
Case 8	3	6.1				
Case 9			Open>15 min	Off>15 min		
Case 10			Open	On		
Case 11						2.0
Case 12						Same
Case 13					Instrument Cable	

[*] For simulations with the door closed, a crack (2.4 m x 0.005 m) at the bottom of the doorway was assumed.
[+]A value in a cell indicates the parameter is varied from the base case.

3 Input Parameters and Assumptions

In accordance with the procedure established for the benchmark exercise presented above, efforts were made by the participants to arrive at a consensus on values for all the input parameters needed for the various codes to be used in the exercise. The following is a summary of the main issues that arose in the consideration of input parameters and assumptions for the scenarios in the exercise, and how participants decided to dispose the issues.

3.1 Summary

Three main issues arose regarding input parameters and assumptions for the fire scenarios in the benchmark exercise:

A.   Specification of the fire source;
B.   Modeling of the target in the compartment; and
C.   Lower oxygen limit (LOL).

The specification of the fire source is fundamental to the input for fire models, and can significantly affect the predicted compartment thermal environment. A consensus was reached on the characterization of the heat release rate (HRR) for the fire scenarios for the benchmark exercise. However, it was noted that presently there is a lack of a consolidated source of information or guidance from where one can select data for heat release rates for different NPP fire scenarios. Although agreement was reached on the specification and values for the target model and LOL to be used for the benchmark exercise, participants did not reach a consensus on the most appropriate specification that could be recommended for model users. The specification of the above three parameters could lead to "user effects," and are the largest sources of uncertainty in the predicted results from the input parameter specification process for the types of fire scenarios examined in the benchmark exercise. These three main issues are summarized below followed by a discussion of other issues of importance.

3.2 Main Issues

1.   <u>HRR Curves for Cable Tray Fires</u>:

Predicting the HRR of a burning cable tray stack is extremely complex, and current models are not capable of realistically predicting such phenomena. Therefore, it is recommended that the HRRs of the burning cable tray stack be defined as input in the problem. For the benchmark exercise, the consecutive ignition and burning of all three cable trays (trays A, C2, and C1) were modeled as one fire. The analyses assumed peak HRRs for the whole cable tray stack between 1 MW and 3 MW. The 1 MW to 3 MW range was chosen as bounding values for a stack of 3 cable trays. Considering a heat of combustion of 25 MJ/Kg and a surface controlled a specific mass loss rate of

about 3 g/(m².s) for cables that pass the IEEE-383 tests, a cable tray 15 m long and 0.6 m wide will have an effective HRR of 0.9 MW. An earlier study (NRC, 1985), and fire tests reported in EPRI (1992) and EPRI (1983) also concluded that the peak HRR for a cable tray is limited from 0.8 MW to 2 MW for a well-ventilated room. The growth characteristic of cable tray fires depends on the fire source, cables ignited with liquid combustibles result in rapid growth, whereas cables ignited by another cable tray fire result in slower growth. Based on tests conducted by EdF (Grondeau, 1997), a t-squared growth was assumed with $t_0 = 600$ s, and $Q_0 = 1$ MW, where:

$$\dot{Q} = \dot{Q}_0 (t / t_0)^2$$

A fire duration of 60 min at peak HRRs was assumed, followed by a t-squared decay with similar constants as for growth. The experiments conducted by EdF have shown that peak HRRs for cable tray fires generally do not last more than 60 minutes.

Given the complexity of modeling flame spread, and the developmental state of flame spread models, it is recommended that current fire modeling analyses use heat release rates derived from tests conducted that have configurations similar to that being analyzed.

The development of a comprehensive database of heat release rate test data for combustible materials in NPPs will be beneficial for the broader application of fire models for NPP fire safety analysis. Further, HRR's to be used for specific NPP fire scenarios will need to be established to avoid "user effects."

2.   Cable Target Model and Dysfunction Temperature

A detailed heat transfer model for a cable tray will be fairly complex. Cable trays generally have a number of cables bundled together in layers, and most cables consist of several conductors. Cables configured in a single layer will get damaged and ignite at a lower flux than cables in a multilayer configuration because the flux to a single layer will not be shielded by cables above that layer. The damage or ignition temperature for cables in a multilayer configuration will depend on the volume-to-surface area ratio. Generally, current fire models are not capable of modeling complex cable configurations. As stated above in Chapter 2, for simplicity the target in the benchmark exercise was assumed to be one power cable conservatively composed only of PVC. Some of the codes used for the benchmark exercise have simple one-dimensional slab models for targets, and others have incorporated a 1-D radial model to approximate radial heat transfer in cables.

As stated in Chapter 2, simulations were conducted for power cables (50 mm diameter), and instrumentation cables (15 mm diameter). For models in which the target is represented as rectangular slabs, the slabs were assumed to be oriented horizontally with a thickness of 50 mm and 15 mm correspondingly. Some participants expressed concern regarding the adequacy of a one-dimensional target model since the

incident radiative flux would vary with the orientation of the slab. Also, the specification of the slab thickness, and selection of the criterion for cable damage (surface temperature versus centerline temperature) would be key to the success of a one-dimensional target model. The cable surface temperature is not indicative of the effects of the thermal environment on cable functionality. Experiments in the PEPSI tests conducted by IPSN indicate that the temperature of the PVC insulation immediately surrounding the electrical conductors reaches about 473 K when cable malfunctions occur (Such, 1997). This corresponds to the temperature at which the PVC insulation softens. Experience from experiments conducted at VTT, indicated that the centerline temperature of a target slab, with a thickness equal to the diameter of the cable, best approximates the temperature of the PVC insulation surrounding the individual conductors. However, some participants felt that the slab dimensions specified for the benchmark exercise may be too thick and result in the simulation of a larger thermal inertia of the target than exists in reality.

This issue is discussed further later in this document when the results of the analyses are presented, and the effect of the cable target model on the results is examined.

3.   Lower Oxygen Limit

In order to conduct a conservative analysis, some participants advocated the use of a value of zero for the LOL. This proposal was put forth based on experimental observations which indicated that it was difficult to determine an LOL value because of the complexity of the combustion phenomena, and effects of ventilation on combustion. Other participants felt that setting LOL at 0% for cases which were developed to examine the effects of ventilation will be contradictory, and for other cases would not yield best-estimate results. Based on this premise, it was suggested that the LOL be set at 12% in order to examine these effects. Several participants in the exercise conducted the analyses of the cases with LOL set at 0% and 12 % to determine the effect. The impact of LOL on the results will be discussed later in this report.

3.3 Other Issues

4.   Chemical Properties of Combustible Sources

Generally, fire models require the specification of the chemical properties of the fire sources, and the species yielded in the combustion process. Such yields affect the emissivity and absorption of radiation by the hot gas and may be important. The content of the trash bag fire source was specified for the benchmark exercise as composed of: (1) straw and grass cuttings(1.55 kg); (2) eucalyptus duffs (2.47 kg); and a (3) polyethylene bag (0.04 kg). These contents were thoroughly mixed, and then placed in the bag in a loose manner before the heat release data was obtained in the tests. However, the chemical properties of the grass cuttings in the trash bag were not available and specified for the exercise. This was a limitation since the chemical properties of the fuel were necessary input for the fire models, especially in the

calculation of radiation from the hot gas. Several analysts assumed the trash bag to contain wood for which the properties were available.

The cable insulation was assumed to be polyvinyl chloride (PVC), and its chemical properties were available. The chemical formula of PVC is C_2H_3Cl, and the oxygen-fuel mass ratio is 1.408. The yields (mass of species/mass of fuel) are 0.46 for CO_2, 0.063 for CO, 0.5 for HCL, and 0.172 for soot.

The development of a comprehensive database of chemical properties of combustible materials in NPPs will facilitate the modeling of specific fire scenarios.

5.   User Effects

As proposed in the procedure for the benchmark exercise, analysts discussed and agreed on the input data for the various codes that will be used in the benchmark exercise. The goal was for participants to analyze the same problem and minimize the variation of results due to differing input data. Even with such efforts to minimize "user effects," some effects were evident in the benchmark exercise. "User effects," and their impacts are discussed later in the document after the results are presented.

6.   Corner/Wall Effects

In practice, cable trays are installed nearer than 0.9 m from walls as specified in the proposed benchmark exercise. Also, transient combustibles may be present in the corner or along walls. In order to minimize the number of cases for the benchmark exercise, corner/wall effects were not examined. Corner/wall effects may be important for specific configurations when combustibles are near a corner or wall, and it is recommended that their impact on the results be examined.

7.   Conditions Outside Compartment

In NPPs, doors in most compartments typically open to another compartment, and not to the outside ambient conditions. In order to simplify and make feasible the evaluation of model effects, multi compartment analysis was not included in the benchmark exercise since that would include additional considerations and effects on the results. In modeling realistic fire scenarios, the conditions outside the compartment may be important, and it is recommended that such effects be examined.

8.   Constriction or Orifice Coefficient for Vents

Based on expert opinion of the participants, it was decided that a value of 0.68 used in some computer codes will be used for the benchmark exercise. The adequacy of this value is discussed later in the document when the results are presented.

9. Convective Heat Transfer Coefficient

Based on expert opinion of the participants, it was decided that the convective heat transfer coefficient would be set at 15 W/m^{2}K for the benchmark exercise. The adequacy of this value is discussed later in the document when the results are presented.

4 Results of Analyses

The following presents a summary of the results that were sought in the benchmark exercise presented in Chapter 2. The main results for the ignition of a cable tray by the trash bag fire, and damage of cable trays of redundant safety systems are presented in Section 4.2. This is followed by a discussion in Section 4.3 on an assessment of the adequacy of the physical models used in the codes for the specific scenario by examining and comparing the trends of the output variables.

The detailed results of the analyses for the benchmark exercise conducted by participants using different fire models are presented in Appendices A through I.

4.1 Summary of Results

4.1.1 Part I

None of the analyses conducted for the benchmark exercise predicted the ignition of the target cable (at 643 K) by the postulated trash bag fire for any of the ventilation conditions in the room. The predicted temperatures for all the cases in Part I are very similar. Given the dimensions of the room and the heat release rate of the trash bag, the maximum surface temperature of the target outside the fire plume region for all the cases analyzed is less than 350 K. The target cable may ignite only if it is in the fire plume region of the fire. The temperature of the target cable is predicted to significantly increase when the distance between the trash bag and cable is between 0.4 m and 0.5 m and the target becomes exposed to the high plume gas temperature. The predicted maximum surface temperature of the target in this region is predicted to be ≈ 550 K. Although the maximum predicted heat flux from the plume incident on the target is predicted to be ≈ 14 kW/m², the duration of the exposure is not long enough to increase the surface of the cable to the ignition temperature. Based on this, one could establish a minimum horizontal safe separation distance[6] of 1.0 m between the trash bag and the target cable. A fire of similar intensity sustained over a longer period could ignite the cable.

4.1.2 Part II

The predicted maximum temperatures of the target cable were below 400 K for all the cases analyzed in Part II. The cable tray fire was limited between 10 min and 15 min by the depletion of oxygen near the cable tray. Given the elevation of the fire source and the predicted extinction of the fire, cable damage is unlikely for the scenarios examined. The analysis of an elevated fire source is key to the accuracy of the predicted result.

---

[6]The concept of safe separation distance is not directly applicable in all countries.

4.2 Verification of Sub-models

This section mainly discusses the verification of the sub-models based on an examination and comparison of the trends from the different fire models used in the exercise. Verification is defined here as the process of determining that a model implementation accurately represents the developer's conceptual description of the model and the solution to the model. Validation, which is discussed in Section 4.3, is defined as the process of determining the degree to which a model is an accurate representation of the real world from the perspective of the intended uses of the model (AIAA, 1998). This section includes the comparison of the magnitudes of the parameters predicted by different fire models. These comparisons will be summarized and discussed in Section 4.3.

The benchmark exercise was aimed mainly at comparing zone models since there is more experience with these models in NPP applications. Therefore, this report mainly addresses zone models and their sub-models. In some instances, comparisons are made with CFD and lumped-parameter models in order to derive insights regarding the model assumptions in the different approaches. Experience with fire models that have been used for the first time for the type of problem posed in the benchmark exercise is discussed. The advantages of more advanced approaches, compared to the two-zone approach, are discussed in Chapter 5.

The following is a list of the major sub-models implemented in the two-zone fire computer codes for modeling the physical phenomena in the scenarios:

- combustion chemistry (tracking concentrations of oxygen and combustion products)
- plume and ceiling jet flow
- mass and energy balance in the two zones (stratification)
- ventilation through doors and cracks
- forced ventilation
- heat transfer to boundaries
- heat transfer to targets
- thermal response of the target

4.2.1 Part I

The measured heat release rate of the trash bag fire which was used as input for Part I is shown in Figure 2. The peak heat release rate for the trash bag fire is ≈ 350 kW, and peaks at ≈ 150 s.

Base Case

Figure 3 shows the plume flow development during this scenario predicted by some of the fire models used in the exercise. The main plume flow increases rapidly at the

initiation of the fire, and does not follow the fire heat release rate, as expected. This is due to the nature of the correlations used in the codes. CFAST over predicts mass entrainment at the initial stages of the fire because of the plume height used in the calculation of the entrained air. Initially, the plume height is assumed to be from the fire to the ceiling. This leads to an over prediction of the initial mass flow to the upper layer, and the rate of descent of the gas layer interface. The peak plume flow from the CFAST (BRE) analysis is less than that from the CFAST (NRC) analysis because of the assumed height of the fire (on the floor in CFAST (NRC) versus at the height of the top of the garbage bag (0.62 m) in CFAST (BRE)). This difference is caused by a "user effect" and is discussed further in Section 5. The peak plume flow predicted by FLAMME_S is less than CFAST by a factor of $\approx$ 2. Table 10 lists the peak plume flow predicted by the various fire models that were used in the exercise. Plume flow is not a normal output parameter from MAGIC. Plume flow is not directly computed in CFD and lumped-parameter models.

Figure 4 shows the predicted hot gas layer development predicted by some of the fire models used in the exercise. The interface height decreases rapidly initially due to high plume flow (see Figure 3). The rate of descent of the interface height decreases after $\approx$ 230 s when the HGL temperature has peaked (see Figure 8). Because of the two-zone assumption, the hot gas layer is prevented from reaching the floor due to air inflow at the crack below the door caused by a negative pressure in the compartment (see Figure 7). In reality, the hot gas layer is expected to reach the floor in parts of the room farthest from the door. CFAST predicts a more rapid descent of the HGL interface than FLAMME-S because of the higher predicted plume flow as shown in Figure 3. The trend of HGL development predicted by the fire models used in the exercise are as expected, given the two-zone assumption in the zone models. The HGL interface height is not directly computed in CFD and lumped-parameter models.

Figure 5 shows the oxygen depletion for the Base Case predicted by the fire models used in the exercise. The oxygen concentration in the upper layer decreases by $\approx$ 1% to 19.2 % generally[7]. The oxygen depletion predicted by the various models is similar. The fire will not be limited by oxygen in this fire scenario for the assumed HRR of the fire and dimensions of the room.

Figure 6 shows the pressure development predicted by the fire models used in the exercise, and Figure 7 shows the resulting flows in and out of the compartment. The pressure is predicted to peak at $\approx$ 150 s when the fire heat release rate peaks, as would be expected. At some point after the fire peaks, the heat released into the compartment by the fire is less than the heat loss through the concrete walls (see Figure 10 for a

---

[7]The oxygen concentration output by the MAGIC code is the mass fraction, whereas the other codes output the mole fraction.

typical heat loss trend[8]) resulting in the decrease of compartment temperature and pressure. The pressure swings to a negative value resulting in flow into the compartment through the door crack. The predicted peak in the outflow is consistent with the pressure profile, and the outflow goes to zero when the pressure in the compartment is less than the outside. The predicted initiation of inflow is consistent with the pressure profile, and is much less than the outflow. Table 10 lists the peak pressure and lower layer outflows that were predicted by the various fire models used in the exercise. The peak over-pressure predicted generally varies between 600 Pa to 2000 Pa, resulting in an outflow of 0.4 kg/s to 0.6 kg/s from the crack under the door. The pressure evolution predicted by JASMINE is discussed by Miles (Appendix G) and was found to be sensitive to the heat release mechanism and amount of heat lost to the boundaries. The trends of pressure and vent flow predicted by zone, CFD, and lumped-parameter fire models used in the exercise vary by a factor of $\approx$ 3 and 1.5, respectively.

Figure 8 shows the hot gas layer (HGL) temperature. The upper layer temperature peaks at $\approx$ 200 s, about 50 s after the fire peaks, when the heat released into the compartment is less than the heat loss from the concrete walls. Table 10 lists the peak HGL temperatures predicted by the various fire models that were used in the exercise. The predicted peak temperature is between 330 K to 360 K. Therefore, in this scenario, the upper layer temperature is predicted to increase by only about 30 K to 60 K. The maximum temperature in the HGL under the ceiling is predicted to be between 400 K to 450 K by JASMINE, FDS, and COCOSYS. The trend of the HGL temperature predicted by the various fire models (zone, CFD, and lumped-parameter) used in the exercise is similar and as expected. The predicted peak HGL average temperature varies by up to 50 %.

One important difference in the results from the zone, CFD, and lumped-parameter codes for the type of scenarios examined for the Benchmark Exercise is the hot gas temperature. A two-zone code, calculates the *average* temperature of the hot gas layer, whereas CFD codes compute the entire temperature profile in the compartment. The peak average HGL temperature predicted by zone models for the Base Case is $\approx$ 350 K. The temperature profiles that were predicted by CFD codes for this case ranges from $\approx$ 350 K in the lower region to $\approx$ 400 K in the upper region of the hot gas. This temperature gradient in the hot gas will determine the convective heat flux to the cable tray depending on its vertical position and may become more prominent and important for scenarios with a high fire intensity.

Figure 9 shows the target surface temperatures predicted by the fire models used in the exercise. The target temperature is predicted to peak at $\approx$ 250 s, approximately 100 s after the fire and target flux reaches its peak due to the thermal inertia of the target. The trend of the target surface temperature predicted by the various fire models used in

---

[8]The unsteady behavior of the curve is due to the numerical derivation of the integral heat inside the wall and door structure.

the exercise is similar and as expected. Table 10 lists the peak flux and temperature of the target. The low thermal conductivity of PVC induces a strong temperature gradient between the surface and center of the cable. The target surface temperature is generally predicted to only increase ≈ 20 K for this case. It should be noted that, although not evident in the results for this case, the fire models utilize different approaches for calculating the heat flux incident on the target. The target is modeled as a slab in CFAST. The orientation specified for the slab will determine the incident flux on it (Miles:Appendix G) and may be a source of "user effects." This is discussed further in Chapter 5. The target is also modeled as a slab in FLAMME_S (see Bouton:Appendix A). MAGIC and COCOSYS employ a 1-D radial model for cable targets in order to eliminate the need to specify the orientation of a slab and improve the predictive capability. CFX includes a 3-D conduction model for the target. The predicted fluxes on the target by these models will vary because of the different assumptions and approaches embedded in them.

Cases 1, 2 and 3: Effect of Distance

Cases 1, 2 and 3 examine the effect of the distance between the target and fire on target heating. The heating of the cable in this scenario is mainly due to the radiative heat flux from the fire and the convective heat transfer from the hot gas. Figure 11 shows the typical evolution of the target surface temperature for various distances (d) between the fire and target. The target surface temperature peaks at ≈ 200 s, ≈ 50 s after the fire reaches its peak intensity due to the thermal inertia of the target. The increase in target surface temperature between distances (d) of 0.9 m and 0.5 m is due to the increase in radiative flux from the fire that is incident on the target. Figure 12 shows the typical strong effect of distance on the radiative flux incident on the target. The target is within the plume region at a distance of ≈ 0.4 m and is heated by convection by the hot plume gas. Target heating in the plume region is not currently modeled in CFAST. The MAGIC code provides an option for a side calculation of target heating in the plume region. The heating can be calculated by hand using plume correlations. CFD codes can calculate target heating based on the principal formulations in the approach which does not explicitly require an empirical plume model. In lumped-parameter approaches, the plume is not really modeled and therefore the form of the plume is dependent on the nodalization around the fire (Klein-Hessling:Appendix F). Also, momentum is not balanced in the lumped-parameter approach. Figure 13 graphically illustrates the exposure of the target in the plume region in a CFD analysis.

Tables 11, 12 and 13 lists the peak fluxes and target surface and centerline temperatures predicted by the fire models used in the exercise. The Tables indicate that the target does not reach the ignition temperature even when it is in the plume region according to the criteria established for ignition, i.e., target centerline temperature of 643 K. The tables again indicate the strong gradient between the target surface and centerline due to the low thermal conductivity of PVC. As indicated above, it should also be noted here that the fire models used for the benchmark exercise utilized

different approaches for calculating the heat flux incident on the target. The result of the different approaches is evident in Tables 11, 12 and 13. In Case 1, some of the fire models include a calculation for target heating in the plume region (e.g., FLAMME_S and CFX).

Cases 4 and 5: Effect of Natural and Mechanical Ventilation

The following presents some key features of the results of Cases 4 and 5. Figure 14 shows a typical development of the interface height for Case 4 versus the Base Case. The interface height approaches a constant value at $\approx$ 140 s, after the HGL reaches the top of the door at $\approx$ 100 s. Figure 15 shows a typical development of the upper layer outflow and lower layer inflow after the HGL interface reaches the door at $\approx$ 100 s, indicating the establishment of a neutral plane below the top of the door (at $\approx$ 2.2 m). Figure 18 is a typical vector plot of temperature in a plane parallel to the cable trays at the midpoint of the room (and the door), and illustrates the typical flow patterns predicted by a CFD code for Case 4 in which the door is open. Outflow and inflow at the door around the neutral plane are illustrated, as also predicted by the zone models. Figure 16 shows typical HGL temperature development for Cases 4 and 5. The HGL temperature for Case 4 is less than the Base Case after $\approx$ 270 s because of the outflow of hot gas from the upper layer (which reaches its peak value at $\approx$ 200 s) through the door, and higher plume flow. The HGL temperature for Case 5 is less than that in the Base Case after $\approx$ 100 s when the HGL reaches the mechanical vents, and ambient air is injected into and hot gas ejected from the hot gas layer in the two-zone formulation.

Figure 17 shows a typical development of flows in the mechanical ventilation system (for Case 5) simulated by zone models. The transitions in flows from the mechanical vents in and out of the gas layers occurs at about $\approx$ 100 s when the HGL reaches the mechanical vents. Figures 19, 20, and 21 show typical flow patterns predicted by CFD models that can be caused by the mechanical ventilation. This type of information will be useful for examining the local effects of ventilation on target heating, where assuming the target is exposed to the average conditions of the HGL will yield conservative results.

The above indicates that the predicted flow patterns for natural and mechanical ventilation by both zone, CFD, and lumped-parameter models are similar, as expected. CFD models have the advantage of providing more detailed flow information for examining local effects.

Tables 14 and 15 list the peaks of some parameters predicted by the fire models used in the exercise. The natural ventilation through the door (Case 4) and mechanical ventilation (Case 5) do not have a strong effect on the target temperature which is in the HGL. The target surface temperature for Case 4 and 5 is less than in the Base Case because of cooler hot gas layer temperatures, but by only 2 K to 4 K of a total increase of 20 K. The predicted peak outflow from the door for Case 5 ranges from 0.4 to 1.3 kg/s. The variation in the predicted outflow is generally consistent with the variation in

the plume flows listed in Table 10. The predicted oxygen concentration in Case 5 is consistently slightly higher than the Base Case due to inflow of ambient air into the HGL. The maximum variation in the predicted HGL temperature by the various codes is ≈ 45 % for Case 4, and ≈ 30 % for Case 5.

Conclusion

The international panel determined that the above analysis of the results for Part I demonstrate that current zone, CFD, and lumped-parameter fire models provide a comprehensive treatment of most physical phenomena of interest in the scenarios analyzed. The results indicate that the trends predicted by the sub-models are reasonable for the intended use of the models for analyzing the specified scenarios. The results of the analyses for the specified scenarios provide useful insights for nuclear power plant fire safety analysis.

4.2.2 Part II

Base Case

Figures 22 to 26 show the predicted results of the main parameters of interest with the fire models used for the benchmark exercise. Figure 27 shows a typical result of the species concentrations predicted by the fire models, and Figure 28 shows the pyrolysis rate specified for the case.

The predicted trends for the heat release rate, interface height, and oxygen concentration in Figures 22, 23, and 24 are collectively examined. The fire models predict the HGL lowers to the fire source (at an elevation of 3.4 m) between 200 s and 400 s. This variation is due to the different approaches used in modeling the fire source (e.g., the cable tray is divided into 10 fire sources in the FLAMME_S analysis). The fire models predict the heat release rate decreases rapidly between 500 s and 700 s when the oxygen concentration in the HGL reaches the LOL of 12 % specified for the exercise. The variation of the predicted time at which the fire is extinguished is due to slight variations of the predictions of oxygen concentration in the HGL. It should be noted that the MAGIC (CTICM) and COCOSYS utilized LOL values of 0 % and 4 % for the analyses. The effect of a lower LOL on the heat release profile is evident in Figure 22 which shows the fire is sustained over a longer period. The HRR predicted by COCOSYS is sustained even longer due to the higher predicted oxygen concentration as seen in Figure 24. Fluctuations in the HRRs predicted by CFAST (shown in Figure 22) are due to the movement of the interface height around the fire source as shown in Figure 23. The extinction models utilized in all the computer codes are approximations of the interaction of the complex combustion process with a limited oxygen environment. Therefore, the results represent an approximation of the conditions expected for this fire scenario.

The HGL profiles shown in Figure 25 are consistent with the HRR profiles shown in Figure 22. As listed in Table 16, the fire models generally predict a peak HGL temperature of ≈ 450 K. The MAGIC (CTICM) and FLAMME_S profiles indicate a decrease in the slope of the HGL temperature when the HRR becomes constant at 1 MW (see Figure 22). The change in the slope is due to the dynamic balance of heat addition to the HGL and loss to the boundaries. The peak temperature predicted by JASMINE and COCOSYS under the ceiling is ≈ 500 K and ≈ 650 K respectively. The higher prediction by COCOSYS is due to the lower LOL value (4 %) used for the analysis, however, other modeling assumptions may also account for the difference.

Table 16 lists the peak flux on the target, and Figure 26 shows the target surface temperature profiles. As indicated earlier, the fire models utilize different approaches for computing the heat flux on the target. For example, the effect of the orientation of the slab in CFAST analyses is seen in Table 16 and Figure 26. The heat flux reported for COCOSYS is only from convection since radiative fluxes are not calculated for Part II (Klein-Hessling:Appendix F). The variation of the peak target surface temperature

predicted by models with similar predictions of heat flux on the target are due to the fire HRR and HGL temperature profiles, i.e., the target temperature increase is based on the duration of its exposure to the environment.

The species concentration predicted by FLAMME_S shown in Figure 27 is consistent with its predicted HRR profile shown in Figure 22. The production of the species from combustion is terminated at ≈ 700 s when the fire is extinguished.

The analysis demonstrates the complexity in modeling an elevated fire source which can be affected by a limited oxygen environment. The assumption for the LOL will have a significant effect on the predicted peak target temperature. Conservative assumptions are warranted due to the uncertainty in the extinction models used in the computer codes.

Cases 1 and 2: Effect of Distance

Tables 17 and 18 list the peak heat fluxes and target temperatures for Cases 1 and 2 reported by the fire models used for the exercise. A consistent trend in the effect of distance on target heating is not evident from the Tables due to the different approaches used for computing heat fluxes. The typical strong effect of the distance between the fire and target on the radiative flux incident on the target was discussed in Section 4.2.1.

Cases 3 to 8: Effect of Fire Intensity and Distance

As discussed above, the cable tray fire in the Base Case is limited by the oxygen depletion in the environment. Cable tray fires that could be potentially more intense (as specified by the pyrolysis rate for these cases) are also limited, i.e., the HRRs are similar to that specified for the Base Case. Therefore, these cases are not discussed further here.

Case 10: Effect of Ventilation

Table 19 lists the peak values of the heat flux, and HGL and target temperatures for Case 10. The peak values predicted by the zone models are generally similar to those for the Base Case because the fire source is in the HGL. The mechanical ventilation system inserts ambient air and ejects air for the lower layer in the two-zone formulation without affecting the HGL. The two-zone approach establishes an artificial boundary between the two zones. In reality, there will be some mixing of mass between the zones. Figures 19, 20, and 21 graphically present the effects of mechanical ventilation on the plume and flow patterns in the compartment predicted by CFD codes. The fire source could be exposed to higher concentrations of oxygen than the HGL average predicted by zone models, if the fire source is near a mechanical ventilation inlet vent. Conservative values of the LOL could be assumed in analyses with zone models to account for this uncertainty.

Cases 11 and 12: Effect of Cable Tray Elevation

Table 20 and 21 lists the peak values for heat flux and target temperatures for Cases 11 and 12. The model used for the target cable will determine the manner in which the target elevation affects the incident heat flux and heating of the cable. As indicated earlier, different approaches are utilized by the fire models used in the exercise leading to the variation in results listed in the tables. Generally, a higher target elevation would expose it to the HGL for a longer period leading to higher temperatures. However, the effect of target elevation is not significant. It should be noted that the target remains outside the ceiling jet layer in this scenario. None of the zone models used in the exercise include a model to predict target heat by the ceiling jet. It will be useful to have this capability for other scenarios in which the target is located in the ceiling jet.

Case 13: Effect of Target Structure

Table 22 lists peak target surface and centerline temperatures that were predicted by the fire models used in the exercise. The structure of the cable has a strong effect on its thermal resistance and heating. The power cable has more thermal inertia and resists heating for a longer period as compared to the instrumentation cable. Table 22 shows that the peak centerline temperatures for the instrumentation cable for Case 13 are much higher than those for the power cable in the Base Case. Figure 29 shows the typical temperature profiles for the power and instrumentation cables. The difference between the core temperature profiles for Case 13 and the Base Case are evident in the figure. The core temperature of the target is much less than the surface temperature due to the low thermal conductivity of the cable insulation, PVC (0.092 W/m.K), except for Case 13. In Case 13, the core temperature is much higher because the diameter of the instrumentation cable is less than that of the power cable by a factor of three. Also, note that the core cable temperature continues to increase after the surface temperature has peaked for all the cases. The figure shows that the maximum temperature (core or surface) is less than the specified damage temperature of 473 K for all the cases in Part II.

A comparison of the fire duration with the time needed for heat to reach the core of the target provides an insight as to why the target is not damaged (Bouton:Appendix A). An estimate of the time taken for the rear face of the target to increase in temperature when the front face is exposed to a heat flux is given by the formula:

$$t_p \approx \frac{e^2}{16(\lambda/\rho c)}$$

where e is the wall thickness, λ the thermal conductivity, ρ the density, and c the specific heat. This equation provides a thermal penetration time of 200 s and 20 s for the power and instrumentation cables, respectively. The duration of the fire is $\approx$ 720 s

for all the cases. For the power cable, the thermal penetration time and fire duration are of the same magnitude. Therefore, the core of the power cable does not approach the surface temperatures. For the instrumentation cable, the thermal penetration time is much less than the fire duration. Therefore, with a short delay, the temperature profile of the cable centerline is similar to that at the surface.

Special Cases

Since the fire was extinguished after ≈ 720 s and well before 4800 s, the expected duration of the fire, several participants in the exercise analyzed special cases. These cases varied slightly but mainly analyzed a cable tray fire at an elevation below the top of the door. Natural ventilation of the hot gases through the door prevented the HGL from reaching and extinguishing the cable tray fire. Therefore, a fire that was sustained at the specified intensity for 3600 s was achieved. Table 23 lists the results of the analyses. All the cases listed analyzed similar conditions, except Case S3 which analyzed a 3 MW fire and a shorter distance between the fire and the cable target. Case S4 analyzed similar conditions but with LOL set at 0 %.

Figure 30 shows the HGL and target surface temperature development for typical results from two fire models. Both models predict an initial rapid rise in the HGL temperature followed by a less rapid increase after the fire intensity has peaked. As indicated earlier, the change in the slope is due to the dynamic balance of heat addition to the HGL from the fire and loss to the boundaries. The target surface in these cases approaches the HGL temperature due to longer exposure of the target to the thermal environment in the compartment. The difference in the peak HGL temperatures predicted by the two models is 35 %. The peak HGL temperatures predicted by other models listed in Table 23 vary by less than this, e.g., the difference between the CFAST and FLAMME_S predictions is ≈ 17 %. Case S4 produces a less severe condition than Case S5 because the fire is extinguished after ≈ 900 s even though LOL is set at 0 % (see MAGIC (CTICM) results in Figure 22).

Table 23 shows that the cable centerline temperatures approach the surface temperatures for these cases because of the long duration of the fire. The thermal penetration time of the power cable, 200 s, is much less than the duration of the fire (sustained for 3600 s) in these cases. Table 23 also shows that the target centerline temperature exceeds the specified damage criteria of 473 K only for Case S3 which analyzed a target 3.1 m from a 3-MW fire sustained for 3600 s.

Conclusion

The international panel determined that the above analysis of the results for Part II demonstrates that current zone, CFD, and lumped-parameter fire models provide a comprehensive treatment of most physical phenomena of interest in the scenarios analyzed. The results indicate that the trends predicted by the sub-models are reasonable for the intended use of the models for analyzing the specified scenarios.

The analyses of the scenarios also demonstrate the complexity in modeling an elevated fire source which can be affected by a limited oxygen environment. The extinction sub-models utilized in all the computer codes are approximations of the interaction of the complex combustion process with a limited oxygen environment. Therefore, the results from the extinction sub-models represent an approximation of the conditions expected for the fire scenarios. The assumption for the LOL will affect the predicted peak target temperature. Therefore, conservative assumptions are warranted due to the uncertainty in the extinction models used in the computer codes. Also, as indicated earlier, the target sub-model in some of the computer codes requires the specification of target orientation by the user. This may result in non-conservative results and "user effects." This limitation may be overcome by establishing procedures for the use of the models to obtain conservative and consistent results. The results of the analyses for the specified scenarios provide useful insights for nuclear power plant fire safety analysis.

4.3 Validation of Models

This section presents a brief discussion of model validation which was defined above as the process of determining the degree to which a model is an accurate representation of the real world from the perspective of the intended uses of the model.

4.3.1 Validation Studies and Uncertainty Estimate

The fire models used in the benchmark exercise have all been compared with test data for fires ranging from 100 kW to 2.5 MW in compartments with volumes ranging from 10 m^3 to 1300 m^3 . These comparisons are summarized and referenced in the individual reports for the fire models included in the appendices. The comparisons are generally satisfactory, with different accuracies reported for the range of data sets. Gautier (Appendix C) reports that the difference in temperatures between those predicted by the model and measured for steady fires is rarely less than 10 K, but predictions that are 50 K or higher are common. The data sets in the validation database include data for the configuration (power, compartment volume) analyzed in the benchmark exercise reported here. IPSN has reported (Such, 1997) tests conducted in a compartment with a volume of 400 m^3 volume and a 1 MW fire for 4200 s. The relative variation of pressure, temperature, and oxygen concentration predicted by FLAMME_S with test data was within 20 %. The comparison of cable surface temperature evolution was less successful due to the compartment vertical temperature gradient in the test data and the difficulty in measuring the cable surface temperature. The validations of the fire models conducted to date indicates that they generally provide a reasonably accurate representation of the real world for the types of scenarios in the benchmark exercise.

Although the exercise reported here did not include comparison of model results with test data, the analysis reported above did include the comparison of the magnitudes of the parameters predicted by different fire models. Generally, the predictions were similar. Models developed independently, if based on the same fundamental laws, are expected to produce similar results.

A distinction is made here between the variability of results due to different assumptions of input data, either for model coefficients, compartment configuration, or fire source data, and the uncertainty of model predictions given the inherent approximations contained in them. As indicated earlier, different assumptions of fire source power can significantly affect the results from the models. Other important input data are the thermophysical parameters, e.g., the convective heat transfer coefficient. The international panel judged that differences in model results due to the uncertainty of the models is less than differences that can be caused by variations in input data and assumptions.

4.3.2 Benefit of Extending Validation Database

Although the above discussion proposes a certain degree of confidence in the current fire models, there are benefits to extending the validation database. As discussed in previous sections, the sub-model for the target, and issues regarding the thermal environment of the target, is a source of uncertainty for these types of scenarios. As indicated in the analysis of the results, the target response is sensitive to the magnitude and duration of the heat flux incident on it. A target may be more sensitive to the duration of the exposure than the magnitude of the heat flux and intensity of the thermal environment if it has a high thermal inertia. It will be useful to conduct international collaborative validation exercises in which the sensitivity of target response is explored and the predictive capability of target damage is the main focus of the program. Also, more refined measurements and data analyses will be useful to estimate the quantitative uncertainties of the parameters predicted in the analyses of these fire scenarios. The computer code results, with quantitative estimates of the uncertainties in the predicted parameters, will extend the confidence in the models for supporting engineering judgments in nuclear power plant fire safety analysis.

5 General Conclusions and Recommendations

This final chapter provides a discussion of the general conclusions and issues derived from the benchmark exercise.

5.1 Capabilities and Limitations

As indicated above, the international panel determined that the analysis of the results of the benchmark exercise demonstrates that current zone, CFD, and lumped-parameter fire models provide a comprehensive treatment of most physical phenomena of interest in the scenarios analyzed. The results indicate that the trends predicted by the sub-models are reasonable for the intended use of the models for analyzing the specified scenarios. The results obtained from these fire models can provide useful insights for nuclear power plant fire safety analysis for the type of scenarios analyzed.

Capabilities

The constitutive equations for mass and energy in the fire models provide a reasonable prediction of the hot gas layer development and temperatures in the compartment. The fire models generally provide an adequate method to balance and estimate the concentration of oxygen and combustion products in the compartment. Mass flows that result from the pressurization of the compartment, and natural or mechanical ventilation, are reasonably predicted for the zone, CFD, and lumped-parameter models. Convective and radiative heat fluxes to the boundaries and target are comprehensively treated in the models. The thermal response of the target is also adequately estimated in the models.

Limitations

Fire Source

The mass loss rate in the models is generally not coupled with the thermal behavior of the source. This limitation necessitates the specification of the mass loss rate profile. The heat release rate is then calculated in the model based on the availability of oxygen. The coupling of mass loss and heat release, which entails modeling the combustion process, is complex and difficult, especially for solid fires. Until further research is conducted and accurate models developed to overcome this limitation, characteristic mass loss rate profiles will need to be developed and specified. An international effort to develop standardized mass loss profiles is recommended.

A related limitation exists for the extinction sub-models utilized in the computer codes. The sub-models used are approximations of the interaction of the complex combustion process with a limited oxygen environment. The results from the extinction sub-models represent an approximation of the conditions expected for the fire scenarios. Some

tests have shown that fires can be maintained at low oxygen concentrations through the establishment of flames distant from the source. Conservative assumptions for the LOL may be warranted to compensate for the limitations in the extinction models used in the computer codes. Participants in the exercise reported here used an LOL value ranging from 0 % to 12 % based on their experience and judgment, and degree of conservatism needed for the analysis. It is recommended that users of fire models determine an appropriate value based on the ventilation conditions for their application, scenario configuration (single versus multi-compartment), and desire for conservatism in the analysis. A sensitivity analysis for different LOL values may be appropriate for a best-estimate calculation.

Target Model

The fire models generally include a simple sub-model for the target that allows the modeling of one cable. This is acceptable as long as the goal of the analysis is to provide a conservative estimate. The modeling of a cable bundled with other cables in a tray will result in lower cable temperatures. The ability to model bundled cables, and the structure of the cable tray may be beneficial. The target sub-model in some of the computer codes requires the specification of target orientation by the user. This may result in non-conservative results (for a single cable) and a "user effect." This limitation may be overcome by including a 1-D radial heat transfer model for the target, or establishing procedures for the use of the slab model in a consistent manner. The ability to model a target with more than one material may also be useful to determine the temperature gradient in the cable, otherwise the property of the single material to be specified needs to be developed. Target heating in the plume and ceiling jet is not included in most of the models, thereby limiting the analysis of certain types of scenarios.

Given the above complexity in estimating cable damage, an evaluation should be conducted to determine whether consistent results can be obtained in modeling cable damage directly (modeling heat conduction into a cable or tray of cables) or defining a conservative safety criterion based on gas temperature and/or incident flux may be prudent.

Two-Zone Approximation

The two-zone approximation may limit the analysis of certain types of scenarios and issues. This includes issues for which the local effects of natural and mechanical ventilation need to be examined (e.g., under ventilated scenarios), or the local temperature in the HGL is necessary to calculate the target temperature.

Other Modeling Issues

The following is a summary of modeling issues that are discussed in the reports by the analysts in the appendices, or that were raised and discussed at the 4th meeting when

the results of the analyses were presented.

Radiation from Hot Gas

Radiation from the hot gas in the upper layer or the plume region is likely to be the main contributing factor to cable damage for the types of scenarios analyzed in the exercise. The predicted concentration of soot is an important factor in calculating the radiation from the hot gas. A sensitivity study is recommended to examine the impact of soot concentration on the overall radiative flux from the hot gas. A review should also be conducted to assess the need for additional data for soot yields.

Plume Models

The plume correlation in zone models provides the driving force for the generation of hot gases. Certain limitations in the plume model for CFAST were noted earlier. Although plume correlations and calculations have been extensively reviewed and used in the development of zone, CFD, and lumped-parameter models, they should be examined for any limitations for the types of fire sources of interest in nuclear power plants.

Convective Heat Transfer Coefficient

During the development of input data for the models, it was decided that the convective heat transfer coefficient would be set at 15 W/m^2 K for the benchmark exercise. This value may be too high and unrealistic, especially for some surfaces. This parameter should be reviewed to determine if another value based on a free convection correlation should be used, and if different values should be used for the floor, wall, ceiling, and cable.

5.2 User Interface

The following are recommendations made regarding the user interface.

As evident from the discussions in this document, users of fire models should have knowledge of basic heat transfer, thermodynamics, and fluid mechanics. A fundamental course in fire dynamics, available at the graduate level in several universities, will provide additional beneficial knowledge for the use of the models. It is not necessary to be a developer or an expert to use the models. Short courses that provide basic training in the use of specific models will also be beneficial.

In order to prevent misuse, the fire models should be adequately documented with a technical reference manual, user's guide, and verification and validation report. The documentation should include sample problems which include input data and results for the scenarios analyzed so that the user is able to replicate the analyses. The inclusion of several sample problems will allow the user to verify the correct installation of a code,

gain confidence in the use of the model, and have access to input data for a range of fire scenarios. Allowable options in the models should be adequately explained, e.g., constrained versus unconstrained fire in CFAST, to prevent misuse of the options for conditions for which they were not intended (Will:Appendix H). Specific parameters that may be subject to "user effects" should be identified and discussed, e.g., target orientation in CFAST and the mesh for the conduction calculation in MAGIC.

Results may vary if different versions of the code are used. The legacy of the fire models should be documented to identify the differences between various versions of the code. The compatibility of older codes with newer operating platforms should be identified, e.g. CFAST version 3.1.6 is not compatible with Windows NT (Will:Appendix H). The effect of different compilers on the model installation should also be discussed.

The fire models should have a graphical user interface (GUI) to allow users to efficiently input data for the models and minimize errors in this process. The lack of a GUI for CFAST Version 4.0 may have led to errors (Will:Appendix H). The GUI should provide automatic controls for the input of data and alert the user when values are beyond recommended ranges, or are incorrect. A GUI with this type of feature to check for errors will minimize the input of incorrect data, and the improper use of the model.

5.3 Benefits of Hand Calculations

Although hand calculations can provide bounding results for many scenarios, the results discussed above showed the strong coupling between the target response and the thermal environment created by the fire. Therefore, for the types of scenarios analyzed in the exercise reported here, zone models provide the minimum simulation capability to examine the dynamic response of the target to the fire environment.

5.4 Need for Model Improvements

Several of the models used may benefit from an improved target model, especially to address the "orientation" issue discussed above. However, the benefit from such an improvement will need to be examined given zone models do not provide local temperatures of the hot gas around the target. There may be a steep vertical temperature gradient in the hot gas, especially for large fires. The fire models generally include a simple sub-model for the target that allows the modeling of one cable. This is acceptable as long as the goal of the analysis is to provide a conservative estimate. The modeling of a cable bundled with other cables in a tray will result in lower cable temperatures. The ability to model bundled cables, and the structure of the cable tray, may be beneficial. The ability to model a target with more than one material may also be useful to determine the temperature gradient in the cable. Target heating in the plume and ceiling jet regions may also be beneficial improvements to the models that do not have this feature.

5.5 Need for Advanced Models

The mass loss rate in the models is generally not coupled with the thermal behavior of the source. This limitation necessitates the specification of the mass loss rate profile. The coupling of mass loss and heat release, which entails modeling the combustion process, is complex and difficult, especially for solid fires like cables. Several efforts are underway to address this issue. CFD codes provide the opportunity to address this issue because of the availability of localized information that is necessary for coupling mass loss and heat release. A related benefit of this improvement will be the ability to more accurately predict the point of extinction in under ventilated fires.

CFD models may be beneficial to verify the results of a zone model study. CFD models, which are computationally more expensive, may be used following the analysis of the problem with a zone model, including sensitivity calculations. A few important scenarios can then be analyzed with a CFD model to provide a comparison and verification of the results obtained from the zone model.

CFD models may also be beneficial for analyzing issues when local effects are important. Figures 19, 20 and 21 illustrated the ability of CFD models to provide detailed information of the flow patterns in the compartment. This type of information can be useful in calculating target heating in the plume region, and for determining effects of ventilation on the fire source and target. Lumped-parameter models also provide local information to determine the effects of ventilation. Also, both CFD and lumped-parameter models provide information on the temperature gradient in the hot gas layer which may be important for determining target response.

The prediction of radiative fluxes from the plume in the near field is a complex problem. CFD models, in combination with a radiation model, can provide a better estimate of the radiative fluxes from the flaming region and hot gas layer. The radiation model may be as important as the fluid dynamics for thermal damage analysis. In order to maintain efficiency in the computations, radiation fluxes and gas temperatures could be stored at target locations, and used later in a separate conduction model.

5.6 Need for Additional Test Programs

The need for additional test programs for supporting the use of fire models may be divided into three categories.

1. Fire Model Validation

The need for additional fire model validation was discussed in Section 4.3.2. The sub-model for the target, and issues regarding the thermal environment of the target, is a source of uncertainty for the types of scenarios that are important in nuclear power plants. It will be useful to conduct international collaborative validation exercises in

which the predictive capability of target damage is the main focus of the validation. Also, more refined measurements and data analyses will be useful to estimate the quantitative uncertainties of the parameters predicted in the analyses of these fire scenarios. The data from tests can also be used for improving target models, and developing models for target heating in the ceiling jet and plume regions.

2. Mass Loss Rate Data

Given the complexity of modeling flame spread, and the developmental state of flame spread models, it was recommended earlier that current fire modeling analyses use mass loss rates derived from tests conducted with configurations similar to that being analyzed. The development of a comprehensive database of mass loss rate profiles for combustible materials in NPPs will be beneficial for the broader application of fire models in fire safety analysis.

3. Cable Damage Criteria

The temperature at a specific point in the cable was used in the exercise to specify the criterion for cable damage. Information regarding cable damage criteria is limited. It will be beneficial to generate damage criteria for cables and a broad range of equipment of interest. This information is essential for fire safety analysis. The full benefit of fire models in nuclear power plant fire safety analysis can be achieved by establishing a broad database for damage criteria.

5.7 Generic Applicability of Conclusions

Most of the insights gained and conclusions drawn from this benchmark exercise are applicable to a broad range of fire scenarios expected in nuclear power plants. However, further benchmark and validation exercises are necessary for some specific configurations such as large compartments (like the turbine building) with large pool fires, multi compartments with horizontal and vertical vent connections, and control room configurations. Insights on some further specific issues are likely to be developed from such exercises.

Table 10 Comparison of Results for Part I, Base Case

O₂ Conc. in HGL at 600 s (Vol. %)	Peak Plume Flow (kg/s)	Peak Pressure (Pa)	Peak LL Outflow (kg/s)	Layer Ht. at 240 s (m)	Peak HGL Temp. (K)	Peak Flux on Target (W/m²)	Peak Target Temp. (K) Surface	CL
cb: 19.0 cn: 19.3 f: 19.9 me: 22[6] j: 19.9 o: 19.3	cb: 3.6 cn: 4.7 f: 2.2 o: 0.3	cb: 1770 cn: 2057 f: 1444 me: 961 o: 975 h: 210 j: 46 s: 600[4]	cb: 0.54 cn: 0.59 f: 0.41 me: 0.39 o: 0.40 H: 0.35 j: 0.08	cb: 1.37 cn: 0.82 f: 1.83 me: 1.37 h: 0.3	cb: 359 cn: 357 f: 347 me: 336 mc: 336 o: 449[1] h: 349 x: 360 j: 400[3] s: 400[5]	cb: 1330 cn: 1257 me: 1839 o: 472 x: 210 j: 4287 s: 1197	cb: 317 cn: 322 mc: 319 o: 312 s: 333 me: 318 x: 360	f: 303[2] me: 301 mc: 300 o: 301 h: 310 x: 300

[1]COCOSYS reported temperatures are maximum values at the ceiling.
[2]FLAMME_S reported target temperatures for Part I are at the end of calculation (600 s).
[3]JASMINE reported temperatures are the "center top" values which are higher than average "hot layer" temperatures.
[4]The crack area was twice the area specified due to grid size used in simulation.
[5]FDS reported temperature is the maximum value at the ceiling.
[6]The oxygen concentration from MAGIC are reported as mass percent.
cb: CFAST-BRE
cn: CFAST-NRC/NIST
f: FLAMME_S
me: MAGIC-EdF
mc: MAGIC-CTICM
o: COCOSYS
h: HADCRT
j: JASMINE
s: FDS
x: CFX

Table 11 Comparison of Results for Part I, Case 1

Peak Flux on Target (W/m^2)	Peak Target Temp. (K) Surface	CL
cb: 3120 cn: 1932 me: 12,855 o: 26,763 x: 210 j: 4029	f: 773[1] cb:353 cn:332 mc:346 o: 327 x: 550[1]	f: 349 me: 303 mc: 300 o: 300 x: 300

[1]Target calculations by FLAMME_S and CFX account for the convective heat transfer from the hot gases in the plume region to the target.

Table 12 Comparison of Results for Part I, Case 2

Peak Flux on Target (W/m^2)	Peak Target Temp. (K) Surface	CL
cb: 2430 cn: 1808 me: 4665 o: 711	cb:340 cn:329 mc:333 o: 315	f: 308 me: 302 mc: 300 o: 300

Table 13 Comparison of Results for Part I, Case 3

Peak Flux on Target (W/m^2)	Peak Target Temp. (K) Surface	CL
cb: 1770 cn: 1537 me: 2732 o: 648	cb:329 cn:321 mc:323 o: 314	f: 308 me: 302 mc: 300 o: 300

Table 14 Comparison of Results for Part I, Case 4

Peak UL Outflow (kg/s)	Layer Ht. at 240 s (m)	Peak HGL Temp. (K)	Peak Flux on Target (W/m^2)	Peak Target Temp. (K)	
				Surface	CL
cb:0.92 cn:1.36 f: 0.50 me:0.86 o: 1.26 h: 0.4 j: 0.90	cb: 1.86 cn: 1.67 f: 2.03 me:1.77 h: 1.5	cb: 365 cn: 357 f: 348 me:336 mc:336 o: 452 j: 400	cb: 1340 cn: 1298 me:1845 o: 486 j: 4560 s: 981	cb:322 cn:318 mc:320 o: 311 s: 325	f: 303 me:301 mc:300 o: 301 h: 306

Table 15 Comparison of Results for Part I, Case 5

O$_2$ Conc. in HGL at 600 s (%)	Peak Pressure (Pa)	Layer Ht. at 240 s (m)	Peak HGL Temp. (K)	Peak Flux on Target (W/m^2)	Peak Target Temp. (K)	
					Surface	CL
cn: 19.7 f: 20.3 me:22.5 m: 19.7 o: 19.7	cn: 2200 f: 1071 me: 714 o: open h: ≈ 0	cn: 0.82 f: 1.83 me: 1.43 h: 1.0	cn: 348 f: 348 me: 334 mc: 334 o: 451 x: 350	cn: 1239 me: 2042 o: 396 x: 210 s: 890	cn: 319 s: 319 mc:318 o: 308 x: 360	f: 303 me: 301 mc: 300 o: 300 h: 309 x:300

Table 16 Comparison of Results for Part II, Base Case

O_2 Conc. of HGL at 600 s (%)	Peak Pressure (Pa)	Peak HGL Temp. (K)	Peak Flux on Target (W/m²)	Peak Target Temp. (K) Surface	CL
cb: 12.5 cn: 13.2 me: 17.0[2] f: 17.2[2] f: 17.6 j: 16.1 o: 17.6[2]	cb: 715 cn: 805 me: 721 f: 676 o: 2104 j: 305	cb: 524 cn: 441 f: 465 me:440 o: 646[1] x: 680 j: 500	cb: 3170[4] cn: 1594[5] me: 3785 o: 2400 x: 840 j: 2420	cb: 357 cn: 323 o: 436 f: 403	f: 325[3] o: 374 me: 311 x: 301

[1]COCOSYS reported temperatures are maximum values at the ceiling.
[2]Reported at 500 s.
[3]FLAMME_S reported target temperatures for Part II are at the end of calculation (1200 s).
[4] Reported fluxes are incident on top side of target slab for Part II results
[5]Reported fluxes are on bottom side of target slab for Part II results

Table 17 Comparison of Results for Part II, Case 1

Peak Flux on Target (W/m²)	Peak Target Temp. (K) Surface	CL
cb: 2740 j: 2620 me: 3784 o: 814	cb: 357 o: 438 f: 427	f: 325 me: 311 o: 374

Table 18 Comparison of Results for Part II, Case 2

Peak Flux on Target (W/m²)	Peak Target Temp. (K) Surface	CL
cb: 2500 me: 3784 j: 2530 o: 2368	cb: 349 o: 435 f: 427	f: 325 me: 311 o:373

Table 19 Comparison of Results for Part II, Case 10

Peak HGL Temp. (K)	Peak Flux on Target (W/m²)	Peak Target Temp. (K) Surface	CL
cn: 448 f: 465 me: 441 o:702 x: 525 j: 550	cn: 2234 me: 3792 o: 2158 x: 500 j: 3310	cn: 373 o: 555	f: 324 me: 311 o:472 x: 335

Table 20 Comparison of Results for Part II, Case 11

Peak Flux on Target (W/m²)	Peak Target Temp. (K) Surface	CL
cb: 4080 cn: 2155 me: 3784 o: 2527 j: 3250	cb: 387 cn: 343 o:446	me: 311 o: 379

Table 21 Comparison of Results for Part II, Case 12

Peak Flux on Target (W/m²)	Peak Target Temp. (K) Surface	CL
cb: 2570 cn: 1626 me: 877 o: 1827 j: 1570	cb: 345 cn: 326 o: 398	me: 302 o: 355

Table 22 Comparison of Results for Part II, Case 13

Peak Flux on Target (W/m^2)	Peak Target Temp. (K) Surface	CL
cb: 3170 o: 2400	cb: 358 o: 482 f: 421	f: 400 me: 352 o: 473

Table 23 Comparison of Results for Part II, Special Cases

	Peak HGL Temp. (K)	Peak Flux on Target (W/m^2)	Peak Target Temp. (K) Surface	CL
Case S1	cn: 457	cn: 2172	cn: 435	
Case S2	f: 489		f: 483	f: 458
Case S3	mc: 623		mc: 603	mc: 533
Case S4	me: 441	me: 4250	me: 408	me: 323
Case S5	me: 543		me: 531	

Case S1: Part II, Base Case with fire source at 1.8 m, and door open.
Case S2: Part II, Case 10 with fire source at 2.3 m (elevation of tray A).
Case S3, Part II, HRR = 3 MW; D = 3.1 m; door open and ventilation system on; fire source at 2.1 m, and LOL = 0 %.
Case S4: Part II, Base Case with LOL = 0 %.
Case S5, Part II, Case 10 with fire source at 1.0 m.

All dimensions are in meters

Figure 1 Representative PWR Room

45
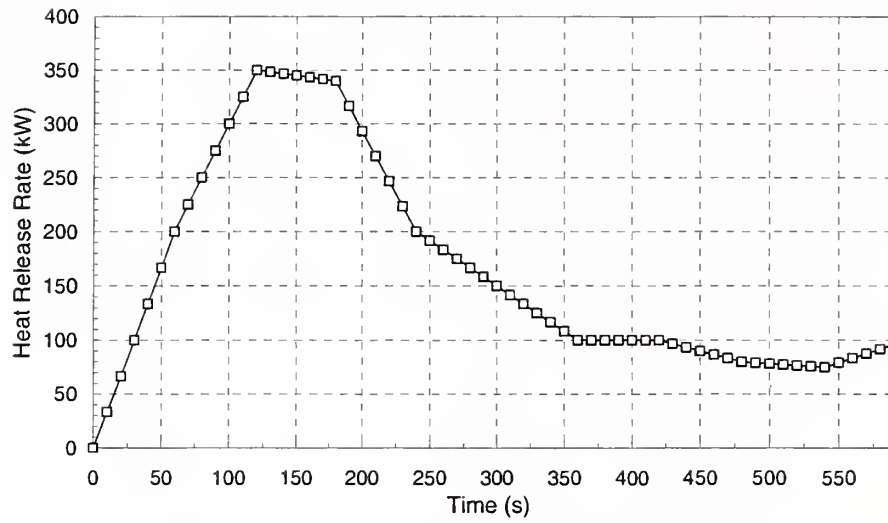
Figure 2 Trash Bag Fire (Part I)
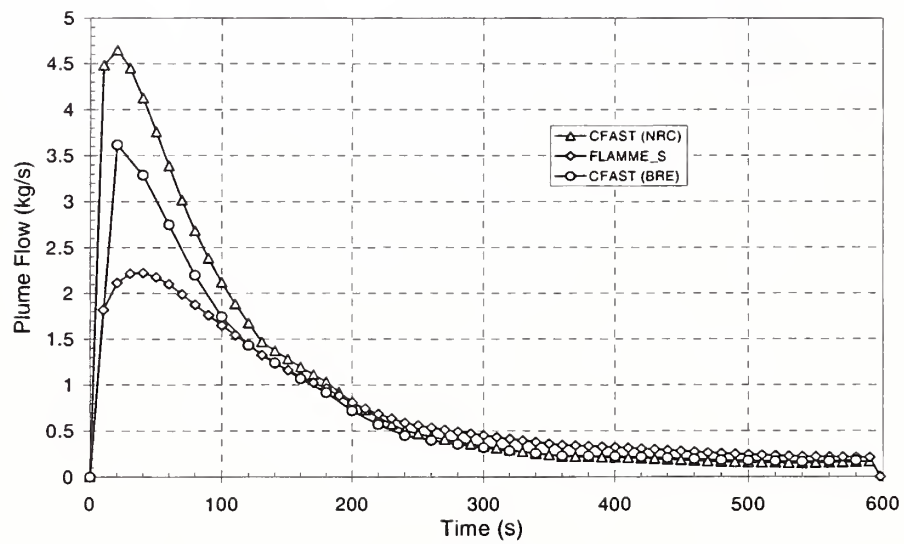
Figure 3 Plume Flow (Part I, Base Case)

46
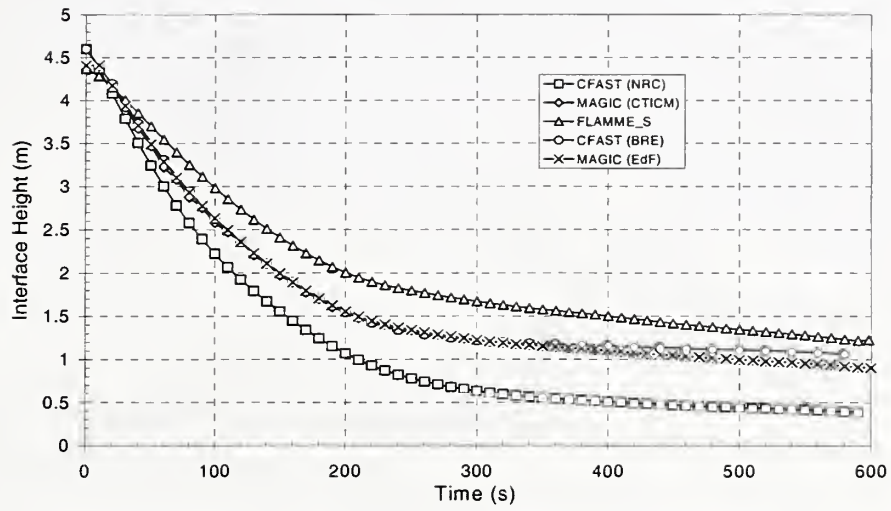
Figure 4 HGL Development (Part I, Base Case)
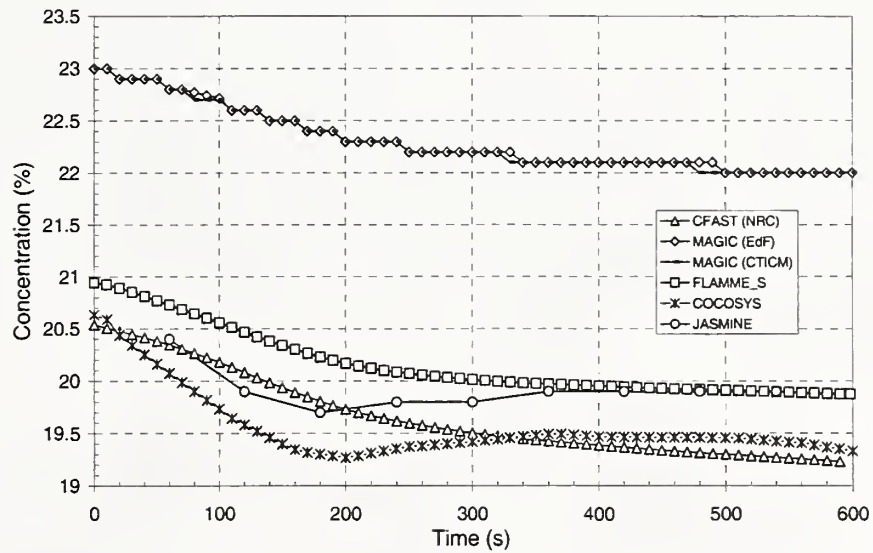
Figure 5 Oxygen Concentration (Part I, Base Case)
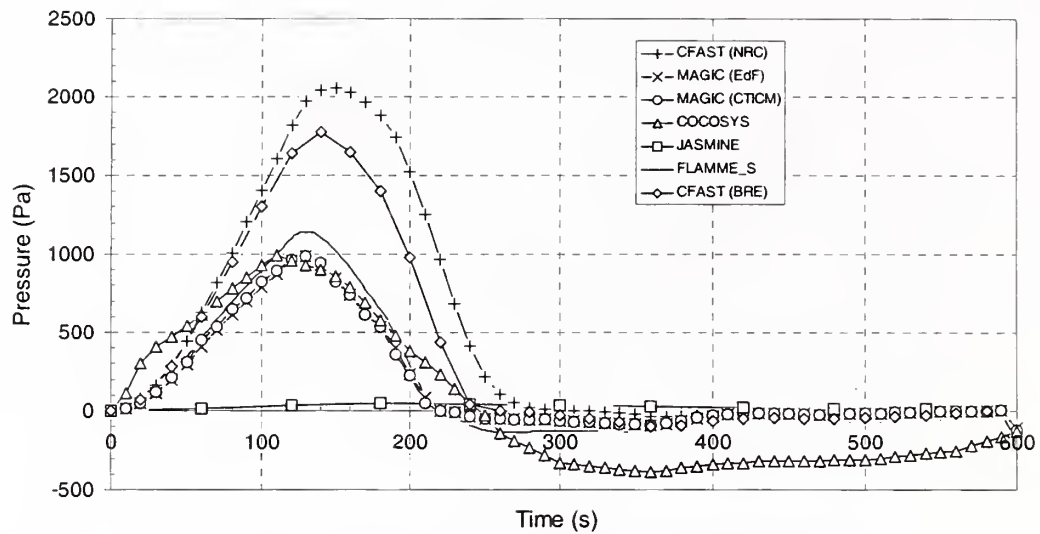
Figure 6 Pressure Development (Part I, Base Case)
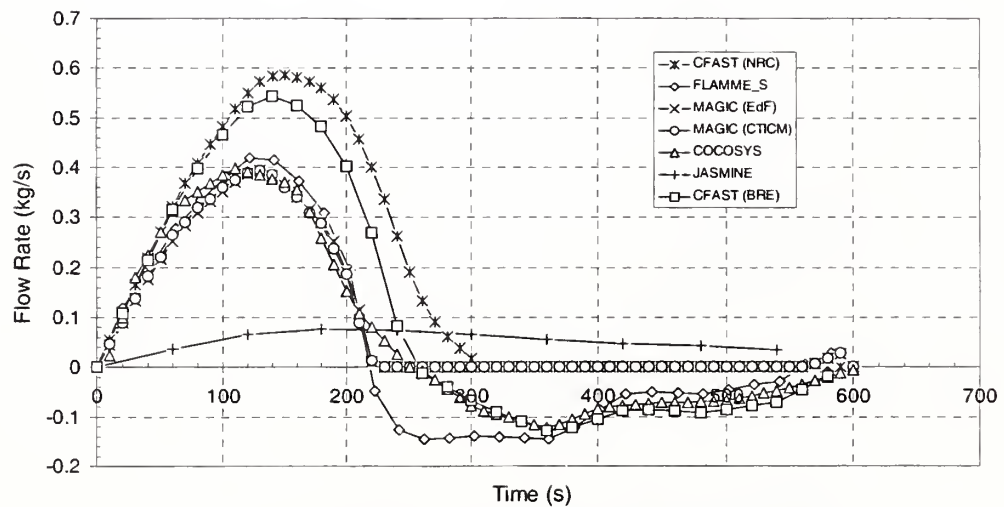
Figure 7 Flow from Crack (Part I, Base Case)
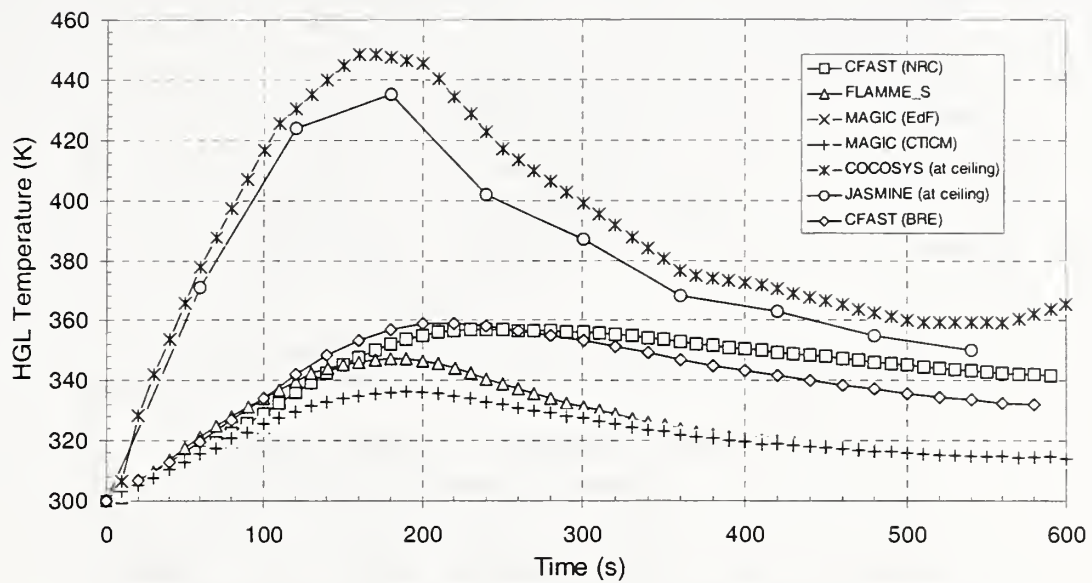
Figure 8 HGL Temperature (Part I, Base Case)
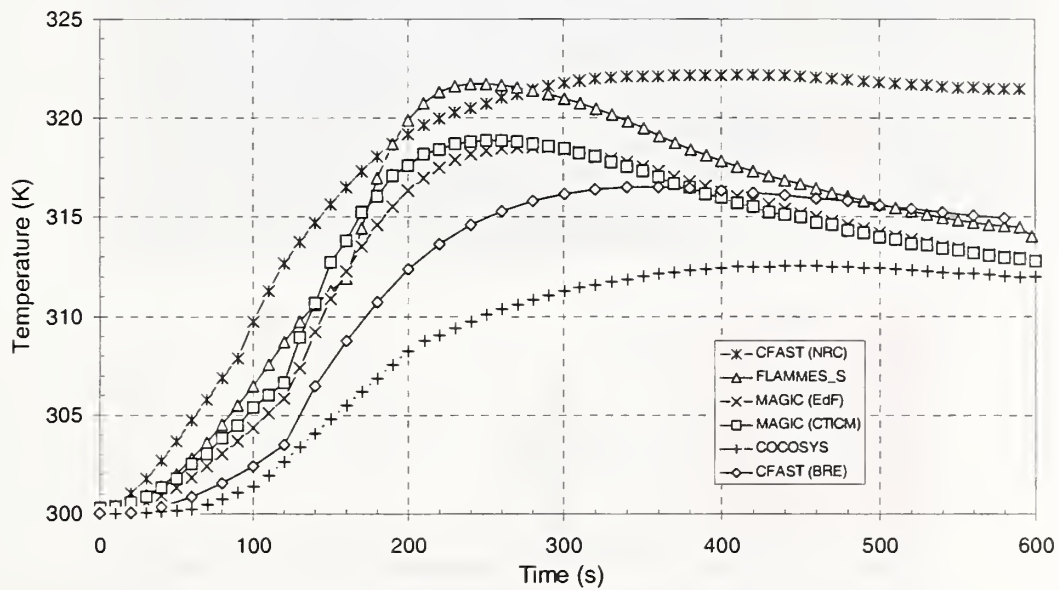
Figure 9 Target Surface Temperature (Part I, Base Case)

(cocV1.2AA) pyrolysis benchmark p1bs
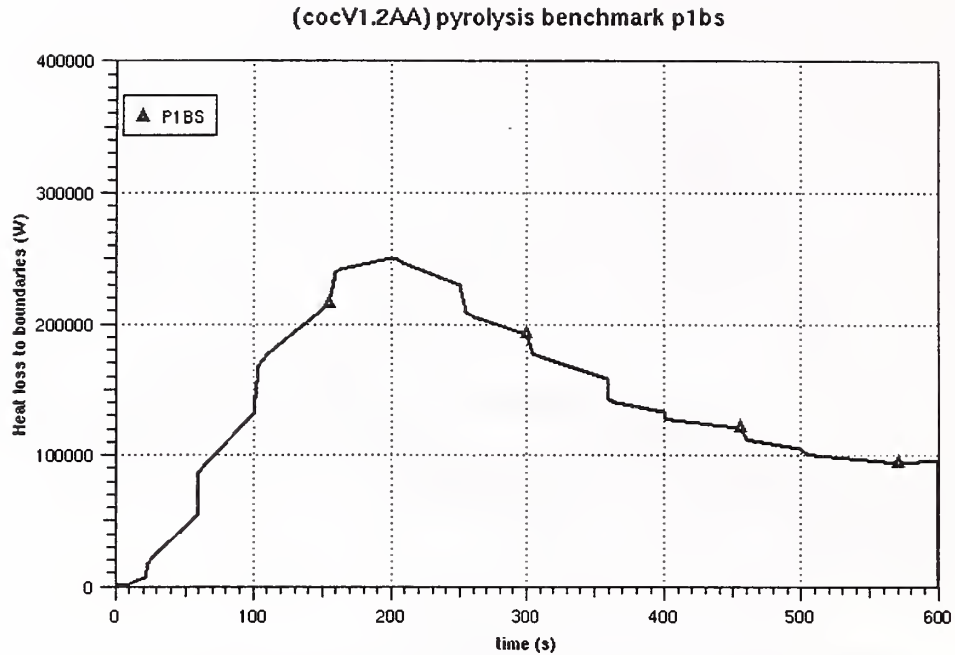
Figure 10 Total Heat Loss from Boundaries - COCOSYS
(from Klein-Hessling (Appendix F))
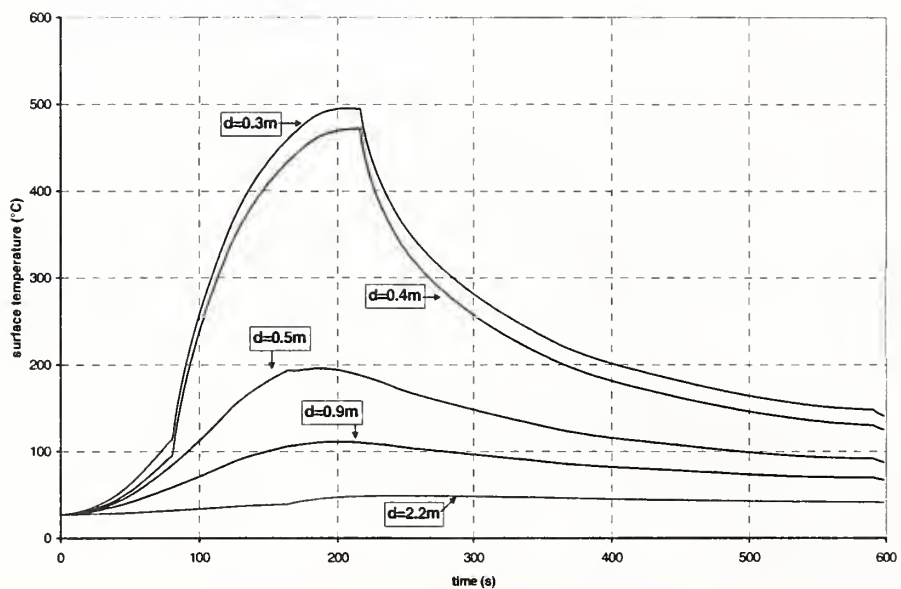
Figure 11 Effect of Distance between Fire and Target -
FLAMME_S (from Bouton:Appendix A)
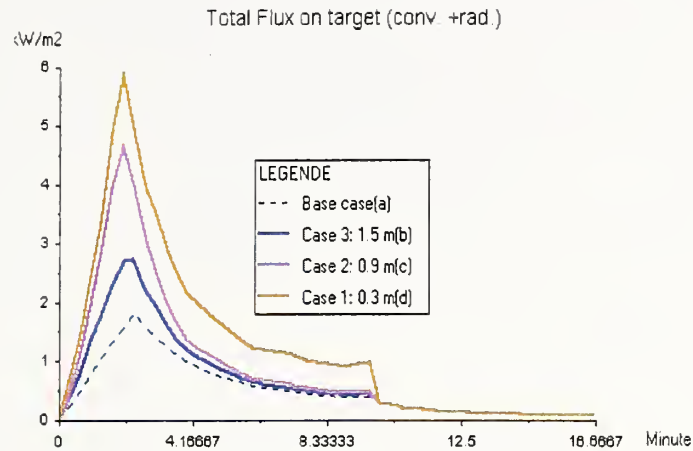
Figure 12 Effect of Distance on Radiative Flux - MAGIC (from Gautier:Appendix C)

Cable Tray Fires of Redundant Safety Trains
Benchmark Part I
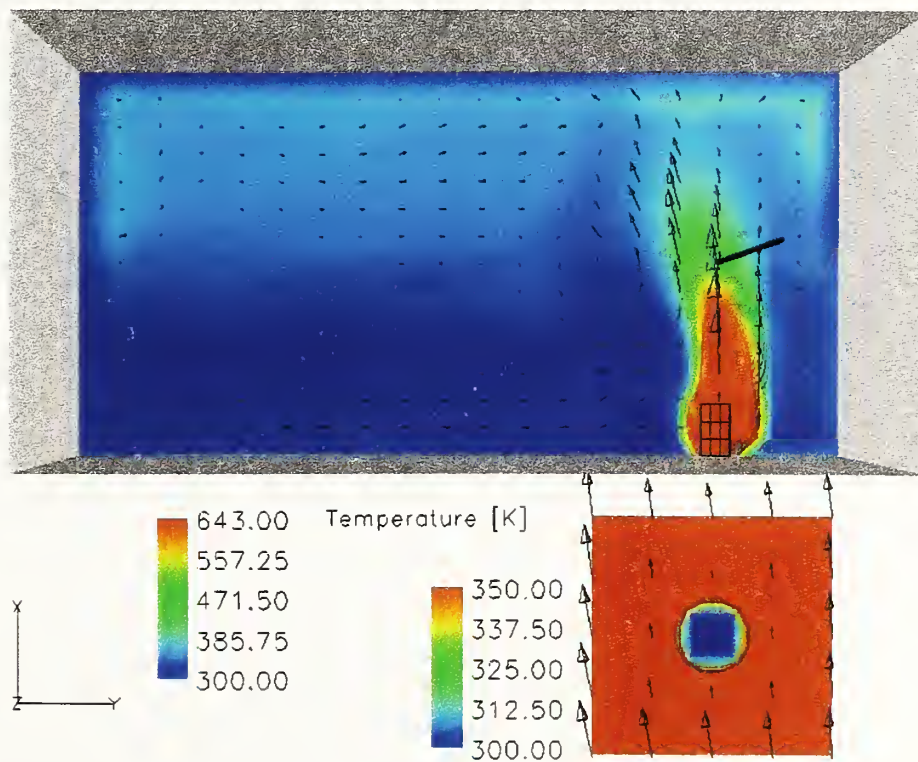
Figure 13 Target Exposure in Plume Region in CFD Analysis - CFX
(from Heitsch (Appendix D))
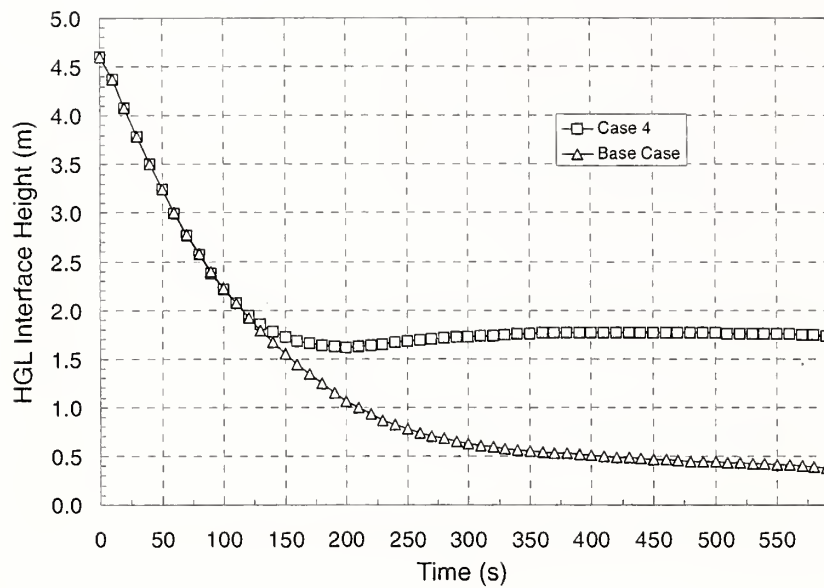
Figure 14 HGL Development (Part I) - CFAST
(from Dey (Appendix B))
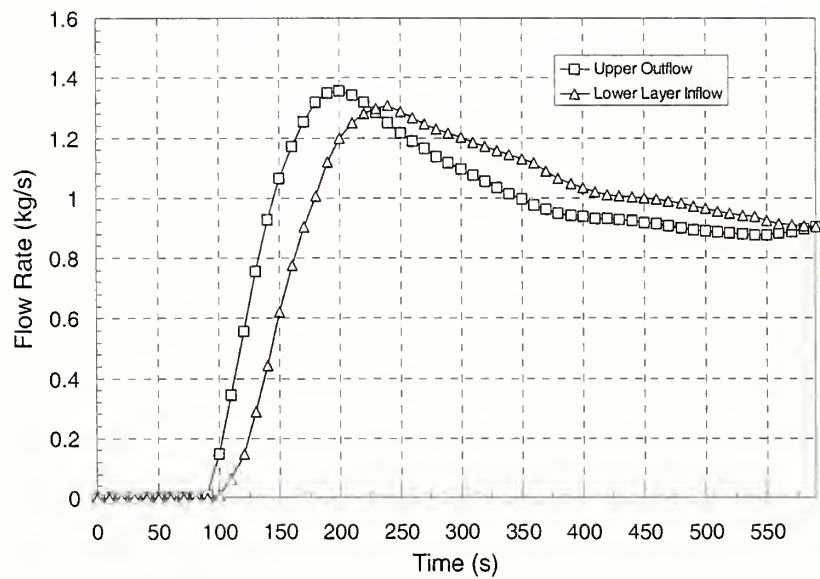
Figure 15 Door Flows (Part I, Case 4) - CFAST
(from Dey (Appendix B))
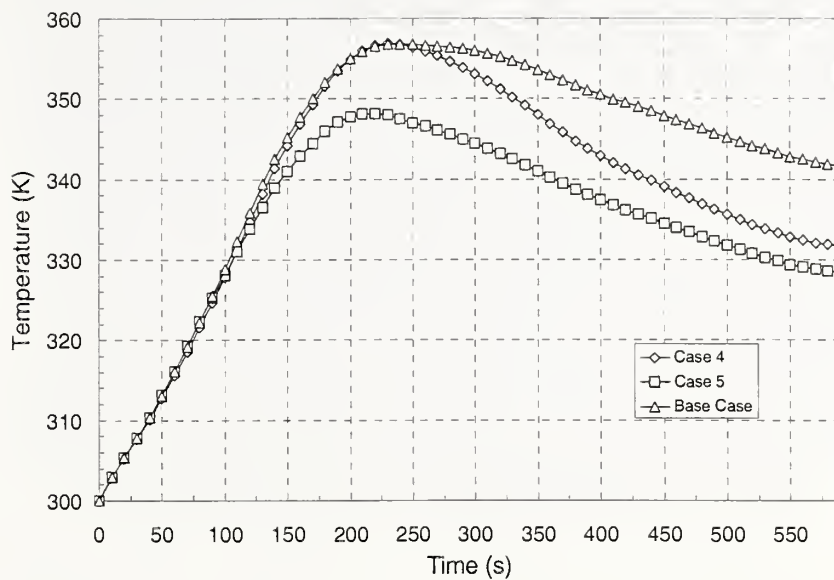
Figure 16 HGL Temperature (Part I) - CFAST
(From Dey (Appendix B))
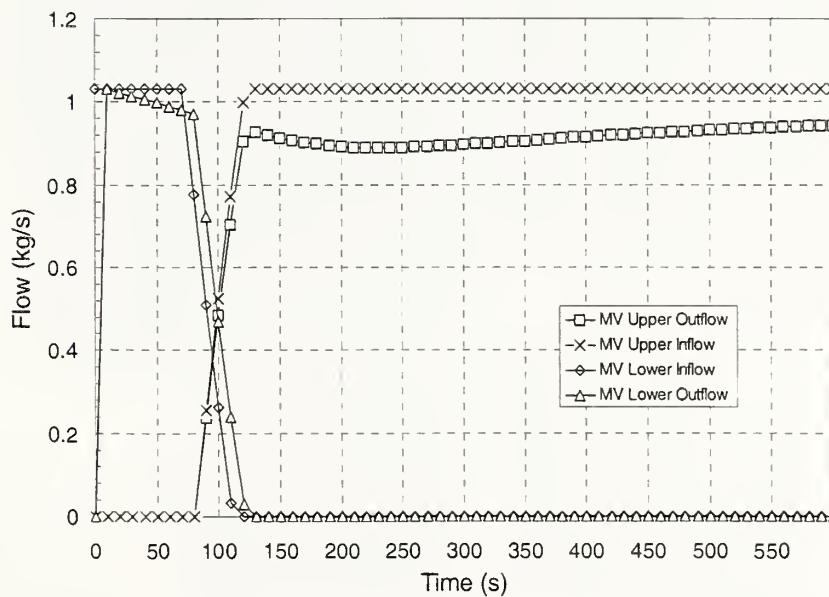
**Figure 17 Mechanical Ventilation Flows (Part I, Case 5) -
CFAST** (from Dey (Appendix B))
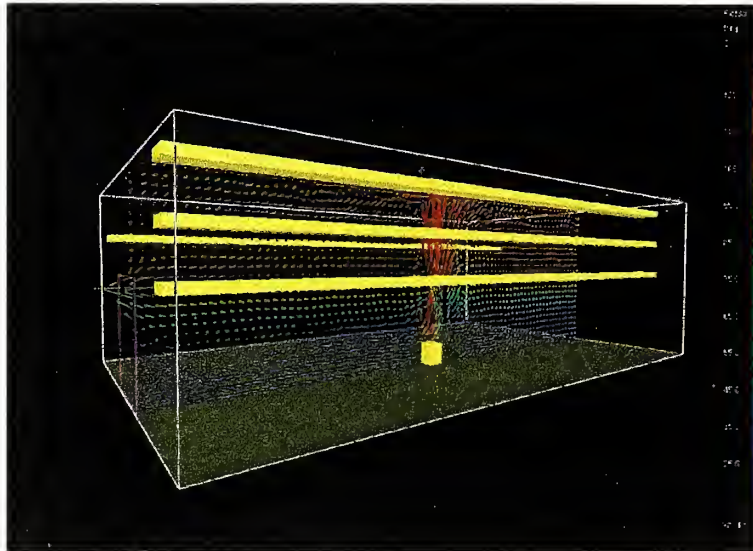
Figure 18 Door Flows (Part I, Case 4) - FDS
(from Dey (Appendix B))

Part I base case – no mechanical
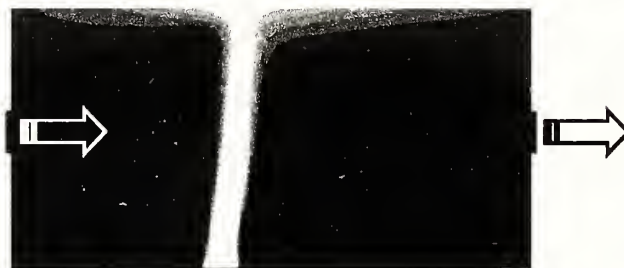
Part I case 5 - with mechanical ventilation

**Figure 19 Effect of Mechanical Ventilation
- JASMINE** (from Miles (Appendix G))
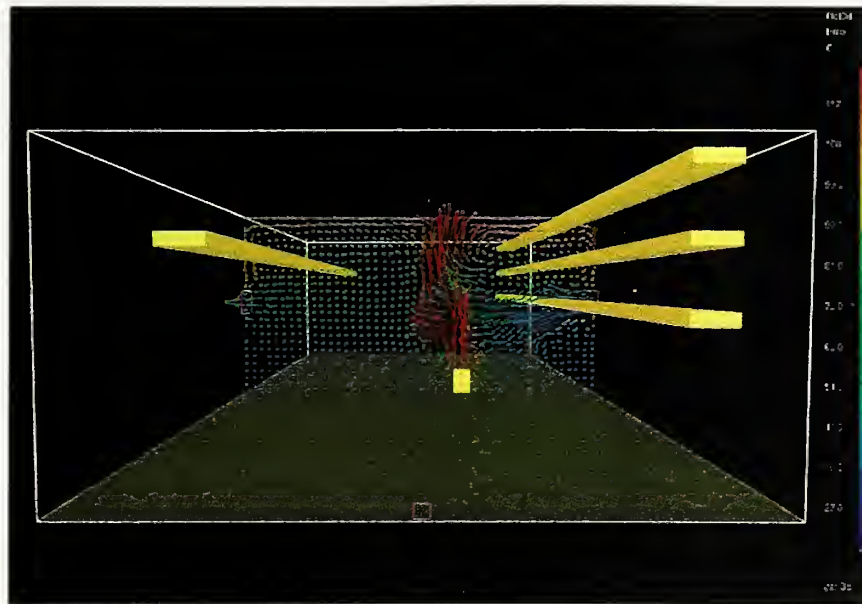
**Figure 20 Effects of Mechanical Ventilation
(Part I, Case 5) - FDS** (from Dey (Appendix B))

Cable Tray Fires of Redundant Safety Trains
Benchmark Part I

Time=180.35s

Case 5
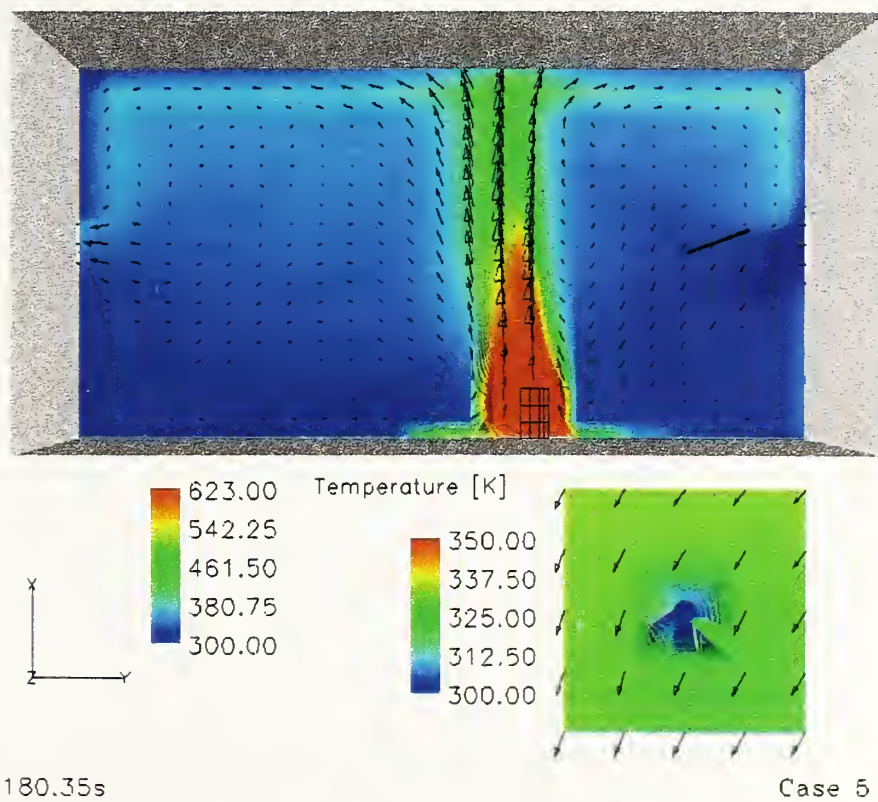
Figure 21 Effects of Mechanical Ventilation - CFX
(from Heitsch (Appendix D))
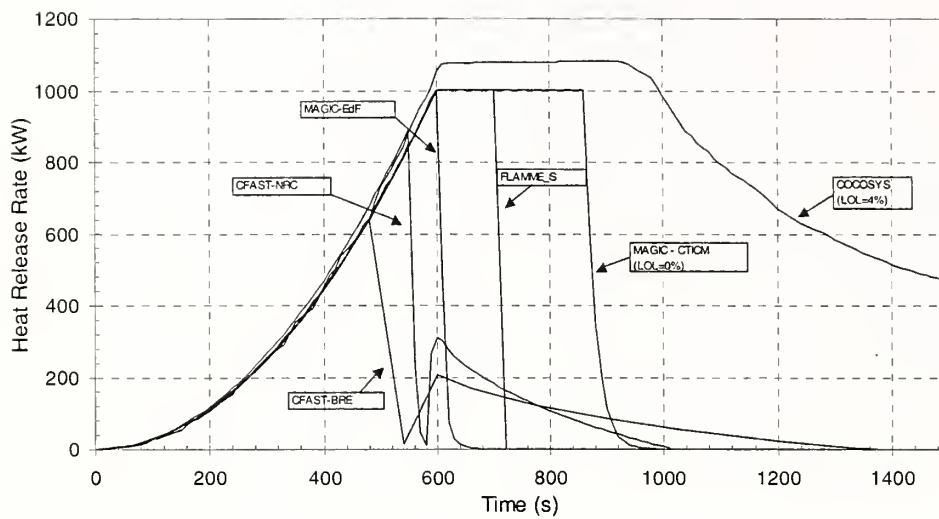
Figure 22 Heat Release Rate (Part II, Base Case)
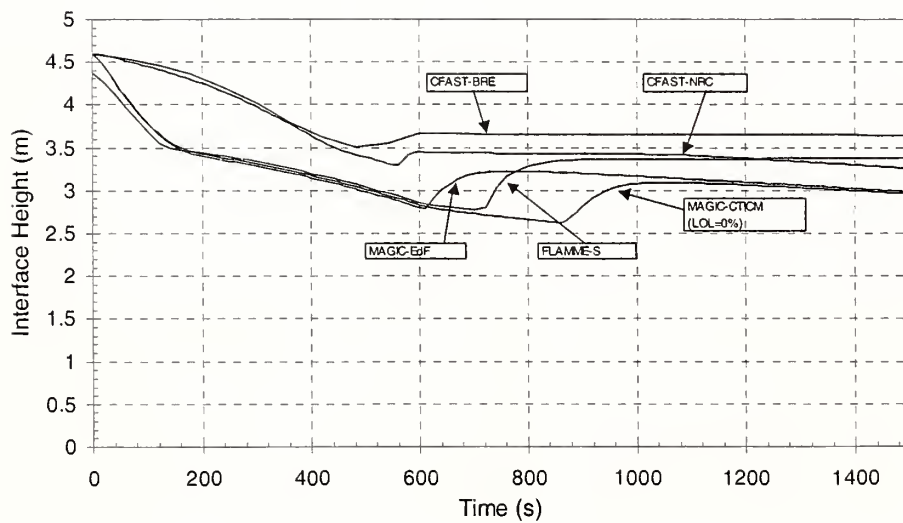
Figure 23 HGL Development (Part II, Base Case)

56
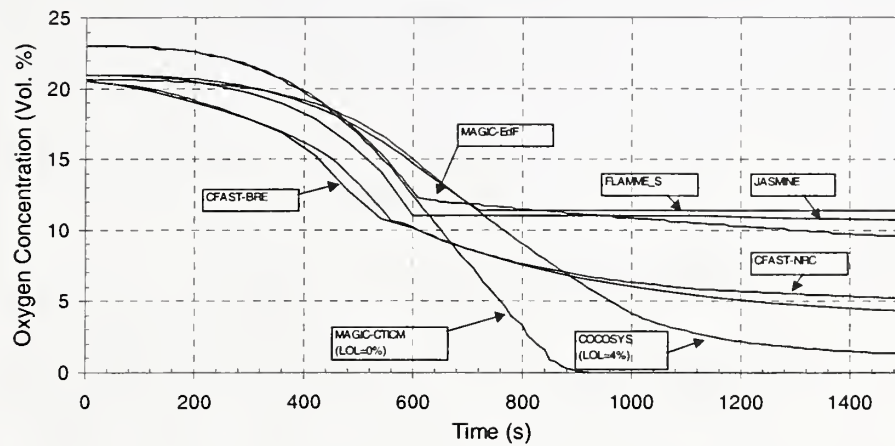
Figure 24 Oxygen Concentration (Part II, Base Case)
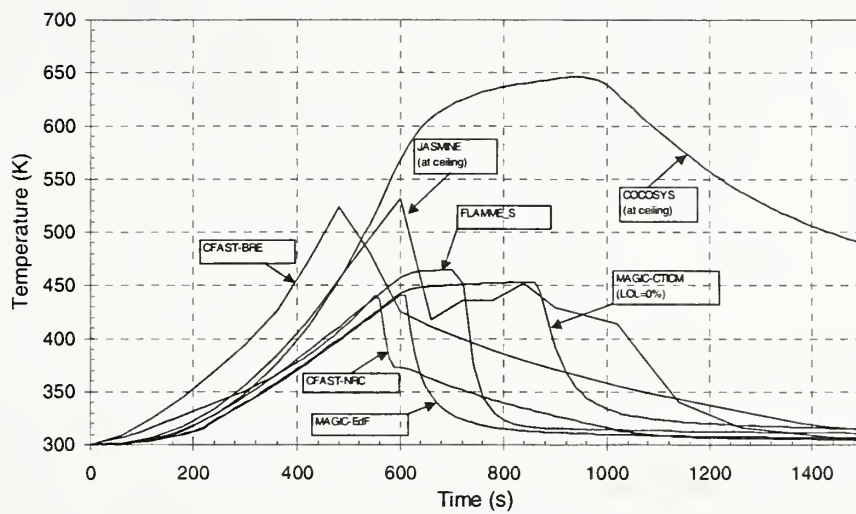
Figure 25 HGL Temperature (Part II, Base Case)

57
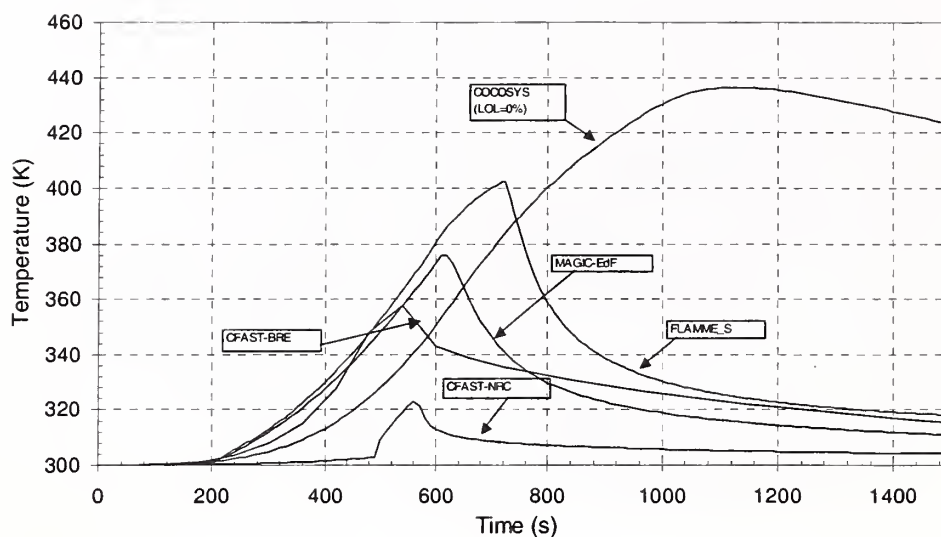
Figure 26 Target Surface Temperature (Part II, Base Case)
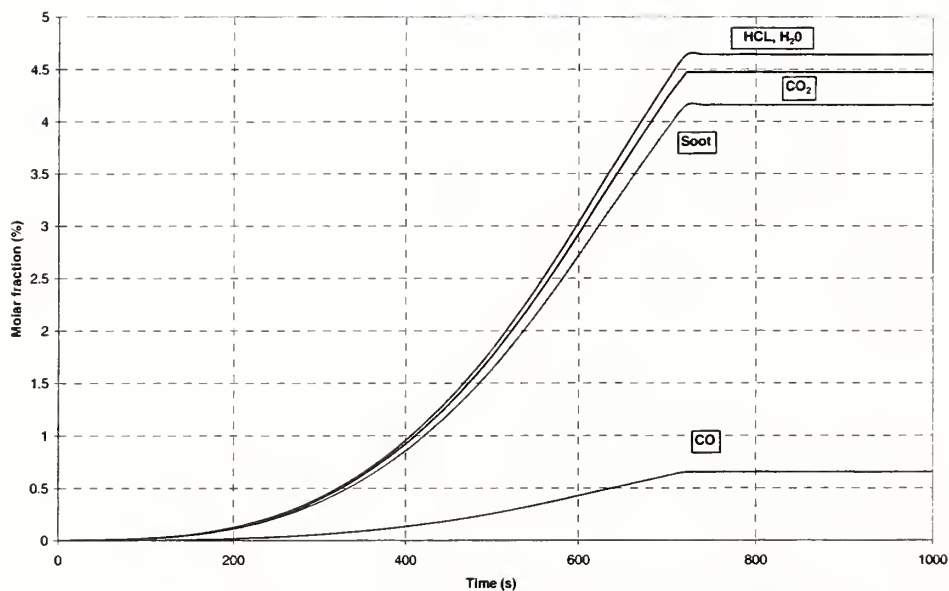
Figure 27 Species Concentration (Part II, Base Case)
(from Bouton (Appendix A))
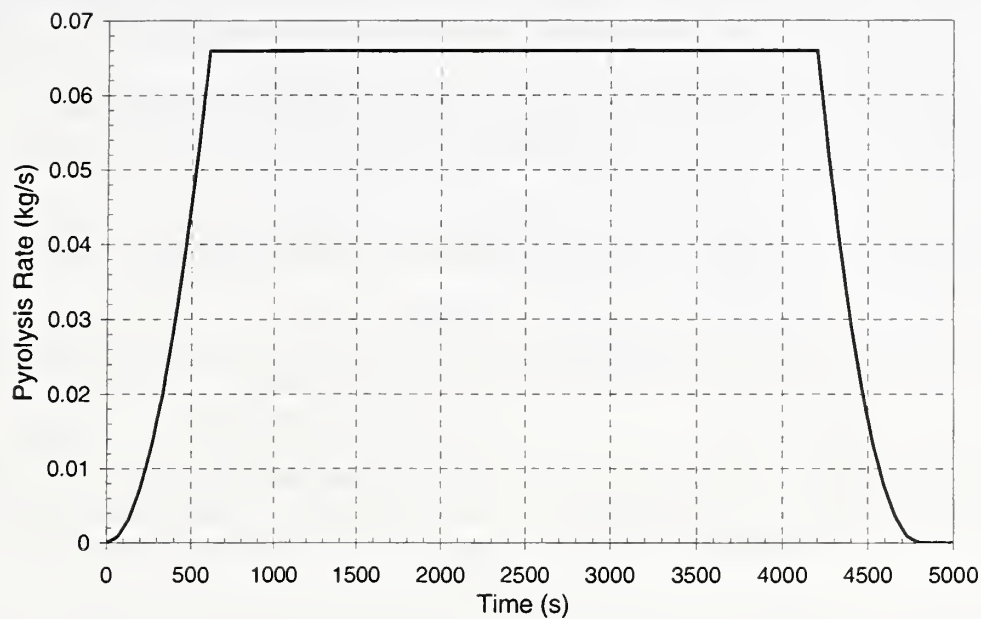
Figure 28 Pyrolysis Rate (Part II, Base Case)
(from Dey (Appendix B))
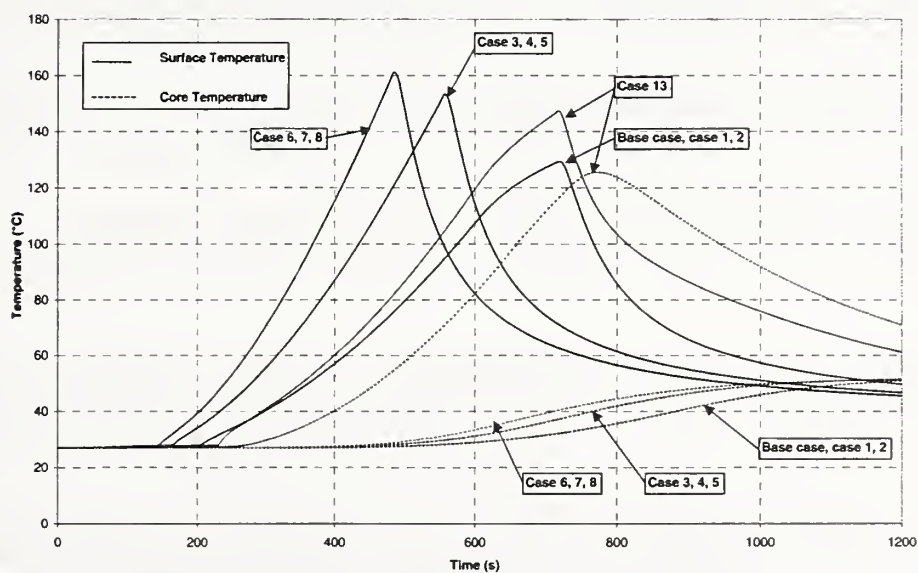
Figure 29 Effect of Cable Structure
(from Bouton (Appendix A))

59
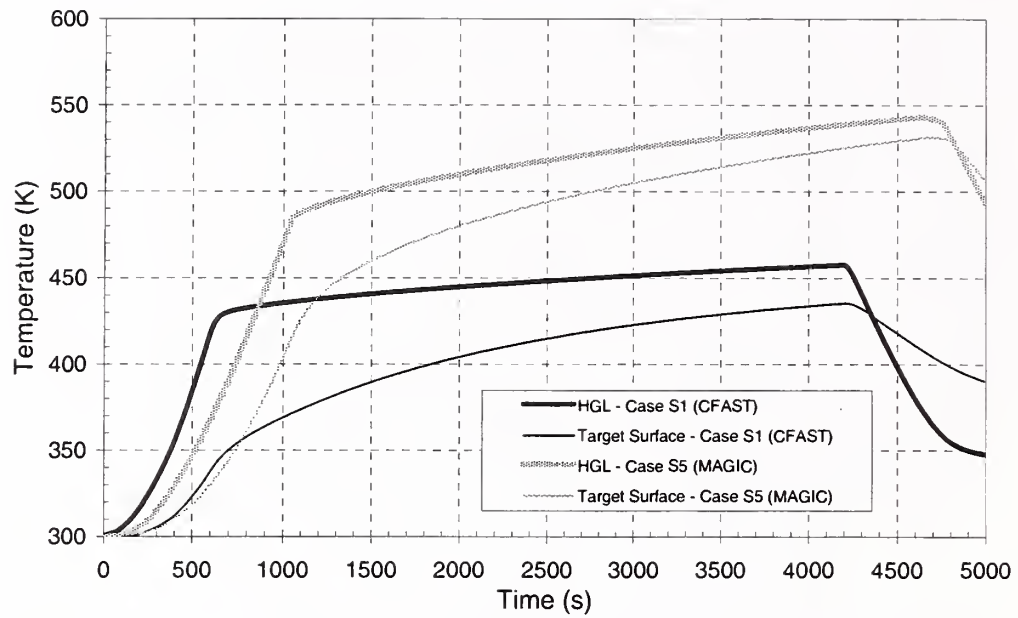
Figure 30 Temperature Development (Special Cases)

6 References

American Institute of Aeronautics and Astronautics, "Guide for Verification and Validation of Computational Fluid Dynamics Simulations," AIAA, Guide G-077-1998.

Electric Power Research Institute, "Fire Tests in Ventilated Rooms: Detection of Cable Tray and Exposure Fires," J.S. Newman, EPRI NP-2751, Palo Alto, California, 1983.

Electric Power Research Institute, "Fire Tests in Ventilated Rooms: Extinguishment of Fire in Grouped Cable Trays," EPRI NP-2660, Palo Alto, California, December 1992.

Grondeau, P., "Rapport de Essai: Etude de la Evolution d'un Incendie dans des Cables Electriques en Nappes Horizontales," No. PE965045 P1-P2, CNPP Vernon, 1997.

Keski-Rahkonen, O., "CIB W 14 Round Robin on Fire Simulation Code Comparisons," Proceedings of the 2nd International Seminar on Fire and Explosion Hazard of Substances and Venting of Deflagrations, 11-15 August 1991, Moscow, Russia, All-Russian Research Institute for Fire Protection, pp. 87-101, 1998.

Lee, B. T., "Heat Release Rate Characteristics of Some Combustible Fuel Sources in Nuclear Power Plants," NBSIR 85-3195, National Bureau of Standards, 1985.

Such, J. M., "Programme Etude Probabilste de Surete Incendie (PEPSI), essai no. 1, Resultats experimentaux (Probabilistic Study Program of Fire Safety (PEPSI), Test no. 1, Experimental results, Report LEMF EF.30.15.R/96.442, 1997.

Tewarson, A, "Generation of Heat and Chemical Compounds in Fires," SFPE Handbook of Fire Protection Engineering, 2nd Edition, 3-53 to 3-124, Bethesda, Maryland, 1995.

Van Volkinburg, D. R. et al, "Toward a Standard Ignition Source," Paper No. 78-64, Lawrence Berkeley Laboratory, University of California, Berkeley, California, 1978.

U.S. Nuclear Regulatory Commission, "Probability-Based Evaluation of Selected Fire Protection Features in Nuclear Power Plants,"Azarm, A. and Bocio, J.L., NUREG/CR-4230, May 1985.

U.S. Nuclear Regulatory Commission, "International Collaborative Project to Evaluate Fire Models for Nuclear Power Plant Applications: Summary of Planning Meeting," Dey, M., NUREG/CP-0170,, Washington, DC, April 2000.

U.S. Nuclear Regulatory Commission, "International Collaborative Project to Evaluate Fire Models for Nuclear Power Plant Applications: Summary of 2nd Meeting," Bertrand, R., and Dey, M., NUREG/CP-0173,, Washington, DC, July 2001.

Appendix A: Benchmark Analysis with FLAMME_S, Eric BOUTON, and Bruno TOURNIAIRE, IPSN, France

IPSN/DRS/SESHP/GMEF
SESHP/GME/IPS/FLS/C60/RP/
00.930

Study of cable tray fires of redundant safety trains with the
Flamme_S code.

INSTITUT DE PROTECTION ET DE SURETE NUCLEAIRE

DEPARTEMENT DE RECHERCHES EN SECURITE

	REDACTION	VERIFICATION	ING. AQ.	APPROBATION
NOM	**E. BOUTON B. TOURNIAIRE**	**C. CASSELMAN**	**P. SOUSSAN**	**R. GONZALEZ**
DATE				
VISA				
REV. A				
REV. B				
Titre	Study of cable tray fires of redundant safety trains with the Flamme_S code.			
Auteur(s)	**E. BOUTON - B. TOURNIAIRE**			

Type Rapport	Numéro SESHP/GME/IPS/FLS/C60/RP/00.930

Service d'Essais de Sûreté Hors Pile
Groupe Modélisation et Etudes des Feux

IPSN/DRS/SESHP/GMEF
SESHP/GME/IPS/FLS/C60/RP/
00.930

Study of cable tray fires of redundant safety trains with the
Flamme_S code.

IPSN/DRS/SESHP/GMEF   Cadarache, le 06/10/00

Rapport - SESHP/GME/IPS/FLS/C60/RP/00.930

Study of cable tray fires of redundant safety trains with the Flamme_S code.

E. BOUTON - B. TOURNIAIRE

IPSN/DRS/SESHP/GMEF
SESHP/GME/IPS/FLS/C60/RP/
00.930

Study of cable tray fires of redundant safety trains with the
Flamme_S code.

SERVICE D'ESSAIS DE SURETE HORS PILE		
Groupe Modélisation et Etudes des Feux		
Nat. Document	Rapport	
TITRE	**Study of cable tray fires of redundant safety trains with the Flamme_S code.**	
Auteur(s)	E. BOUTON - B. TOURNIAIRE	
Type de diffusion : Normale	"Mots clés" : Flamme_S - Cable fires	Nbre de pages : 37 Nbre de figures : 47

RESUME :

Ce document présente les résultats de simulations numériques réalisées avec le code Flamme_S pour des scénarios de feu de chemin de câbles (voie de relais devant entrer en service en cas de dysfonctionnement de la voie principale). Ce travail a été réalisé dans le cadre d'un projet international visant à évaluer les modèles incendie appliqués à des feux dans des installations nucléaires.

ABSTRACT :

This report presents the results of numerical simulations achieved with the Flamme_S code on cable tray fires of redundant safety trains. This work has been done in the frame of an international collaborative project to evaluate fire models for nuclear power plant applications.

Repère bureautique : 00-930

TABLE OF CONTENTS

1. INTRODUCTION.

This report presents the results of the numerical simulations achieved with the two-zone model code Flamme_S on cable tray fires of redundant safety trains. This work has been done in the frame of an international collaborative project to evaluate fire models for nuclear power plant applications.

2. DEFINITION OF THE PROBLEM.

2.1 Room size and geometry.

A representative PWR emergency switchgear room has been selected for the benchmark exercise [1]. The room is 15.2 m deep, 9.1 m wide and 4.6 m high (see Figure 1). The room contains the power and instrumentation cables (trays A, C1, C2) for the pumps and valves associated with redundant safe-shutdown equipment (tray B). Both cable trays run the entire depth of the room, and are arranged in separate divisions and separated horizontally by a distance d.

The room has a door 2.4 m x 2.4 m located at the midpoint of the front wall and assumed to lead to the outside. The room also has a mechanical ventilation system with a flowrate of 5 volume changes per hour in and out of the room. The flowrate is assumed to be constant in the mechanical ventilation system. The midpoint of the vertical vents for the supply and exhaust air are located at an elevation of 2.4 m and have area of 0.5 m^2 each. The vents are supposed to be square and connect the room to the outside.
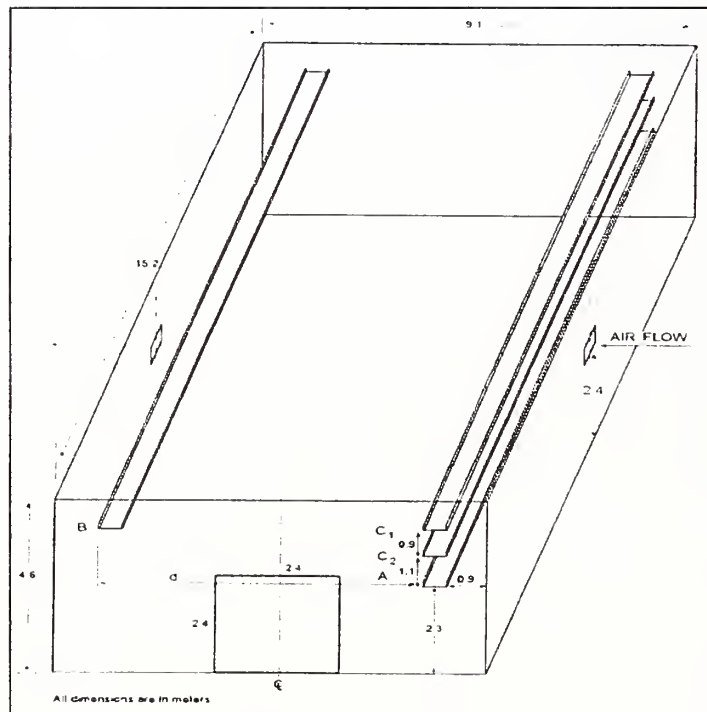
Figure 1: Geometry.

2.2 Wall, floor and ceiling.

The walls, floor and ceiling are 15.2 cm thick. The thermophysical data used in the numerical simulations are:

Specific heat	1000 J/kg.K
Thermal conductivity	1.75 W/m.K
Density	2200 kg/m^3
Emissivity	0.94

The convective heat transfer coefficient is the same for all the surfaces: 15 W/m^2.K.

2.3 Cables.

The cable trays are 0.6 m wide and 0.08 m deep. As can be seen on the Figure 1, a horizontal distance d separates tray B from tray A. The thermophysical data used for cables are :

Heat of Combustion	16 MJ/kg
Fraction of flame heat released as radiation	0.48
Specific heat	1040 J/kg.K
Thermal conductivity	0.092 W/m.K
Density	1710 kg/m^3
Emissivity	0.8

3. PART I.

3.1 Main purpose and scenario.

The objective of the Part I is to determine the maximum horizontal distance between a specified transient fire and the tray A that results in the ignition of the tray A (643 K). In this part, the transient fire is assumed to be a trash bag fire whose heat release rate is represented on the Figure 2:
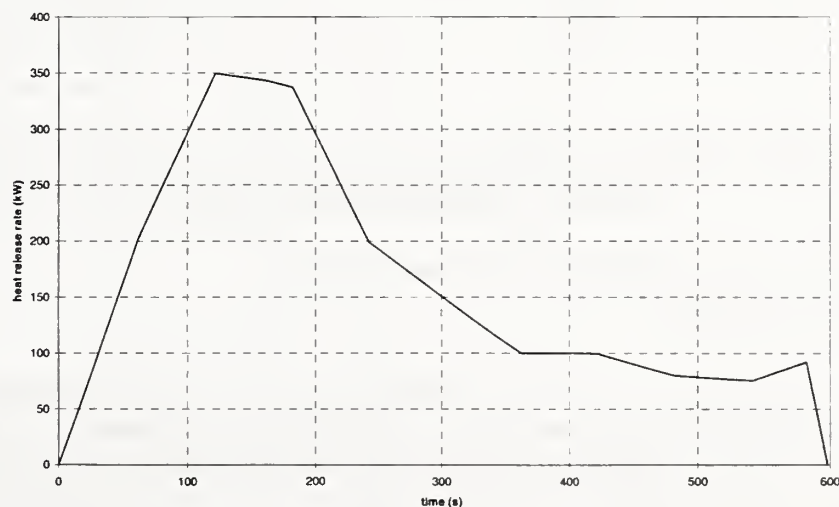
Figure 2: Trash bag fire - Heat release rate.

The trash bag is approximated by a cylinder with a diameter of 0.49 m and a height of 0.62 m. The mass of fuel is 4.06 kg and its heat of combustion is 24.1 MJ/kg with a fraction of 0.3 released as radiation.

The trash bag and the target (representing tray A) are located at the centre of the cable tray length. The target is assumed to be a single power cable with a diameter 50 mm at the bottom left corner of the cable tray A (see Figure 3).
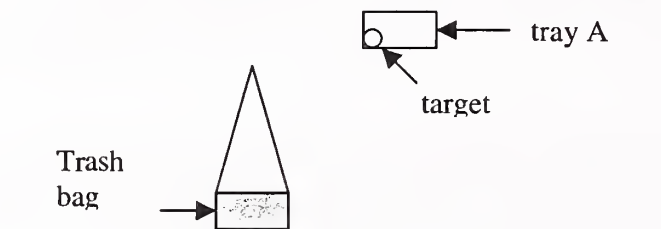
Figure 3: Part I - Trash bag fire.

In this first part, the following calculations are achieved:

1/ The horizontal distance between the midpoints of the trash bag and the tray A is successively 0.3 m, 0.9 m, 1.5 m and 2.2 m. In these simulations the ventilation system is off and the door is closed.

2/ The horizontal distance between the trash bag and the tray A is 2.2 m and the door is open.

3/ The horizontal distance between the trash bag and the tray A is 2.2 m and the ventilation system is on.

All the simulations of the Part I are summed up in the following table:

	Distance from fire (m)	Door	Ventilation system
Base case	2.2	Closed[1]	off
Case 1	0.3[2]		
Case 2	0.9		
Case 3	1.5		
Case 4		open	
Case 5			on

Table 1 : Summary of cases for part I

3.2 Modelling of the problem with the Flamme_S code.

3.2.1 The trash bag fire.

The fuel is assumed to be a trash bag containing wood (fir). The thermophysical data for wood are issued from the fuel data library available with the Flamme_S code. The data concerning the heat of combustion and the fraction of heat released as radiation have been

---

[1] For simulation with the door closed, a crack (2.4 m x 0.005 m) at the bottom of the doorway is assumed

[2] A value in a cell indicates the parameter is varied from the base case

changed and are equal to the data advised in the definition of the benchmark exercise (24.1 MJ/kg for the heat of combustion[3], 0.3 for the fraction of heat released as radiation).

The flame and the plume above the trash bag are described with the Heskestad model [2].

3.2.2 The cable.

In the Flamme_S code, a target such as a cable is represented by a rectangular slab. This slab can be divided in several meshes in the three directions. Hence, a complete description of the temperature field in the cable is available. In the modelling of a slab, the heat exchanges between the slab and its surroundings are only possible with the upper and lower faces of the slab[4] (see Figure 4). That is why, the dimensions of the slab (width and depth) must be estimated in order (a minima) to:

1/ have the same mass between the true cable and the slab,
2/ have the same surface for heat exchanges.
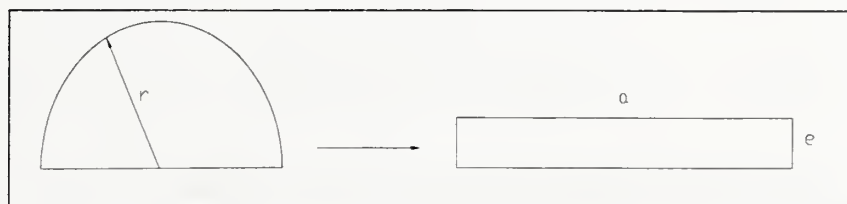
Figure 4: Modelling of the target with a rectangular slab.

Those two conditions impose the following dimensions for the slab:

$$a=width=\pi.r \qquad e=depth=r$$

In all the simulations of the Part I, the slab is divided in 1 (width) x 30 (depth) x 29 (length) meshes. With this cutting, the first mesh at the centre of the slab is 0.42 mm deep[5].

3.3 Numerical results.

3.3.1 Enclosed room.

The first part of this study is devoted to the numerical simulations in the cases with no mechanical nor natural ventilation. We are interested here in the results of the calculations of the base case and cases 1, 2, 3.

---

[3] The actual value of the heat of combustion of the wood is equal to 19.6 MJ/kg.

[4] This comes from the fact that the "object" used to model the slab was initially devoted to the modelling of the wall, floor and ceiling.

[5] More meshes in the "deep direction" induce high restriction in the time step (CFL like condition).

Heat release rate.

The Figure 5 shows the evolution of the heat release rate of the fire. Given the high volume of the room and the relatively low heat release rate of the fire, the oxygen molar fraction is always enough high to ensure the combustion until t=590s. At this time, the fire self extinguished for lack of fuel.
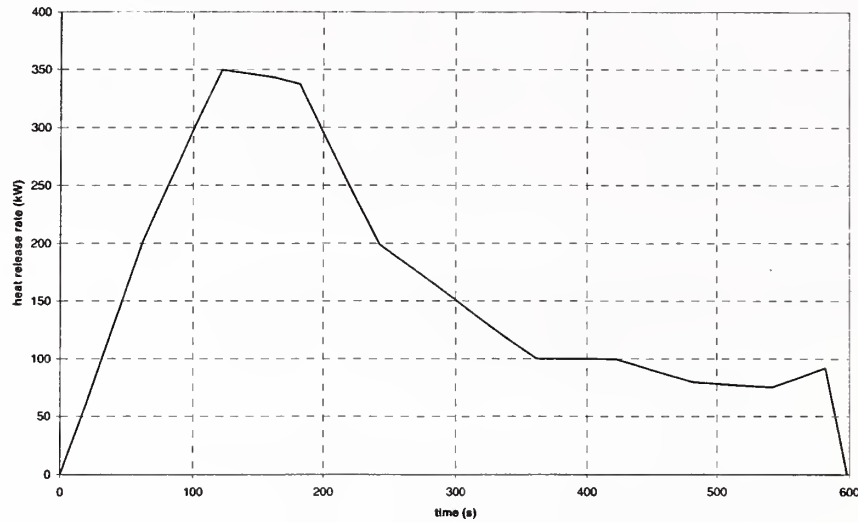
Figure 5: Heat release rate of the fire.

Temperature.

The analysis of the numerical results shows that the temperatures in the room are the same in all the enclosed room simulations. This observation shows that the localisation of the cable has a negligible effect on the whole thermal behaviour of the room. The Figure 6 shows the evolution of the room temperature. As shown in this figure, the high volume of the room associated with a relatively low heat release rate of the fire (<350 kW) induce low maximum temperatures in the room (T_{max}<80°C). This observation means that any failure or ignition of the target may be due either to radiant heat transfer from the flame or from convective heat transfer with the plume, but not from convective heat transfer with the hot gas layer.
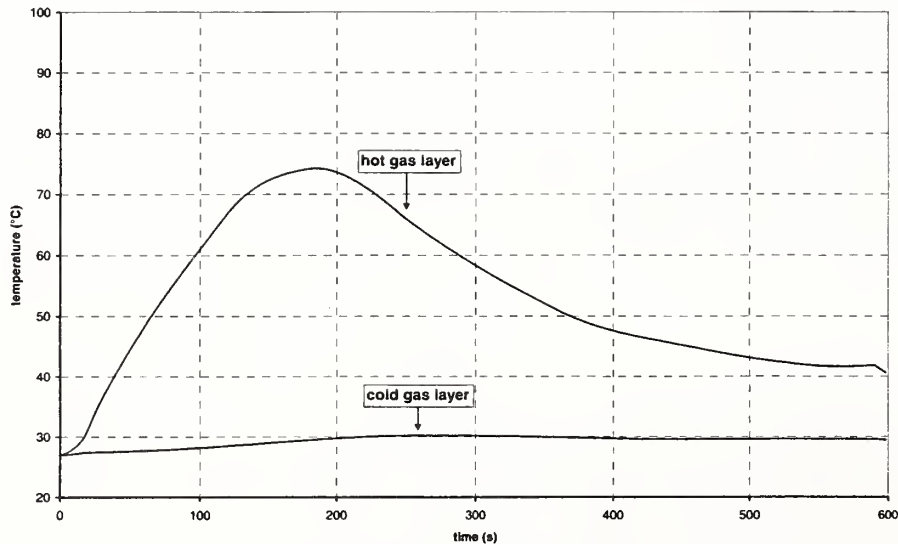
Figure 6: Room temperature.

The Figure 7 shows the evolution of the hot and cold layer depth. As can be seen on this figure, the target is in the hot gas layer from t=160s.
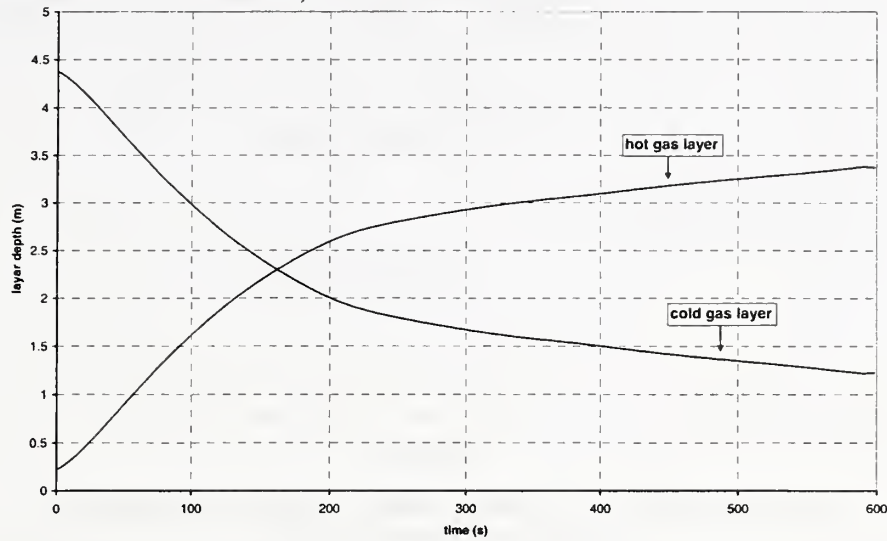
Figure 7: Gas layer depths.

The target.

As mentioned before, the heating of the cable is principally due to the radiant heat released by the flame and, given its position, to the convective heat transfer with the hot gas of the plume. The Figure 8 shows the temperature of the first mesh at the centre of the target. In the following of the text it will be referred as the maximum surface temperature of the target. The evolution of the temperature surface of the cable follows the heat release rate of the fire and starts decreasing when t≈150s. As can be seen on the Figure 8 and on the Figure 9 the ignition temperature is reached when the distance between the midpoints of the trash bag and tray is between 0.4m and 0.5m.
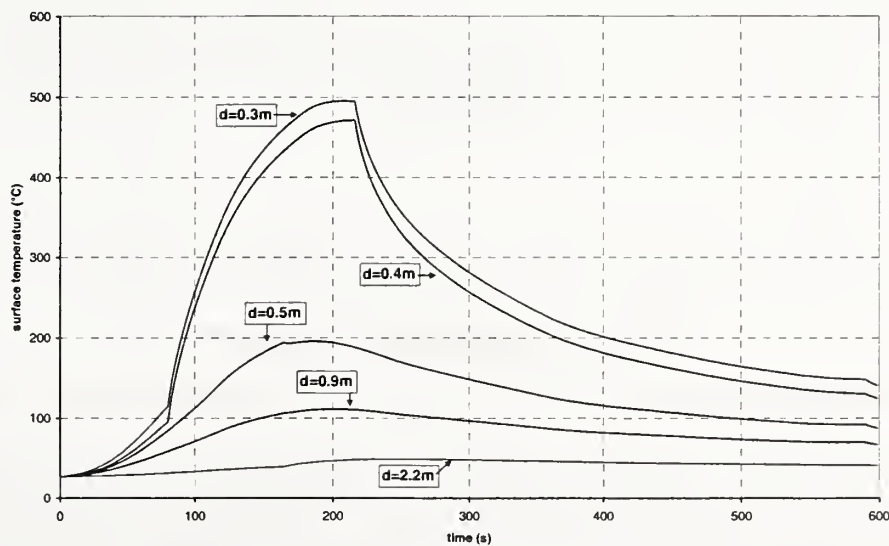
Figure 8: Temperature "surface" of the cable.
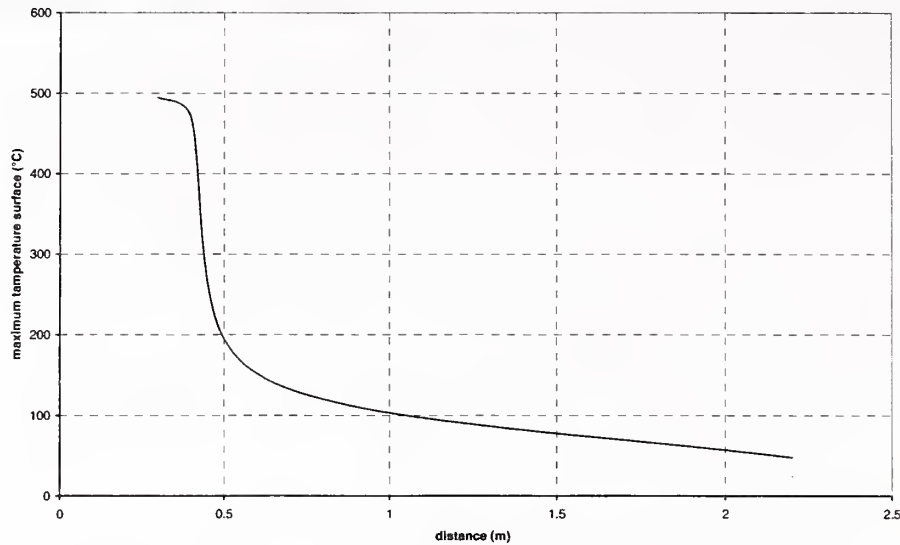
Figure 9: Maximum temperature "surface" of the cable.

The strong difference between the results with d=0.4 m and d=0.5 m comes from the fact that in the last case the cable is never in the plume of the fire (according to the calculations). The increase in the temperature for d>0.5m is only due to the radiant heat released by the flame.

The Figure 10 shows the temperature of the central mesh. The low thermal conductivity of PVC induces a strong temperature gradient between the surface and the centre of the cable.
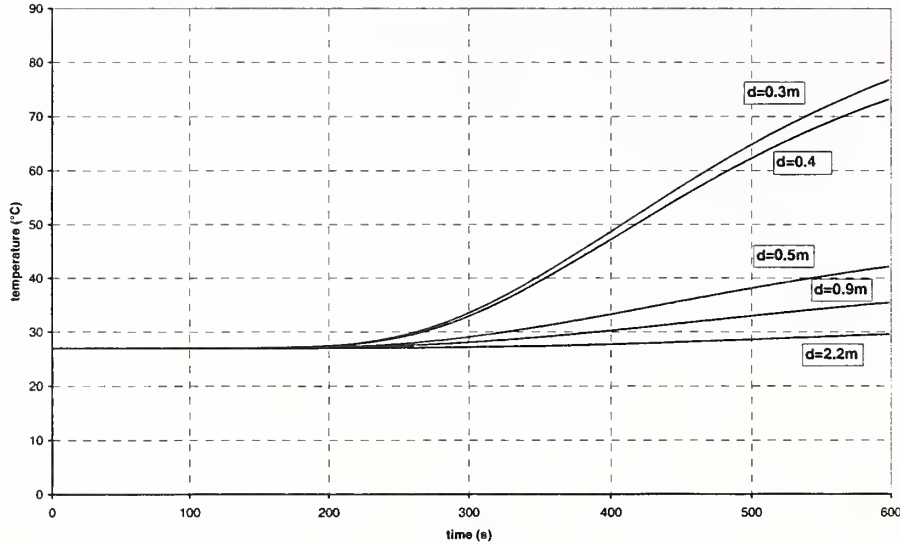
Figure 10: Temperature inside the cable.

3.3.2 Ventilated room.

The results obtained in ventilated configurations and with d=2.2 m are nearly the same as in the base case. As can be seen on Figure 11, the temperature in the room does not exceed 80°C. The results of both calculations are very near until t=160 s ; before this time the interface height is above the vents and the door and the mass flows due to ventilation only concern the lower layer.
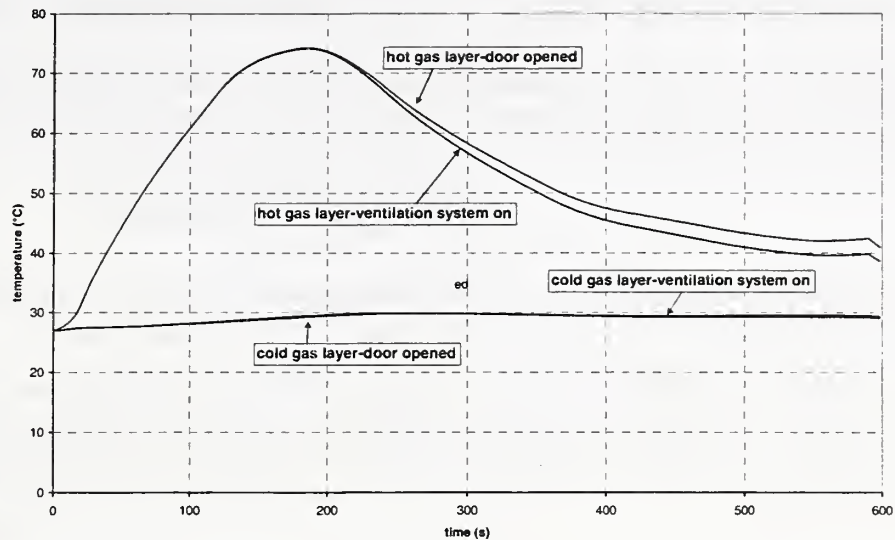
Figure 11: Temperature profiles for the cases with the door open and ventilation system on

The Figure 12 shows the cable temperature. The maximum temperature surface of the target is less than 60°C in both cases far from the ignition temperature. The break in the slope at t≈160 s corresponds to the time when the cable enters the hot gas layer (cf. Figure 35). From this moment, convective heat transfer with the gas of the room quickly increases since upper layer's gas are hotter than lower layer's ones.
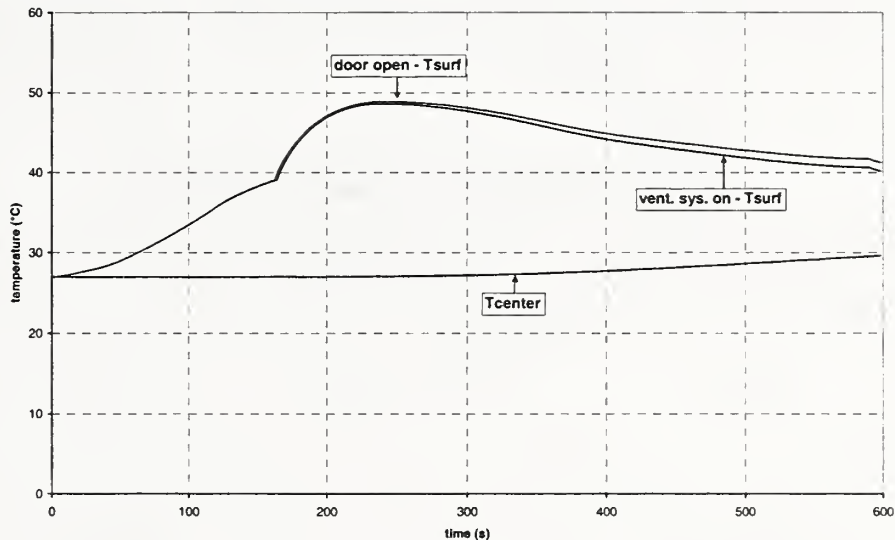
Figure 12: Cable temperature.

All the other results concerning the case 4 and the case 5 are reported in the Appendix 2.

3.3.3 Complementary study.

The calculation of the radiant heat transfer between the flame and the target is based on a classical point source approach. If r is the distance between the point source and the cable, the radiation heat on the cable is expressed as:

$$\Phi_{target} = \Phi_{flame-rad} \cdot \frac{\Omega}{4\pi} = \Phi_{flame-rad} \cdot \int \frac{dS}{4\pi r^2} \text{ (in W)}$$

where Ω is the solid angle, ϕ_{target} is the radiant heat on the target, $\phi_{flame-rad}$ the radiant heat released by the flame and dS the surface of the target "seen" by the point source.

When the target is cylindrical, dS remains constant and the solid angle decreases as the distance between the fire and the cable. The radiation heat on the cable only depends on r. On the other hand, when the cable is modelled as a slab (see Figure 13), the solid angle decreases as r increases and because of the decrease of dS. The radiation heat on the cable no more depends directly on r^6.
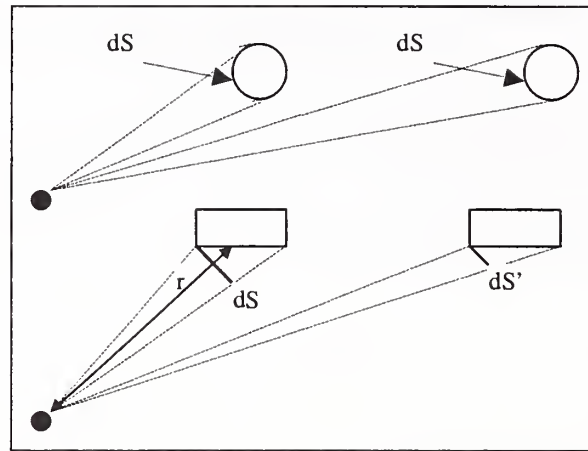
Figure 13: Radiant heat released on the target

In order to avoid this phenomenon, the problem has also been modelled in the following way: the target is located upon the fire source, the distance between the top of the fuel and the target being the same as in the real geometry.
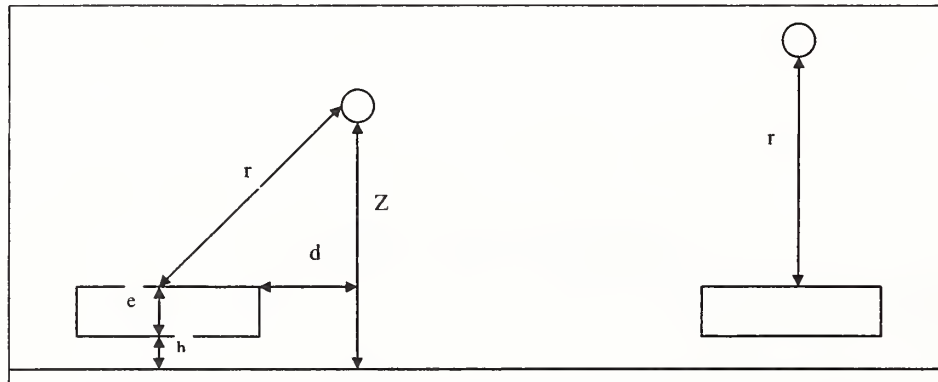
Figure 14: Real geometry (left) and modelled problem (right).

---

[6] Remember that in our modelling, only two opposite faces are involved in heat transfer.

The distance between the fuel surface and the target is given by :

$$r^2=(R+d)^2+(Z-h-e)^2$$

Where:　　　　R = the radius of the fuel surface,
　　　　　　　e = the depth of the fuel (=0.048m),
　　　　　　　h = the height of the fuel (=0.62m).

If H is the absolute height of the target in the modelled problem, the relation between d and H is:

d (m)	0.15	0.3	0.9	1.5	2.2
H (m)	2.36	2.40	2.69	3.09	3.65

Comments:

1/ In this approach convective heat exchange between the hot gas layer and the cable depends on the distance between the fire source and the target. The consequences of this difference are probably low since, as can be seen in the previous parts, the decrease of the interface height is quite fast and the increase of the temperature of the hot gas layer is relatively small.

2/ The source of the code has been modified in order that the convective heat exchanges on the target, which is now in the fire plume, are not calculated with the plume temperature.

The Figure 15 shows the maximum temperature surface of the cable when heated by radiant heat from the flame.
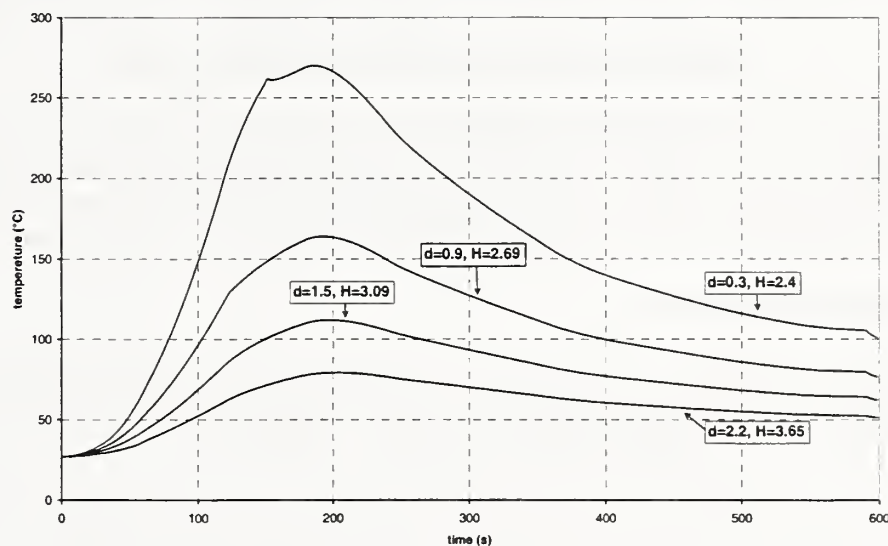
Figure 15: Temperature "surface" at the centre of the target.

Several comments can be made:
1/ The maximum temperature surface never reaches the ignition temperature (370°C).

2/ The maximum temperature surface decreases when the distance between the fire and the target increases.

3/ The sudden slopes changes in the temperature profiles correspond to the time when the target enters the hot gas layer (ex: d=0.3 m, t=150 s). At this time, a part of the radiant heat released by the flame is absorbed by the gas.

4/ For t>200 s the maximum surface temperature decreases. This corresponds to the fact that the heat release rate of the fire decreases and that the gas of the hot gas layer is colder than the target.

The Figure 16 shows the radiant heat flux on the mesh at the centre of the target. The strong decreases observed at t=150 s for d=0.3 m and at t=120 s for d=0.9 m correspond to the time when the target enters the hot gas layer (see also Figure 7).
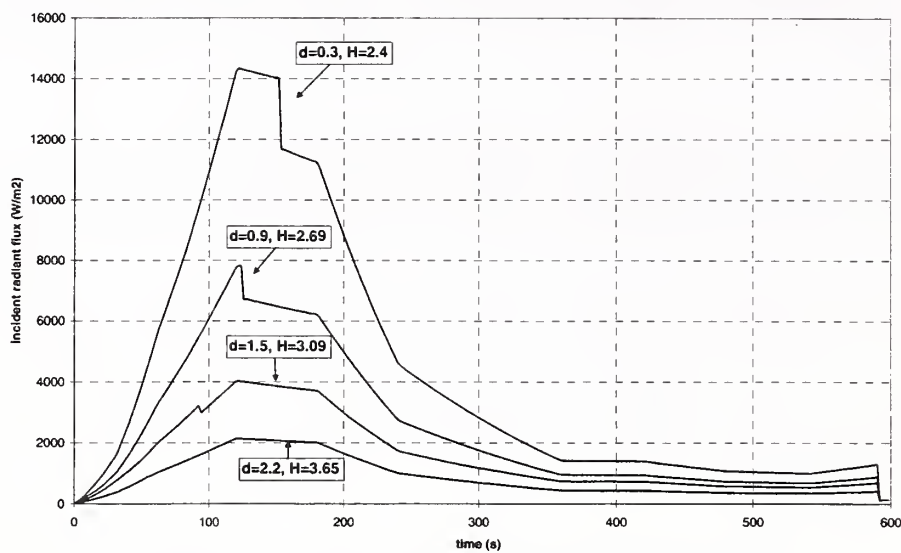
Figure 16: Incident radiant heat flux on the target.

It is also interesting to highlight that the maximum heat flux calculated for d=0.3m is only slightly higher than 14 kW/m^2 and that the target receives this flux only during a short time. This radiant heat flux is equal to the critical heat flux found in the literature for the PVC [4]. May be this explains the reason why the ignition temperature is never reached in this study.

3.4 Conclusion of the first part

The numerical simulations of the first part show that, given the dimensions of the geometry and the relatively low heat release rate of the fire, the ignition or damage of the cable is unlikely except when it is located in the fire plume.

4. PART II.

4.1 Main purpose and scenario.

The objective of the part II is to determine the damage time (t_d) of the cable tray B for several heat release rates of the cable tray stack fires (trays A, C1 and C2) and horizontal distance, d (see Figure 1). The effect of target elevation and ventilation will also be examined.

In this part the fire is supposed to be a burning cable tray stack. As the modelling and the prediction of the heat release rate of such a fire are extremely difficult (pyrolysis, flame propagation, …), the heat release rate is considered as an input of the problem. The peak heat release rate (Q_0) for the whole cable tray stack is between 1-3 MW. The ignition period is modelled as a t-squared growth:

$$Q(t) = Q_0 \, (t/t_0)^2 \qquad \text{where } t_0 = 10 \text{ min}$$

The fire duration (Δt) is 60 min at peak heat release rate and then the decay period is described in the same way as the ignition growth:

$$Q(t) = Q_0 \left[(1 - \frac{x_e}{x_e - 1})(\frac{t}{t_0 + \Delta t})^2 + \frac{x_e}{x_e - 1}(\frac{t}{t_0 + \Delta t}) \right]$$

where

$$x_e = \frac{(2 \, t_0 + \Delta t)}{t_0 + \Delta t}$$

The theoretical heat release rate for the burning cable tray stack used in this part is displayed on the Figure 17.
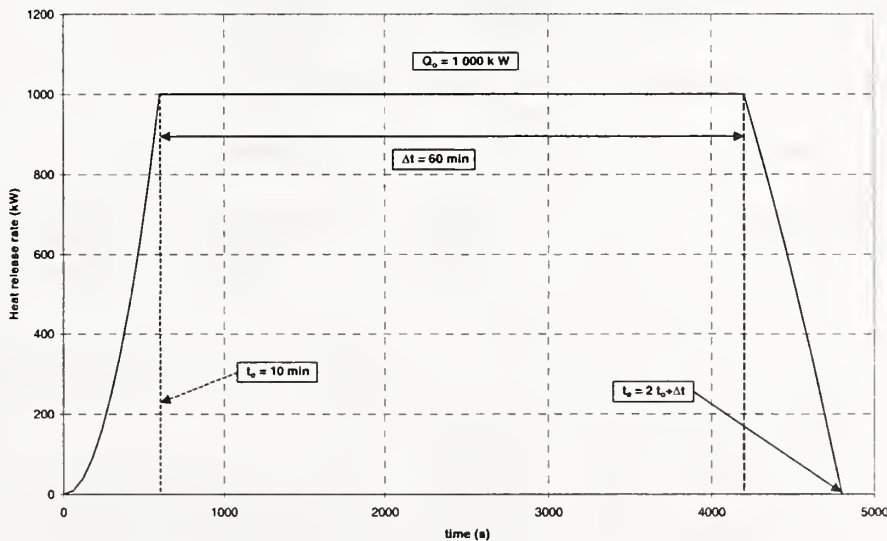
Figure 17 : Burning cable tray stack - theoretical heat release rate

The ignition and burning of the cable tray stack is modelled as one fire. The heat source (trays A, C1 and C2) is at the centre of the cable tray length and width and at the elevation of the

bottom tray C2 (3.4 m). The fire source is assumed to be the entire length of tray C2 (15.2 m), width (0.6 m) and height (0.24 m). In this part, the target is a single power cable (like in part I) or an instrumentation cable made of PVC with a diameter of 50 mm or 15 mm respectively. The cable is assumed to be damaged when its core reaches 200°C. The target is located at the bottom right corner of cable tray B (see Figure 18).
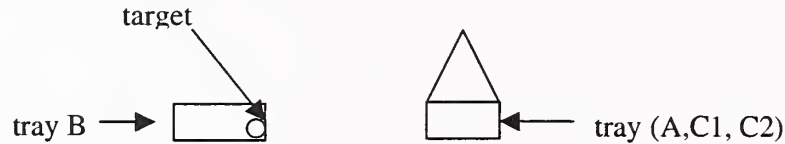
Figure 18 : Part II – Burning cable tray stack (A, C1, C2)

In this section, the following calculations are performed:

1/ The peak heat release rate for the cable tray stack is equal to 1 MW; the horizontal distance (d) between the fire and the target is successively 3.1 m, 4.6 m and 6.1 m.

2/ The peak heat release rate varies from 2 to 3 MW at a horizontal distance d =3.1 m, 4.6 m, 6.1 m.

3/ The door is closed and the ventilation system initially runs; the door is open and the ventilation system shuts after 15 min.

4/ The door is open and the ventilation system is on throughout the simulation.

5/ The tray B is 2.0 m above tray A or at the same elevation as the tray A.

6/ The target is an instrumentation cable with a diameter of 15 mm.

All the cases considered in this part are summarised in the table thereafter:

	HRR (MW)	d (m)	Door	Vent Sys.	Target	Elev[7]. (m)
Base case	1	6.1	Closed[8]	Off	Power	1.1
Case 1		3.1[9]				
Case 2		4.6				
Case 3	2	3.1				
Case 4	2	4.6				
Case 5	2	6.1				
Case 6	3	3.1				

[7] Height above tray A

[8] For simulations with the door closed, a crack (2.4m x 0.005 m) at the bottom of the doorway is assumed

[9] A value in the cell indicates the parameter is varied from the base case

Case 7	3	4.6				
Case 8	3	6.1				
Case 9			Open>15 min	Off>15 min		
Case 10			Open	On		
Case 11						2.0
Case 12						Same (0.)
Case 13					Instrument	

Table 2 : Summary of cases for part II

4.2 Modelling of the problem with the Flamme_S code.

4.2.1 The burning cable tray stack

The fuel is assumed to be a cable tray stack made of PVC. The thermophysical data for PVC are derived from the fuel data library available with the Flamme_S code except those provided by the definition of the benchmark (see § 2.3). The burning cable tray stack has been divided into ten smaller fire sources that are 1.52 m long, 0.6 m wide and 0.24 m high. This modelling of the fire source leads to a better description of the radiative exchanges between the flame and the target than with only one radiative source point set in the middle of cable tray A. Besides, the Flamme_S code prohibits the use of the Heskestad's correlations for the linear fire source (i.e length/width > 3). In the calculations, the given mass fractions for CO and soot have been used to deduce the others. The molar fractions of the combustion species introduced in the Flamme_S data files are listed in the following table :

Species	Molar fraction
CO_2	0.9636
CO	0.1406
Soot	.8958
H_2O	1.0
N_2	5.8647
HCl	1.0

The lower oxygen limit in the calculations is set to 12 %.

4.2.2 The cable target (tray B)

The target (tray B) has been represented by a vertical rectangular slab (see § 2.3). Its thickness and width depend upon its nature:

	Width (m)	Thickness (m)
Power cable	0.078	0.025
Instrumentation Cable	0.0236	0.0075

In all the calculations performed in the second part, the target has been divided in 30 (width) x 1 (depth) x 10 (length) meshes.

4.3 Numerical results.

4.3.1 Enclosed room.

The first part of the study deals with the simulations devoted to the enclosed room (base case, cases 1 to 8 and case 13). Remember that there is only a crack at the bottom of the doorway (2.4 m x 0.005 m).

Actual heat release rate

The evolution of the actual heat release rate as a function of time is shown in the Figure 19. The fire is quickly into the upper layer (see Figure 22). Given the volume of the room and the lower oxygen limit (12 %), the fire self-extinguishes due to the lack of oxygen in the upper layer (see Figure 20). As expected, the extinction delays decrease with the increase of the mass burning rate (i.e. with the peak heat release rate). The different extinction times are listed in the following table :

Q_o (MW)	Extinction delay (s)
1	720
2	556
3	484

After the fire extinction, the oxygen molar fraction in the upper layer remains constant because the interface height behaves as a fictitious solid surface[10] (see Figure 20). In the cooler zone, the oxygen concentration remains constant to its initial value.
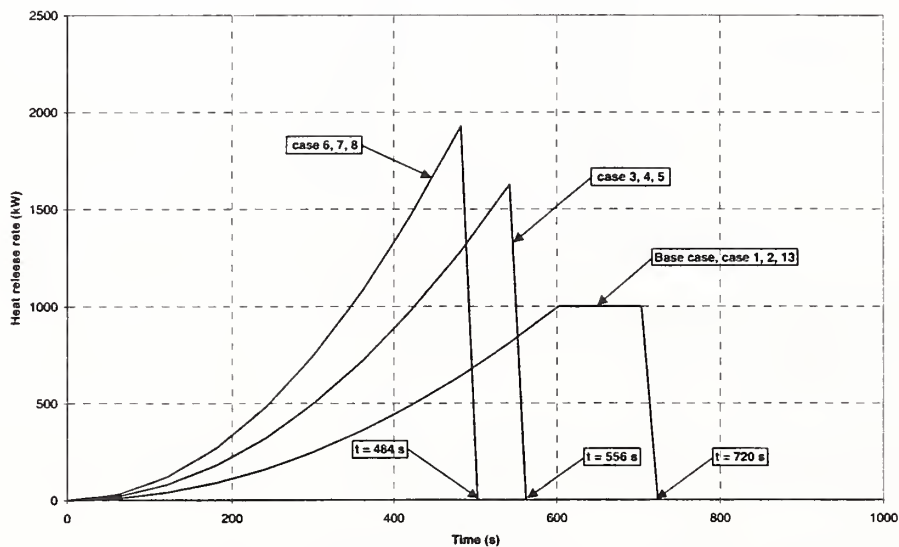
Figure 19 : Actual heat release rate

---

[10] No mass flow enter or leave the layers
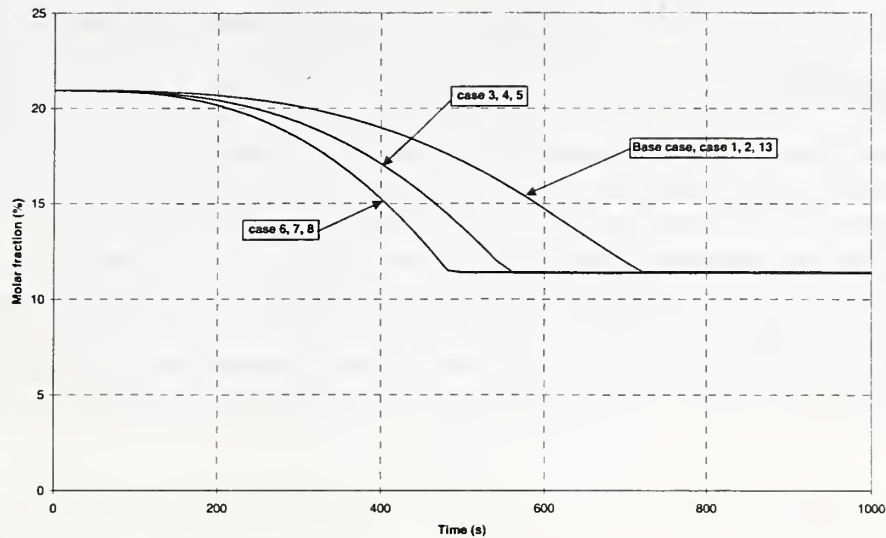
Figure 20 : Oxygen molar fraction in the upper layer

Upper and lower layer temperature

The analysis of the numerical results shows that the temperature profiles in the upper layer display the same tendency as the heat release rate (see Figure 21): the higher the peak heat release rate, the higher the maximum temperature in the upper layer. These temperatures are summed up in the following table :

Case	Maximum Upper layer temperature (°C)
Base case, Case 1, 2, 13	192
Case 3, 4, 5	244
Case 6, 7 , 8	267
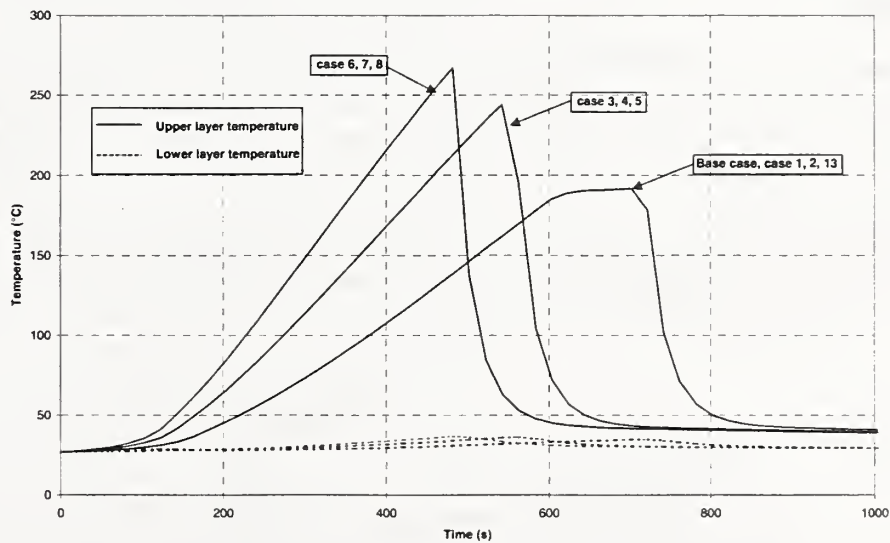
Figure 21 : Upper and lower layer temperatures

The Figure 22 also shows that the shift for the lower zone temperature is weak.

Gas layer depth

The Figure 22 displays the gas layer depth for all cases corresponding to the enclosed room. As shown in the figure, each curve has two inflexion points. The first one is reached when the interface height is near the upper surface of the burning cable tray stack. Beyond this moment, there isn't any more fresh air going into the upper layer from the cooler region throughout the plume. Nevertheless, due to the burning of the cable tray the combustion products go on filling out the upper layer. Therefore, the thickness of the lower layer decreases far below the fire place. When the fire self-extinguishes, the second inflexion point is reached. Beyond this moment, the quick cooling of the hot gases results in an increase of the interface height.
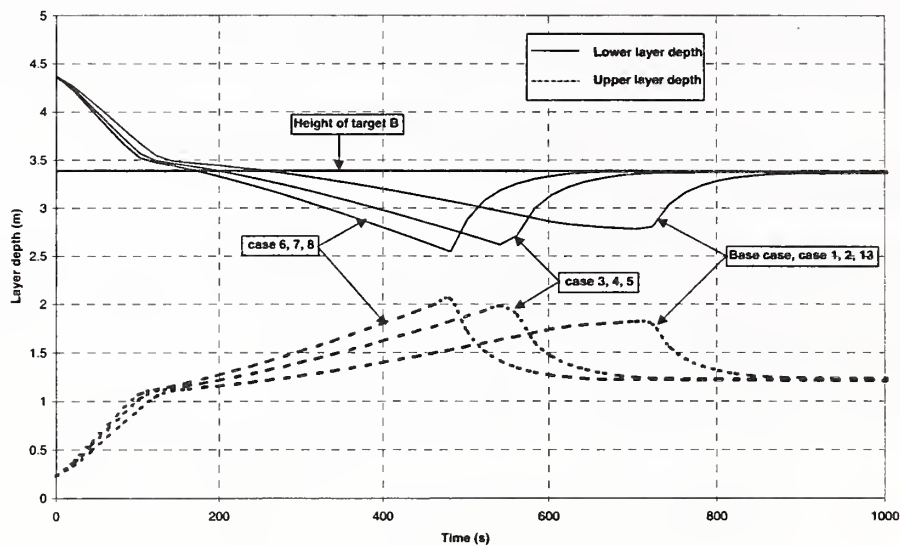
Figure 22 : Gas layer depth

The target

The temperature profiles at the surface and centerline of the target are displayed on the Figure 23. Each surface temperature profile displays a sudden change in its slope soon after the ignition of the cable. At this time, the target is plunged into the upper layer. The emissivity of the hot gases is around 0,5 and tends to increase. A non negligible amount of the fraction of heat released by the flame as radiation is absorbed by the hot gases. Thus, the increase of the target temperature is mainly due to the convective and radiative heat exchange between the target and the gases. Whatever the case, the maximal surface temperature of the target is always lower than the damage temperature (200°C) (see the following table) :

	Target maximal surface temperature (°C)
Base case, Case 1, 2	130
Case 3, 4, 5	154
Case 6, 7 , 8	161
Case 13	148

Besides, the core temperature of the target is also far below the surface temperature due to the value used for the thermal conductivity coefficient for PVC (0.092 W/mK) except for the case13. In the case 13, the core temperature is much higher (see Figure 23) because the diameter of the instrument cable is indeed three times less than that of the power cable.

For the base case and the cases 1, 2, 13, the maximal upper layer temperature is even less than 200°C . Obviously, the target won't never be damaged. For the other cases, the comparison of the fire duration with the time needed for heat to reach the core of the target gives an insight of the reasons why the target will likely never be damaged. Remember that a rough estimate of how long it will take the back of the wall to feel an increase in the temperature on the front face is given by the following formula : $t_p \approx \dfrac{e^2}{16(\lambda/\rho c)}$ [3].

where e is the wall thickness, λ the thermal conductivity, ρ the density and c the specific heat.

	Thermal penetration time (s) (to reach the core of the cable)	Fire duration (s)
Power cable	200	720 (base case)
Instrument cable	20	720 (case 13)

For the power cable, both characteristic times have the same magnitude. It consequently takes a non negligible amount of time to heat the whole cable (see Figure 23). For the instrument cable, with a short delay, the centerline temperature profile displays the same tendency as the surface temperature profile because the thermal penetration time is small in comparison with the fire duration.
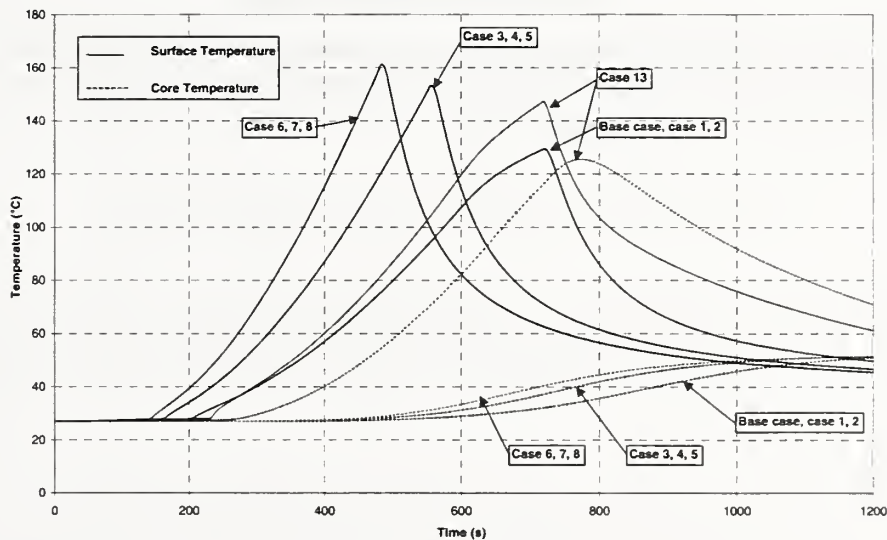
Figure 23 : Cable temperature profiles (target)

A-23

As the heat of the tray B mainly results from the thermal exchanges with the hot gases, the distance d between the target and the burning cable tray stack has no effect upon the temperature profiles in the target.

Additional results are given in the Appendix 2.

4.3.2 Ventilated room.

Case 9.

This case is different from the base case because of the ventilation conditions. The door is closed until 15 minutes at the time when the mechanical ventilation is stopped. The Figure 24 shows the evolution of the heat release rate of the cable fire. Despite the mechanical ventilation, the fire self-extinguishes at t=720 s for lack of oxygen.
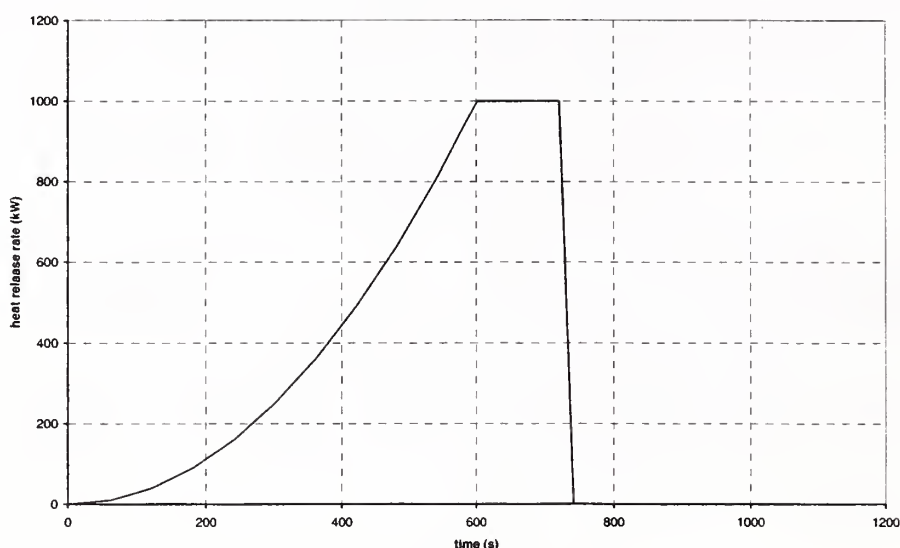
Figure 24: Heat release rate.

As can be seen on the Figure 25 the fire source is quickly (t=200s) in the upper layer where the oxygen concentration reaches 12% at t=720s (Figure 26). In this case the fire duration is too short for the ventilation effects to be felt.
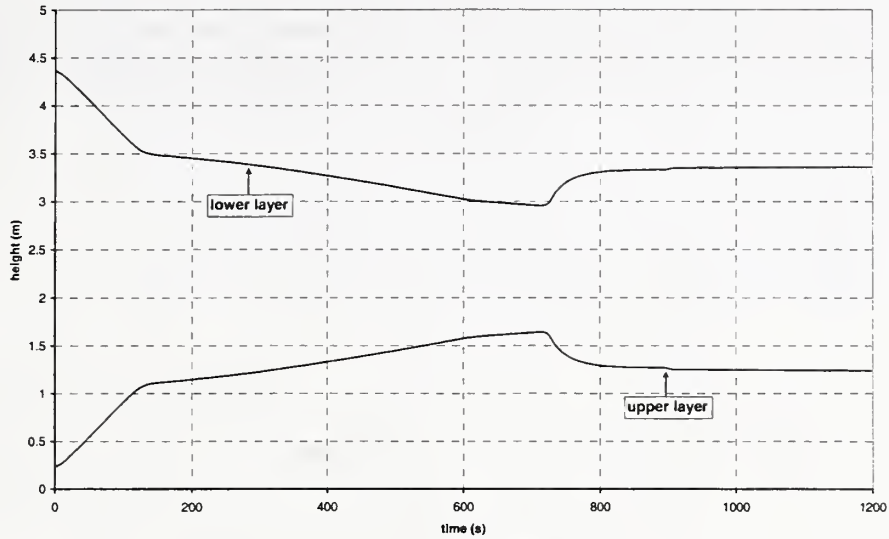
Figure 25: Depth of upper and lower layers.
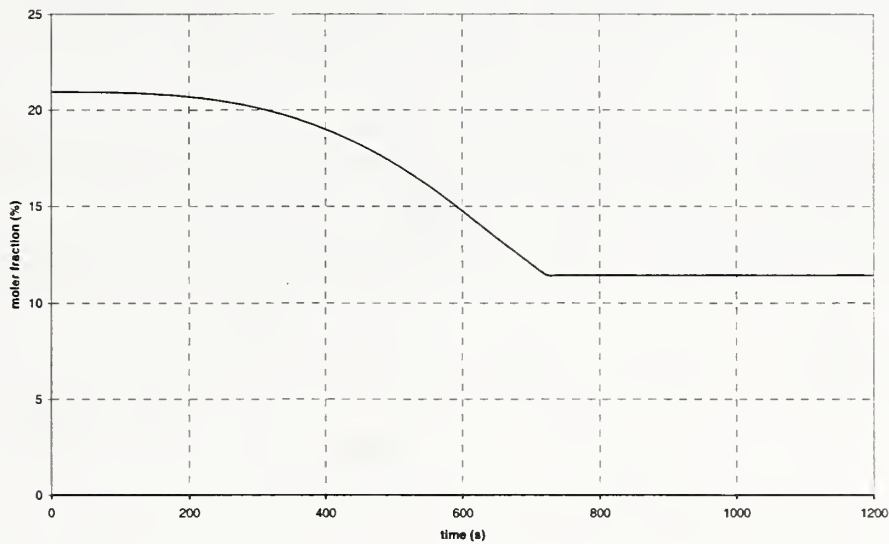
Figure 26: Oxygen molar fraction in the upper layer.

The temperature profiles in the room (Figure 27) show the same tendency as the heat release rate of the fire. The maximum temperature does not exceed 200°C and this explains the reason why the target remains far under the damage temperature (Figure 28).
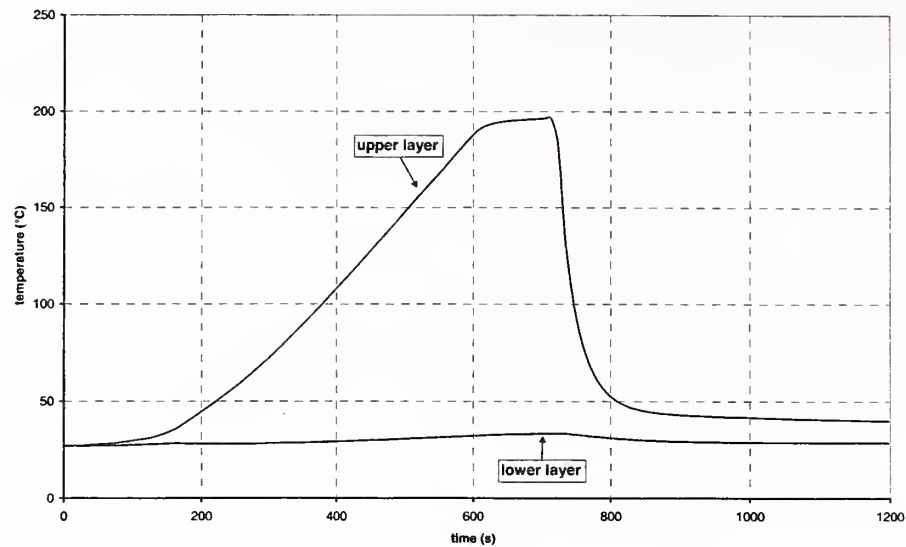
Figure 27: Room temperatures.

The sudden slopes change in the cable surface temperature at t=200s corresponds to the time when the target enters the upper layer. At this time the convective heat exchange between the cable and the gas quickly increases because of the relatively high temperature of the gas of the upper layer.
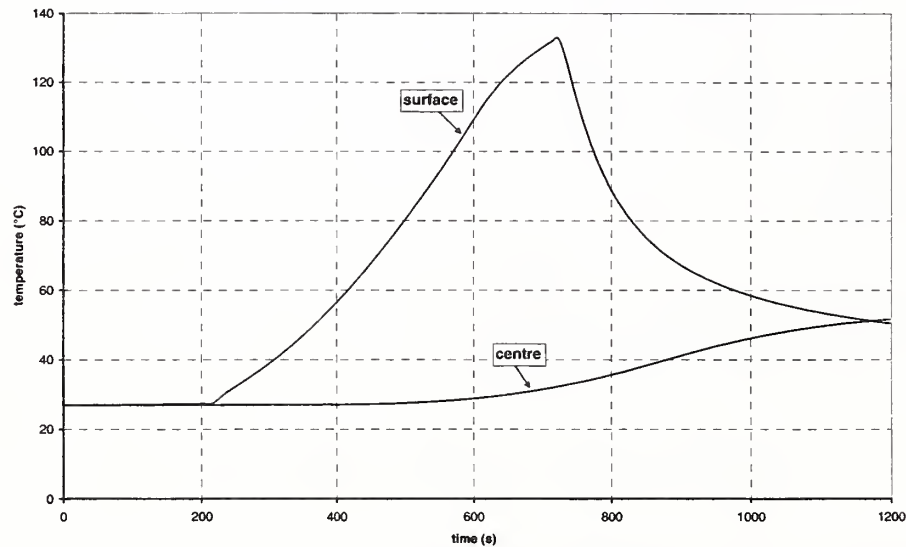
Figure 28: Cable temperature (target).

Complementary results are presented in the Appendix 2.

Case 10 and 10b.

In the case 10, the door is open and the ventilation system is on during all the fire duration. The case 10b is a complementary simulation in which the elevation of the cable fire is 2.3 m (height of the cable tray A). This last simulation aims at studying the effect of the fire elevation in the model.

The Figure 29 shows the heat release rate of the fire in the cases 10 and 10b. In the first case, the fire self extinguishes at t=720 s for lack of oxygen whereas in the second case the fire reaches the end of the imposed HRR.
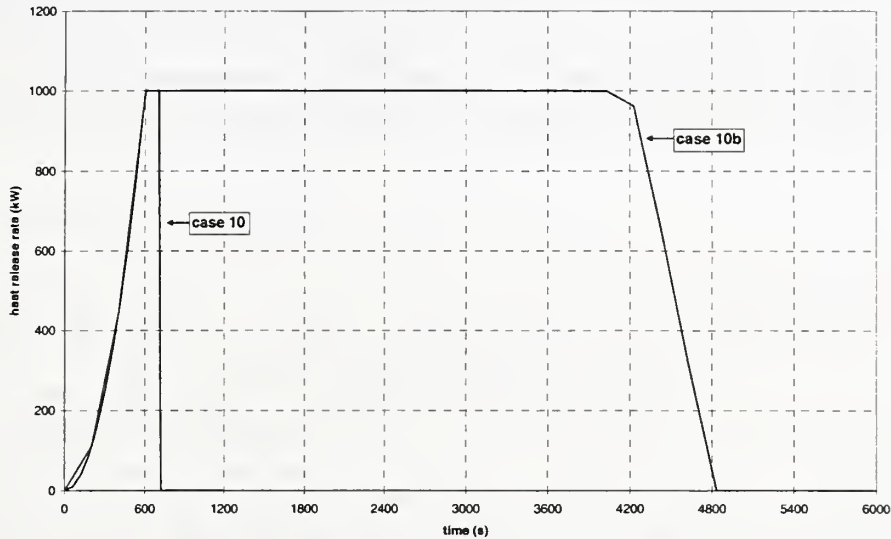
Figure 29: Heat release rate of the fire.

This difference is directly involved to the elevation of the fire source. In the case 10, the fire enters rapidly the upper layer of the room where the oxygen molar fraction reaches 12% at t=720s. In the case 10b, the interface height reaches the bottom of the mechanical vents before the fire self-extinguishes for lack of oxygen (Figure 31). From this time, the upper layer is supplied with fresh air from the outside and the oxygen molar fraction remains enough to ensure the combustion (Figure 30).
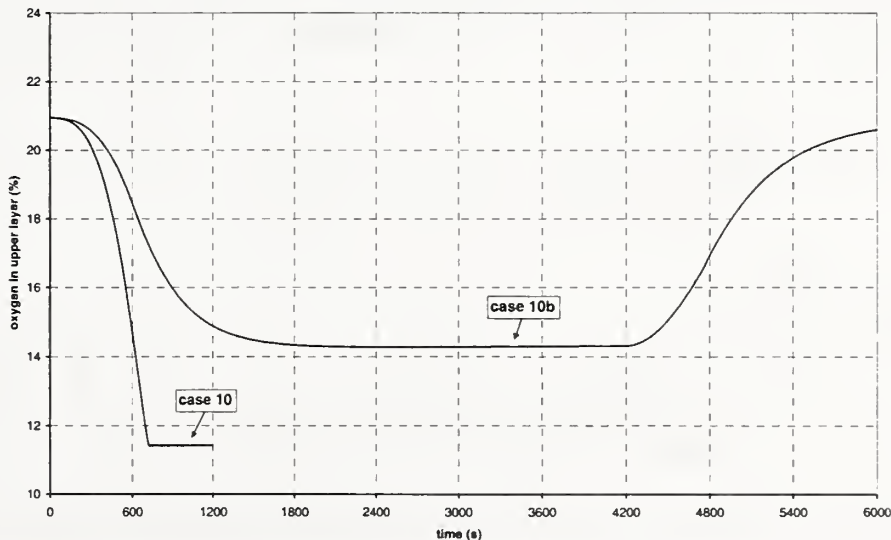
Figure 30: Oxygen molar fraction in the upper layer.
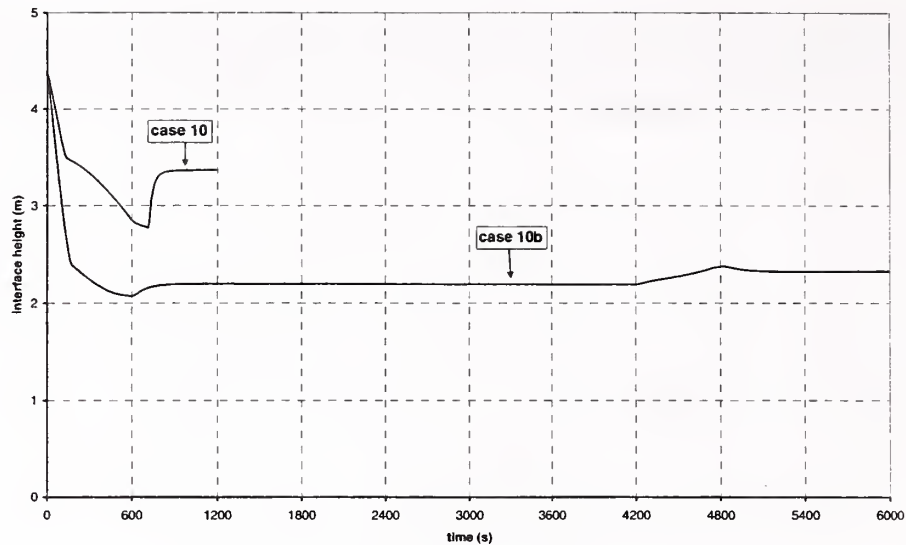
Figure 31: Interface height in the room.

The temperature profiles in the room show the same evolution as the heat release rate of the fire. The temperature increase in the room is quicker in the case 10 than in the case 10b at the onset of the fire. This comes from the fact that in the second case the dilution of the combustion products with the air entrained by the plume in the upper layer is more important. On the other hand, one can observed that in the case 10b the cable surface temperature exceeds 200°C at the end of the fire. In the case 10, the cable surface temperature does not reach 150°C because of the short duration of the fire.
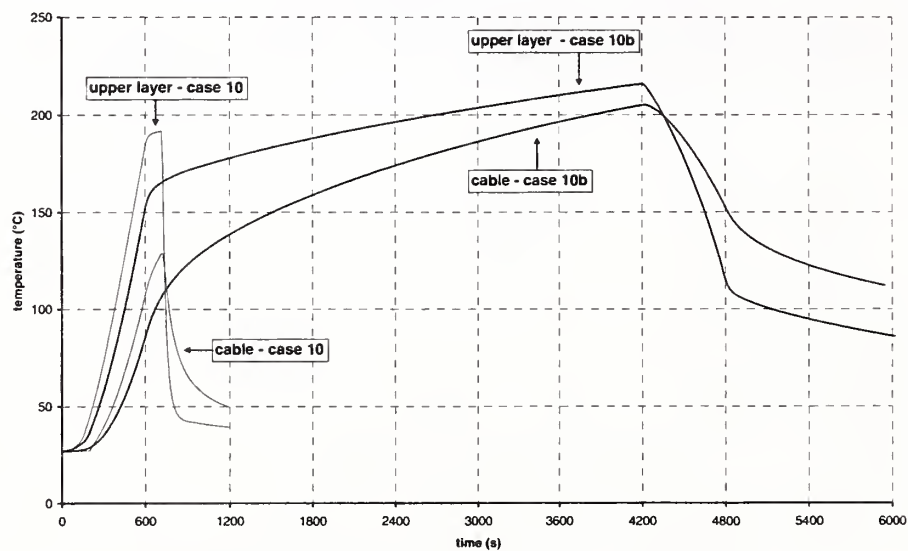
Figure 32: Cable surface and room temperature.

These simulations show the strong influence of the fire elevation in the current modelling of the problem.

Complementary results for the case 10 are reported in the appendix 2.

Cases 11, 12

The difference between these cases and the base case is the elevation of the target which is 2 m (case 11) or 0 m (case 12) above the cable tray A. The elevation of the target has no effect on all the properties of both layers. Furthermore, for the same elevation as the cable tray A, the target is always in the cooler zone during all the simulation. Thus, the temperature of the whole target keeps nearly constant (around 30°C).

As the ceiling jet phenomenon is not modelled in the Flamme_S code, a rise in the elevation of the target (2 m above the tray A) leads to the same results as those obtained for the base case.

4.4 Conclusion of the second part

In the second part, the heating of the cable tray B is mainly due to the thermal exchanges with the hot gases. Whatever the case, the tray B is likely never damaged because the surface temperature of the target is below the damage temperature advised for the cable (200°C). For the enclosed room, the elevation of the target doesn't matter for the calculations because the ceiling jet effect is not taken into account.

From a calculation point of view, the elevation of the fire seems to be much more important. For example, when the fire is set to the elevation of cable tray A (Q_0 = 1 MW), the fire reaches the end of the imposed heat release rate leading to higher temperatures in the hot gases. In this case, near the end of the fire, the surface temperature of the target is slightly above the specified damage temperature. But even in this case, the target is not damaged.

5. CONCLUSION.

This report is devoted to a study of cable tray fires of redundant safety trains with a two-zone model. The aim of this work is to evaluate fire models for nuclear power plant applications. All the calculations have been performed with the 2.2 version of the FLAMME_S / SIMEVENT code.

The power and instrument cables trays (tray A) associated with the redundant safe shutdown equipment (tray B) are set in a representative PWR emergency switchgear room. They are arranged in separate divisions and separated horizontally by a distance d.

The study is divided in two parts. The purpose of the first one is to determine the maximum distance between a specified transient fire and the cable tray A which results in the ignition of the cable tray. The fire is assumed to be a trash bag containing wood. The aim of the second part is to evaluate the damage time of the redundant safe shutdown equipment (tray B) for several peak heat release rates of the cable tray stack A (1 - 3MW) and various horizontal distance d (3.1 m, 4.6 m, 6.1 m). In this part the cable trays are supposed to be made of PVC. The ignition of the cable fire is modelled of as a t-squared growth. The same modelling is used for the extinction of the fire.

The calculations achieved in the part I show that the heating of the cable tray A is mainly due to the fraction of energy released by the flame as radiation and, given the location of the trash in the room, to the convective exchanges with the plume. The main results of the numerical

simulations are that, given the size of the switchgear room and the relatively low heat release rate of the transient fire (350 kW), the ignition or damage of the cable tray A is unlikely except when it is in the plume of the fire.

In the second part, the analysis of the numerical results shows that the heating of the cable tray B principally results from the thermal exchanges with the hot gases of the upper layer. As in part I, the damage of the redundant cable B is unlikely. Furthermore, the elevation of the target in the room has no effect upon the results because in the Flamme_S code the ceiling jet phenomenon is not modelled.

6. REFERENCE.

1. MONIDEEP DEY
   "Benchmark exercise #1 - Cable tray fire of redundant safety trains."
   International Collaborative Project to Evaluate Fire Models for Nuclear Power Plant Application - Revised september 11 - 2000.

2. HESKESTAD G.
   "Fire Plumes"
   The SFPE Handbook of Fire protection Engineering -1995.

3. QUINTIERE J. G.
   "Heat Transfert"
   Principles of Fire Behavior - 1998

4. TEWARSON A.
   "Generation of heat and chemical compounds in fire."
   The SFPE Handbook of Fire Protection Engineering - 1995.

7. APPENDIX.

7.1 Appendix 1.

This appendix presents the results of the door open and ventilation system on cases.

7.1.1 Case 4 - Door open.
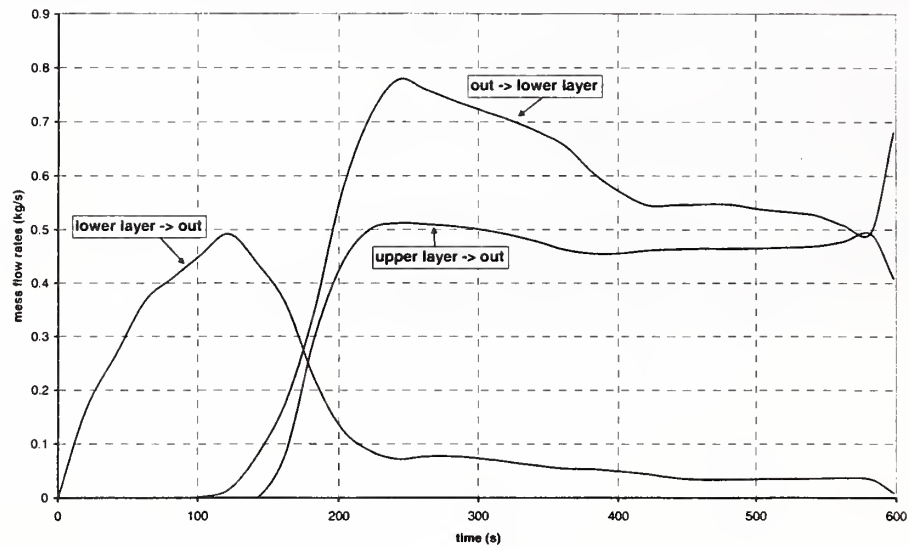
Figure 33: Mass flow rate through the door.
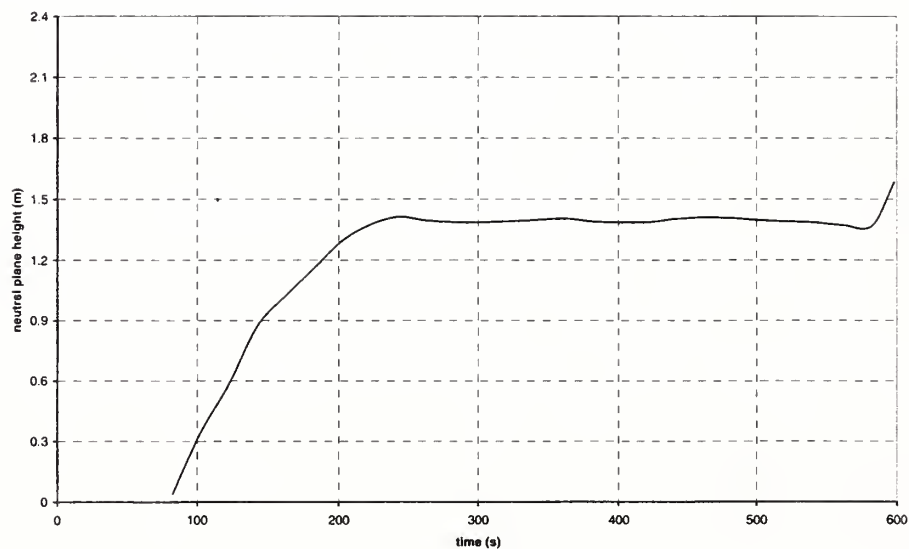
Figure 34: Neutral plane height.

Figure 33, Figure 34, Figure 35 and Figure 36 illustrate how mass flows take place through the door. For t < 80 s, the slight increase of the room temperature induces a flow from the lower layer of the room toward the outside. At t ≈ 80 s a neutral plane occurs (Figure 34);

mass flow leaves and enters the lower layer of the room. For t > 140 s, the interface height in the room reaches the top of the door (Figure 35) ; mass flows leave the lower and upper layers of the room and enter the lower layer.
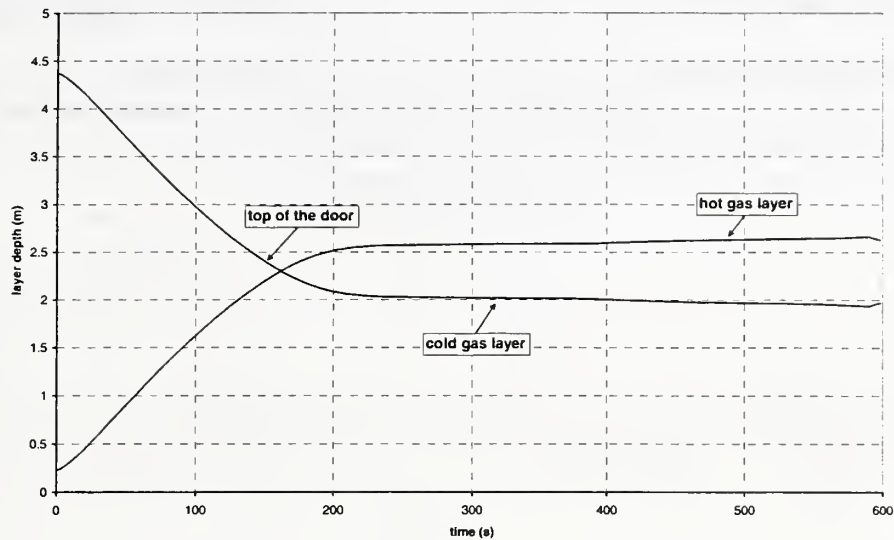
Figure 35: Depth of the upper and lower layers.
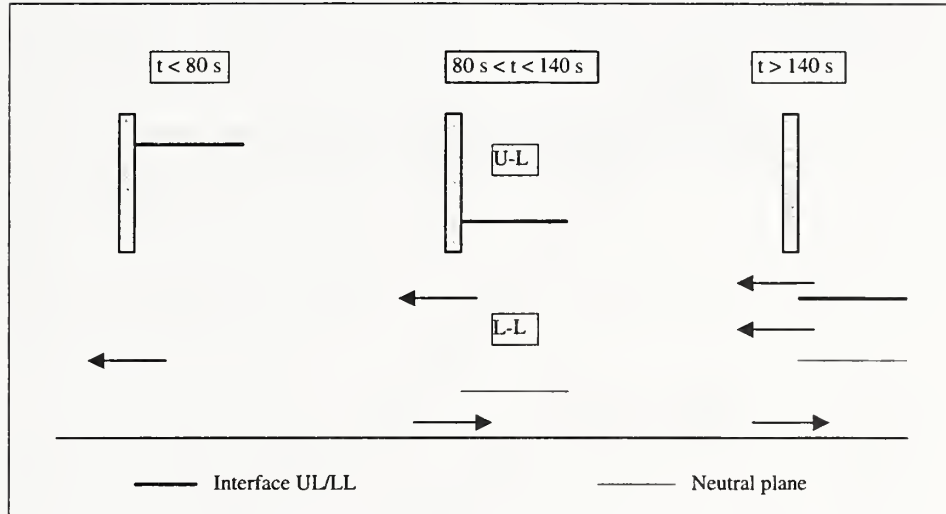
Figure 36: Mass flow rate through the door.

7.1.2 Case 5 - Ventilation system on.

The Figure 37 and the Figure 38 show the mass flow rates through the air supply and exhaust vents. Since the density of the ambient air is 1.17 kg/m^3, it corresponds exactly to a flowrate of 5 volume changes per hour.

The distribution of the flows between the upper and lower layers depends on the height of the interface. Before t = 180 s, the interface height is higher than the top of the vent and all the flows enter and leave the lower layer. On the contrary, for t = 480 s the interface reaches the bottom of the vents and flows enter and leave the upper layer.
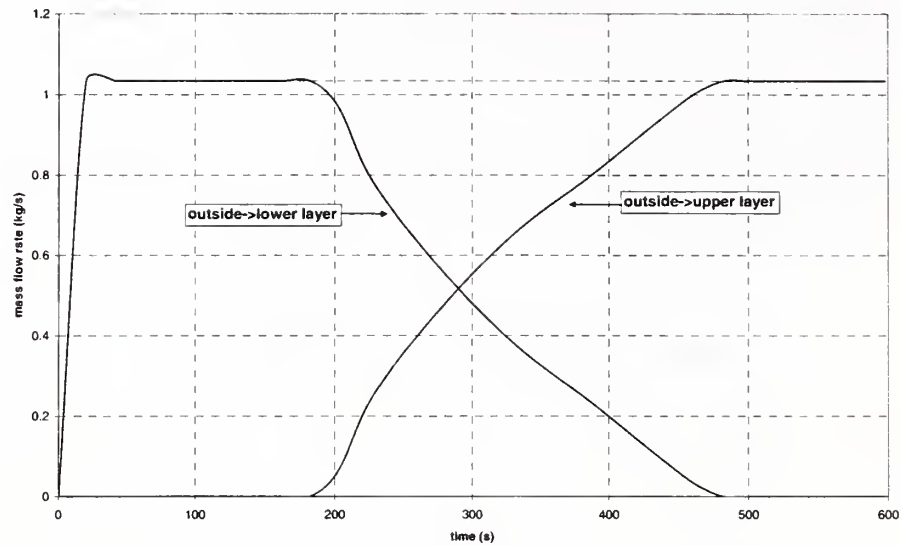
Figure 37: Mass flow rate through the supply vent.
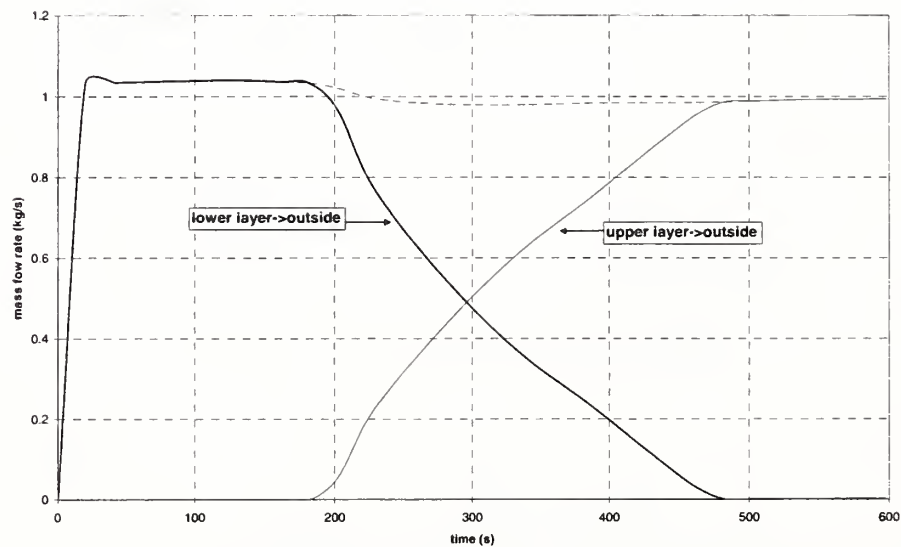
Figure 38: Mass flow rate through the exhaust vent.

7.2 Appendix 2.

7.2.1 Enclosed cases (1,2,3,4,5,6,7,8,13)

Combustion species concentration.

The Figure 39, Figure 40 and Figure 41 display the molar fraction of the chemical species in the upper layer for the base case and the cases 1 to 8 and 13.

As previously observed the fire duration does not exceed:
- 720 s for the cases 1,2,13,
- 556 s for the cases 3,4,5,
- 484 s for the cases 6,7,8.

From these times, the interface behave as a "solid" boundary that separates the upper and lower layers. No exchange between the layers occur and the molar fraction of the chemical species remain constant.
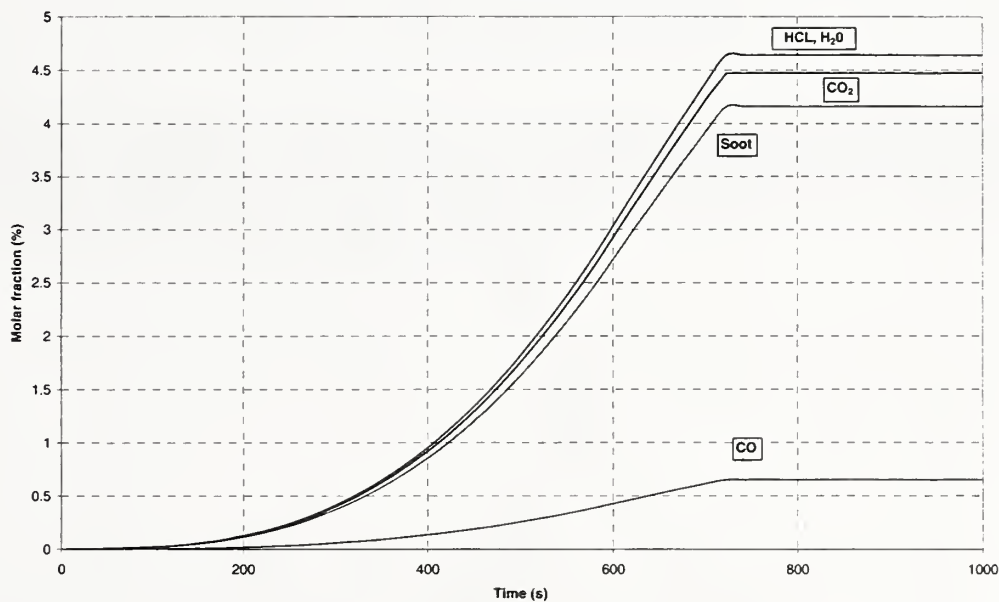
Figure 39 : Chemical species in the upper layer
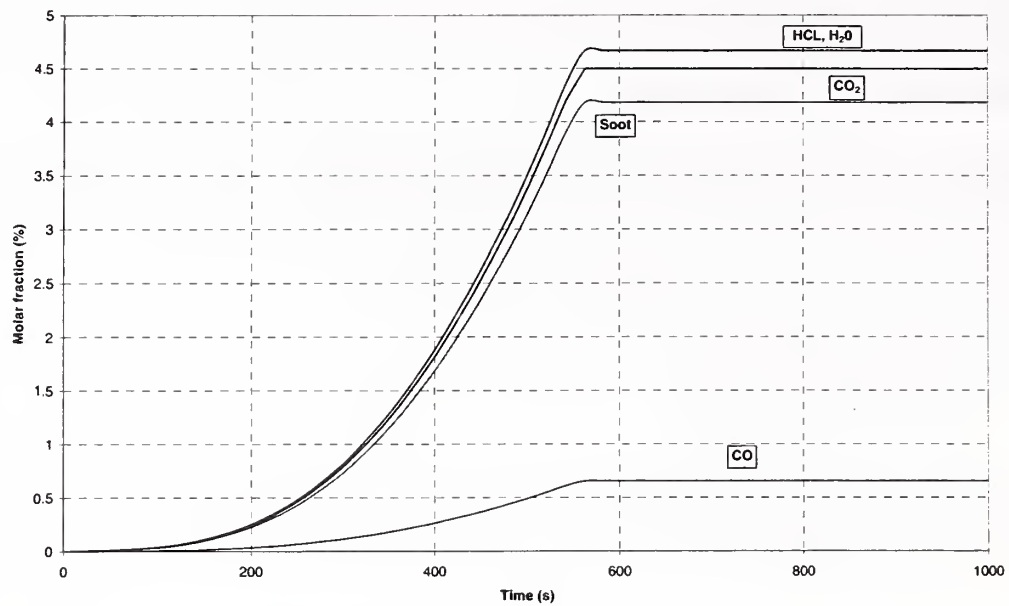
Figure 40 : Chemical species in the upper layer
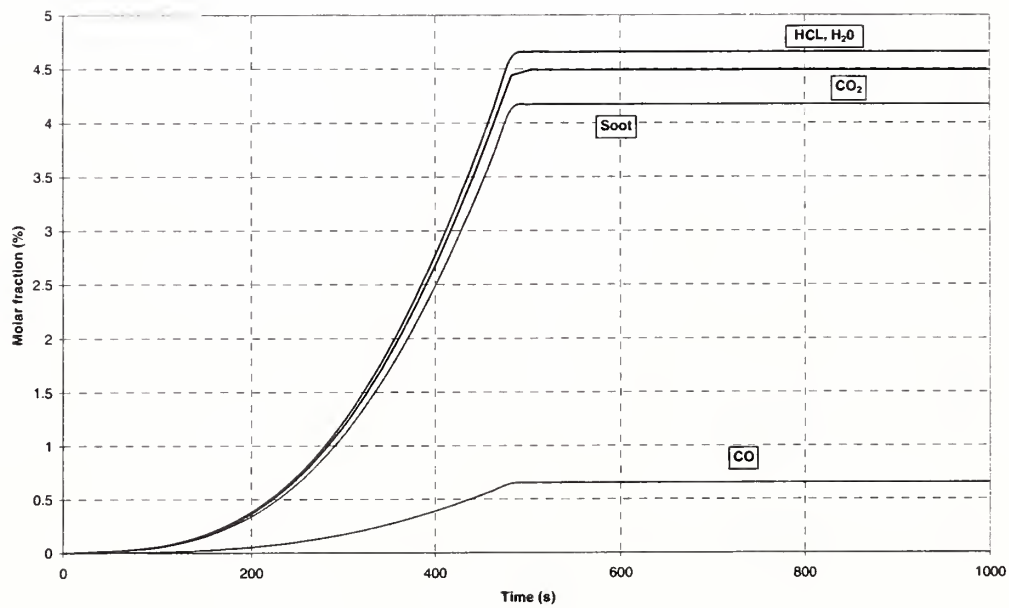
Figure 41 : Chemical species in the upper layer

Incident Radiant flux on the target (cable tray B)

The Figure 42 shows the incident radiant flux on the target. As previously explained, the profiles display a sudden slopes change corresponding to the time when the cable tray B enters in the upper layer.
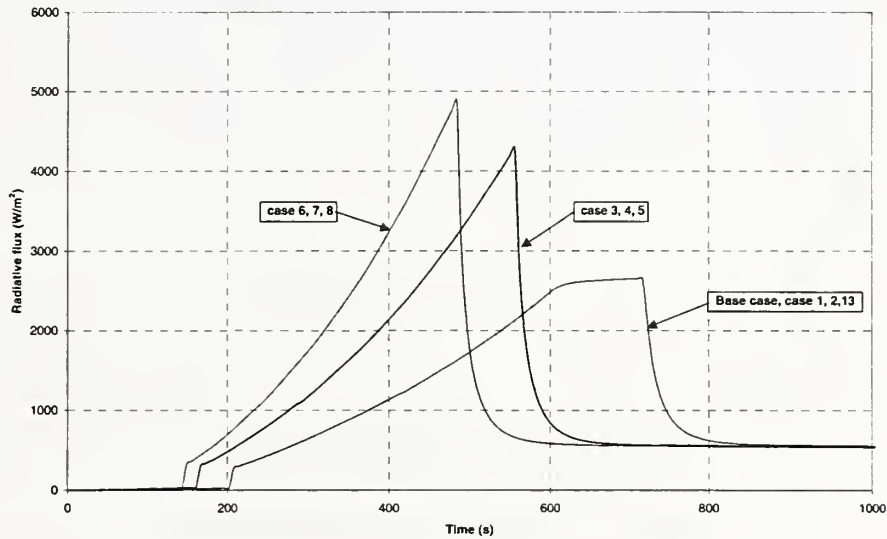
Figure 42 : Incident radiant flux on the target

7.2.2 Case 9.

The Figure 43 shows the molar fraction of the chemical species in the upper layer. As previously observed the fire duration does not exceed 720s and, from this time, the heights of the upper and lower layers are nearly constant. This explains the reason why no decrease of the molar fraction in the upper layer is observed.
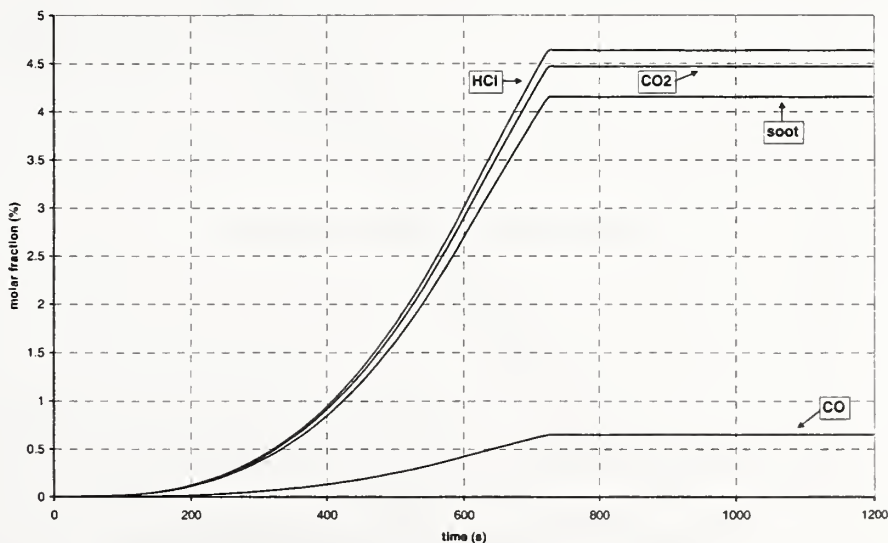
Figure 43: Chemical species in the upper layer.

The following figure is reported only to check that the ventilation system ensures a flowrate of 5 volume changes per hour in and out of the room.
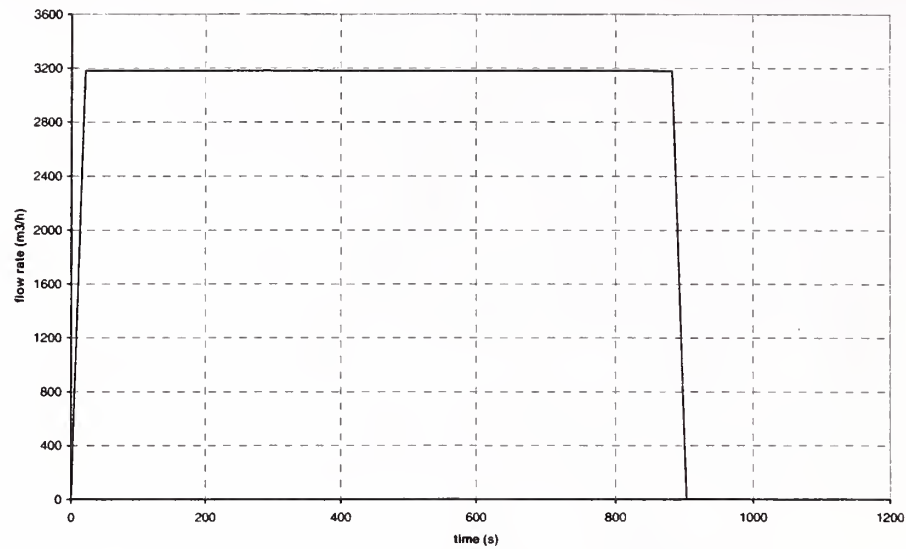
Figure 44: Flowrate in and out of the room.

7.2.3 Case 10.

The Figure 45 shows the molar fraction of the chemical species in the upper layer. As previously observed the fire duration does not exceed 720s and, from this time, the heights of the upper and lower layers are nearly constant (cf. Figure 31). This explains the reason why no decrease of the molar fraction in the upper layer is observed.
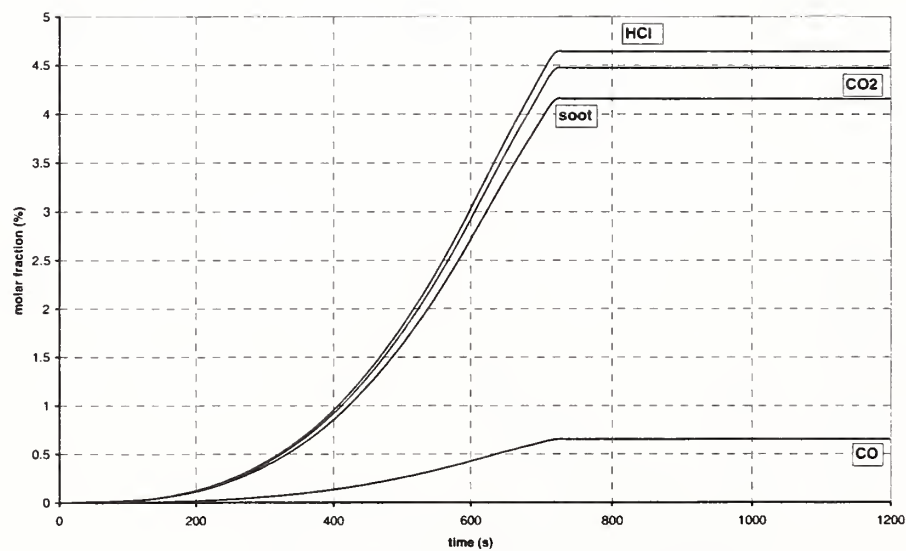
Figure 45: Chemical species in the upper layer.

The Figure 46 shows the mass flow rate through the door. Since the interface height never reaches the top of the door, only the lower layer is concerned with these flows.
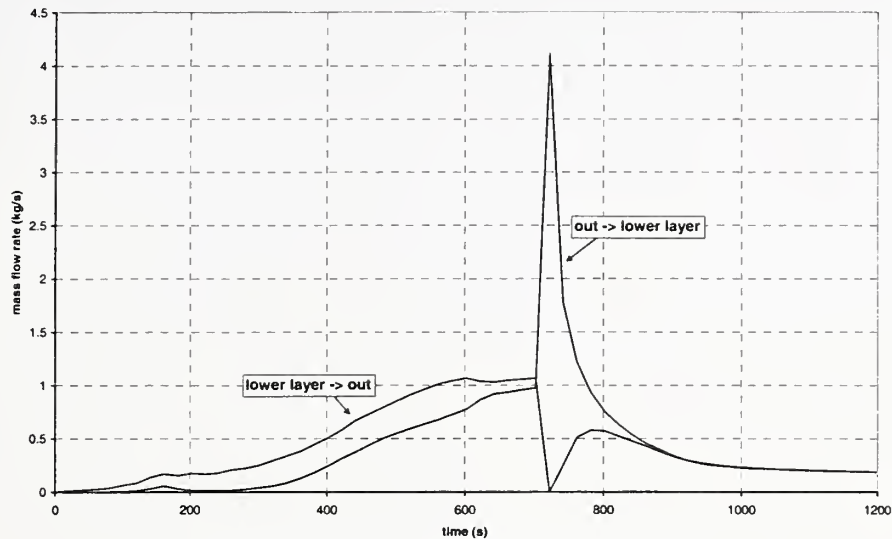
Figure 46: Flow rate through the door.
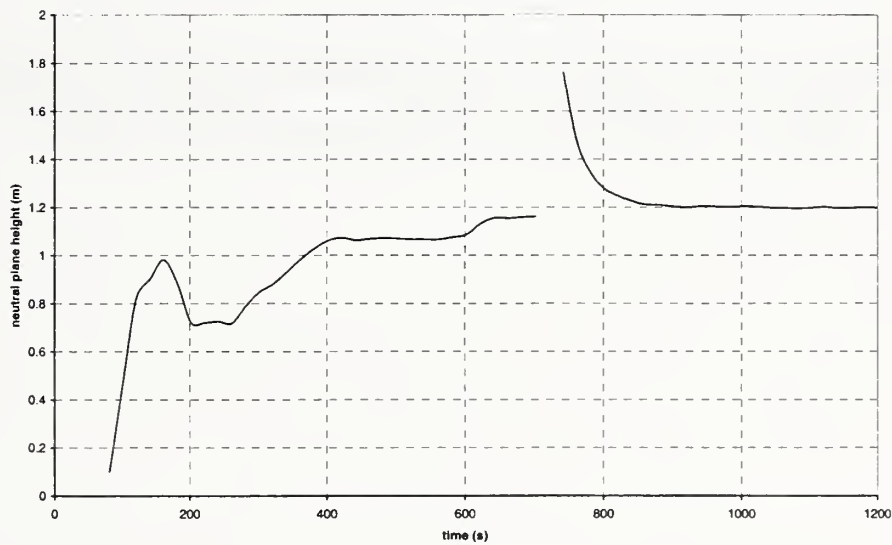
Figure 47: Neutral plane height.

Appendix B: Benchmark Analysis with CFAST and FDS, Monideep DEY, NRC/NIST, USA

SUMMARY

This Appendix presents analyses conducted with the CFAST and FDS fire models for an international benchmark exercise aimed at evaluating the capability of current fire models to simulate cable tray fires of redundant safety systems in nuclear power plants. The exercise involved simulating fire scenarios in a large nuclear power plant compartment with cable trays as targets in varying ventilation conditions. The analyses demonstrate that both the CFAST and FDS codes provide a treatment of most physical phenomena in the scenarios analyzed. The predicted time scale and magnitude of the main parameters of interest in these scenarios by both codes are similar. The sub-model for the target, and issues regarding the thermal environment of the target, are the largest source of uncertainty for these types of scenarios. It will be useful to conduct validation exercises for CFAST and FDS in which the predictive capability of target damage is the main focus of the validation. These exercises will provide information to allow the development of quantitative estimates of the uncertainties for the major parameters of interest.

INTRODUCTION

The analysis presented in this Appendix was conducted as part of a benchmark exercise in the International Collaborative Project to Evaluate Fire Models for Nuclear Power Plant Applications (Dey, 2000). The objective of the collaborative project is to share the knowledge and resources of various organizations to evaluate and improve the state of the art of fire models for use in nuclear power plant fire safety and fire hazard analysis. The project is divided into two phases. The objective of the first phase is to evaluate the capabilities of current fire models for fire safety analysis in nuclear power plants. The second phase will implement beneficial improvements to current fire models that are identified in the first phase, and extend the validation database of those models. Currently, twenty-two organizations from six countries are represented in the collaborative project.

The first task of the international collaborative project is to evaluate the capability of fire models to analyze cable tray fires of redundant safety systems in nuclear power plants. The safety systems are required to safely shutdown the reactor during abnormal and emergency events in the plant. A specified distance separates cable trays of redundant safety systems if they are located in the same compartment in which a single fire could potentially damage both systems. Therefore, the analysis of fires that could damage redundant safety trains is an important part of nuclear power plant fire hazard analysis. The evaluation of the capability of fire models to analyze these scenarios is being conducted through an international benchmark exercise.

The benchmark exercise (Bertrand and Dey, 2001) is intended to simulate a basic scenario defined in sufficient detail to allow evaluation of the physics modeled in the fire computer codes. An assessment of appropriate input parameters and assumptions, interpretation of results, and determining the adequacy of the physical sub-models in the codes for specific scenarios will establish useful technical information regarding the capabilities and limitations of the fire computer codes. This valuable information will be documented in a technical reference manual for fire model users. Generic insights regarding the capabilities of the models will also be developed in this process and documented. The comparisons between codes can be used to understand the modeling of the physics in them, i.e. if all the codes

produce similar results over a range of scenarios then the physics modeled in the codes is probably adequate for this scenario. However, the compounding effects of different phenomena will also need to be examined as part of this evaluation. Some variations in the results may be acceptable depending on how the results will be used. Uncertainties in the predictions based on validations of each code will provide a basis for the confidence on the set of results developed in the exercise.

This Appendix presents the analyses for the benchmark exercise conducted using the Consolidated Fire And Smoke Transport [CFAST] (Jones, 2000), and Fire Dynamic Simulator [FDS] (McGrattan, 2000) computer codes developed by the National Institute of Standards and Technology, U.S. Department of Commerce. The paper provides the results of an assessment and verification of the capability of these computer codes to analyze the fire scenario specified for the benchmark exercise.

DEFINITION OF SCENARIO

A representative emergency switchgear room for a Pressurized Water Reactor (PWR) has been selected for this benchmark exercise. The room is 15.2 m (50 ft) deep x 9.1 m (30 ft) wide and 4.6 m (15 ft) high. The room contains the power and instrumentation cables for the pumps and valves associated with redundant safety systems. The power and instrument cable trays run the entire depth of the room, and are separated horizontally by a distance, d. The cable trays are 0.6 m (≈24 in) wide and 0.08 m (≈3 in) deep. A simplified schematic of the room, illustrating critical cable tray locations, is shown in Figure 1. The room has a door, 2.4 m x 2.4 m (8 ft x 8 ft), and a mechanical ventilation system with a flow rate of 5 volume changes per hour in and out of the room.

There are two parts to the exercise. The objective of Part I is to determine the maximum horizontal distance between a specified transient (trash bag) fire and tray A that results in the ignition of tray A. Part II examines whether the target cable tray B will be damaged for several heat release rates of the cable tray stack (A, C2, and C1), and horizontal distance, d. The effects of the fire door being open or closed, and the mechanical ventilation on or off, are examined in both parts of the benchmark exercise.

VALIDATION OF THE CFAST AND FDS FIRE CODES

The CFAST and FDS fire codes have been compared to several data sets from experiments, including those with configurations and fire intensities similar to that specified for the benchmark exercise. However, none of the tests included cable trays as target material to measure the response of the target to the physical environment in the compartment.

Results from the CFAST code have been compared to several tests of fires in spaces ranging from small compartments to large aircraft hangers. Peacock (1993) compared predictions of CFAST to four fire tests in a single compartment, multi-compartment on a single floor, and a seven-story building. The magnitude and trends (time to critical conditions and general curve shape) are reported. The comparisons ranged from a few percent to a factor of 2 to 3 of the measured values.

Results from the FDS code, Version 1, has been compared with experimental data for open plumes, back draft, flashover, a warehouse fire, pool fires in a Navy Hangar, and fires in a decommissioned nuclear reactor containment. These comparisons demonstrated the enhanced predictive capability of this code for a wide range of fire scenarios, and also identified areas for improvement. Specifically, the modeling of radiation from the hot gases and walls is an important effect in nuclear power plant compartment fires. The modeling of this effect has been included in Version 2, which was released in December 2001. Significant improvements in the predictions of the tests in the decommissioned containment building have been achieved with FDS, Version 2.

Although several comparisons of these codes to experimental data are available, it is not possible at this stage to translate this research to quantitative estimates of uncertainties of the predicted results from the codes for the benchmark exercise. A complete analysis of past validation research, including an examination of the effect of the specifics (compartment configuration, fire source intensity, ventilation, etc.) of a fire scenario on the predictive capability of the codes is planned.

RESULTS OF THE ANALYSES

Part I

CFAST Analyses

The major sub-models used in CFAST for the scenarios specified in the benchmark exercise are (1) combustion chemistry (tracking O_2, and species); (2) plumes and layers; (3) vent flow, including forced ventilation; and (4) heat transfer, especially radiation and convection to the target.

The following presents the major highlights of the results obtained for the analysis of the benchmark exercise. The trends of various parameters are examined to verify the adequacy of the basic sub-models for the specific scenarios. The general conclusions from the exercise are also presented, although as indicated above, quantitative estimates of the uncertainties associated with the predictive capability of the codes for the specific parameters examined are not available at this time.

The measured heat release rate (Lee, 1985) of a large trash bag was used as input for the simulation as shown in Figure 2. In order to conduct a simplified and conservative analysis, the target is assumed to be a single power cable with a diameter of 50 mm at the bottom left corner of the cable tray A. Consistent with the target models in CFAST and FDS, the target cable is represented as a rectangular slab oriented horizontally with a thickness of 50 mm. The cable is assumed to ignite when the centerline of the cable reaches 643 K. Table 1 summarizes the cases for Part I of the benchmark exercise. The peak heat release for the trash bag fire (Figure 2) for Part I is $\approx$ 350 kW, and peaks at $\approx$ 150 s.

Table 1. Summary of Cases for Part I

	Distance between Trash Bag & Cable	Door	Ventilation System
Base Case	2.2 m	Closed*	Off
Case 1	0.3+		
Case 2	0.9		
Case 3	1.5		
Case 4		Open	
Case 5			On

* For simulations with the door closed, a crack (2.4 m x 0.005 m) at the bottom of the doorway was assumed.

+A value in a cell indicates the parameter was varied from the base case.

Base Case

Figure 3 shows the predicted oxygen depletion for the Base Case. The oxygen concentration in the lower layer stays approximately constant, as would be expected. The oxygen concentration in the upper layer decreases by ≈ 1 % to 19.2 %. Therefore, the fire will not be limited by oxygen in this fire scenario.

Figure 2 also shows the plume flow development during this scenario. The main plume flow increases rapidly at the initiation of the fire, and does not follow the fire heat release rate, as expected. CFAST over predicts mass entrainment at the initial stages of the fire because of the plume height used in the calculation of the entrained air. Initially, the plume height is assumed to be from the fire to the ceiling. This leads to an over prediction of the initial mass flow to the upper layer, and the rate of descent of the gas layer interface.

Figure 4 shows the hot gas layer (HGL) temperature and the interface height development. The upper layer temperature peaks at ≈ 230 s, about 80 s after the fire peaks, due to the lag time for the heating of the gas by the fire. In this scenario, the upper layer temperature increases only about 50 K. After peaking, the upper layer temperature decreases with time due to the heat loss to the boundaries. The interface height decreases rapidly initially due to high plume flow (see Figure 2). The rate of descent of the interface height decreases after ≈ 230 s when the HGL temperature has peaked. The hot gas layer is prevented from reaching the floor due to air inflow at the crack below the door caused by a negative pressure in the compartment (see Figure 5).

Figure 5 shows the pressure development, and the resulting flows in and out of the compartment. The pressure peaks at ≈ 150 s when the fire heat release rate peaks, as would be expected. The pressure decreases after the fire peaks due to outflow from the compartment at the crack under the door, and swings to a negative value. The small oscillations in the pressure after ≈ 250 s is due to the small fluctuations in the heat release rate. The peak in the outflow is consistent with the pressure profile, and the outflow goes to zero when the pressure in the compartment is less than the outside. The initiation of inflow is consistent with the pressure profile, and is much less than the outflow. The small oscillation of the inflow is caused by the fluctuations in the pressure.

Figure 6 shows the components of the heat flux to the target. The radiative flux on the target from the fire follows the fire heat release rate curve, as expected. The radiative flux on the target (lower side) from the hot gas increases at the point ($\approx$ 100 s) when the interface height reaches the target. The radiative flux from the hot gas on the target peaks at $\approx$ 280 s, 50 s after the upper layer temperature peaks, and decreases in a similar manner to the upper layer temperature. The lag between the peak in the radiative flux from the hot gas and the upper layer temperature is because of the time needed for hot gas layer growth under the target. The convective flux is negative initially because the target temperature is greater than the lower layer temperature. The convective flux becomes positive and starts to increase at $\approx$ 100 s when the hot gas layer interface reaches the target, as expected. The convective flux peaks at $\approx$ 230 s when the upper layer temperature peaks, as expected.

Cases 1 to 3

Figure 7 shows the target surface temperatures versus time for the Base Case and Cases 1 -3. For the Base Case, the target temperature peaks at $\approx$ 290 s, $\approx$ 140 s after the fire and target flux reaches its peak due to the thermal inertia of the target. The target surface temperature only increases $\approx$ 20 K for this case. Figure 8 is a plot of the maximum surface temperatures of the target versus the distance between the fire and target. The plot could be approximated by a straight line and does not show a rapid increase in temperature with decreasing distance between the fire and the target. This can be explained by examining Case 1. The radiative flux from the hot gas layer is the same as the Base Case since the only difference between the cases is the fire location. The radiation from the fire is the largest in Case 1 because the fire is closest to the target; however, the peak convective flux is half of that in the Base Case (100 vs. 200 W/m^2). The decreased peak convective flux is caused by a smaller difference in temperature between the hot gas layer and the target surface (the target surface temperature is higher due to higher radiative flux).

Cases 4 and 5

The following presents some key features of the results of Case 4 and 5. Figure 9 shows the development of the interface height for Case 4 versus the Base Case. The interface height approaches a constant value at $\approx$ 140 s, after the HGL reaches the top of the door at $\approx$ 100 s. Figure 10 shows the development of the upper layer outflow and lower layer inflow after the HGL interface reaches the door at $\approx$ 100 s, indicating the establishment of a neutral plane below the top of the door (at $\approx$ 2.2 m). Figure 11 shows the HGL temperature development for Case 4 and 5. The HGL temperature for Case 4 is less than the Base Case after $\approx$ 270 s because of the outflow of hot gas from the upper layer (which reaches its peak value at $\approx$ 200 s) through the door, and higher plume flow. The HGL temperature for Case 5 is less than that in the Base Case after $\approx$ 100 s when the HGL reaches the mechanical vents, and ambient air is injected into and hot gas ejected from the hot gas layer.

Figure 12 shows the development of flows in the mechanical ventilation system for Case 5. The transitions in flows from the mechanical vents in and out of the gas layers occurs at about $\approx$ 100 s when the HGL reaches the mechanical vents. The mass flow rate into the upper layer is larger than the mass flow rate out of the upper layer because mechanical

ventilation flows in CFAST are specified as volumetric flow rates. The temperature of the flow out of the compartment is higher than the ambient conditions of the flow into the compartment. Figure 3 shows that the oxygen concentration in the HGL layer is greater in Case 5 than the Base Case after $\approx$ 160 s when the HGL reaches the mechanical vents, and air at ambient conditions is injected in to the upper layer. Figure 7 shows the target surface temperature for Case 4 and 5 along with the other cases. The target surface temperature for Case 4 and 5 is less than in the Base Case because of cooler hot gas layer temperatures. The cable temperature does not approach the point of ignition (643 K) in any of the cases analyzed.

The above analyses of the results for Part 1 demonstrates that CFAST provides a treatment of most physical phenomena of interest in the scenarios analyzed. The results indicate that the trends predicted by the sub-models in CFAST are reasonable and provide insights beneficial for nuclear power plant fire safety engineering.

FDS Analyses

The following presents a summary of the analyses that was conducted with the FDS code in order to allow a comparison with the results from CFAST. Direct comparison between CFAST and FDS for several parameters discussed above is difficult. The total flow through vents is not a direct output from the FDS code. Plume flow and the hot gas layer interface height are computed directly in a zone model, but not in CFD models.

Figure 13 is an output image from the Smokeview (Forney, 2000) graphical interface to the FDS code, which allows a comprehensive visual analysis of the code output. The specific image in Figure 13 is a slice file, which shows the development of system parameters versus time for a particular plane in the 3-D geometry simulated. This specific figure shows a snapshot of the temperature profile at the midpoint of the room (where the trash bag is located) for the Base Case at 230 s. Although it is not possible to obtain an accurate determination of the interface height from images such as shown in Figure 13, a visual examination of the slice file versus time showed that the time scales for hot gas layer development and peak temperatures (at $\approx$ 230 s for the Base Case, Case 4, and Case 5) predicted by CFAST and FDS are similar. Similar observations of the pressure slice file simulations indicated that the magnitude and timing of the pressure peak (at $\approx$ 150 s for the Base Case) were also similar.

Figure 14 is a vector plot of temperature in a plane parallel to the cable trays at the midpoint of the room (and door) and illustrates the flow patterns for Case 4 in which the door is open. Outflow and inflow at the door around the neutral plane is illustrated, as also predicted by the CFAST code. Figure 15 is a similar plot in a plane perpendicular to the cable trays at the midpoint of the room (and fire) and illustrates the flow patterns caused by the mechanical ventilation system in Case 5. This information will be necessary to examine the local effects of target heating.

One important difference in the results from the CFAST and FDS codes for the type of scenarios examined for the Benchmark Exercise is the hot gas temperature. CFAST, a two-zone code, calculates the *average* temperature of the hot gas layer, whereas FDS computes the entire temperature profile in the compartment. The peak average HGL temperature (at $\approx$

275 s) predicted by CFAST for the Base Case is 77 C. The temperature profile predicted by FDS for this case (at ≈ 275 s) ranged from 75 C in the lower region to 130 C in the upper region of the hot gas. This temperature gradient in the hot gas will determine the convective heat flux to the cable tray depending on its vertical position. Table 2 compares the results obtained from the CFAST and FDS codes. Most of the results are similar. The largest difference is noted for the convective heat flux to the target in the Base Case. This is expected because the vertical temperature gradient would be the largest for this case with no ventilation. The differences in the target surface temperatures calculated for all the cases analyzed are within 20 %.

Table 2. Comparison of CFAST and FDS Results

	Max. Rad. Flux (w/m^2) At Target		Max. Conv. Flux (w/m^2) At Target		Max. Target Surface Temp. (K)	
	CFAST	FDS	CFAST	FDS	CFAST	FDS
Base Case	587	712	188	485	322	333
Case 4	582	704	186	277	321	325
Case 5	588	710	148	180	318	319

Part II

The following presents the results of analyses with the CFAST code. Due to time constraints, FDS was not exercised for Part II of the benchmark Exercise.

Predicting the heat release rate of a burning cable tray stack is extremely complex, therefore, the mass loss rate of the burning cable tray stack was defined as input in the exercise. The consecutive ignition and burning of all 3 cable trays (trays A, C2, and C1) were modeled as one fire. The analyses were conducted assuming a peak heat release rate for the whole cable tray stack between 1 – 3 MW. A t-squared fire growth with t_0 = 10 min., and Q_0 = 1 MW was assumed, where:

$$Q = Q_0 (t/t_0)^2$$

The cable fire was assumed to last for 60 minutes at the peak heat release rate, and decay in a t-squared manner with similar constants as for growth.

The heat source (trays A, C2, and C1) was assumed to be at the center of the cable tray length and width and at the same elevation as the bottom of tray C2. The target (representing tray B) was assumed to be at the center of the cable tray length. In order to conduct a simplified and conservative analysis, the target was assumed to be a single power or instrumentation cable, without an electrical conductor inside the cable, and with a diameter of 50 mm or 15 mm respectively at the bottom right corner of cable tray B. The target in CFAST is modeled as a rectangular slab, and was assumed to be horizontally oriented with a thickness of 50 mm or 15 mm. The cable was assumed to be damaged when the centerline of the cable reached 473 K.

Table 3 summarizes the cases for Part II of the benchmark exercise.

Table 3 Summary of Cases for Part II

Fire Scenario	HRR (MW)	D (m)	Door Position	Mech. Vent. Sys.	Target	Target Elev. (m)
Base Case	1	6.1	Closed*	Off	Power Cable	1.1
Case 1		3.1+				
Case 2		4.6				
Case 3	2	3.1				
Case 4	2	4.6				
Case 5	2	6.1				
Case 6	3	3.1				
Case 7	3	4.6				
Case 8	3	6.1				
Case 9			Open>15 min	Off>15 min		
Case 10			Open	On		
Case 11						2.0
Case 12						Same
Case 13					Instrument Cable	

* For simulations with the door closed, a crack (2.4 m x 0.005 m) at the bottom of the doorway was assumed.

+A value in a cell indicates the parameter is varied from the base case.

Base Case

Figures 16 to 20 show the predicted results of the main parameters of interest. Figure 21 shows the pyrolysis rate specified for the case. The predicted trend for the heat release rate, interface height, and oxygen concentration in Figures 16, 17, and 18 is collectively examined. CFAST predicts that the HGL interface lowers to the fire source (at an elevation of 3.4 m) at $\approx$ 580 s. The heat release rate decreases rapidly at this time since the oxygen concentration in the HGL is lower than the specified lower oxygen limit of 12 %. The interface height increases at this point due to inflow into the lower layer from the outside caused by a rapid reduction in the heat release rate and pressure. The heat release rate increases after this point due to the fluctuations in the interface height that temporarily expose the fire source to sufficient oxygen in the lower layer. After $\approx$ 600 s, the interface height starts to decrease slowly as a result of continued pyrolysis and the production of hydrocarbons.

The HGL profile shown in Figure 19 is consistent with the HRR profile shown in Figure 16. The HGL temperature reaches its peak of $\approx$ 440 K at $\approx$ 600 s when the HRR peaks, and decreases rapidly with the heat release rate. The HGL approaches ambient conditions at $\approx$ 1200 s shortly after the HRR goes to zero. The target surface temperature is shown in Figure 20 and peaks at $\approx$ 600 s at a value 323 K, only 23 K above ambient conditions. The target temperature then decreases at a less rapid rate than the HGL temperature due to the thermal inertia of the PVC cable.

The above analysis demonstrates the complexity in modeling an elevated fire source which can be affected by a limited oxygen environment. The assumption for the LOL will have a significant effect on the predicted peak target temperature. Conservative assumptions are warranted due to the uncertainty in the extinction model used in CFAST.

Cases 1 and 2

Analysis of the results for Cases 1 and 2 showed that the distance between the fire and target did not have a strong effect on the target temperature. The absence of the typical strong effect of the distance between the fire and target due to the radiative flux incident on the target was discussed earlier.

Cases 3 to 8

As discussed above, the cable tray fire in the Base Case is limited by the oxygen depletion in the environment. Cable tray fires that could be potentially more intense (as specified by the pyrolysis rate for these cases) are also limited, i.e., the HRRs are similar to that specified for the Base Case. Therefore, these cases are not discussed further here.

Special Case

Since the fire was extinguished after ≈ 720 s and well before 4800 s, the expected duration of the fire, a special case was analyzed. The special case was the same as the Base Case, except the fire was located at an elevation below the top of the door at 1.8 m, and the door was open. Natural ventilation of the hot gases through the door prevented the HGL from reaching and extinguishing the cable tray fire. Therefore, a fire that was sustained at the specified intensity for 3600 s was achieved. Figure 22 shows the HGL and target surface temperature development. The HGL and target surface temperatures peaked at 457 K and 435 K.

CONCLUSIONS

The above analyses of the benchmark exercise for cable tray fires of redundant safety systems demonstrate that both the CFAST and FDS codes provide a treatment of most physical phenomena in the scenarios analyzed. For Part I, the time scale and magnitude of the development of the main parameters of interest in these scenarios are similar. The difference in the predicted target surface temperature between the codes is less than 20 % for the scenarios analyzed. Comparisons of these results with those obtained by others using different fire codes in the benchmark exercise will further verify the physical sub-models in these codes. Comparison of code results with data from a test series specifically focused on target damage would broaden the validation database of these codes.

The analysis of the scenarios in Part II demonstrate the complexity in modeling an elevated fire source that can be affected by a limited oxygen environment. The extinction sub-models utilized in CFAST is an approximation of the interaction of the complex combustion process with a limited oxygen environment. Therefore, the result from the extinction sub-model represents an approximation of the conditions expected for the fire scenarios. The assumption for the LOL will affect the predicted peak target temperature. Therefore, conservative assumptions are warranted due to the uncertainty in the extinction model.

It is concluded that the results obtained from these codes can provide insights beneficial for nuclear power plant fire safety analysis for the type of scenarios analyzed, if the limitations of the code is understood. Further analyses of different fire scenarios are planned. The sub-model for the target, and issues regarding the thermal environment of the target, are the largest source of uncertainty for the types of scenarios in Part I. It will be useful to conduct validation exercises for CFAST and FDS in which the predictive capability of target damage is the main focus of the validation. Also, more refined measurements and data analyses are needed to estimate the quantitative uncertainties of the parameters predicted in the analyses of these fire scenarios. The code results, with quantitative estimates of the uncertainties in the predicted parameters, should provide a sound basis for engineering judgments in nuclear power plant fire safety analysis.

REFERENCES

Dey, M.K., "International Collaborative Project to Evaluate Fire Models for Nuclear Power Plant Applications: Summary of Planning Meeting," NUREG/CP-0170, U.S. Nuclear Regulatory Commission, Washington, DC, April 2000.

Bertrand, R, and Dey, M.K., "International Collaborative Project to Evaluate Fire Models for Nuclear Power Plant Applications: Summary of 2nd Meeting," NUREG/CP-0173, U.S. Nuclear Regulatory Commission, Washington, DC, July 2001.

Floyd, J., "Comparison of CFAST and FDS for Fire Simulation with the HDR T51 and T52 Tests," NISTIR 6866, National Institute of Standards and Technology, Gaithersburg, Maryland, April 2002.

Forney, G.P., and McGrattan, K.B., "User's Guide for Smokeview Version 1.0 – A Tool for Visualizing Fire Dynamics Simulation Data," NISTIR 6513, National Institute of Standards and Technology, Gaithersburg, Maryland, May 2000.

Jones, W.W., Forney, G.P., Peacock, R.D., and Reneke, P.A., "A Technical Reference for CFAST: An Engineering Tool for Estimating Fire and Smoke Transport," NIST TN 1431, National Institute of Standards and Technology, Gaithersburg, Maryland, January 2000.

Lee, B. T., "Heat Release Rate Characteristics of Some Combustible Fuel Sources in Nuclear Power Plants," NBSIR 85-3195, National Bureau of Standards, 1985.

McGrattan, K.B., Baum, H.R., Rehm, R.G., Hamins, A., & Forney, G.P., "Fire Dynamics Simulator - Technical Reference Guide," NISTIR 6467, National Institute of Standards and Technology, Gaithersburg, Maryland, January 2000.

Peacock, R.D., W.W. Jones, and R.W. Bukowski, "Verification of a Model of Fire and Smoke Transport," *Fire Safety Journal*, Vol. 21, pp. 89–129, 1993.
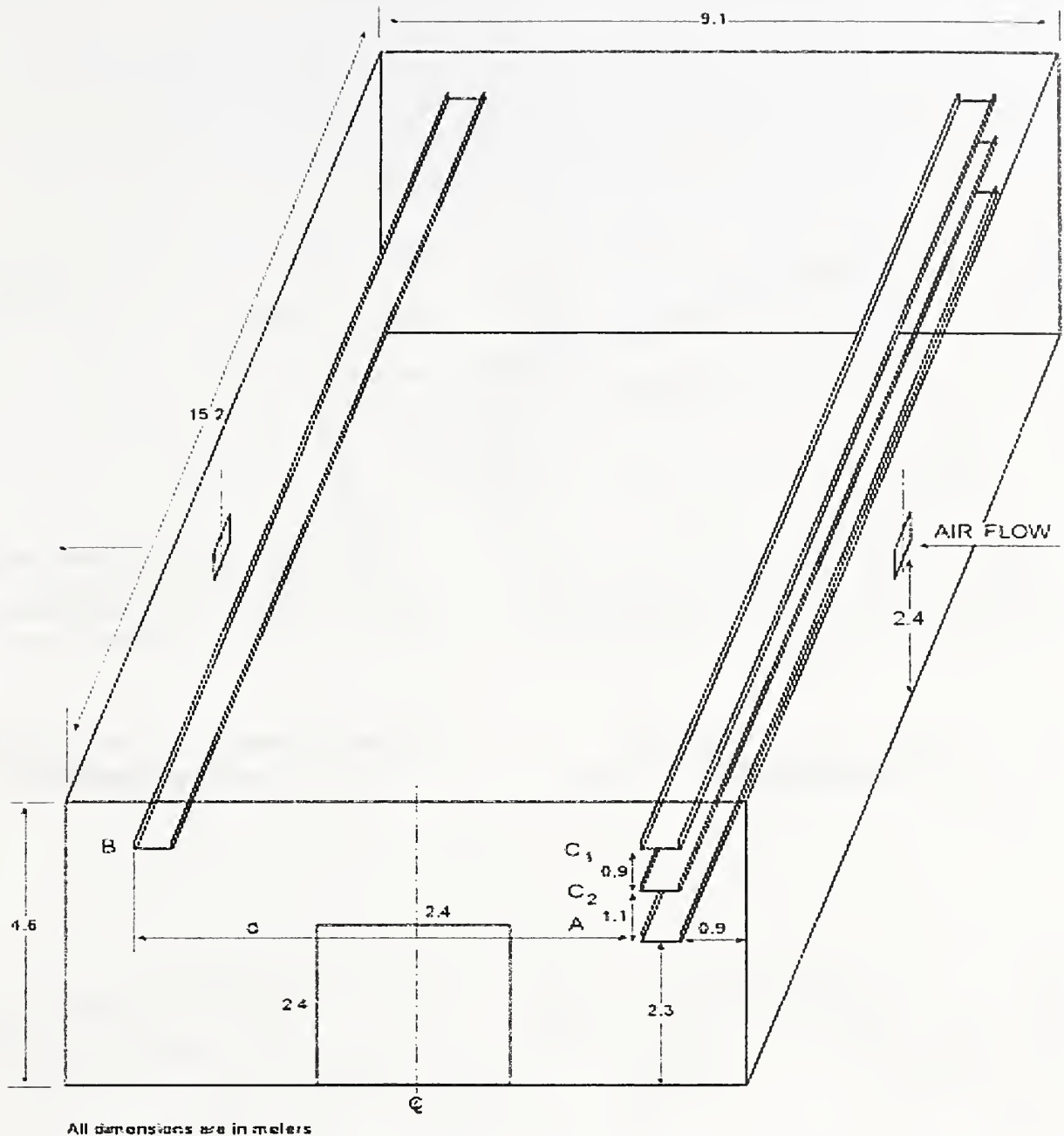
Figure 1 Schematic of PWR Room

All dimensions are in meters
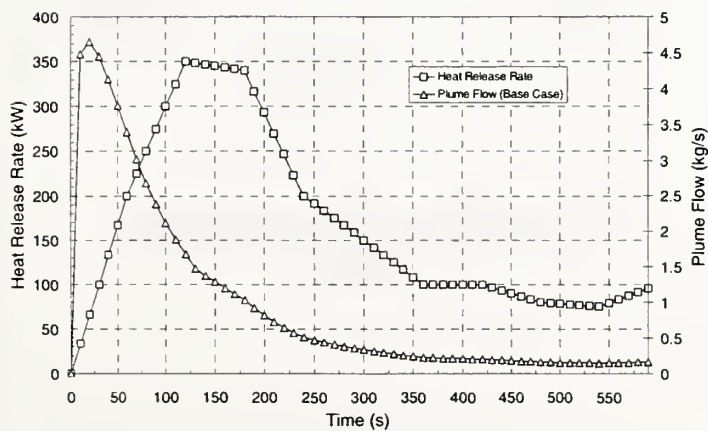
Figure 2 Heat Release Rate and Plume Flow B-12
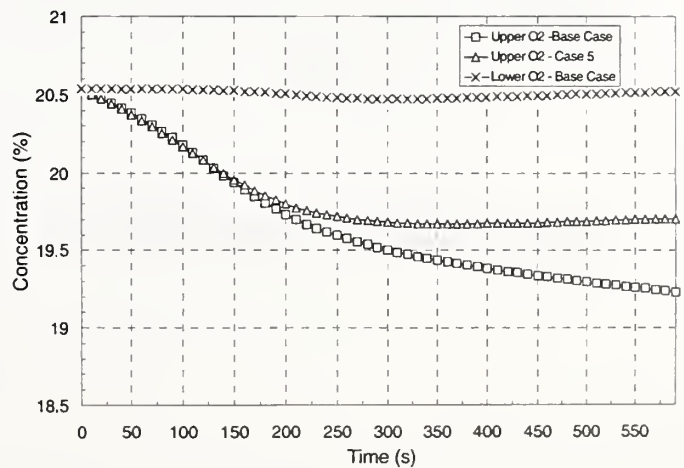
Figure 3 Oxygen Concentrations – Part I
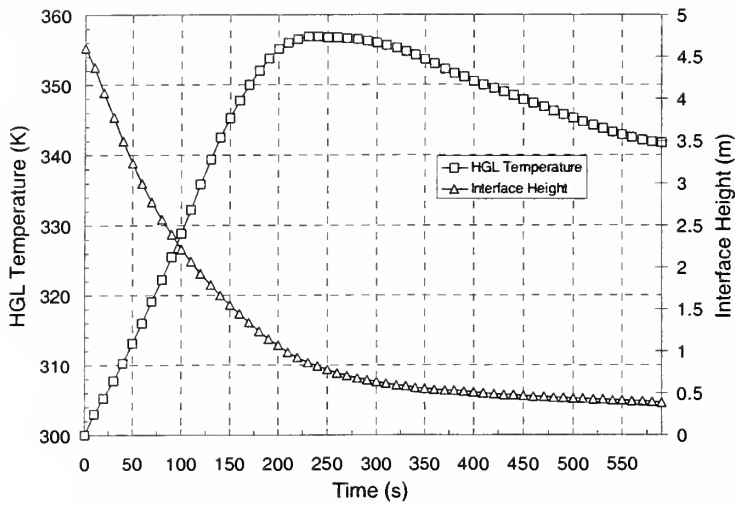
**Figure 4 HGL Development
– Base Case, Part I**
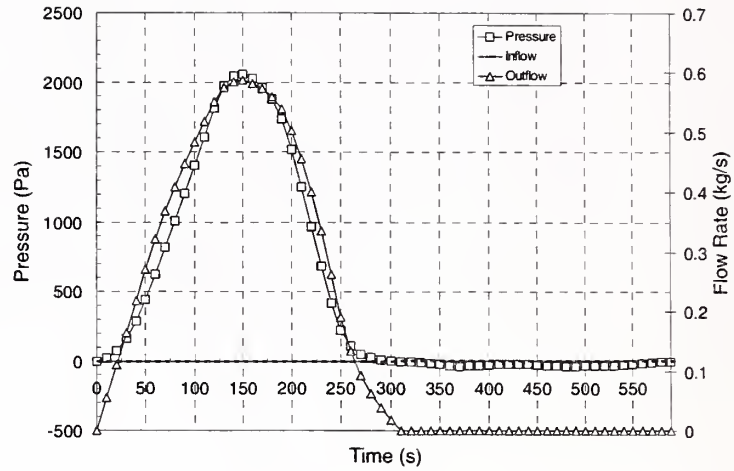
**Figure 5 Pressure and Vent Flow Development
– Base Case, Part I**
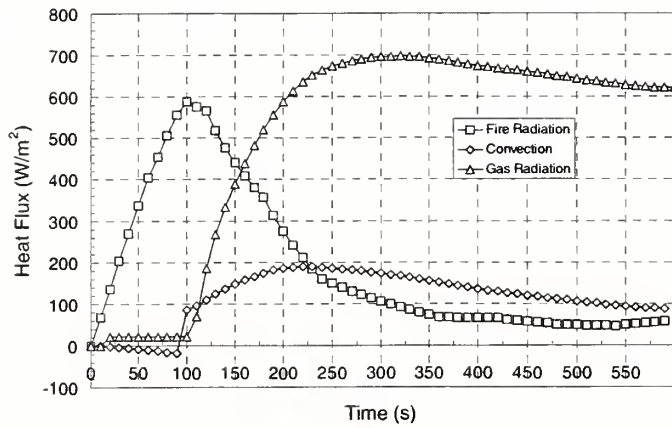
Figure 6 Heat Fluxes – Base Case, Part I
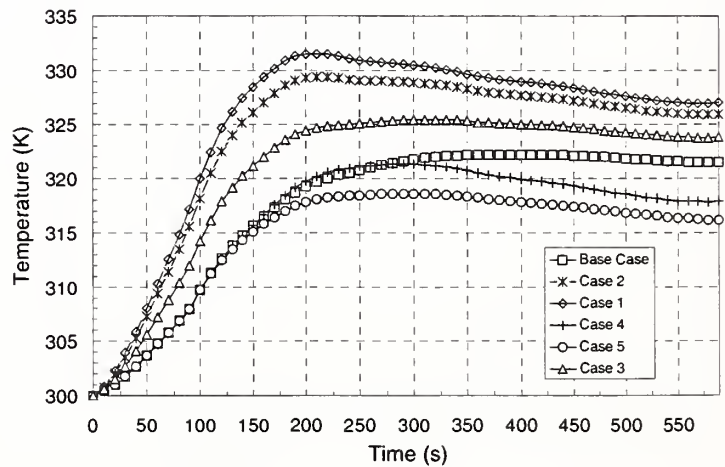
**Figure 7 Target Surface Temperatures,
Part I**
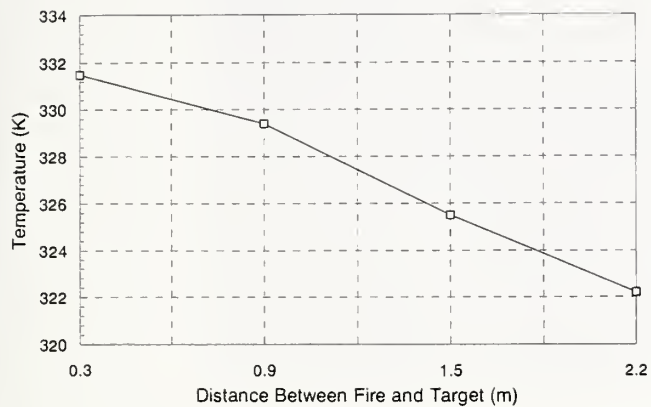
Figure 8 Target Surface Temperatures, Part I
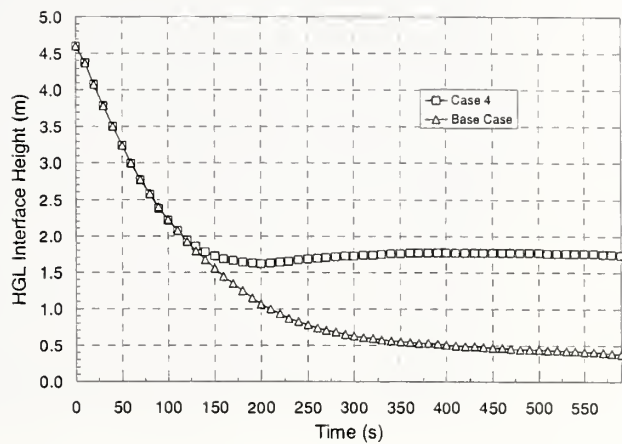
Figure 9 HGL Development – Case 4, Part I
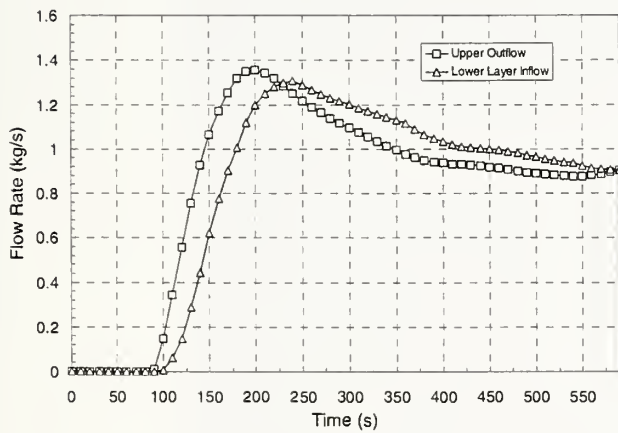
Figure 10 Door Flows – Case 4, Part I
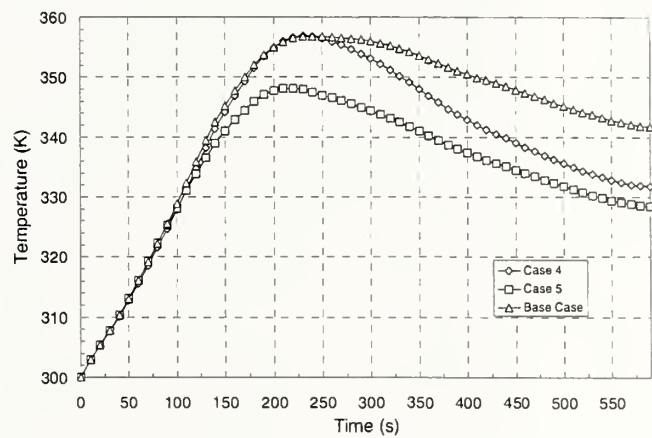
Figure 11 HGL Temperature, Part I
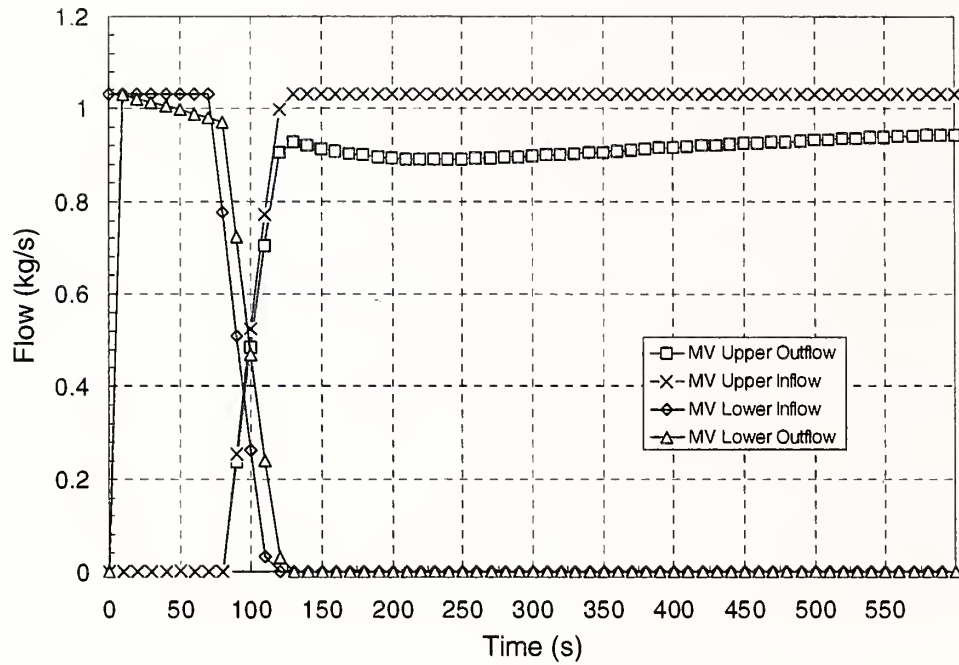
**Figure 12 Mechanical Ventilation Flows – Case 5,
Part I**
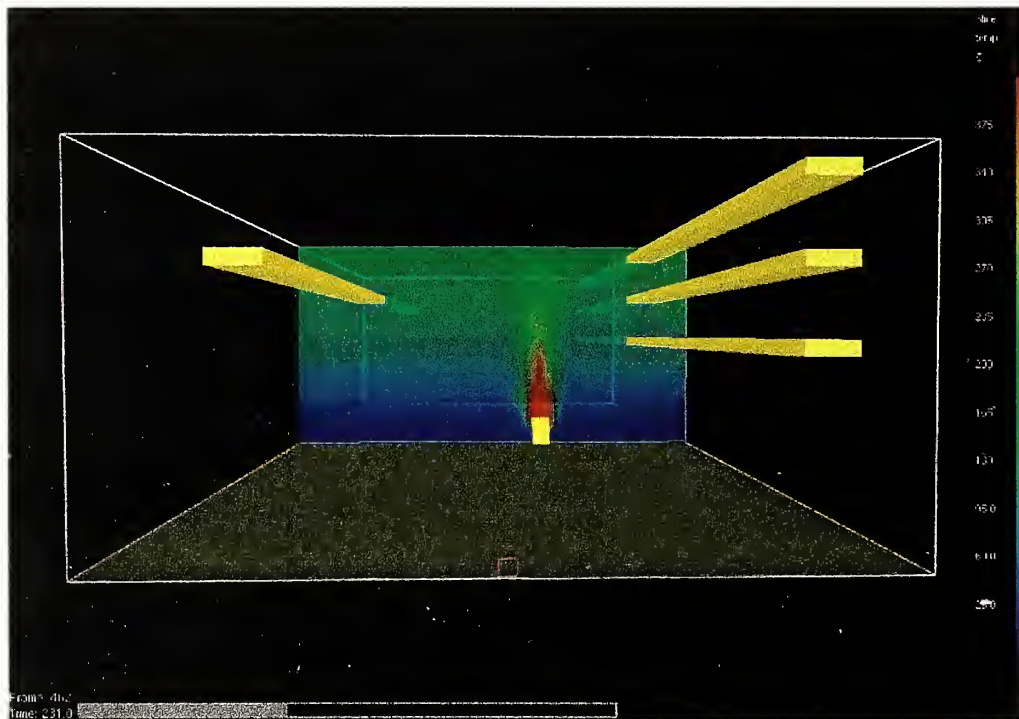
**Figure 13 Temperature Profile –
Base Case, Part I at 230 s**
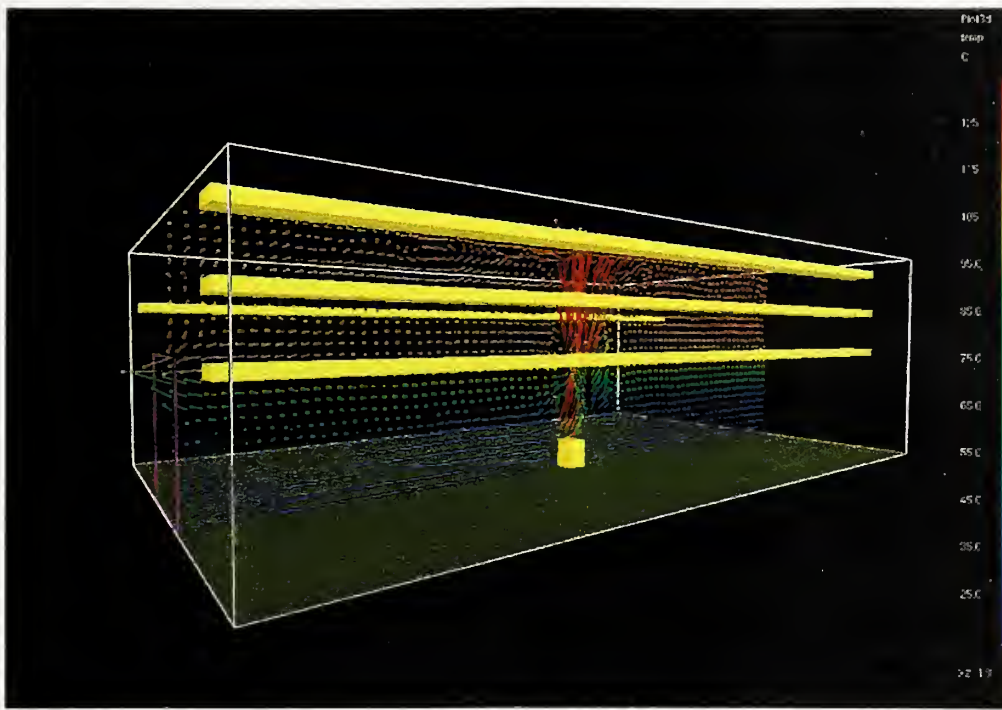
Figure 14 Door Flows – Case 4, Part I
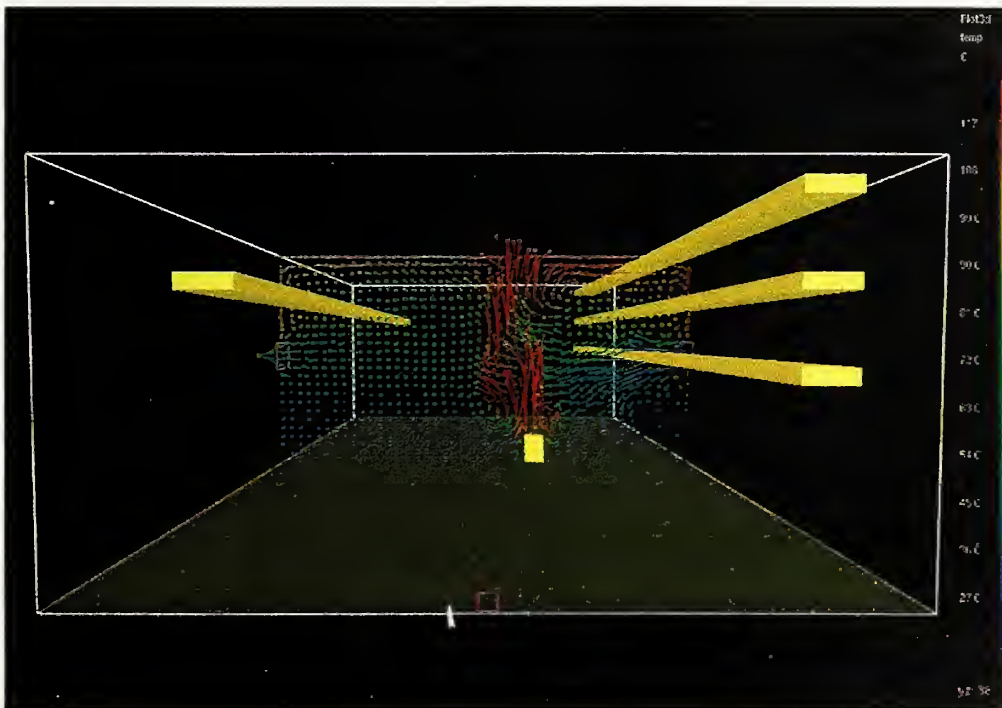
Figure 15 Effects of Mechanical Ventilation –Case 5, Part I
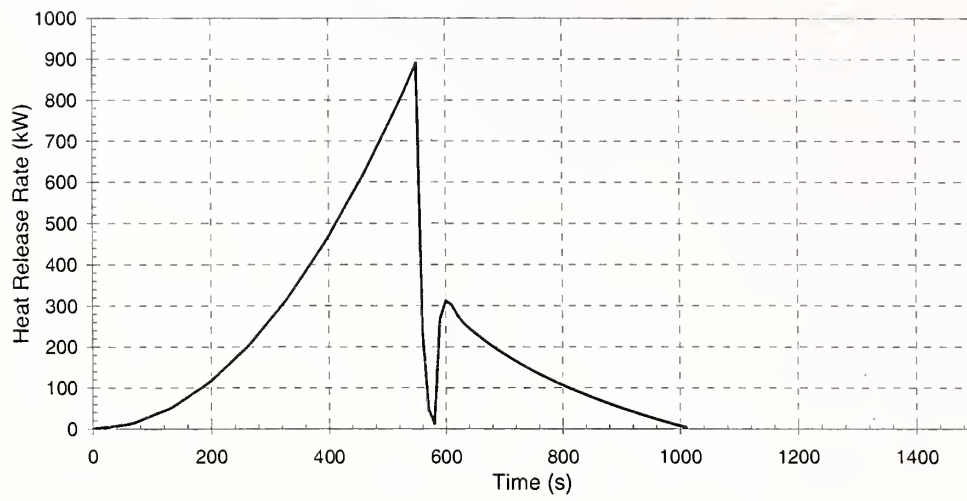
Figure 16 Heat Release Rate, Base Case, Part II
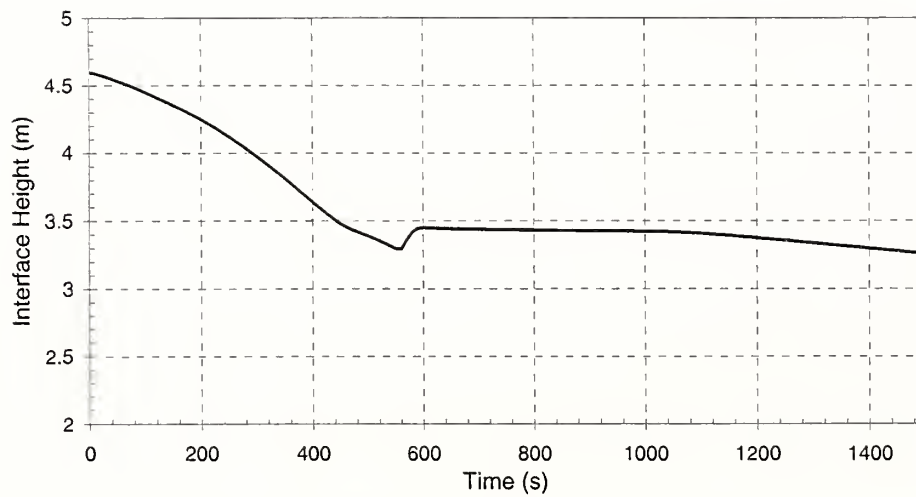
Figure 17 Interface Height, Base Case, Part II
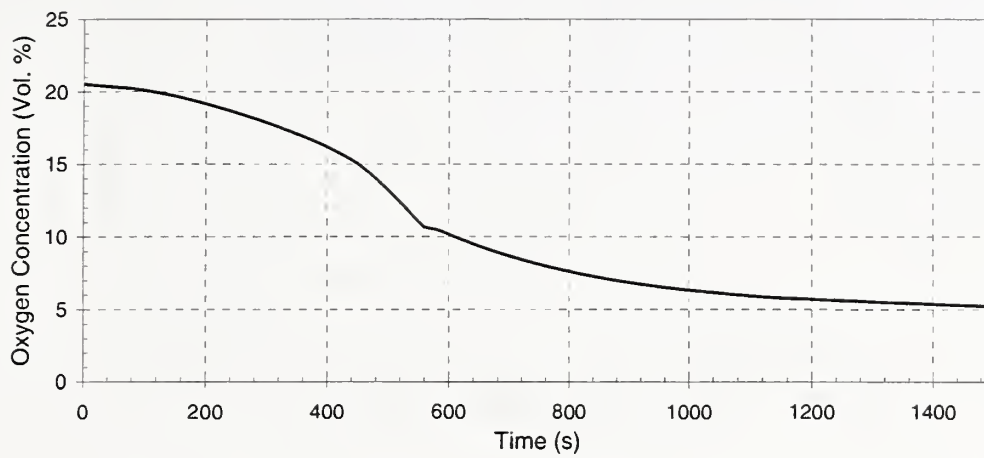
Figure 18 Oxygen Concentration, Base Case, Part II
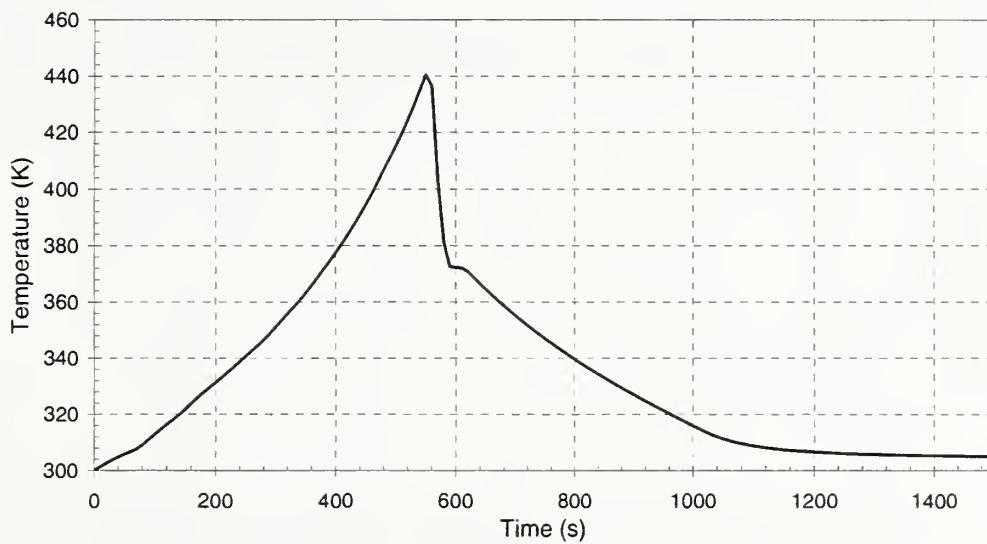
Figure 19 HGL Temperature, Base Case, Part II
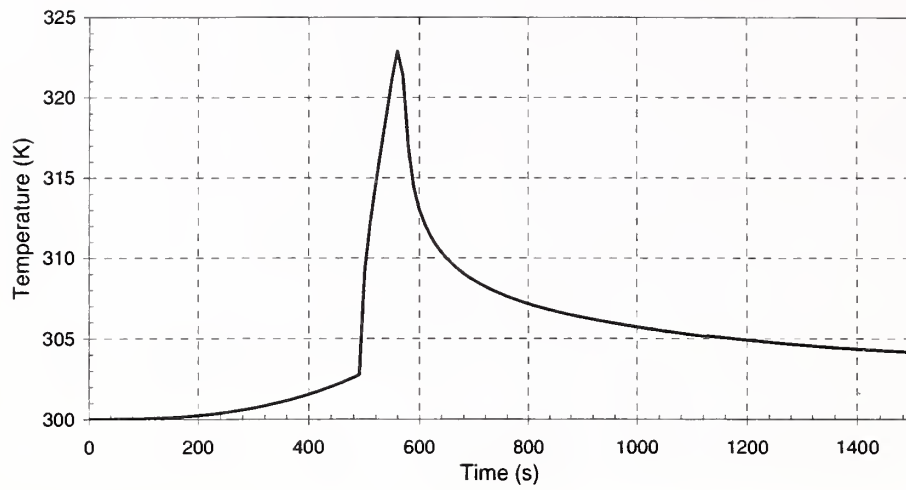
Figure 20 Target Surface Temperature, Base Case, Part II
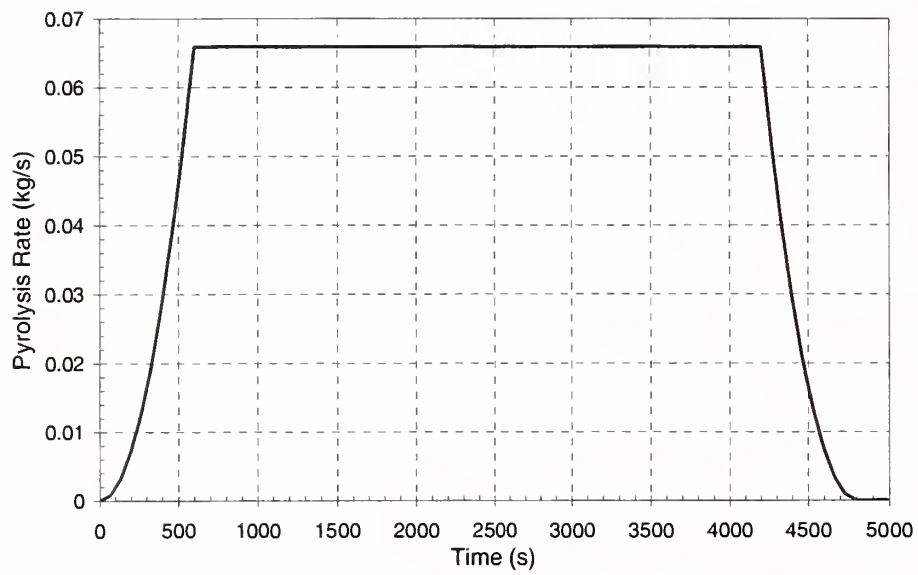
Figure 21 Pyrolysis Rate, Base Case, Part II
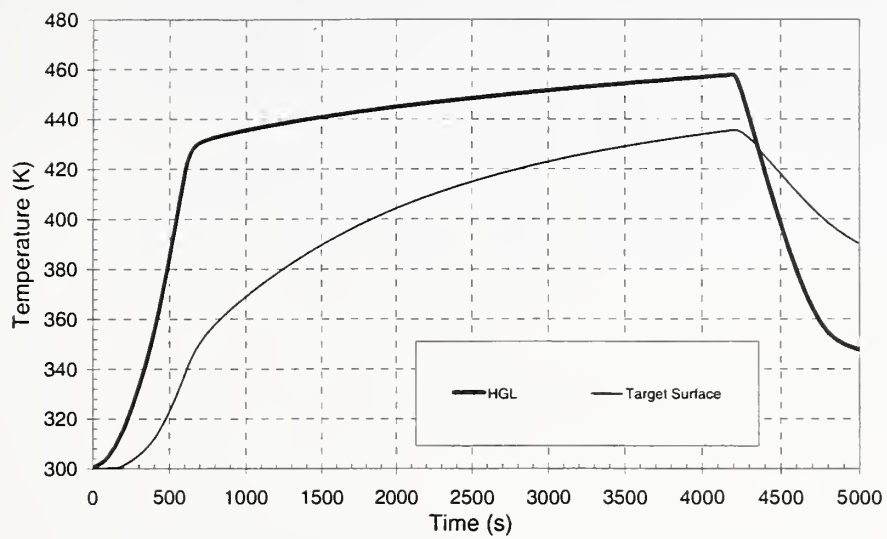
Figure 22 Temperature Development, Special Case, Part II

Appendix C: Benchmark Analysis with MAGIC, Bernard GAUTIER, Helene ERNANDORENA, and Maurice KAERCHER, EdF, France

International Collaborative Project to Evaluate Fire Models for
Nuclear Power Plant Applications
Benchmark Exercise # 1
Cable Tray Fires of Redundant Safety Trains

Simulation of a single room problem using code MAGIC

Bernard GAUTIER - Hélène ERNANDORENA
EDF R&D 6 quai Watier 78401 Chatou FRANCE
Maurice KAERCHER
EDF SEPTEN 12-14 Avenue Dutrievoz 69628 Villeurbanne FRANCE

Introduction

The calculations presented here were done with MAGIC V 3.4.7. The code was used in its standard version. MAGIC uses a two-zone model including most of the classic features:

- Gaseous phase combustion, governed by pyrolysis rate, product properties and oxygen feeding (plume entrainment)
- Two homogeneous smoke and gas layer temperature and concentration stratification, mass and energy balances into gases
- Heat transfers by contact and radiation between flame, gases and smoke, walls and surrounding air, thermal conduction in multi-layer walls, obstacles to radiation
- Mass flow transfer: Fire-plumes, ceiling-jet, openings and vents
- Thermal behavior of targets and cables, secundary source ignition, unburnt gas flames across opening

A data base for combustibles and materials is also available. A description of the code features can be obtained in [1]. The validation file of the code [2] is based on full-scale experiment data.

This file is used to improve the validated range of the code: volumes from 11 to 1300 m^3, fires from 100kW to 2.5 MW, mono-compartment and multi-compartment varied configurations, liquid fires, solid fires, pool fires, linear fires

Two case were proposed to the participants (figure 1 - [4]). Simulation were done with Version 3.4.7 of MAGIC with a LOL (Low Oxygen Limit) of 12%, then of 0%.
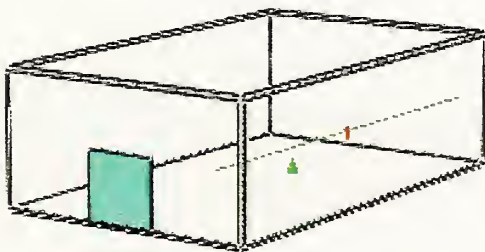
| Part 1: fluxes on a target exposed to a bag fire (5 cases studied) | Part 2: redundant tray B exposed to a trash tray A cable fire (13 cases studied) |
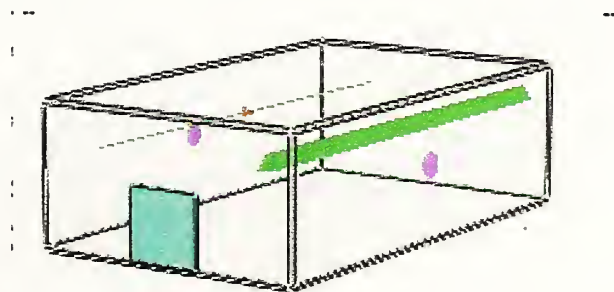
Figure 1 : the proposed cases

Input parameters

The data used for input was directly provided by the benchmark definition of scenario [4].

Some of the requested parameters were not taken into account :

> - the wall emissivity (0.94 wanted) is fixed to 0.9 in MAGIC
> - air humidity (Magic considers dry air)
> - the door structure is not considered in MAGIC (adiabatic material)
> - the specie yields are not considered in MAGIC. Only [O_2], [C_nH_m] and smoke properties are considered in MAGIC, their production is obtained from the source and plume behavior.
> - chemical characteristics of cables were not taken into account: only thermo-physical characteristics are necessary in MAGIC.
> - the tray width and depth were not necessary : we use a single cable to obtain a conservative approach of the cable temperature increase.

Some missing data which had to be set:
> - smoke opacity for the trash-bag fire was fixed to 0.5 m^{-1}
> - the missing stoechiometric ratio for the trash-bag fire was fixed to 1.184 gO2/g

Some other data was not fixed by the text and let to the user choice :

> - wall effect on plume : this option impacts on the plume correlation, using a mirror effect when the plume in confined to a wall.
> - the conduction meshing is not automated in version 3.4.7. The user is supposed to apply the Fourier Law in order to mesh correctly. This last point is one of the most current user effects observed on the code. The meshing is automated and optimized from version 3.4.8.

Least, the time step and the end of simulation time were not specified in [4].

Part I : result analysis
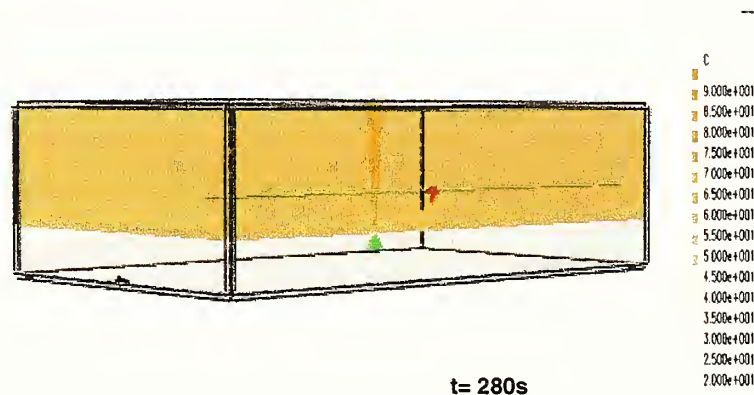
Base case:

t= 280s

figure1: part 1 base Case : smoke filling of the room at t=280s
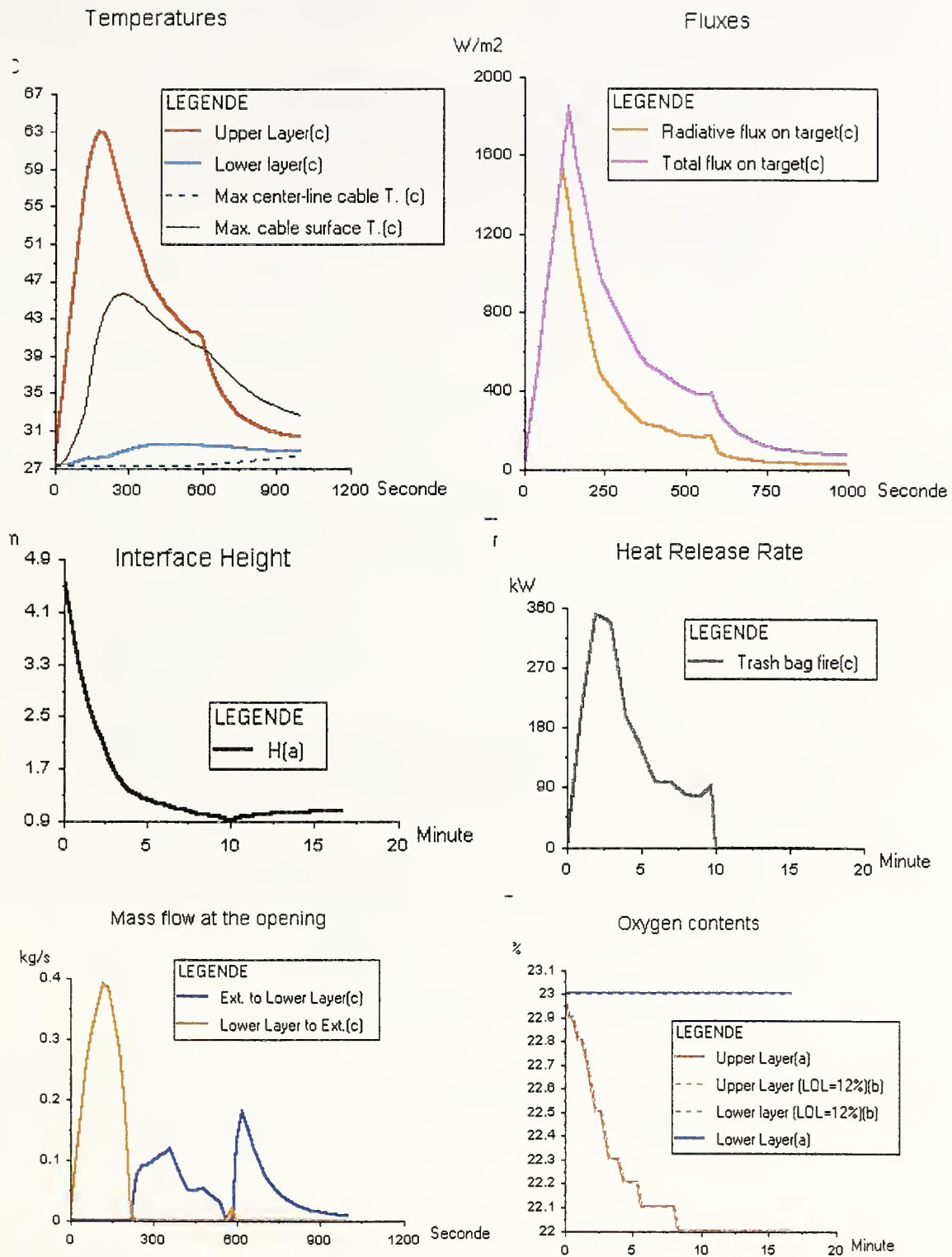
figure 2: part 1 base case

No damage of the target cable is observed in this case . the smoke filling is stabilized (~1m) but temperatures are low. There is not enough consumption of oxygen to show a difference between 0% and 12 % LOL.

Effect of ventilation (case 4 and 5)
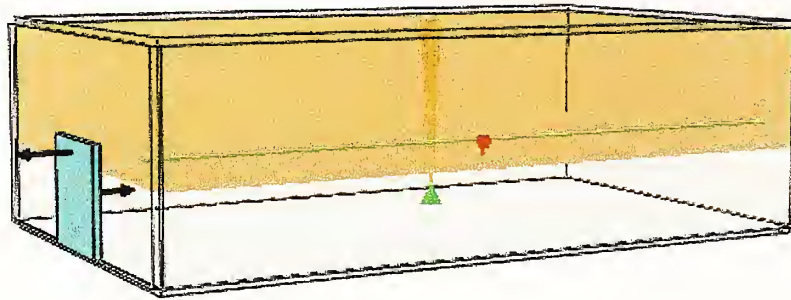
figure 3 : smoke filling in case 4 (door open) at t=800s
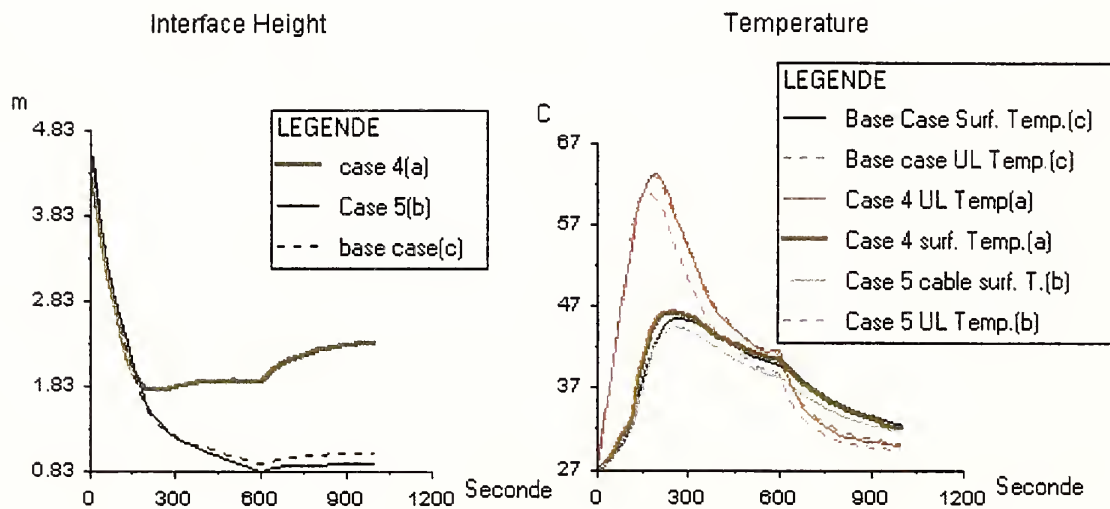
figure 4: ventilation case 4 (door open) and 5 (mechanical vent)

The mass flow balance smoke filling are changed in those two cases: nevertheless, this has no strong effect on the target, which remains in the Upper Layer.

Effect of distance (case 1, 2, 3)
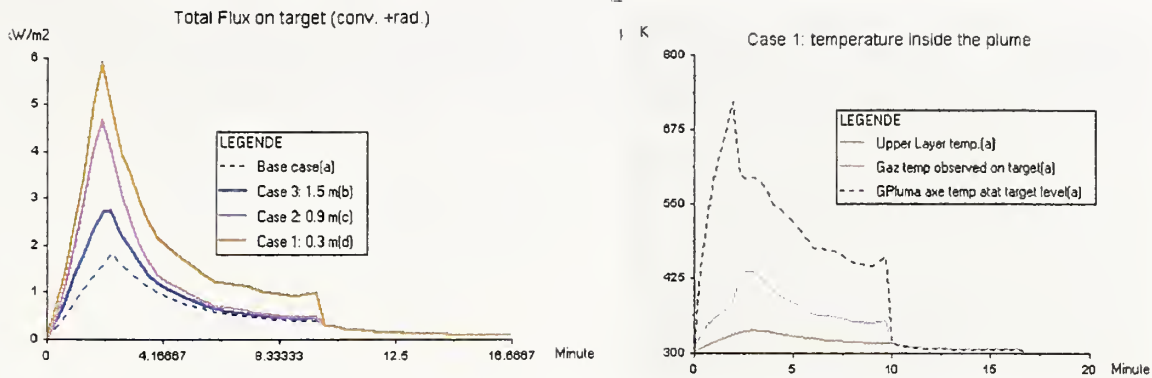
figure 5 : effect of distance

Distance has a strong effect on the radiative flux. The temperature on the target inside the plume is obtained[1] through the Heskestad correlation, taking into account the distance to the axis. As the temperature given by this correlation decreases quickly with the distance to the axis, it can be more conservative to consider the target on the axis (figure 5).

Part II : result analysis
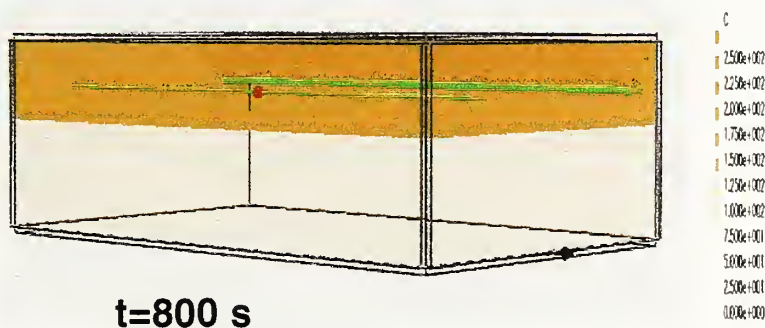
Base case

t=800 s

figure 6: smoke filling in part II base case at t=800s

In the base case of part II, no damage of the redundant cable in tray B was obtained. In fact this is due to the lack of oxygen: even if the source is more important, the heat release becomes quickly weak. Note than in this case, the standard MAGIC thermal model of cable was used.

---

[1] Unlike what was said during the slide presentation...

Figure 7: Part II Base case (LOL=0%)
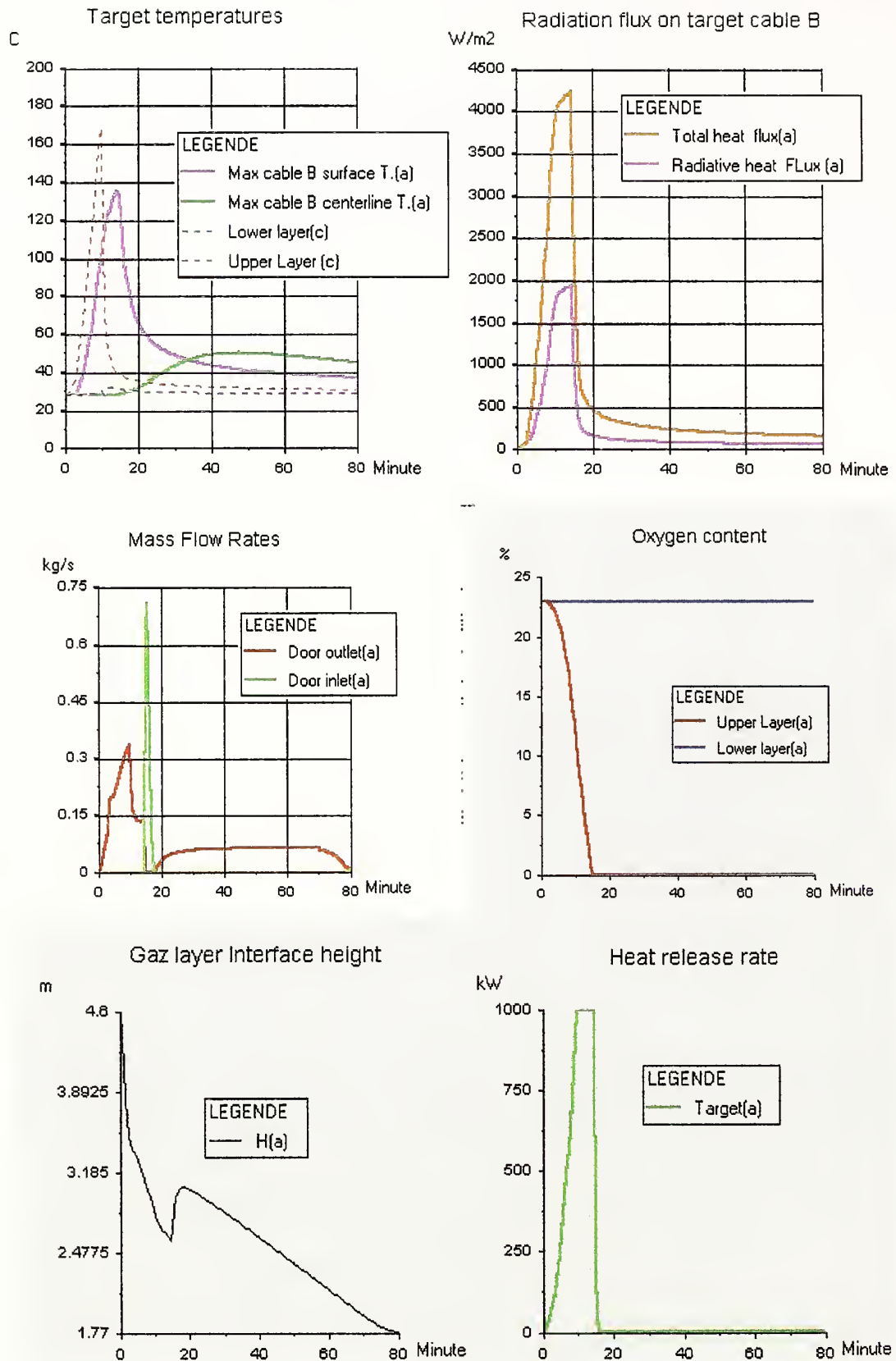
Effect of the LOL

Unlike in part I, the results obtained in part II with a LOL of 12% or a LOL of 0% are quite different. Here, we have an oxygen limited fire, has shown in figure 8. The heat release can be performed further in case LOL=0%, with significant influence on the target temperature peak.
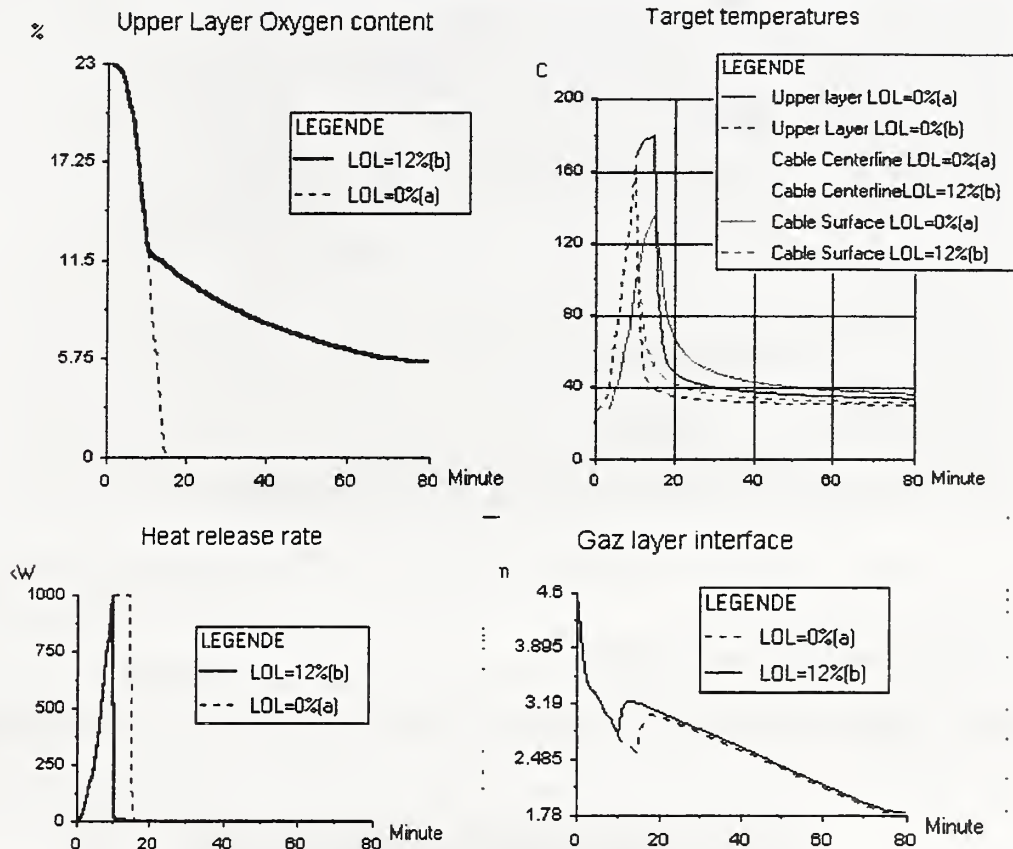
figure 8: effect of the LOL

Mass loss rate increase (case 3-8)

Due to the existing lack of oxygen, the increase of mass loss rate has no significant effect on the fire, which is controlled by the ventilation rate. This is even more true with LOL=12%.
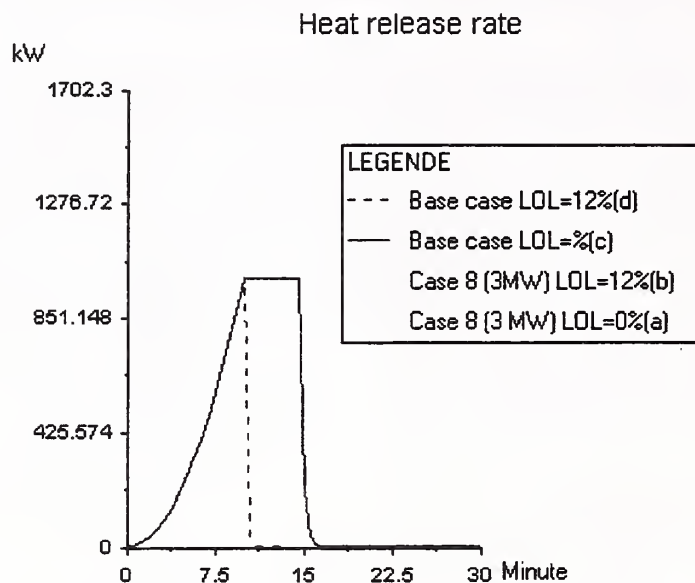
figure 9: mass loss increase

Ventilation effects (cases 9-10)

Due to oxygen rate depletion below the ceiling, the fire conditions are not noticeably changed.
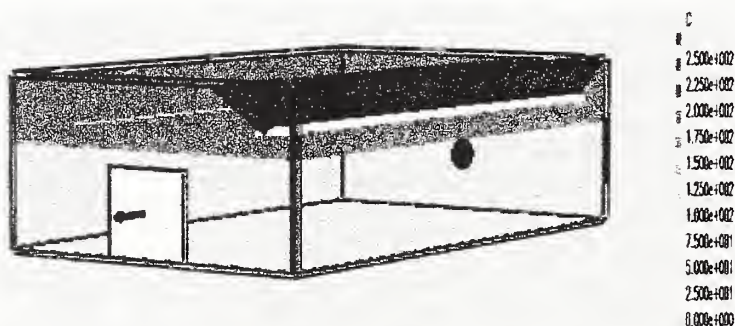
figure 10 : smoke filling at t=600s in case 9

Effect of the cable structure and elevation (cases 13 and 11)

C   Target temperatures

LEGENDE
— Power cable Surf T.(c)
- - - power cable Centerline T.(c)
— Mes cable surf t.(b)
- - - mes cable centerline T.(b)
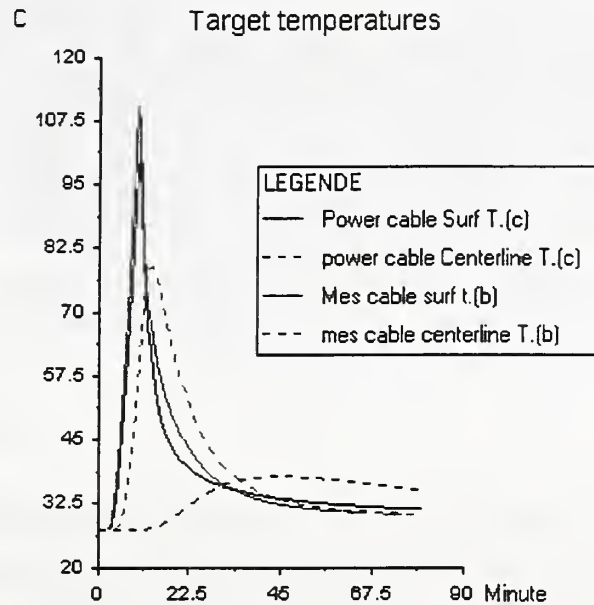
figure 11: effect of cable structure and elevation

The structure of the cable has a strong effect on its resistance: the power cable has more inertia and resists longer (figure 11).

In case 11, the influence of the target elevation is not significant: cable B remains outside of the ceiling-jet region. In fact this point should be discussed further, for the ceiling-jet model is not calculated for R/H > 3, this value being the limit of the validation field (COOPER model [1]). In any case, the target model is not connected to the ceiling-jet model in Version 3.4.7 of MAGIC. In the present case, the cable should be considered lost in a real life risk study.

Result summary

Part I :

Part I	O2 Conc. @ 600s (%)	Max Plume Flow (kg/s)	Max Pressure (Pa)	Max outflow (kg/s)	Layer Ht @ 240s (m)	Max UL Temp. (K)	Max flux on Target (W/m2)	Max. Target CL Temp. (K)
Base Case	R : ZC 22%	NA	R : 961 Pa	R-from LL: 0,389kg/s	R : 1,37m	R : 336 K	Rad :1550,6 W/m2 Total : 1839 W/m2	R : 301,3 K
Case 1							Rad : 11648,8 W/m2 Total : 12855 W/m2	R : 302,9 K
Case 2							Rad : 4654 W/m2 Total : 4665 W/m2	R : 302,3 K
Case 3							R : 2688 W/m2 Total : 2732 W/m2	R : 301,6K
Case 4			R- for neg.peak : -0,1Pa	R - form UL 0.855kg/s	R : 1,77m	R : 336 K	R : 1545 W/m2 Total : 1845 W/m2	R : 301,4 K
Case 5	R :ZC 22,5%		R : 714 Pa		R : 1,43m	R : 333,6 K	R : 1571 W/m2 Total : 2042 W/m2	R : 301,3 K

Part II:

Part II	O2 Conc. (%)		Max Pressure (Pa)		Time @ (s)	Max UL Temp. (K)	Max flux on Target (W/m2)	Max. Target CL Temp. (K)
Base Case	R-@500s : 17%		R-for pos.peak : 721Pa		Layer Ht=3,4m : 206s	R1 : 452,5 K R2 : 440 K	R1 :rad 1920W/m2 Total : 4207 W/m2 R2 : rad 1677W/m2 Total : 3785 W/m2	R1 : 322,6 K R2 : 310,7 K
Case 1							R1 : 1920W/m2 Total : 4208 W/m2 R2 : 1677W/m2 Total : 3785 W/m2	R1 : 322,5 K R2 : 310,7 K
Case 2							R1 : 1920W/m2 Total : 4208 W/m2 R2 : 1678W/m2 Total : 3784 W/m2	R1 : 322,5 K R2 : 310,7 K
Case 5							R1 : 3165 W/m2 Total : 6205 W/m2 R2 : 1678W/m2 Total : 3785 W/m2	R1 : 322,2K R2 : 310,7K
Case 10	R -@ 3800s R1:0% R2:5,77%				Layer Ht=2,4m no value	R1 : 453,5 K R2 : 440,8 K	R1 : 1938,2W/m2 Total : 4238 W/m2 R2 : 1681W/m2 Total : 3792 W/m2	R1 : 322,2 K R2 : 310,7 K
Case 11							R1 : 1920W/m2 Total : 4207 W/m2 R2 : 1677W/m2 Total : 3784 W/m2	R1 : 322,6 K R2 : 310,8 K
Case 12							R1 : 1000,8W/m2 Total : 1119.8 W/m2 R2 : 832,5W/m2 Total : 877 W/m2	R1 : 306 K R2 : 302,6 K
Case 13								R1 : 398,1 K R2 : 351,7 K

Plume flow is not a standard output of MAGIC. All results are in acceptable domain.

Discussions

About uncertainties...

Like the physical models choices are fixed in MAGIC, the calculation uncertainty can be related to the limits and the accuracy observed in the field of validation of the model, and to the user input uncertainties. It is difficult to define a exhaustive rule for the validation field. In the validation file, the experimental configurations present compartments from 10 to 1300m3, fire source from 100 kW to 2,5 MW. The results obtained are globally satisfactory, with different accuracy in each test.

The most significant input parameter are the source power, the thermophysical parameters (k, h, C, ρ) and source characteristics (stoechiometry , radiative part, etc..).

...and user effect

The "User Effect" is limited as much as possible through the graphical (3D) control and the tests performed by the interface (definition range of values, coherency of the building). The stronger user effect has been observed on conduction meshing : significant errors can be committed on gas temperature in the dynamic steps when the meshing is not fine enough. That the reason why this input will be automated in the next version of the code.

The second user parameter identified was the wall effect on the plume . In this case no significant effect (less than 1 °C) can be observed on temperatures.

The interpretation of result data is a strong source of user effects: for instance in MAGIC the cable behavior is not accurately evaluated inside the plume or ceiling-jet. In EDF practice, we consider than a cable is lost when in a plume of Ceiling-Jet. This is an example of the good knowledge of the code feature needed.
Another example is the cable dysfunction criterion. It can vary from one author to another and is very important in safety assessment. This is an example of the good methodology needed.

Models used in MAGIC and significant for the tests

A short summary of the models used in Magic would be:
- the plume and flame experimental entrainment correlation from MAC CAFFREY[a]
- an integrated radial conduction model for cables
- a 1D conduction model into walls, ceiling and floor
- a semi-transparent radiation model for gas, and a radiosity system for walls,
- HESKESTADT correlation for flame height[b] and thermal targets.
- a medium specific area model for opacity of cable smokes[c] (BARAKAT-VANTELON)
- a Ceiling-Jet[d] (L.Y. COOPER)
- "Bernoulli" flow at vertical vent (CURTAT-BODART)

The physical models resulting from the integration of physic laws have no other domain limits than those of the material properties. For (a) (b) (c) and (d) , specific domain limits have been defined in the original experimental works.

Validation of MAGIC

The type of configuration (power, room-size) proposed in the benchmark is well represented in the Validation File of MAGIC [2]. This validation concerns mainly field temperatures and fluxes. The cable center temperature model has been validated at laboratory scale in a "Tewarson" calorimeter device through an EDF experimental program [3].

The validation process of MAGIC gives an idea of the calculation uncertainties. In general, conservative errors are less regarded than "unconservative" ones, for design purpose. For instance, calculated temperature are rarely less than 10°C lower than measurement, but 50°C higher than measurement can be observed.
The flux calculation is less accurate due to many experimental effects. A 50% lower than measurement can be observed. Mass flows are often not available (significant measurement uncertainties).

Effect of the source height

Source height is an important parameter that could have been considered in the benchmark, especially when a door is open (cable trays can be found in lower location). A supplementary calculation has been done in that way (figure 12).
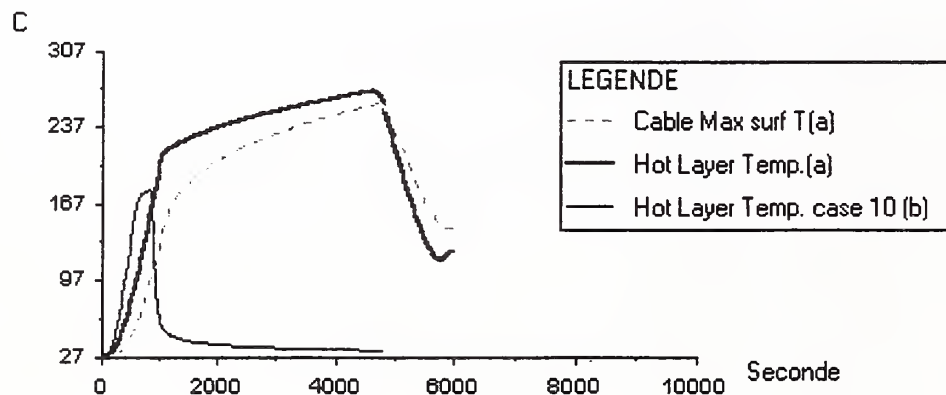
Part II: Effetc of a lower location of cable fire : 1 m above floor in case 10

figure 12: effect of a lower fire source location

The comparison with case 10 shows that the consequences of the fire are quite different: due to the oxygen feeding by the open door, the fire can go on. In this case, cable B would have been probably lost.

Conclusion

The conclusion with follow the suggested guide line [5].

Capability and strength of code MAGIC

From the physical modeling point of view, capability and strength of code MAGIC could be summed up in:
- the global energetic balance done and the good prediction of the level of temperature within the room
- the targets and cable flux and thermal behavior models
- the mass flow prediction by taking into account pressure,
- the calculation of oxygen balance and consumption
- the good level of the radiation model and the wall conduction model
- the good level of information and control provided by the interface (see further).

Weaknesses and limitation:

The behavior of cables is not modeled into plume and flame (cables are considered lost in EDF approach in those cases). This point could be enhanced. The thermal target give a "correlated" response in those cases (Heskestadt model).

The zone model can't represent some 3D aspects like aeraulic "by-pass". A conservative approach is used considering that all the oxygen given to the plume can be used. Some real scale fire tests have shown that confined fires could be maintained with a measured O_2 concentration lower than 10%. In those cases, aeraulic by pass and distant flame were observed. For this reason, EDF does not use the Low Oxygen Limit in safety studies.

The most important criticism one can make about the MAGIC fire model is that mass loss and thermal behavior of source are not coupled. It is the same for most of the existing codes, apart some very specific cases. The problem is that this coupling is really a difficult problem, especially for solid fire. This can be balanced by using characteristic mass loss profile for one given combustible in one given situation. This type of profile is at the center of the methodological discussions for safety assessment.

Need of a more advanced model?

Maybe the most significant progress has to be made on the mass loss rate of the cable. On this aspect a lot of studies have been done [3]. It seems that a complete fire spread model coupling heat release and mass loss could only be proposed in CFD codes, due to the level of local information needed. For common purpose, one will have to use standard profiles and correlation. An important discussion on this data should be held in the nuclear assessment field to agree of the more adapted ones.

Another important point is the target behavior which could be enhanced in the "dynamic" zones (plume, ceiling-jet). Adapted real scale tests would be of interest, especially for thermal behavior of cables.

Could a simpler model be sufficient in those cases?

In some cases a simpler model can be adapted, but cable thermal response, oxygen consumption balance and ventilation effects had to be taken into account in the cases studied here. That means a minimum of balanced model is necessary: zone models are the minimum level of modeling needed here.

Additional type of model needed:

Cable behavior inside the plume or Ceiling-jet would be of interest. Of course, more information would necessary here.

User interface of MAGIC

The user interface is probably one of the most outstanding strengths of code MAGIC. Many automated controls are performed on value definition range, building coherency, and the graphical 3D view provide a powerful visual control to the user. The use of such an integrated interface limits notably the risk of input mistake.

Nevertheless, the user must be aware of some aspects of zone modeling not to forget:
- the conservative approach of phenomena (ex: combustion efficiency)
- the rough representation of air stratification temperature
- some 3D aeraulic and flame effects are not considered (ex: horizontal distance ventilation/source) but over-predicted (always conservative).

Outlook

The most relevant parameter in the deterministic fire modeling is certainly combustible mass rate. There is a great need here for conventional curve profiles or formulas, and experimental process for cable behavior identification. We should define a consensus mass loss profile data file
On that point, from EDF experience we should at least consider:
- not confined cable tray with low ignition (slow spread)
- not confined cable tray with strong ignition (up to ~x00kW: fast spread)
- confined cable trays (in smoke) : "flashover" (global instantaneous ignition)

Cable or component dysfunction is another important parameter
- the cable temperature criterion has to be enhance. Internal temperature of cable seems to be a reliable variable to correlate [7].
- on that point, experimental test benches could be normalized

Multi-room configuration is also an essential issue. For instance, in EDF NPP configuration, component in the first room are always protected if concerned by safety issues : what is important and has to be modeled is what happen to component in secondary rooms. For this reason, it would be of interest to propose more multi-room configurations in the future benchmarks...

To conclude, we should remind the "good way" to process is to go from the more conservative to the more complex: in safety assessment, one should use simple (conservative) formulas or models when sufficient and go into details with zone or CFD codes when necessary. If the methodology is

organized in that way, it will be easier to promote the use of numerical model in the fire risk assessment.

REFERENCES

[1] B. GAUTIER, O. PAGES "MAGIC software version 3.4.1: mathematical model" EDF HT-31/99/007/A.

[2] B. GAUTIER, Ch. LE-MAITRE "Validation file of Software Magic Version 3.4.1". HT-31/99/002/A Feb.99.

[3] E. THIBERT *"Modélisation de la combustion des gaines de câbles électriques"* Thesis from University of Poitier-FRANCE Nov. 1999.

[4] M. Dey "International Collaborative Project to Evaluate Fire Models for Nuclear Power Plant Applications, Benchmark Exercise # 1: Cable Tray Fires of Redundant Safety Trains: definition of scenarios" NRC September 11th 2000.

[5] M. Dey "suggested guideline/questions for presentation of Results of Benchmark Exercise".NRC 2000

Appendix D: Benchmark Analysis with CFX, Matthias HEITSCH, GRS, Germany

CFX Simulations for the Benchmark Exercise #1

- Cable Tray Fires of Redundant Safety Trains -

International Collaborative Project to Evaluate Fire Models

for Nuclear Power Plant Applications

Dr. Matthias Heitsch

Technical Note HET 1/2001

Content

List of Figures and Tables

Abbreviations

CFD	Computational Fluid Dynamics
NPP	Nuclear Power Plant

1 Introduction

A benchmark exercise has been set up to evaluate the capabilities of codes to model relevant phenomena with cable tray fires in a NPP. According to the specification of this Benchmark Exercise part 1 [DEF 00] out of the large number of numerical cases specified a representative selection has been simulated by the help of the general-purpose CFD code CFX 4.3. The motivation of the application of CFX has been to find out how it performs in comparison with other probably more specialised codes. It is also of interest under which conditions the specific characteristics of CFX are beneficial and can justify the higher computing costs. So far, due to restrictions in the computing resources available not the complete suite of specified test cases has been simulated. However, the presented selection is believed to provide a good idea of the capabilities when applying CFX. Work will be continued based on the experience got from the meeting in Palo Alto in January 2001.

2 The CFD Code CFX

The code CFX-4.3 [AEA 99] provides numerical approximations of the Navier-Stokes equations on a finite volume basis. The program version applied here uses a block-structured grid with body fitted coordinates. Block-structured means that all blocks of the computational domain have to be designed with a hexahedral shape. With complex geometries this implies occasionally finer grids than really necessary.

The code offers a number of physical models to simulate a wide range of flow problems. Among these are:

- Arbitrary multi-component mixtures,

- Turbulence models for low and high Reynolds numbers,

- Multi-phase models including a versatile multi-fluid model and a homogeneous two-phase model,

- Particle transport model,

- Complex thermal radiation model based on a Monte-Carlo formulation,

- Chemical reaction capability,

- Convective heat transfer and heat conduction,

- User Interface to modify existing or add own models.

The given benchmark makes use of the turbulence (k-ε) and multi-component models combined with the thermal radiation package. Chemical reactions, although possible, are not included in the simulations so far.

3 Analyses on Part 1

In part 1 of the benchmark exercise a trash bag fire in the vicinity of a cable tray inside an emergency switchgear room (Fig. 1) is to be simulated. The objective "is to determine the maximum horizontal distance between a specified transient fire from the trash bag and tray A (Fig. 1) that results in ignition of tray A" [DEF 00]. For simplicity the cable tray represented by a single power cable of 50 mm. The room has ventilation and a fire proof door. A base case and five related simulations with variations of the distance between cable tray and fire, the door open or closed and the ventilation system on or off are to be investigated. The time to be covered is 600 s. The total heat release from the trash bag is specified in Fig. 3 and the radiative fraction is fixed to be 30%. This specification implies not to simulate the chemical reactions in the trash bag explicitly rather than using the heat release curve and study the convective and radiative flows induced by the fire in the trash bag.

A computer model was developed which is composed of 28400 fluid cells (Fig. 2). The grid resolution could be refined easily but is left on this rather crude level to comply with the number of test cases and the problem time of this exercise. The model contains the trash bag and the target cable (representing tray A) inside the room. In order to save computing time the outer walls are not modeled. This results in an overestimation of the heat losses from the fire room atmosphere because the heat up of inner wall sections is neglected and consequently the temperature difference gas to wall is too large. The given convective heat transfer coefficient of 15 W/m²K is applied. For some of the cases the openings of the ventilation system and the fire door can be opened. In all other cases a crack of specified size around the door is available.

There are several options to implement the heat release from the trash bag. Currently the trash bag is modeled as a solid body with the convective fire heat release from the nearest cells around it and with radiation from its surface. The trash bag could also be a hollow body with the convective heat released from all the internal cells. Because radiation can only be emitted from a surface, in this case the top surface could be used for the radiation source. The benchmark specification does not further localize the heat sources therefore the first option has been implemented. During the simulations it turned out that the shape of the trash bag fire changed from time to time. However if numerical reasons or inherent instabilities cause this behavior has not been further investigated.

Conduction in the target cable is included. The cable itself is represented as a cylinder of appropriate size and can be moved within the grid according to the different test cases.

The atmosphere within the fire room is assumed to be air. Individual gas species are not modeled because the fire chemistry is not included.

3.1 Base Case

In the base case the target cable has a horizontal distance of 2.2 m from the trash bag. The door is closed and the ventilation system is off. It is the first case simulated and is discussed in more detail. The moment of the highest heat release from the trash bag is depicted in Fig. 4. The plume around the trash bag and the induced upwards directed flow is influenced by the option of the heat release chosen and may be different if modeled by the other option (see chapter 3). The target cable is affected by a flow directed downwards as indicated in Fig. 4. At the moment of strongest heat release the warmer gas is concentrated below the ceiling of the room as shown in Fig. 5. Some flow is directed towards the crack in the fire door. After 600 s the temperature distribution in the room is shown in Fig. 6. At this time gas temperatures do not show a remarkable stratification. Close to the walls temperatures are lower due to the heat losses resulting from the high heat transfer coefficient given. This behavior is illustrated in Fig. 7. From bottom to top the temperature does not vary much. Underneath the ceiling it increases considerably (buoyant flow) before wall cooling is dominating. With a higher gas temperature the heat flux to the wall increases and provokes a higher temperature gradient compared with the bottom region. From the temperature profile in Fig. 7 a subdivision

of the room into a hot layer above a cold layer appears to be inadequate. Of interest is the distribution of heat flows to walls and target cable. All flows reach their maximum at the time with the highest heat release. The total heat flux to the cable in comparison with the flow to the walls (Fig. 8) is less than the surface ratio. This may be due to the lower wall temperatures. In Fig. 8 decreases the radiative fraction to the cable to a very small value when the fire heat release decreases after its maximum. The hotter cable then loses energy to the cooler walls. The heat captured by the cable does not lead to a measurable increase of the centerline temperature. The surface temperature develops as shown in Fig. 9 and has almost no further increase after the maximum heat flow from the trash bag is passed.

3.2   Case 1

Case 1 differs from the base case only by another location of the trash bag relative to the target cable. The trash bag is directly below the target cable. The moment of maximum heat release is depicted in Fig. 10. Compared with the base case the cable is now completely inside the hot gas stream from the fire. This results in a higher heat-up of the cable surface as shown in Fig. 12. The maximum is now about 550 K. In the base case it was only 360 K. After the maximum heat is passed the surface temperature goes down as well. The power to the cable over time shown in Fig. 11 has a maximum of about 700 W. This is considerably more than in the base case with 500 W. Another difference is the radiative behavior. With this case in the late phase the cable radiates energy to the surroundings and is therefore cooled.

The centerline temperature remains almost unchanged during the simulation time. Other cases with larger distances of the trash bag than the actual will not be able to create higher cable temperatures with a chance of ignition (643 K).

3.3   Case 5

Case 5 is interesting because of the flow patterns influenced by the ventilation system now on. The position of the trash bag is identical to the base case. Compared with the base case the cable is now in a more upwards flow. This is depicted in Fig. 13. Equally, the heat-up of the cable is very similar and remains low (Fig. 14). The ventilation system with a continuous inflow of cold air does not alter things considerably.

Chemical reactions including oxygen consumption have not been modelled. However, an oxygen depletion which might be avoided by the fresh air entering through the ventilation opening is not realistic because of the short simulation time.

A comparison of all three simulated cases in terms of the cable surface temperature is depicted in Fig. 15. With the given ignition criterion only the location of the fire directly below the target cable would have a chance to ignite the cable over a longer time or with a higher heat release.

4   Analyses on Part 2

This part of the benchmark is to "determine the damage time of the target cable tray B for several heat release rates of the tray stack (A,C2, C1), and horizontal distance D. The effects of target elevation and ventilation will also be examined." [DEF 00]. The duration of the fully developed fire is fixed to be 3600 s (including transitions 4800 s). To perform a reasonable number of simulations in a short time the computational grid was set to have less cells than for part 1. It is shown in Fig. 16. The model now has 11400 cells. This includes the cells to represent the solids of the cable trays and the target cable (instrumentation cable of 18 or 50 mm diameter). The simulated fire heat from the trays A, C1, C2, which are lumped together, follows the shape shown in Fig. 18. The peak can be between 1 and 3 MW. The target cable is considered to be damaged when the centerline of the cable reaches 200 C.

The release of the heat from the assumed fire is implemented similarly to part 1. The convective fraction is placed as volumetric source into the cells closest to the cable trays. The radiative fraction of 48% is emitted directly from the solid surfaces.

With the longer simulation time the heat absorbed by the boundary walls and the subsequent rise of the surface temperature should not be neglected. Therefore a one dimensional heat conduction simulation has been added. Compared with an explicit inclusion of the walls (this means by conducting cells) the computing time is negligible.

Chemical reactions are not treated in the simulations. Hence no check for oxygen depletion has been done in the code. Only a crude hand approximation has been done. From the specifications it remains unclear how to proceed with the fire heat release if oxygen depletes for a time but then recovers by the ventilation system.

4.1 Base Case

This case is distinguished from other cases by a peak heat release rate of 1 MW and a distance of the power cable (diameter 50 mm) of 6.1 m. The door is closed and the ventilation system is off.

With the higher heat release and all openings closed it is likely that the available oxygen is exhausted soon. An approximation indicates a time of about 1200 s. This time has been selected for the illustration in Fig. 17. A global circulation can be observed and the temperature is rather uniform.

It is speculative how the case would further develop if oxygen depletes because this is not modeled currently. To be conservative the simulation over the full time and the heat release according to Fig. 18 has been performed.

The heat flow to the cable which is at the same elevation like the burning cable trays leads to a rapid heat up of its surface (Fig. 19). Therefore radiation from the cable to the colder boundary walls is positive which means that the cable loses energy. Consequently the heat-up of the cable is reduced. A look to the cable temperatures gives Fig. 20. Although at the surface very soon high values are reached, in the central part of the cable only about 50 K increase is obtained. Therefore no damage with the given criterion can be detected. This is true either after 1200 s when the available oxygen tends to deplete or after 4800 s when following the given heat release curve to full extent.

4.2 Case 6

The base case is only capable of producing a relatively low heat-up of the target. Among the specified cases case 6 assumes the highest peak heat value (3 MW) in combination with the nearest placement of the target cable to the fire source. With higher heat output from the fire oxygen will deplete earlier. According to an approximation this may be after 700 s. After this time the flow field and temperature distribution calculated by CFX is shown in Fig. 21. A large vortex has developed with a horizontal flow along the floor. Fig. 23 compares the temperature in the center of the room of case 6 with the base case. For both cases simulations have been extended beyond the oxygen depletion point up to the end of the specified fire duration. Case 6 leads to a much higher room temperature. However the early oxygen starvation prevents a target

damage. The centerline temperature reaches values above the damage threshold of 423 K only in the late phase of the simulation. This is shown in Fig. 22. A summary of the heat flows received by walls and the target is illustrated in Fig. 24. Right from the beginning the target becomes that hot that it constantly loses energy to the outer walls. However, by gas convection it is heated further.

4.3   Case 10

Both cases analysed up to now suffer from early oxygen starvation although the fire power might be strong enough to damage the target cable. A fresh air flow through the room might change the situation. Case 10 is comparable with the base case but the door is open and the ventilation system is working. Oxygen depletion has therefore been excluded. The incoming air is cold and forms therefore a stable stratification in the room. Fig. 25 and Fig. 26 illustrate this from different perspectives. The flows out of the door and the ventilation system can be seen. A cooling effect to the target cable is not expected. If oxygen around the burning cable trays is sufficiently available can not be answered unless the migration and distribution of the species involved would be modeled in detail. Under the assumption of abundant oxygen to feed the fire, the cable centerline temperature is calculated as shown in Fig. 27. There is only little heating-up in the center of the cable.

5   Summary

Following the benchmark specification a selection of six cases out of a total of 20 for both parts has been simulated by the CFD code CFX. Despite this reduced number of cases they were selected with the intention to preserve the scope of the benchmark and to get representative results.

The analyses carried out demonstrate the capabilities of CFD codes in simulating fire situations. They also outline the higher effort with respect to computing resources. On a DEC-Alpha Unix machine with about 350 Mflops simulations needed approximately 64 h and 153 h for part 1 (28400 cells) and part 2 (11400 cells), respectively.

In order to keep computing times manageable it was decided to use relatively coarse grids for both parts of the benchmark.

None of the cases analysed leads to a damage of the target cable according to the specified damage criterion for part 1 and 2. This is true if depletion of oxygen is included in the simulations. If these are carried out following the heat release curves to full extent then case 6 leads to cable damage.

6   Continuation of Work

An obvious continuation of the current work is the simulation of other important test cases. Among these are for part 2 case 9 with partial activation of the ventilation system and opening of the door in the room. This will enable to investigate whether oxygen depletion will occur later than in previous cases. A realistic chance of cable damage may involve case 13 with a cable diameter of 15 instead of 50 mm.

It will be necessary to investigate the quality of the grids for both models applied so far. With finer grid cells at around source and target it can be proved if grid convergence with the solutions found has been achieved.

A crucial point for many cases is the depletion of oxygen. To provide realistic simulations mixing and diffusion of oxygen in combination with the consumption of the fire need to be included into the fire model of CFX. This means that for the relevant species additional conservation equations have to be solved.

References

AEA 99   CFX4.3, Documentation, CFX International, AEA Technology plc, Oxfordshire, United Kingdom, 1999.

DEF 00   Benchmark Exercise, Definition of Problem, Revised June 19-20, 2000.

Figures and Tables
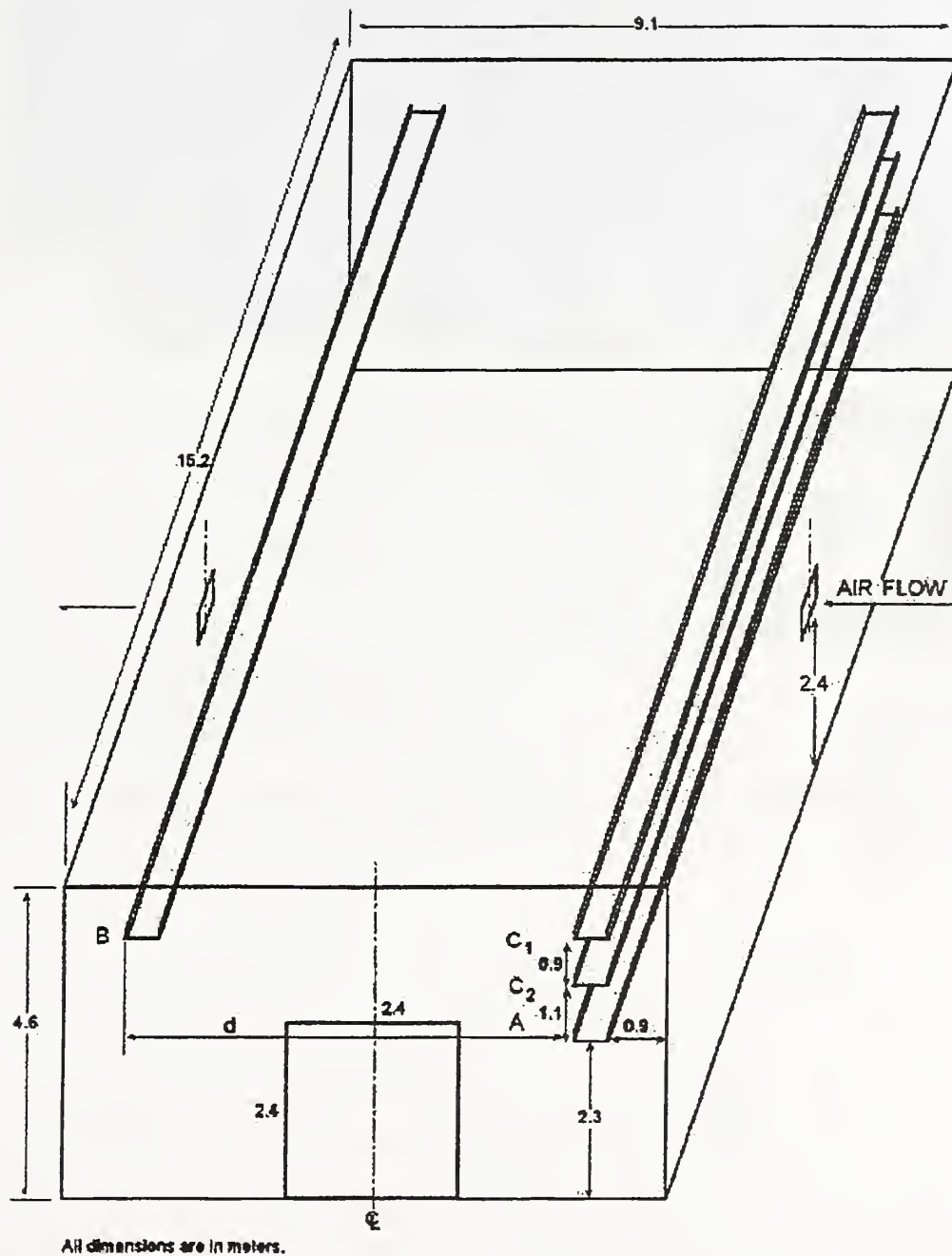
Fig. 1   View of the room to be modeled
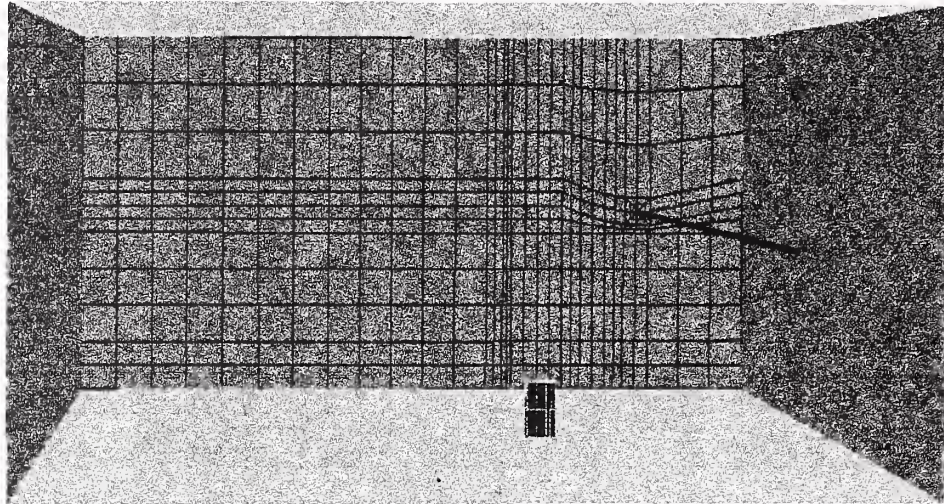
Fig. 2   View of the computer model for part 1
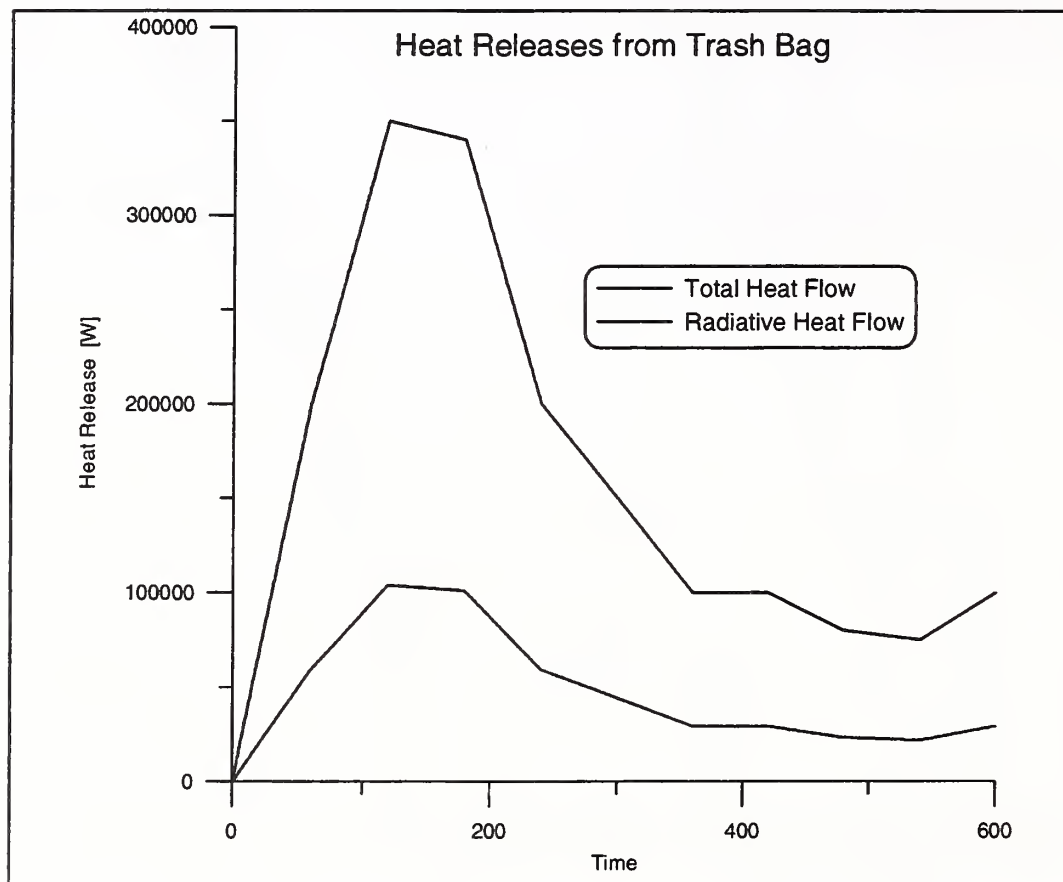
Fig. 3   Overview of given heat release over time (Part 1)
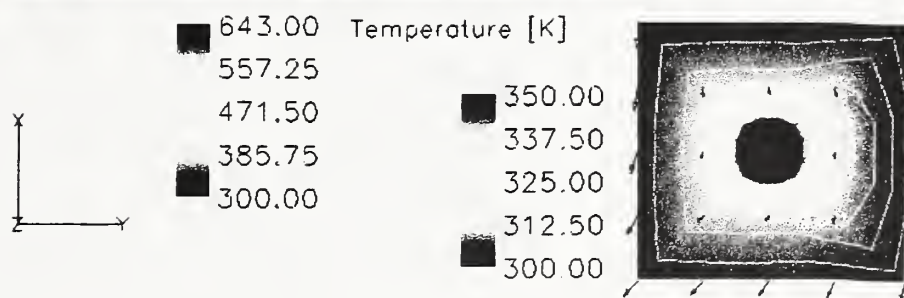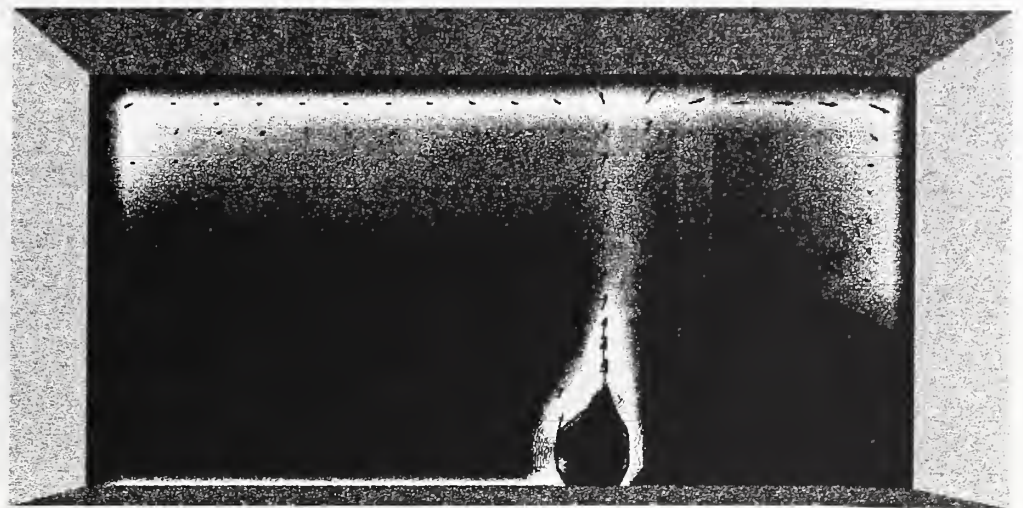
Time=180.35s   Base Case

Fig. 4   Temperature distribution at the time of strongest heat release (base case)

Temperature [K]
643.0
557.3
471.5
385.7
300.0
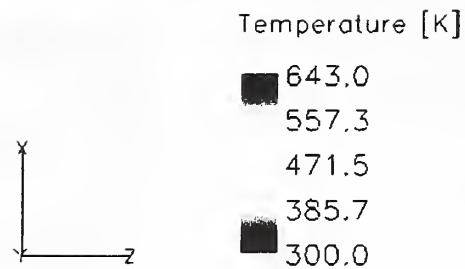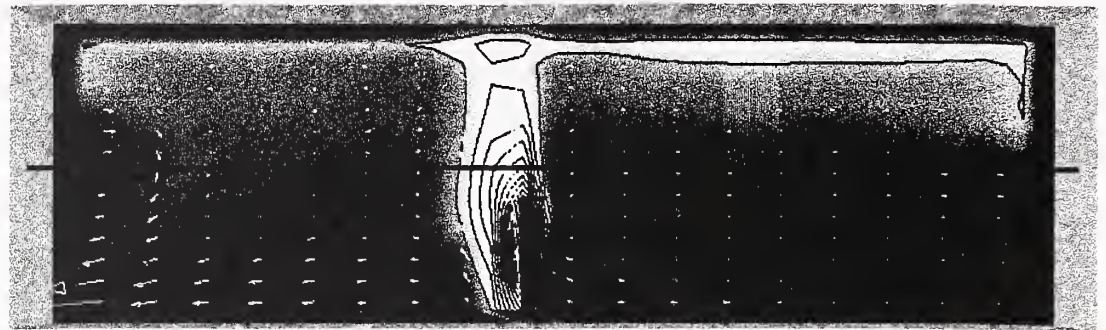
Time=180.35s   Base Case

Fig. 5   Lateral view of the fire room after 180 s (base case)

Temperature [K]
■ 643.0
557.3
471.5
385.7
■ 300.0

Time=600.35s
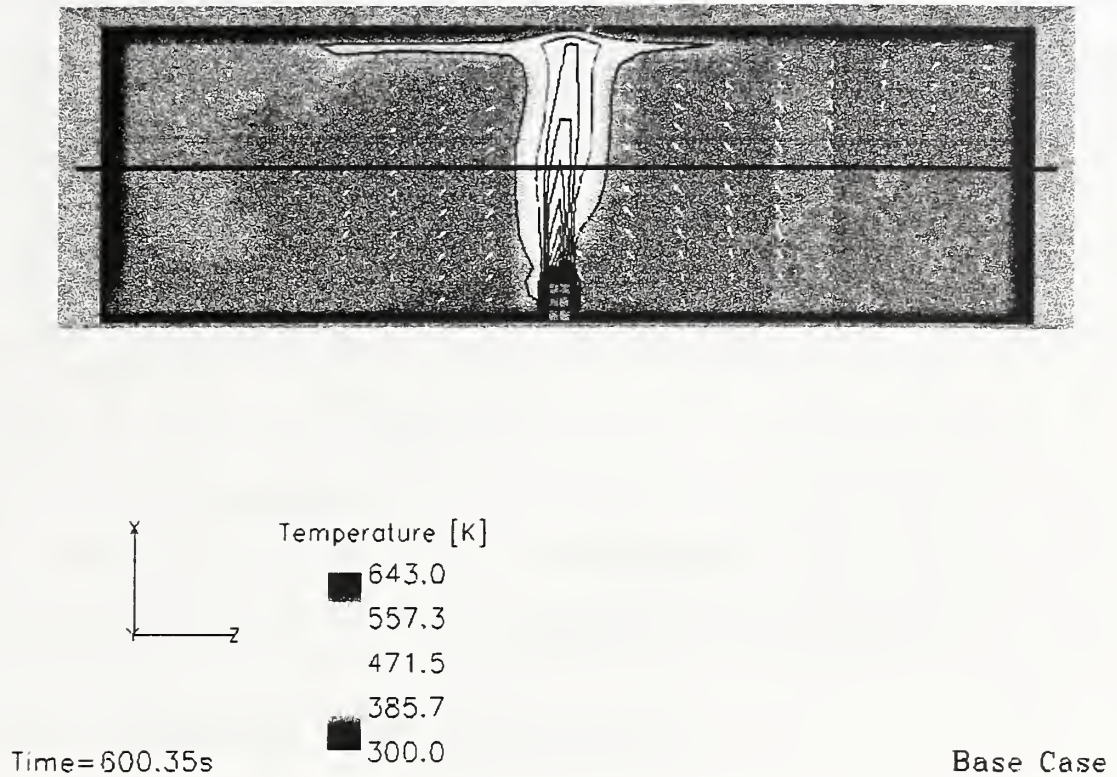
Base Case

Fig. 6   Temperature distribution after 600 s (base case)
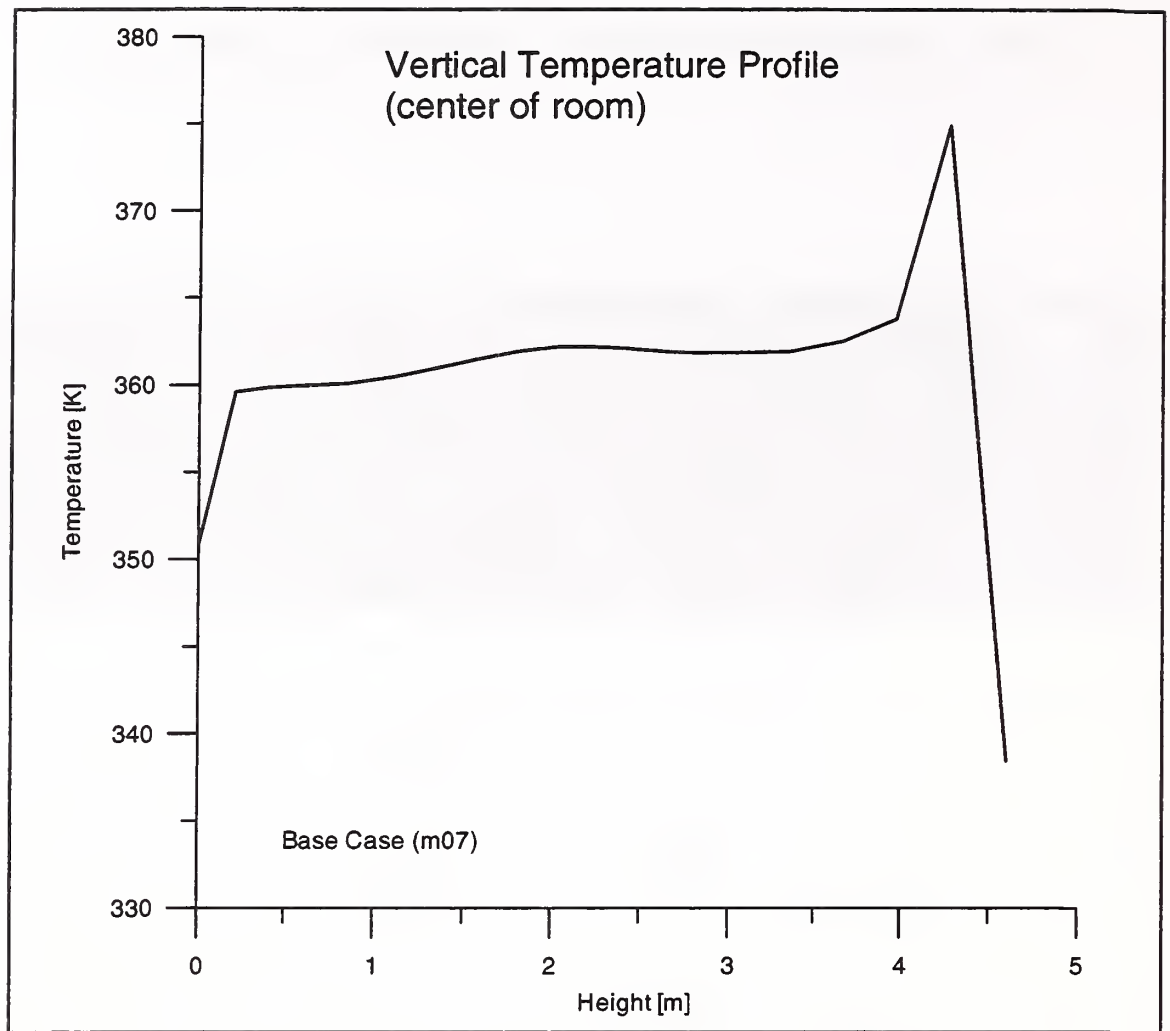
Fig. 7   Vertical temperature profile from bottom to top after 600 s (base case)
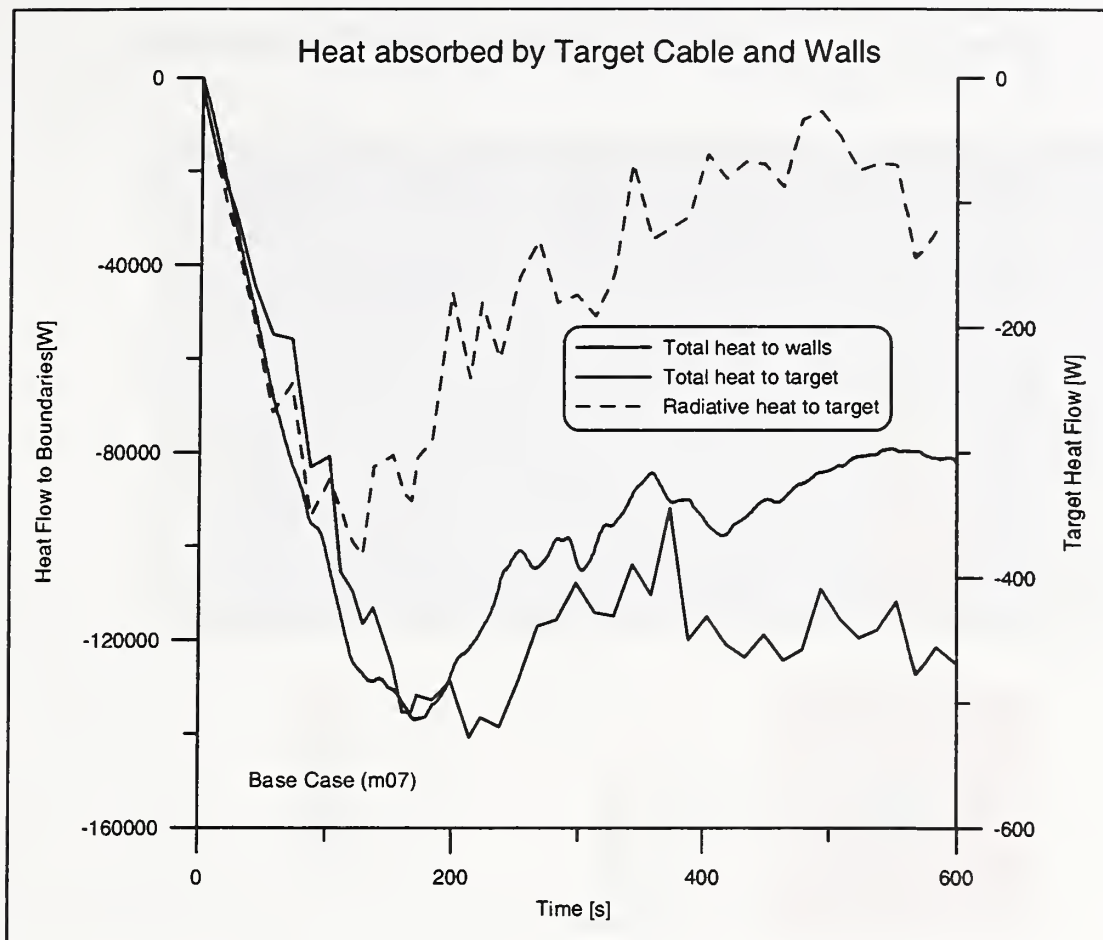
Fig. 8   Heat absorbed by the target cable (base case)
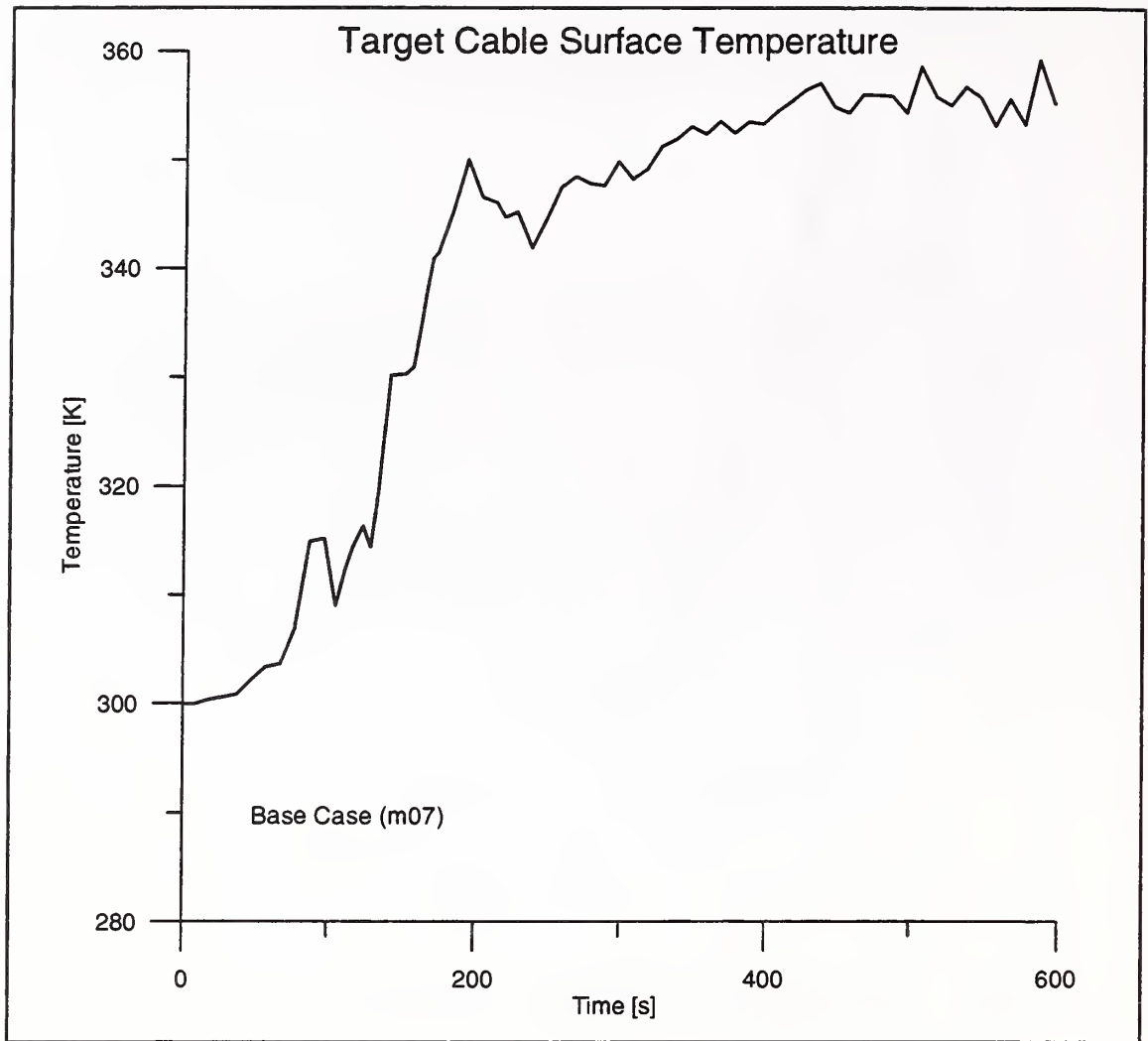
Fig. 9   Target cable surface temperature variation for the base case
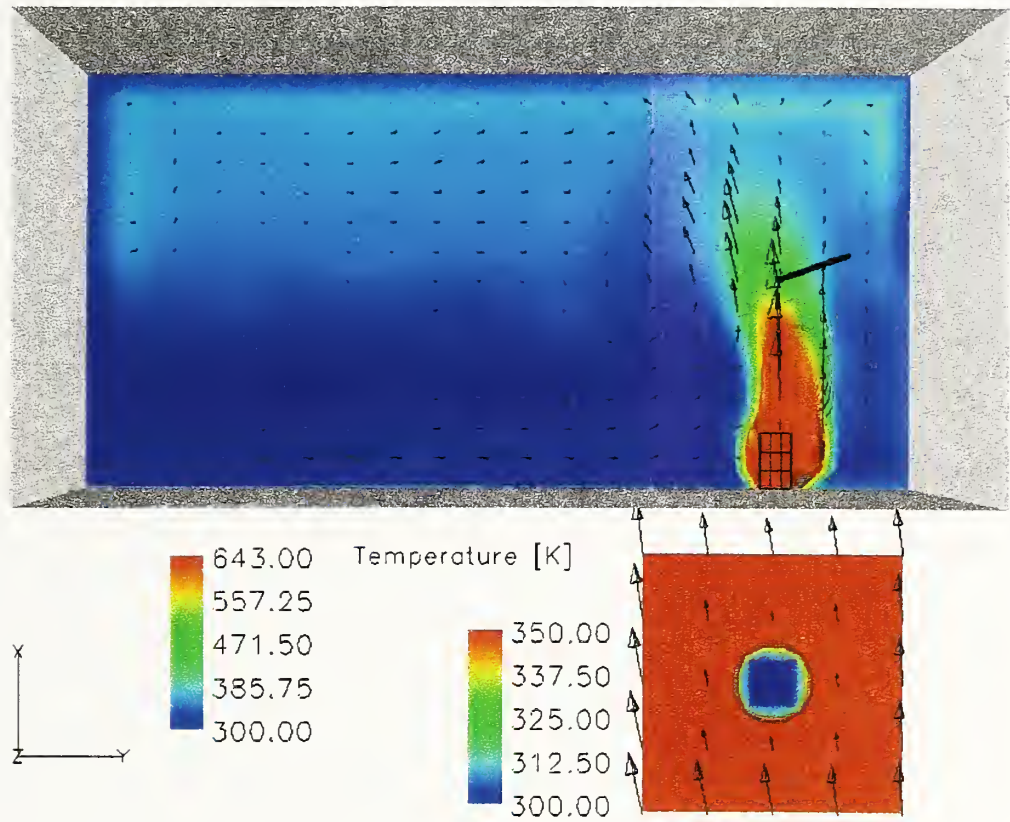
Time=180.1s   Case 1

Fig. 10   Flow field and temperature distribution in the room foe case 1
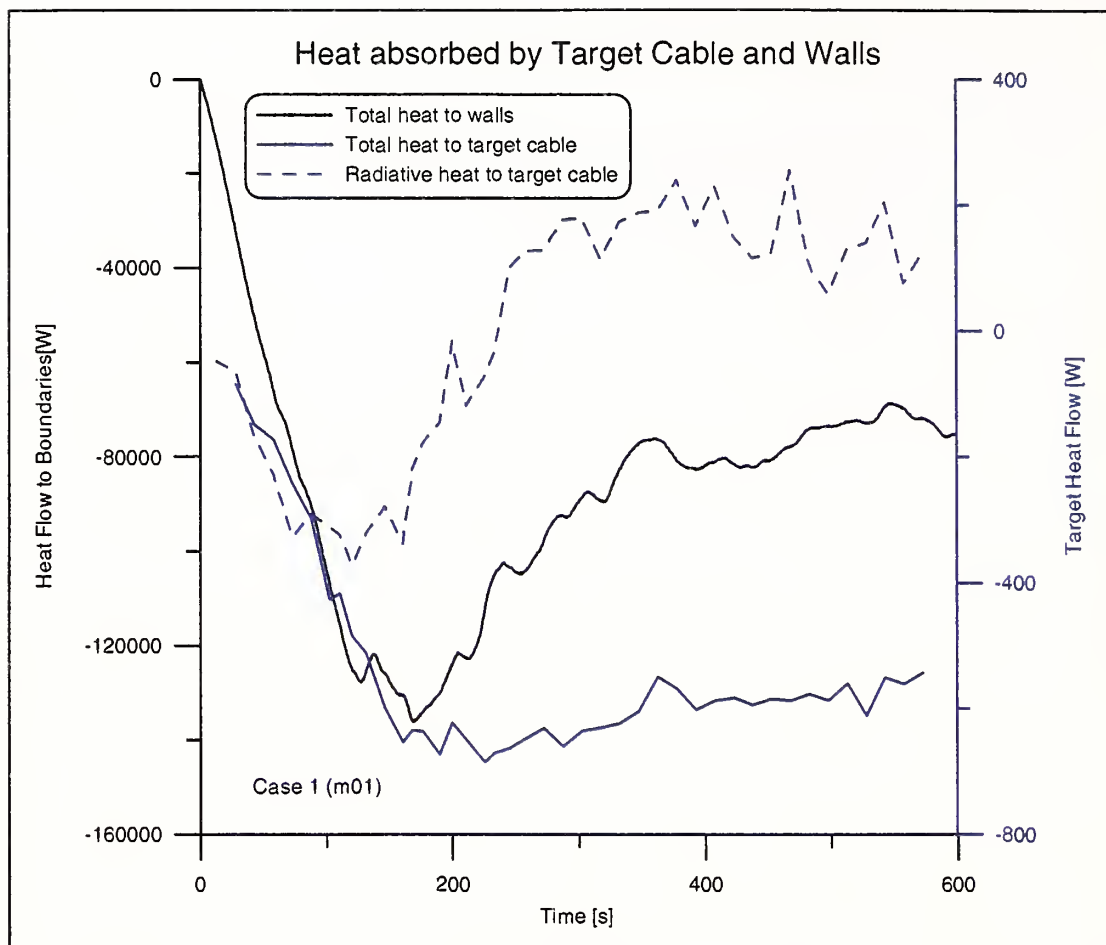
Fig. 11   Heat fluxes for case 1
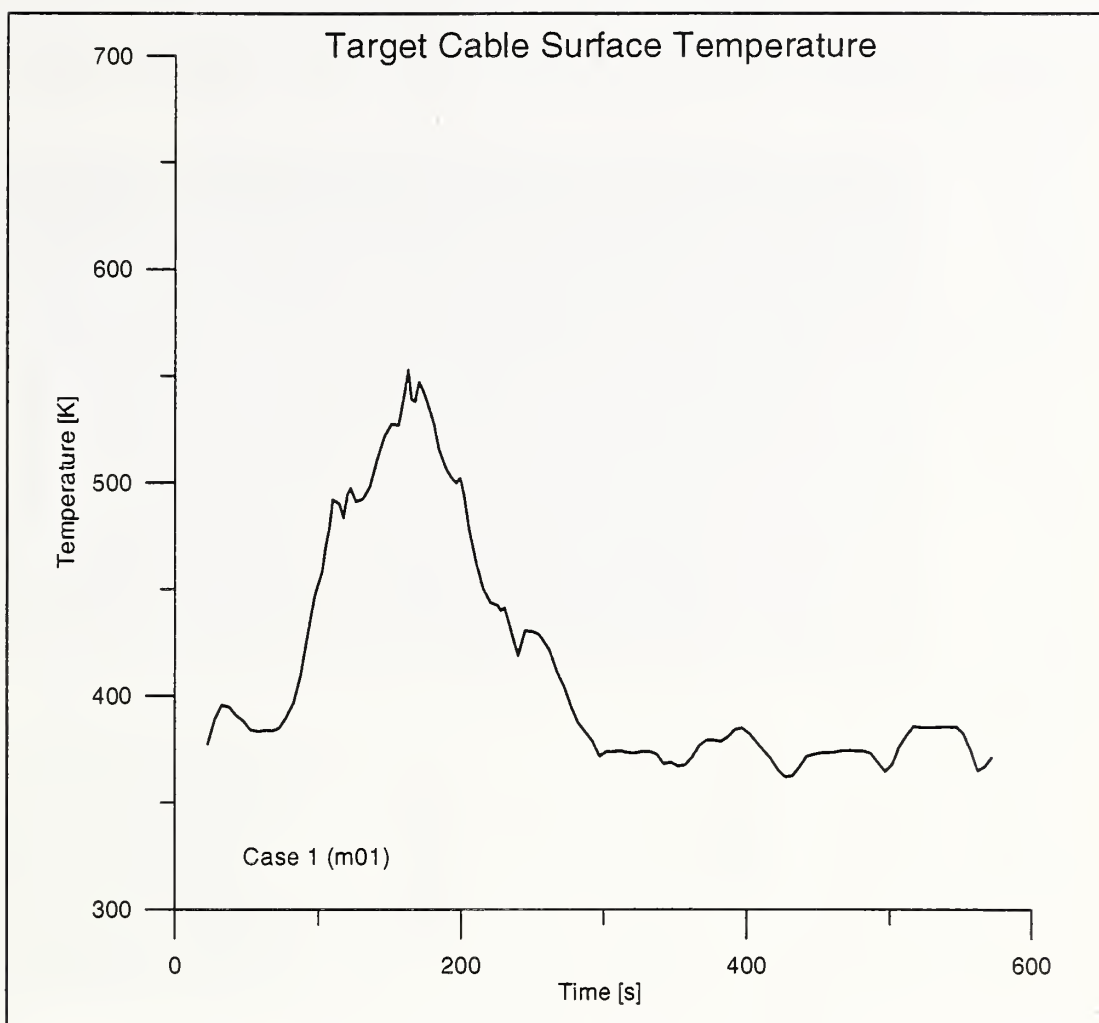
Fig. 12   Surface temperature over time for case 1

Cable Tray Fires of Redundant Safety Trains
Benchmark Part I

623.00
542.25
461.50
380.75
300.00

Temperature [K]

350.00
337.50
325.00
312.50
300.00

Time=180.35s
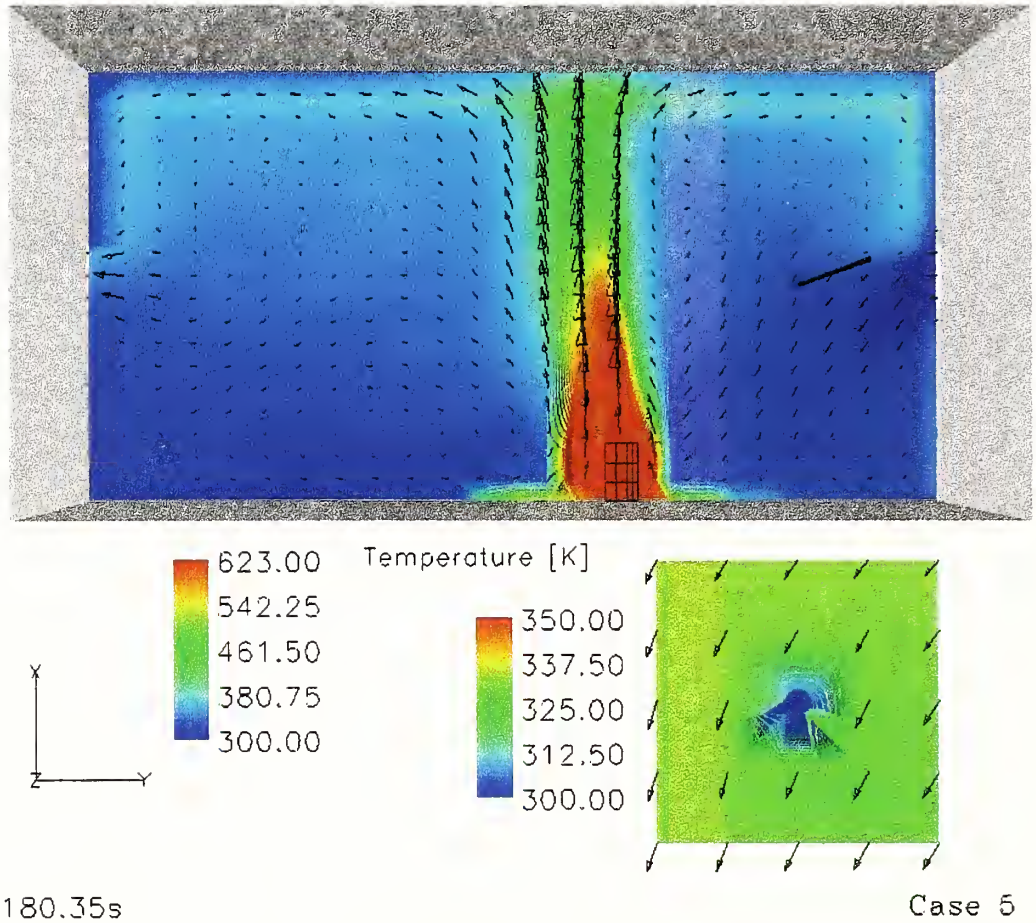
Case 5

Fig. 13   Flow field in the fire room with ventilation system on (case 5)
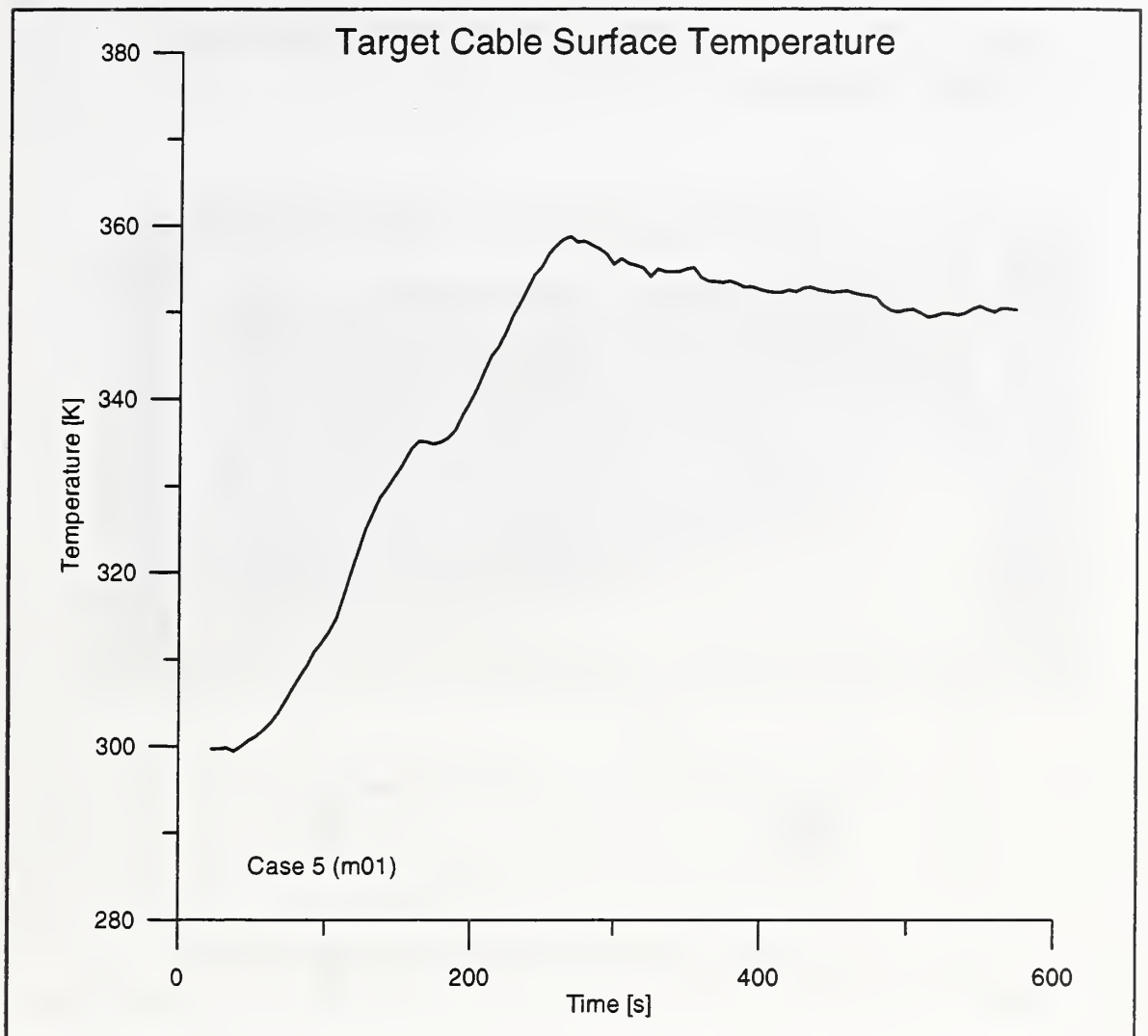
Fig. 14   Cable surface temperature with case 5
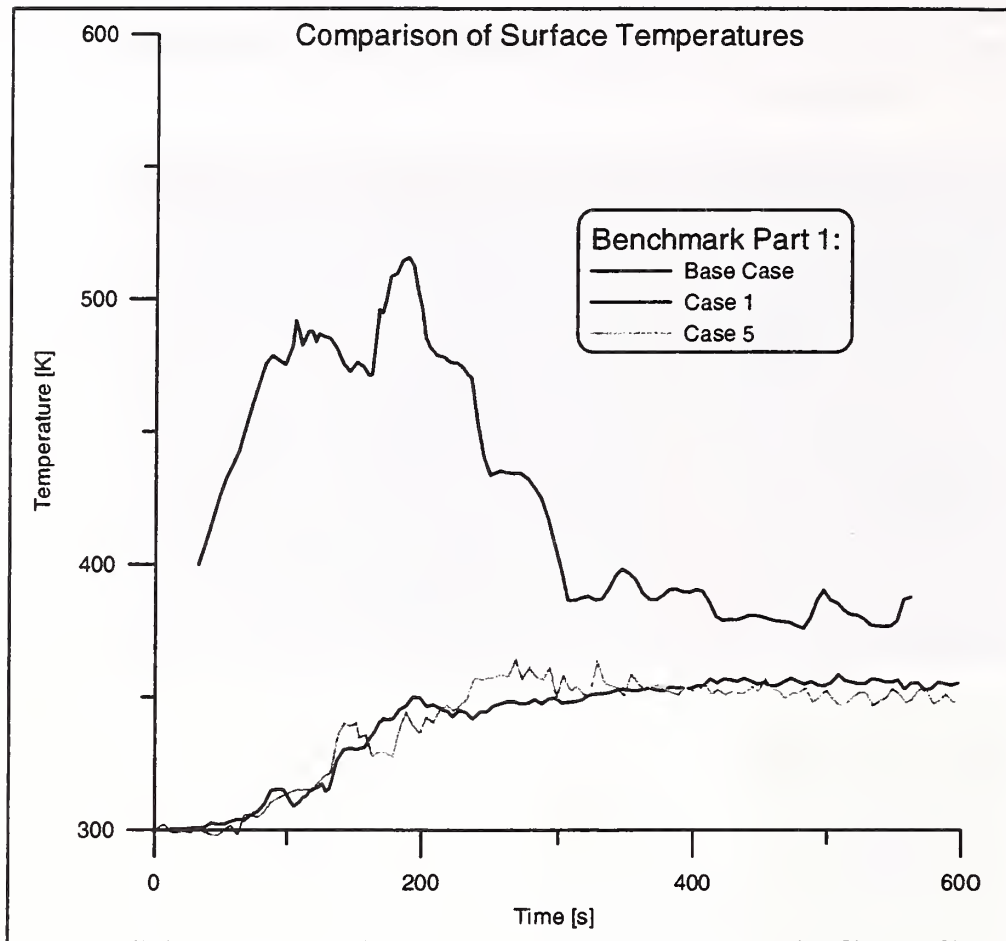
Fig. 15   Comparison of surface temperatures for benchmark part 1
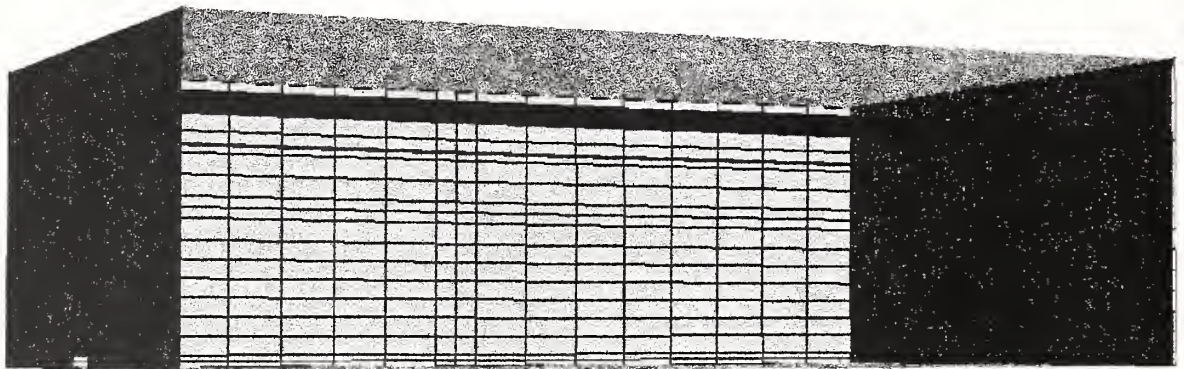
Fig. 16   CFX model for benchmark part 2
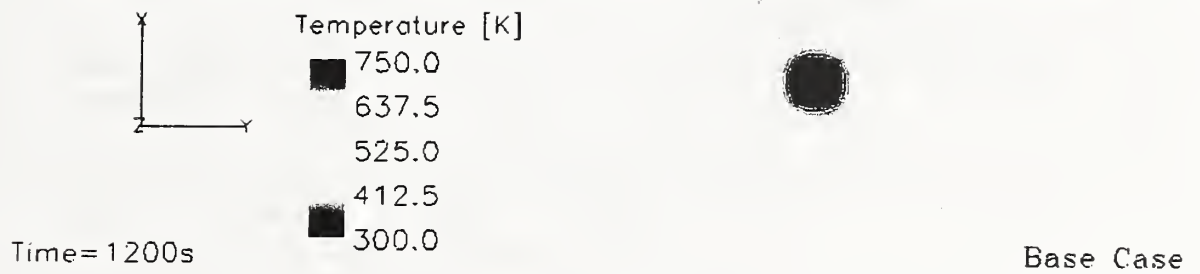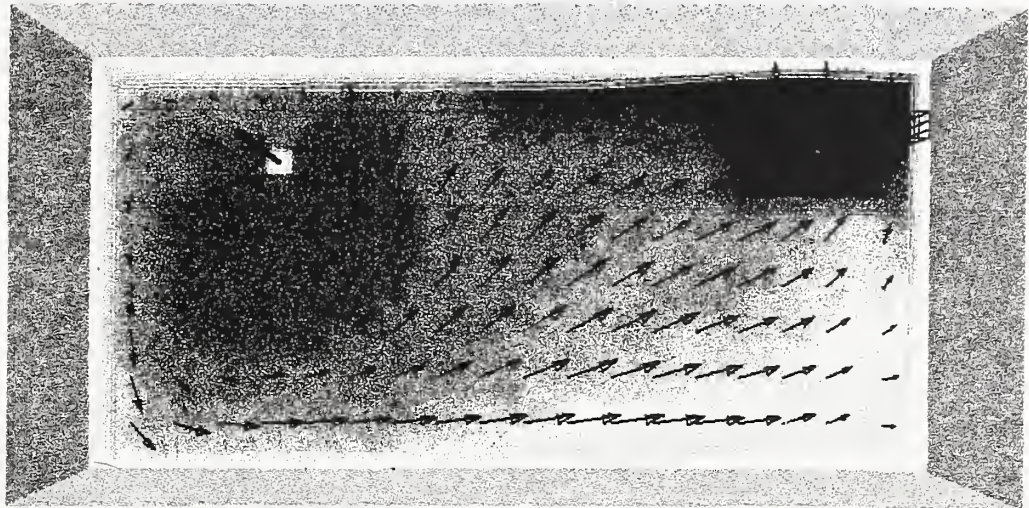
Fig. 17   Temperature distribution after 1200 s (base case)
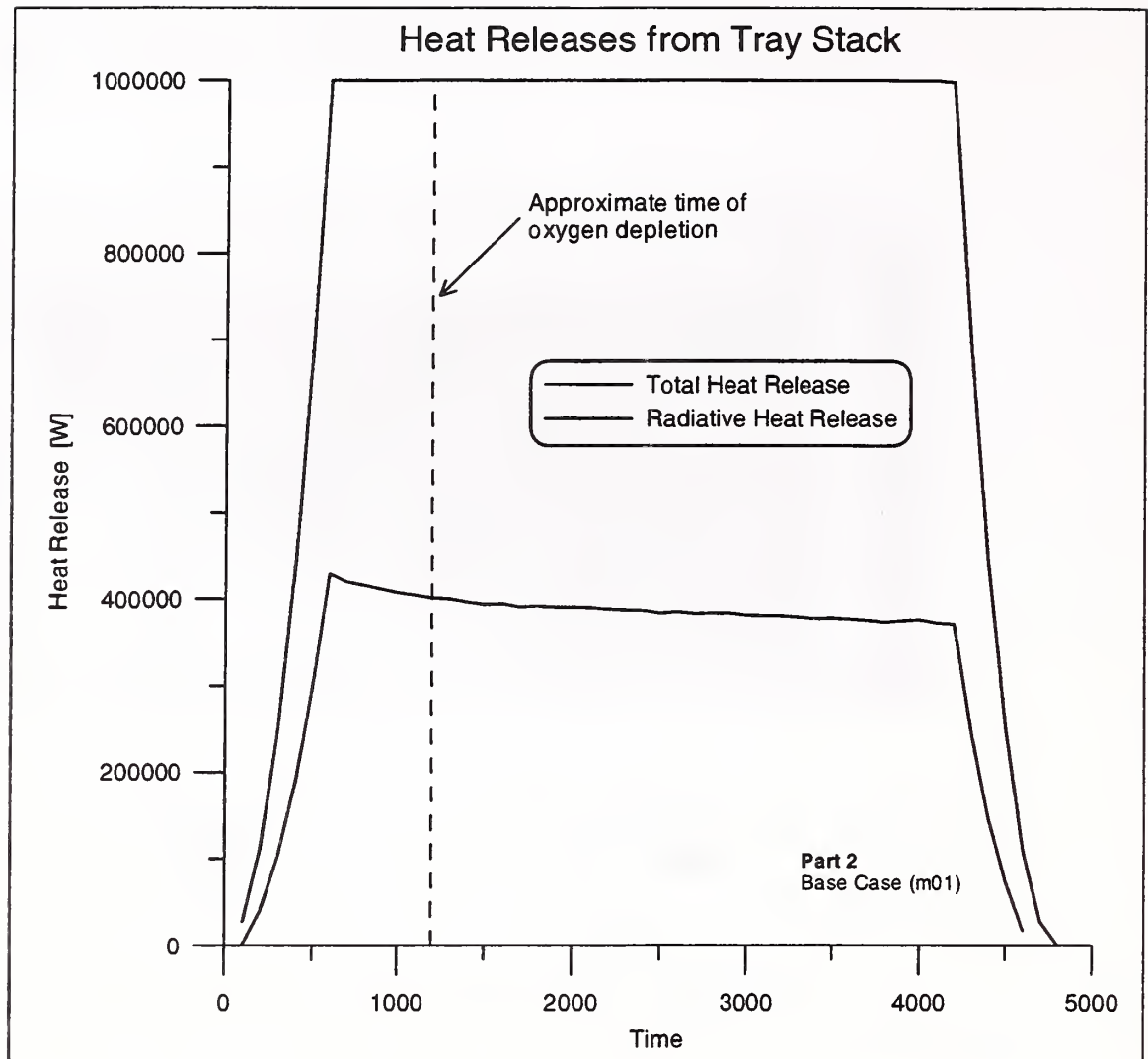
Fig. 18   Given heat release rate over time (part 2, base case)
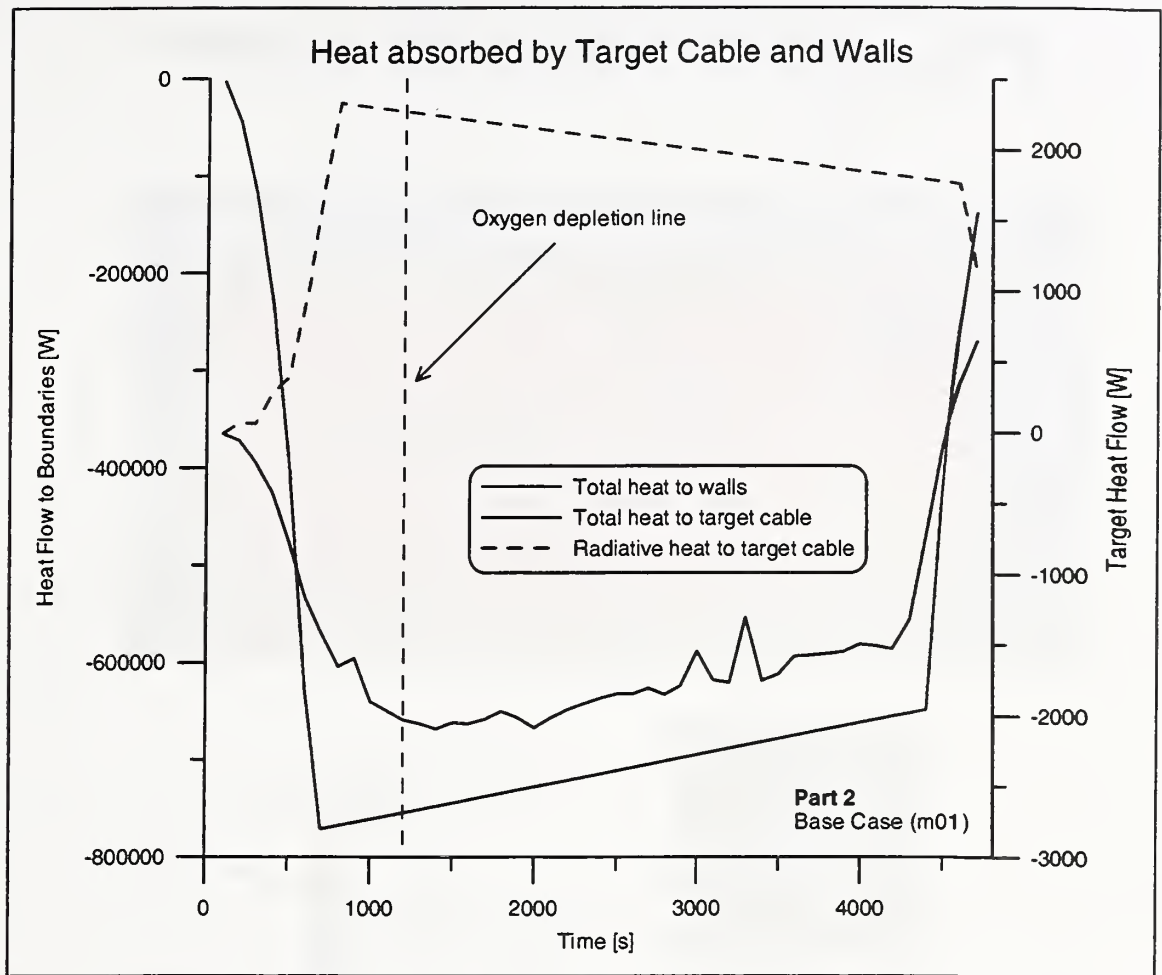
Fig. 19   Heat absorbed by the target cable (part 2, base case)
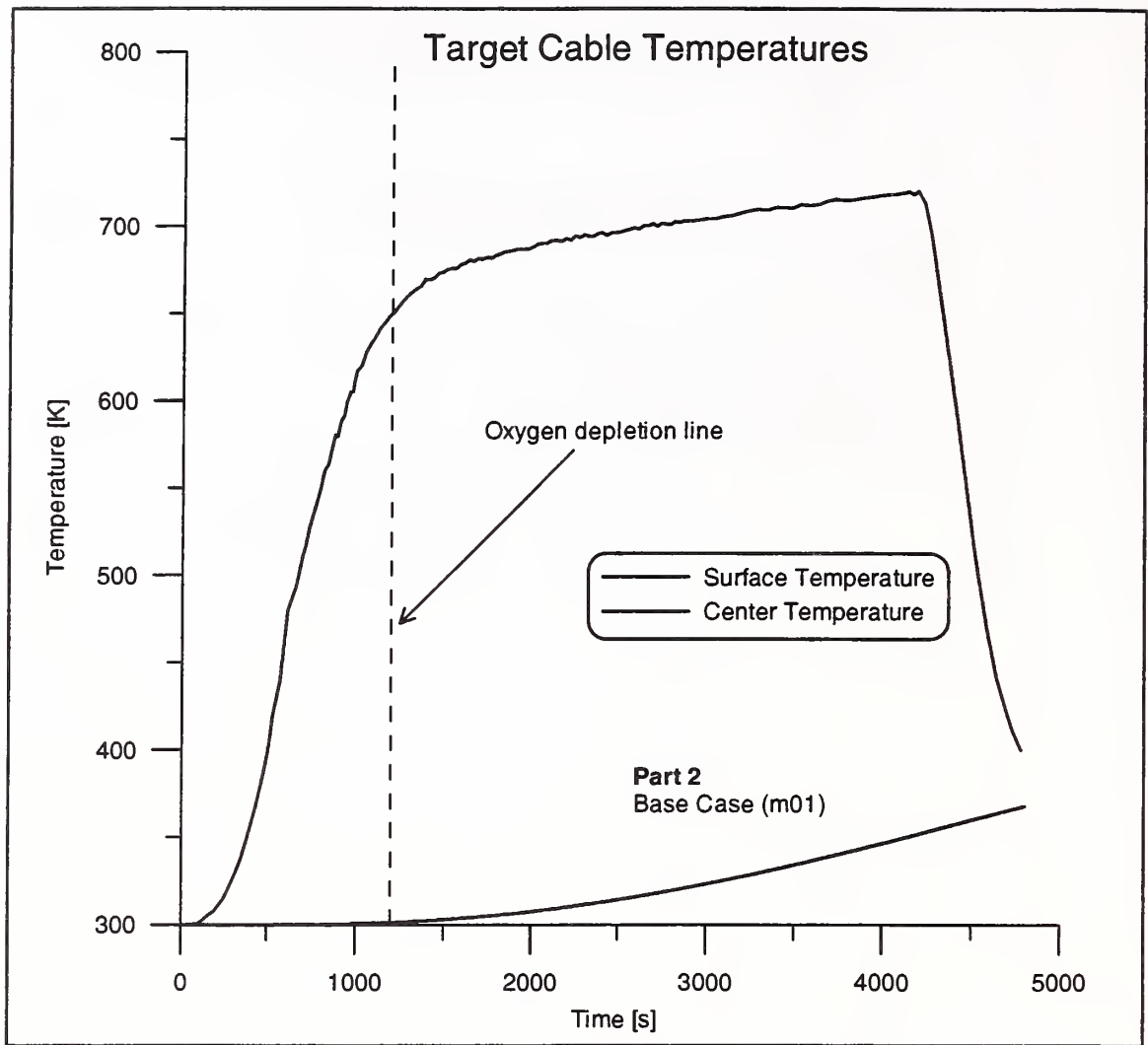
Fig. 20   Target cable temperatures during the base case of part 2
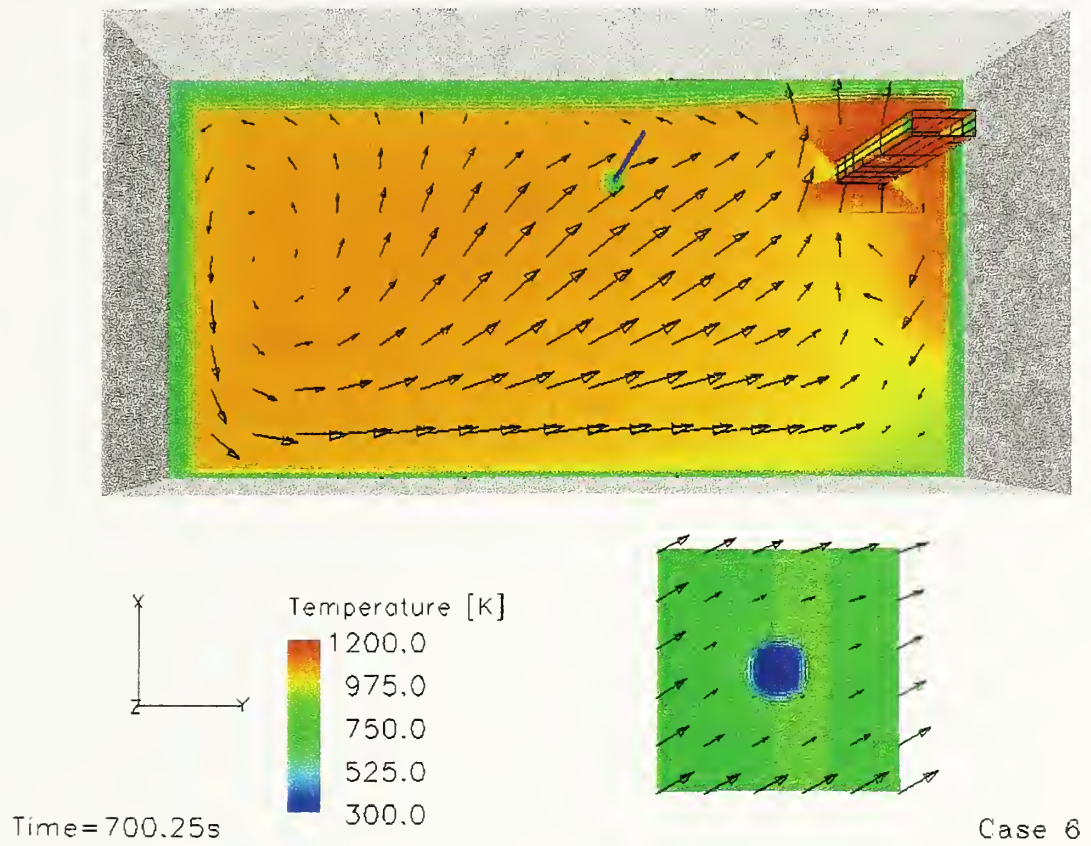
Fig. 21   Temperature distribution after 700 s for case 6

Target Cable Temperatures

Oxygen depletion line

Surface Temperature
Center Temperature

Part 2
Case 6 (m01)

Temperature [K]

Time [s]
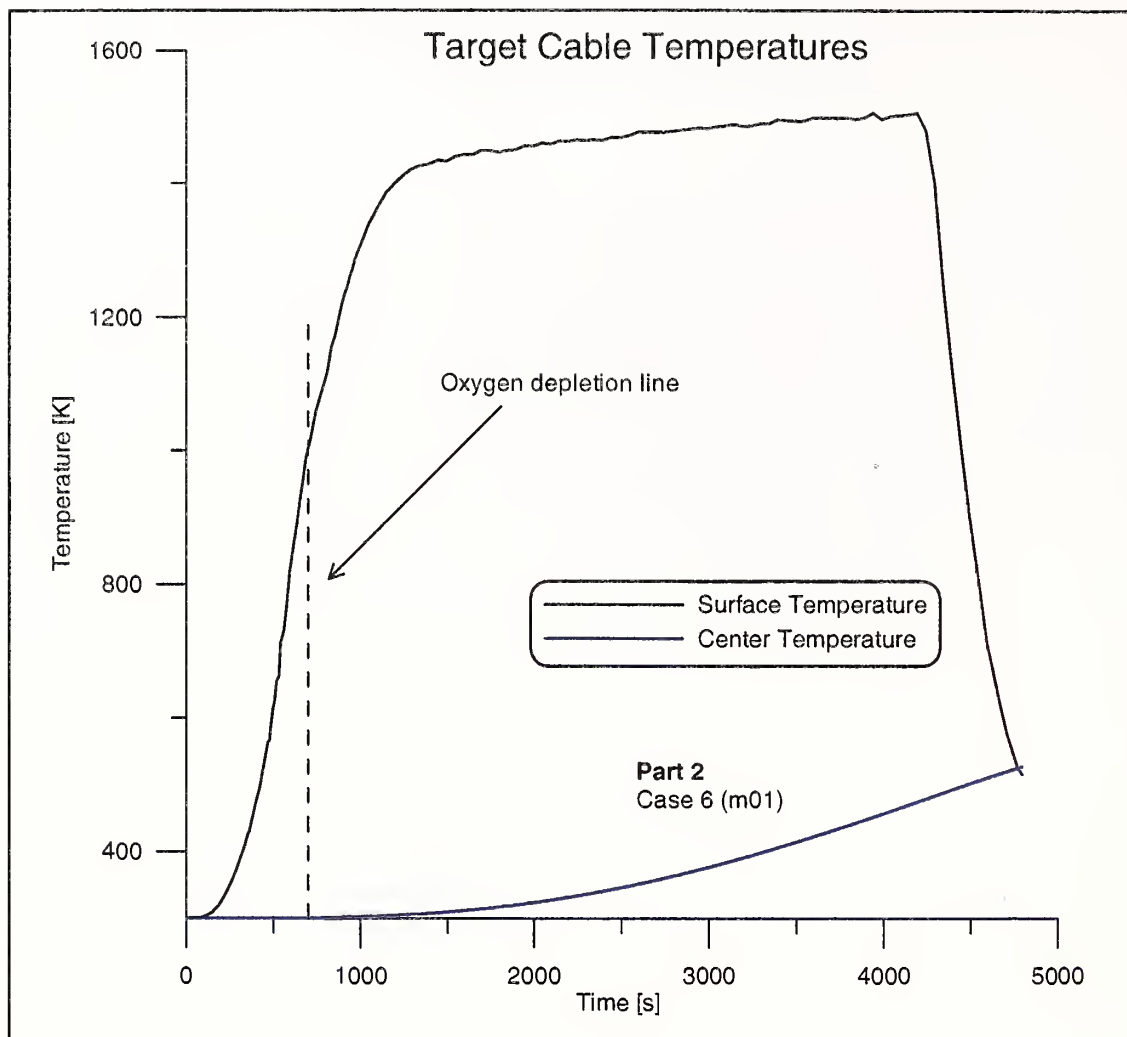
Fig. 22   Target cable temperatures for case 6
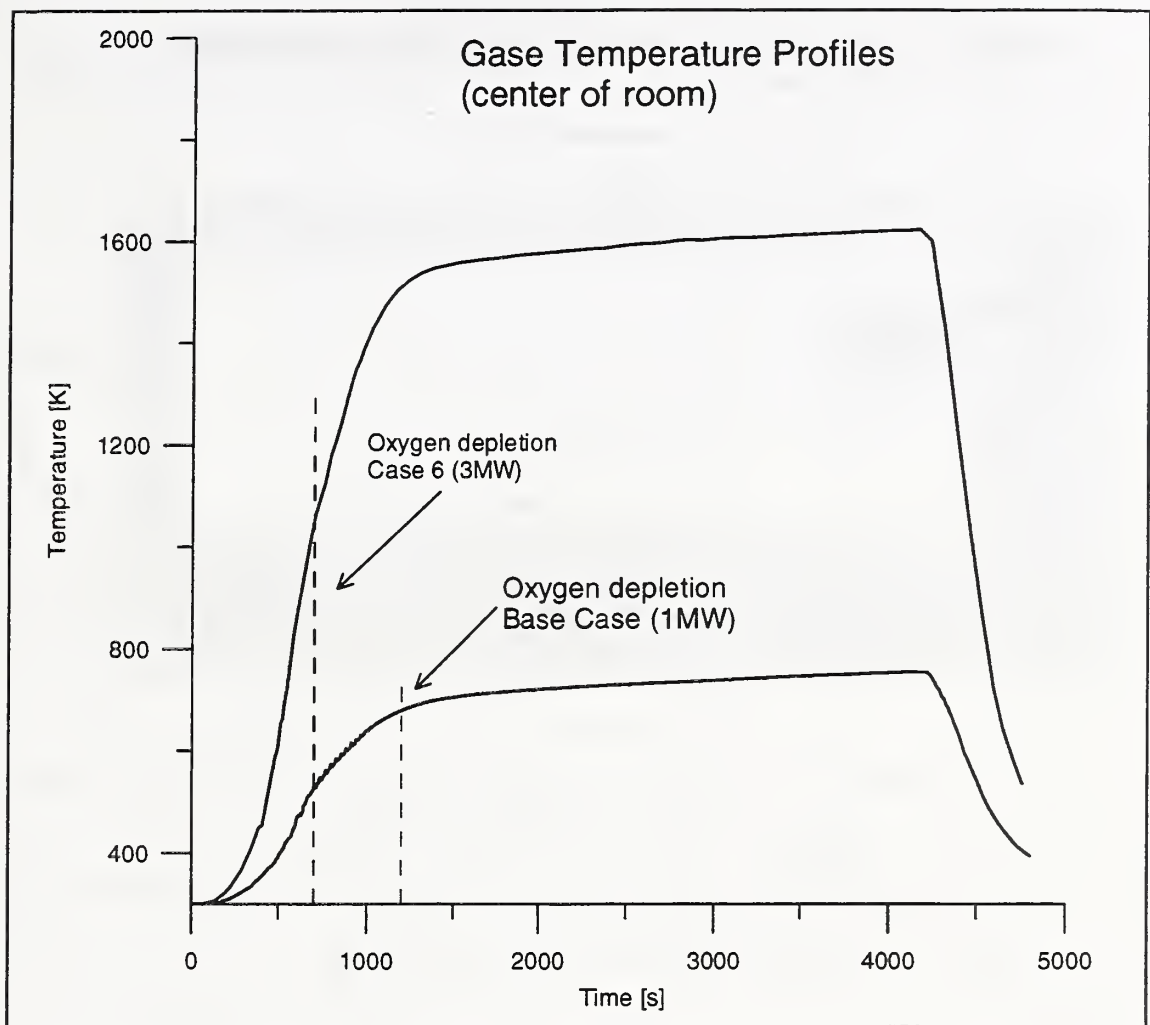
Fig. 23   Profile in the center of the room for base case and case 6

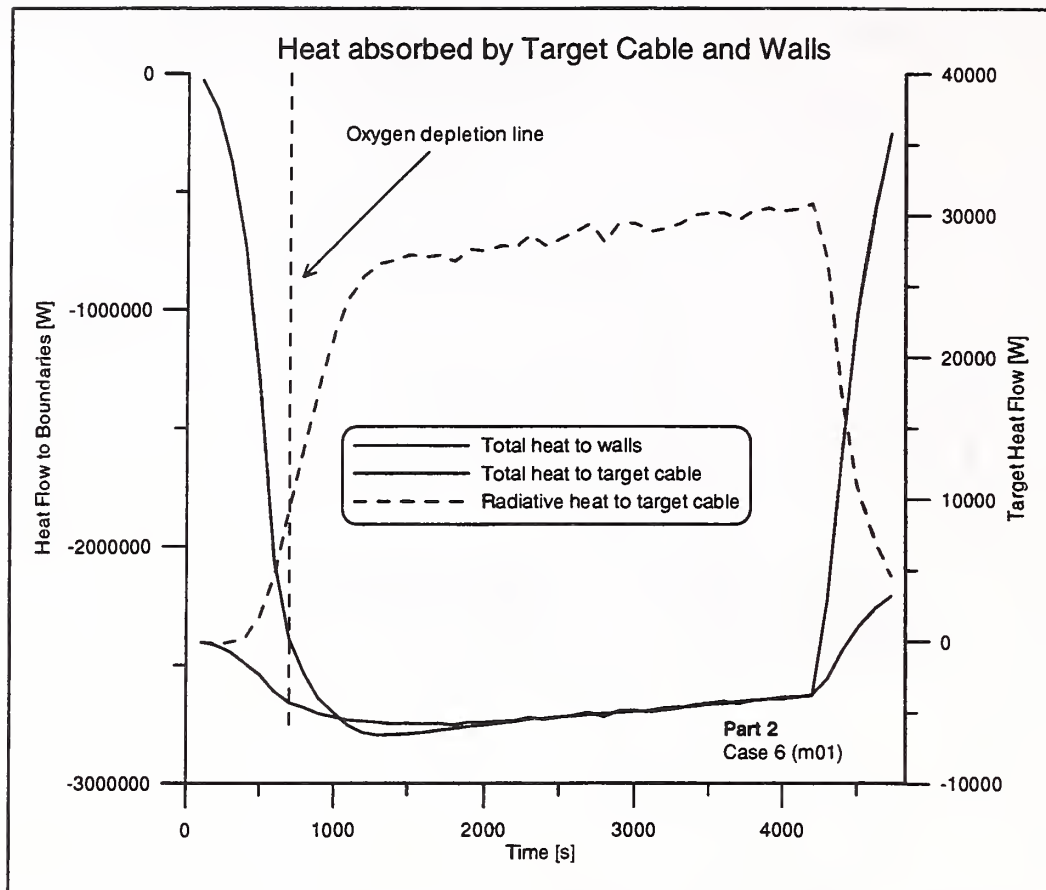Fig. 24   Heat flows to walls and target cable for case 6

Temperature [K]
700.0
600.0
500.0
400.0
300.0

Time=4200.25s
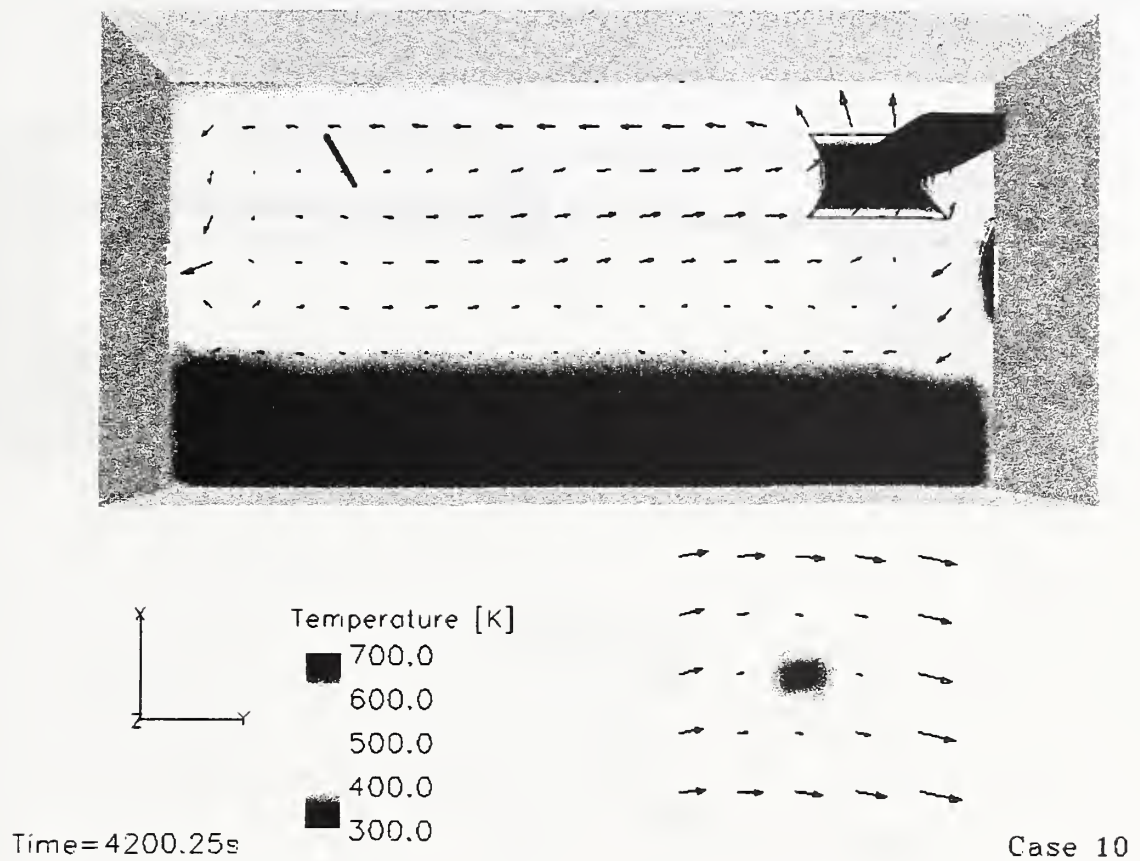
Case 10

Fig. 25   Temperature stratification after 4200 s for case 10

Temperature [K]

700.0
600.0
500.0
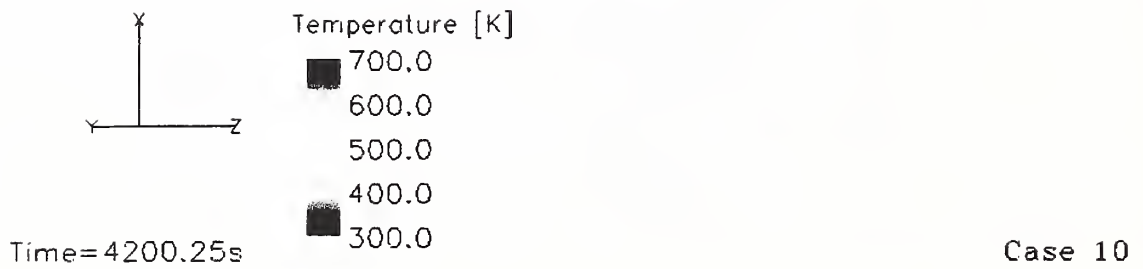400.0
300.0

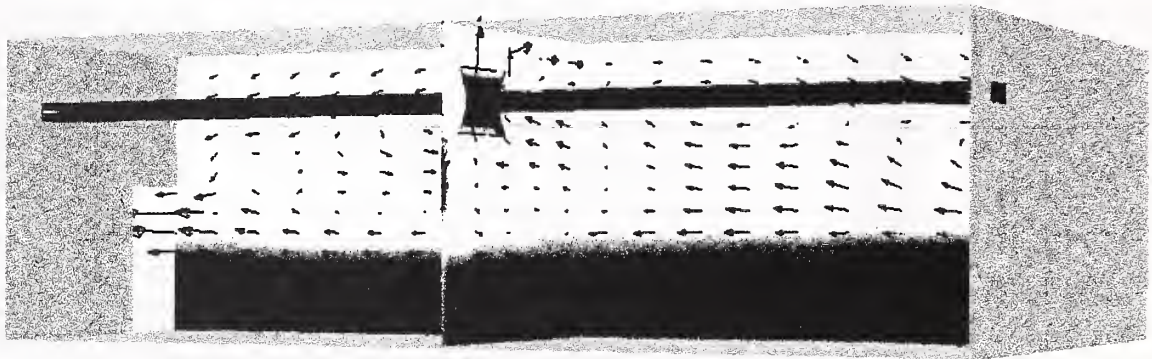Time=4200.25s

Case 10

Fig. 26   Side view of the room at the end of the maximum power release
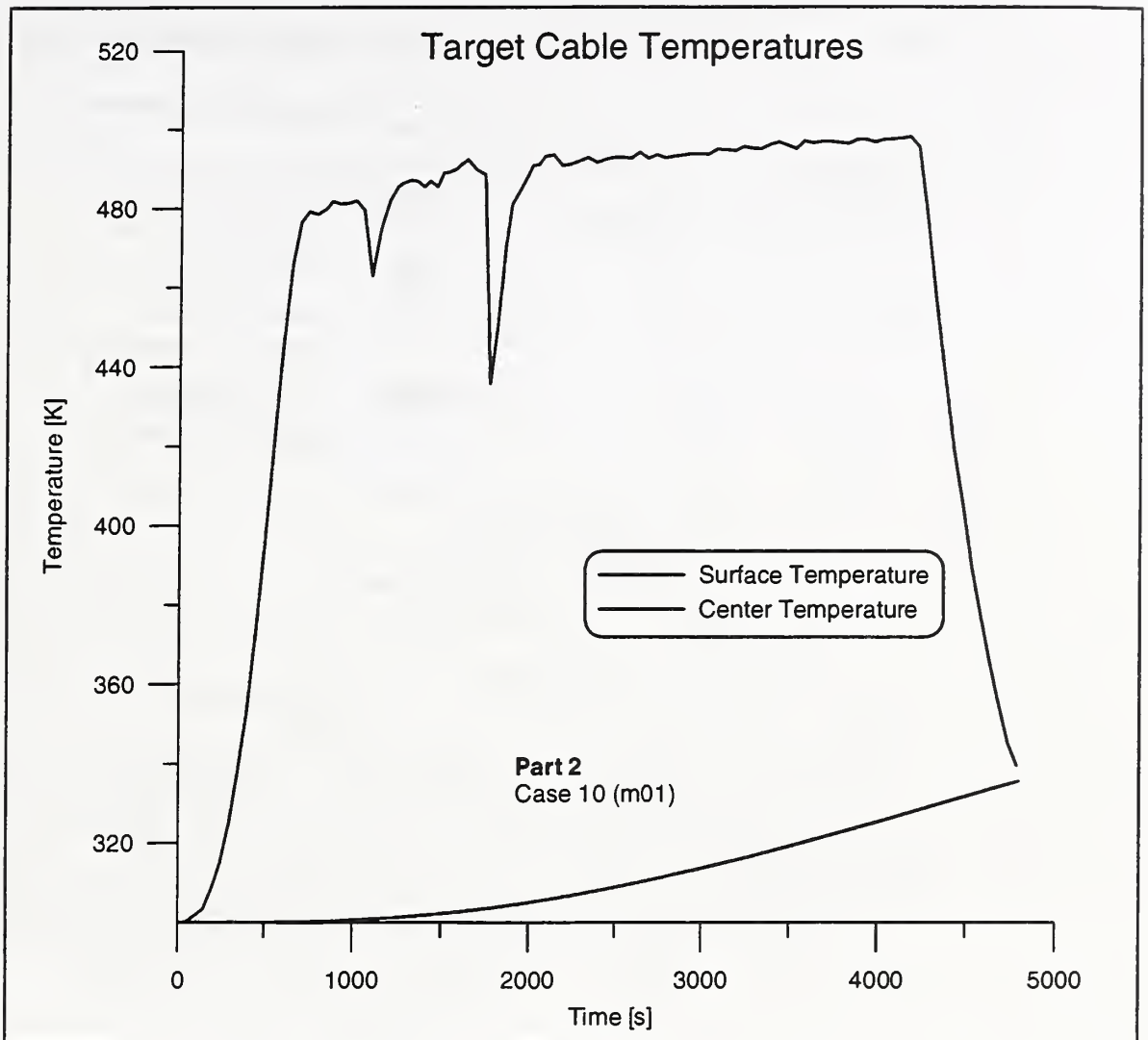
Fig. 27   Target temperatures over time for case 10
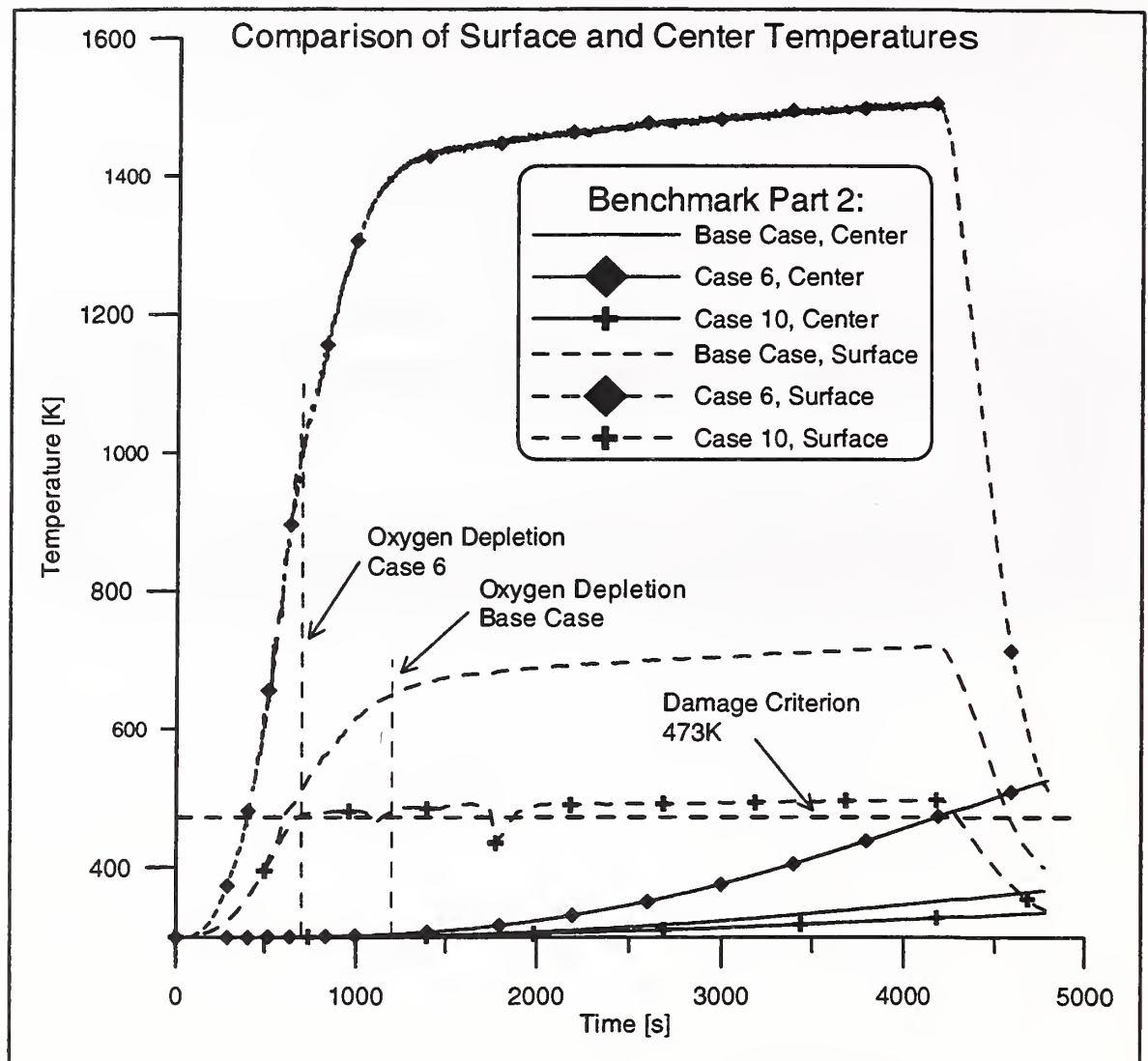
Fig. 28   Comparison of cable temperatures for base case, case 6 and case 10

Tab. 1   Summary of results of simulations

	Max. UL Temp. [K]	Max. Flux on Target [W/m^2]	Max. Target CL Temp [K]
Part 1			
Base Case	360 (180s)	210	300
Case 1	360 (180s)	210	300
Case 5	350 (180s)	210	300
Part 2			
Base Case	680 (1200s)	840	301 (368)
Case 6	1065 (700s)	5800 (700s)	532(4800s)
Case 10	525 (4200s)	500	335

Appendix E: Benchmark Analysis with MAGIC, Daniel JOYEUX, and Olivier LECOQ-JAMMES, CTICM, France

REFERENCES CTICM	INC – 01/222 – OLJ/IM
DATE	June 2001
REVISION	A
PAGES	5

International Collaborative Project to Evaluate Fire Models for Nuclear Power Plant Applications

Benchmark Exercise # 1 - SUMMARY

Cable Tray Fires of Redundant Safety Trains

Simulations with MAGIC (V 3.4.7)
(Revised September 11, 2000)

D. JOYEUX
O.LECOQ-JAMMES

CTICM – DEPARTEMENT INCENDIE ET ESSAIS
Domaine de Saint Paul, BP 64, 78470 SAINT-REMY-LES-CHEVREUSE, FRANCE

Service Recherche et Ingènierie Incendie - Fire Research and Engineering Section

☎: + 33 (0)1 30 85 20 86
📠 : + 33 (0)1 30 85 25 30
E-Mail : incnor@cticm.com

1. INTRODUCTION

We used for the benchmark (references are given in the following text) the 2-zone model MAGIC version 3.4.7. MAGIC is a classic thermal model of fire in multi-compartment building simulation.

The simulations were made according to the document revised in September 2000.

All results have been given in an additional document and only results of three variables are given in this report :

- gas temperature
- surface temperature of target cable
- centerline temperature of target cable

Reference :

International Collaborative Project to Evaluate Fire Models for Nuclear Power Plant Applications
Benchmark Exercise # 1
Cable Tray Fires of Redundant Safety Trains
(Revised September 11, 2000)
Simulations with MAGIC (V 3.4.7)

2. THE MODEL MAGIC

The software MAGIC (Global Analysis Model for fire into Compartments) is a numerical tool which simulates the behaviour and growth of a fire occurring into adjacent rooms.

It is made of modules accessible from the same front panel : a pre-processor, a computation code called MAGIC_M, a post-processor and an animation module.

The version 3.4.7 proposes physical modelling as : modelling improvement of linear fires, modelling improvement of cable thermal behaviour, mass consumption control, improvement of initial condition and density calculation, improvement of the net radiation flux received by a target placed in a room contiguous to fire room, temperature calculation in the ceiling-jet and in the plume.

3. APPLICATION TO THE BENCHMARK EXERCICE : PART I

3.1 RESULTS PART I

The following table gives the results for these four variables in part I.

Part I	$T_{upper\ layer}(°C)$	$T_{lower\ layer}(°C)$	$T_{surface\ target}(°C)$	$T_{centerline\ target}(°C)$
Base case	63.2	29.4	45.7	27.1
Case 1	62.7	29.4	72.8	27.1
Case 2	63.0	29.4	59.9	27.1
Case 3	63.1	29.4	50.3	27.1
Case 4	63.5	28.9	46.6	27.1
Case 5	60.8	29.3	44.7	27.1

Table 1 : Overview of results Part I

3.2 ANALYSIS OF RESULTS PART I

According to the results part I, we can notice the three following points:

- low temperature of gases
- low temperature of target cable
- non ignition of target cable whatever is the distance from fire centerline

4. APPLICATION TO THE BENCHMARK EXERCICE: PART II

4.1 RESULTS PART II

The following table gives the results for these four variables in part II.

Part II	$T_{upper\ layer}(°C)$	$T_{lower\ layer}(°C)$	$T_{surface\ target}(°C)$	$T_{centerline\ target}(°C)$
Base case LOL=0%	180.2	35.7	134.5	49.4
Base case and case 1 at case 8	169.2	31.5	100.7	37.5
Case 9	168.4	30.7	100	37.5
Case 10	169.1	30	100.6	37.5
Case 11	169.2	31.5	101	37.7
Case 12	169.2	31.5	41.4	29.6
Case 13	169.2	31.5	111.7	78.2

Table 2 : Overview of results Part II

4.2 ANALYSIS OF RESULTS PART II

According to the results part II, we can notice the two following points :

- limitation of heat release between 10 and 15 minutes due to the lack of oxygen
- no damage on target because the centerline target cable temperature is below 100°C.

4.3 ADDITIONAL CASE

We added a case on part II (see the table 3 below) with fire source at 2.1 m ; so ventilation is in the upper layer. According to the results of this additional case, we observe no limitation of rate of heat release.

Part II	Rate of heat release (MW)	D (m)	Door	Vent. Sys.	Target	Elev. (m)
Base Case	1 MW	6.1	Closed	Off	Power	3.4
Additional case	3 MW	3.1	Open	On	Power	2.1

Table 3 : Overview of additional case

- The temperature curves are shown in figures 1, 5 and 8.
- The rate of heat release is shown in figure 3.

- The concentration of O_2 is shown in figure 4.
- The flow rate through vents and door is shown in figure 6.
- The radiative flux on target is shown in figure 7.

The following maximum temperatures are reached :

- upper layer temperature = 350°C
- target surface temperature = 330°C

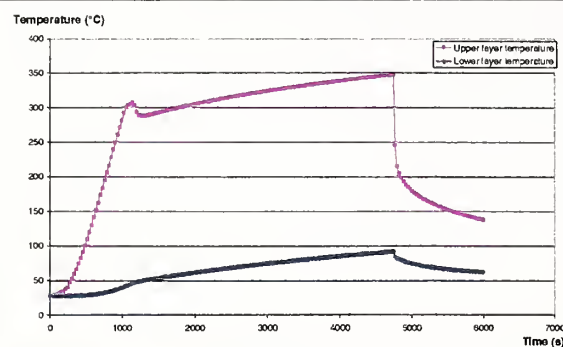## MAGIC V 3.4.7 / BENCHMARK CTICM / PART II additional case
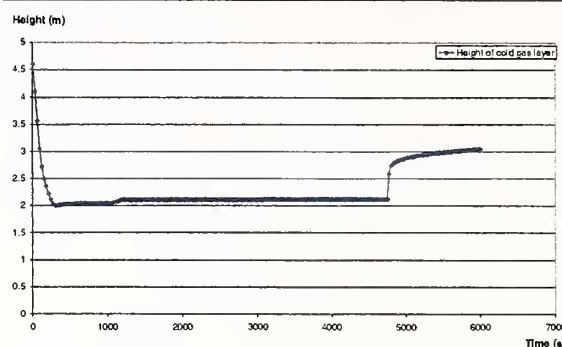
Figure 1 : Upper and lower layer temperature
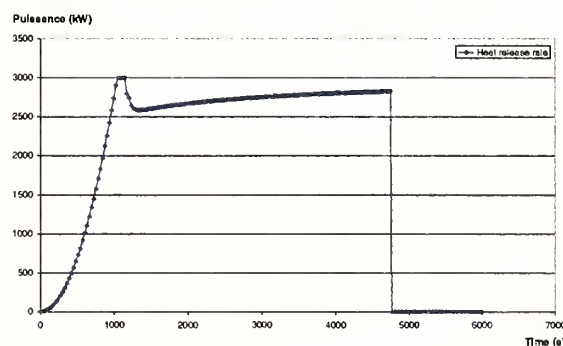
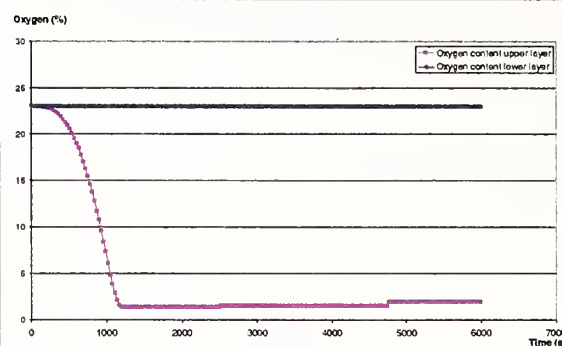Figure 2 : Height of cold gas layer

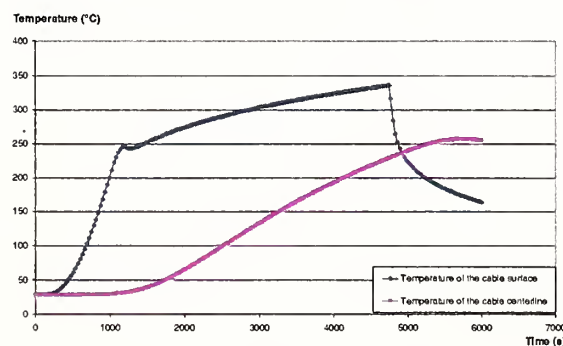Figure 3 : Heat release rate

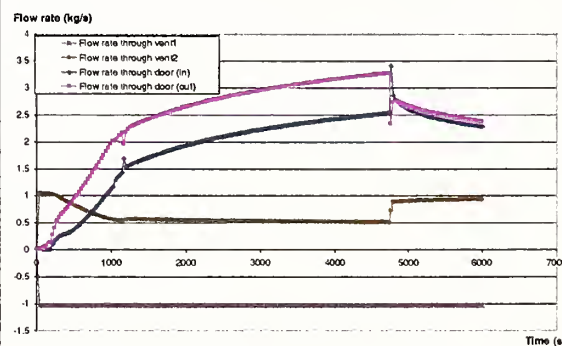Figure 4 : Oxygen concentration

Figure 5 : Cable temperature
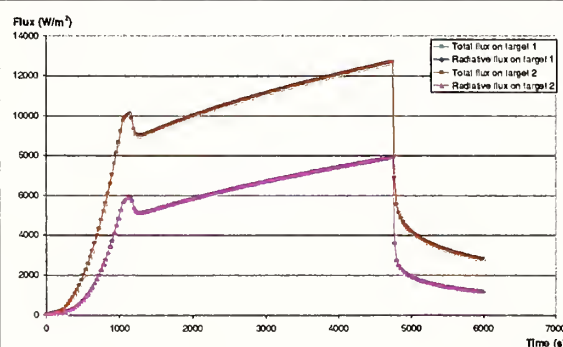
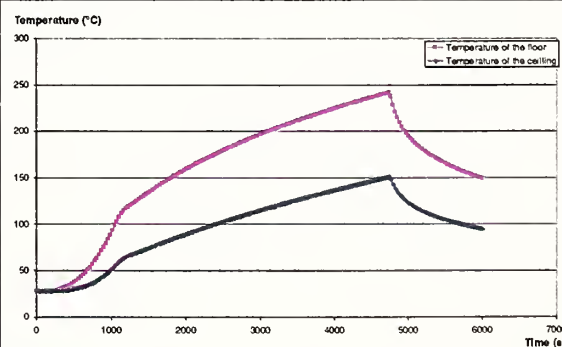Figure 6 : Flow rate through vents and door

Figure 7 : Radiative flux on target

Figure 8 : Floor and ceiling temperature

5. CONCLUSION

According to the simulations, the following comments about the code MAGIC can be given :

- If the target is into the plume, we have a simplified prediction of the target temperature.
- The use of cable target gives better information than the use of a simple target.
- The mechanical ventilation model is an important parameter in this benchmark because it controls the rate of heat release.
- Target centerline temperature = 260°C

According to the criteria for cable damage given by the benchmark (centerline temperature of 200°C), cable damage is observed in this additional case.

According to the different cases of the benchmark, it should be interesting to define more sensitive case for models.

In part I, a higher rate of heat release should be used with a parameter study leading to the ignition or non-ignition of the cable.

In part II, lower source height and ventilation in the hot layer should be used for occurrence of damage criteria.

Appendix F: Benchmark Analysis with COCOSYS, Walter KLEIN-HESSLING, GRS, Germany

Technische Notiz

TN – KLH 2/2000

COCOSYS Calculations for Benchmark Exercise #1
Cable Tray Fires of Redundant Safety Trains

International Collaborative Project to Evaluate Fire
Models for Nuclear Power Plant Applications

W. Klein-Heßling

11. Dezember 2000, Revision 0

1   Introduction

The objective of the fire modelling analyses in a probabilistic risk analysis (PRA) is to estimate the conditional probability of safe-shutdown equipment damage given a fire. Fire modelling results are necessary in order to make this estimate. In the "International Collaborative Project to Evaluate Fire Models for Nuclear Power Plant Applications" different fire codes will be compared and the applicability of the codes for typical questions rising up in PRA's will be evaluated. From the results gained a consensus report will be developed by the participants. The report will be in the format of a user's guide for applying fire models for NPP fire safety design and assessment.

For the comparison of the codes a first benchmark exercise (see Appendix A) has been set up. This benchmark consists of two parts: a trash bag fire to analyse the possibility for an ignition of a cable tray for various distances to the tray, and a cable tray fire to evaluate the possibility of a damage of another tray in a certain distance or on certain evaluations. The comparison between codes can be used to understand the modelling of the physics in them. In project following codes are used (by different institutions): FLAMME-S (IPSN), CFAST (NRC, NIST, VTT, BRE/NII, ???), COCOSYS (GRS), CFX (GRS), MAGIC (EDF), JASMINE (BRE/NII) and WPIFIRE (WPI).

In this technical note the COCOSYS results will be presented.

2   Containment Code System COCOSYS

The Containment Code System (COCOSYS) is being developed and validated for the comprehensive simulation of severe accident propagation in containments of light water reactors [1, 2, 3]. This system is to allow the simulation of all relevant phenomena, containment systems and conditions during the course of design basis accidents and severe accidents. In COCOSYS, mechanistic models are used as far as possible for analysing the physical and chemical processes in containments. Essential interactions between the individual processes, like e.g. between thermal hydraulics, hydrogen combustion as well as fission product and aerosol behaviour, are treated in an extensive way. With such a detailed approach, COCOSYS is not restricted to relevant severe accident phenomena, but will also be able to demonstrate interactions between these phenomena as well as the overall behaviour of the containment.

The complete system is divided into several so-called main modules (Fig. 2-1). Each main module is a separate executable program used for specified topics of the whole process. Between these main modules the communication is realised via a driver program using PVM [4]. The separation into different main modules considers that the strongest coupling between the main modules is on the time step level to avoid a high-frequency data transfer. The amount of data transferred is relatively small, due to a suitable distribution of the complete topology and topics of the systems to the different main modules. The complete separation into several executable programs inhibits side effects from one to other modules. Furthermore, the maintenance effort of the complete system decreases significantly. To reduce the complexity of the whole system, a direct communication between the different main modules is not used. For future versions this concept will be extended to realise parallelism on the main module level.
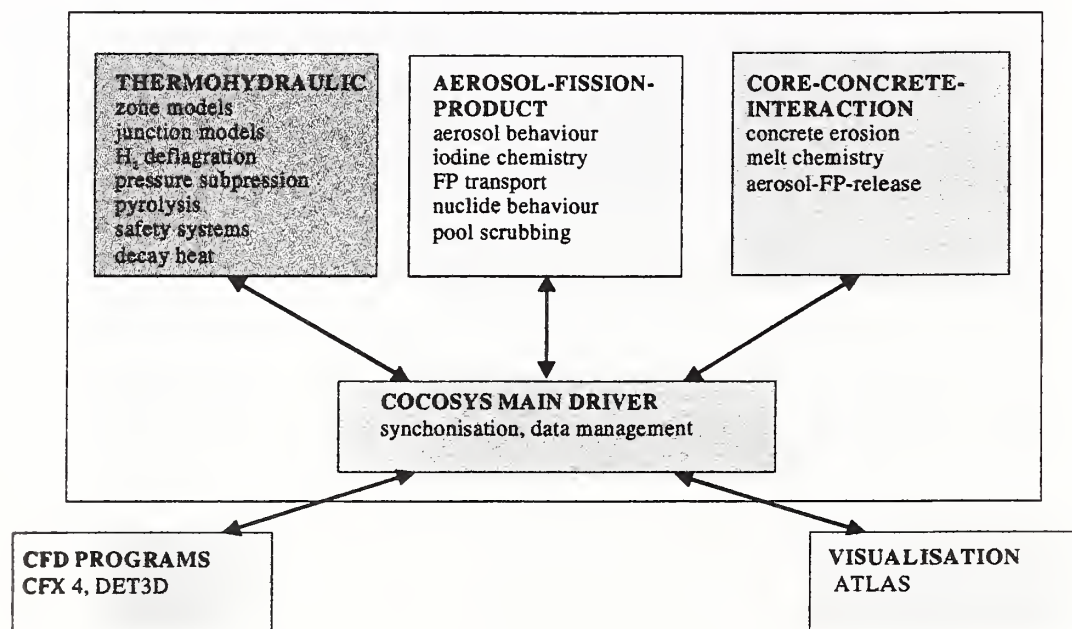

Figure 2-1   Structure of COCOSYS

2.1   Thermal hydraulic main module

The compartments of the considered power plant (or other building types) have to be subdivided into control volumes (zones). The thermodynamic state of a zone is defined

by its temperature(s) and masses of the specified components. This is the so-called lumped parameter concept. The momentum balance is not considered. To realise more complex boundary conditions or processes, a flexible program and data structure is installed. For example, each zone can be split into several so-called zone parts.

The thermal hydraulic main module contains different kinds of **zone models**. These are an equilibrium zone model assuming a homogeneous mixing in the control volume, a non-equilibrium zone model simulating an additional sump volume. For the one dimensional simulation of hydrogen deflagration a separate zone model is used, separating the atmosphere in a burnt and unburned zone part. For the simulation of pressure suppression systems the DRASYS zone model can be used, calculating the hydrodynamic behaviour of the water level inside and outside the pipe and the steam condensation processes.

The **junction models** describe the flow interaction between different zones. In COCOSYS, the simulation of gas flow and water drainage is strongly separated, although water can be transported via atmospheric junctions by gas flow and dissolved gases can be transported via drain junctions. For an adequate simulation of the different systems or boundary conditions, specific junction models are implemented, like rupture discs, atmospheric valves, flaps/doors and specific pressure relief valves used in the VVER-440/213 NPPs. For the simulation of water drainage, several models are realised, describing the sump balance, water flow through pipes and along walls. The implemented pump system model is flexible enough to simulate complete cooling systems (like emergency core cooling systems).

The walls, floors and ceilings of the considered building are represented by **structure objects**. The structure objects include all types of metallic and non metallic heat sinks within zones and between them. The heat flux calculation is one-dimensional, solving the Fourier equation. Plate-type as well as cylinder-type structures can be simulated. The whole wall (heat slab) can be subdivided into layers. Their thermodynamic state is defined by a layer temperature. The arrangement of layers can be chosen freely. Gaps inside a structure are possible, too. The heat exchange between structures and their assigned zones are calculated via convection, condensation or radiation (including wall-to-wall) heat transfer correlations. In these correlations, averaged properties (valid until 3000°C) of the specified components are used. The initial temperature profile and the boundary conditions to the zones can be directly defined by the user.

For a realistic simulation of a severe accident propagation, a detailed modelling of the **safety systems** is important. The THY main module can simulate cooler (including intermediate cooling circuits), spray systems, fan and air conditioning systems, ice condensers and catalytic recombiner systems. Especially for the last topic, a detailed one-dimensional model has been developed.

2.2 Aerosol-fission-product main module

The COCOSYS aerosol-fission-product (AFP) main module is used for best-estimate simulations of the fission product behaviour in the containment of LWRs. Both the thermal hydraulic (THY) and the aerosol-fission-product (AFP) main module consider the interactions between the thermal hydraulics and aerosol fission product behaviour.

The **aerosol behaviour** inside a control volume is solved with the FEBE integration package zone by zone. The condensation on aerosols is solved using a multi-grid method [5]. Especially for hygroscopic aerosols, a very tightly coupled feedback on the thermal hydraulic (especially for the saturation degree) can be considered. The transport of aerosols between the control volumes is solved in a tight way (on time-step level), according to the calculated flow pattern of the THY part. For relative large particles, a different transport velocity is calculated. Heat transfer and condensation influence the deposition rates on wall structures. AFP can calculate up to eight different aerosol components, with their own chemical characteristics and size distribution.

The **FIPHOST** module calculates the transport of fission products carried by so-called hosts in the containment (Fig. 2-2). The mobile hosts are gas, aerosol and water, the immobile hosts are the surfaces in atmospheric and sump spaces. The transport of the hosts will be calculated in other parts of COCOSYS. FIPHOST can handle an arbitrary number of fission product elements, isotopes and/or chemical species in multi-compartment geometry with arbitrary atmospheric and liquid flows between the compartments. All relevant transfer processes of the fission products between hosts are modelled: aerosol depletion by natural processes and by engineered systems like filters, recombiners or spray systems, wash-down from walls into sumps, etc. Host changes as a consequence of chemical reactions or the decay of radioactive isotopes are also taken into consideration.
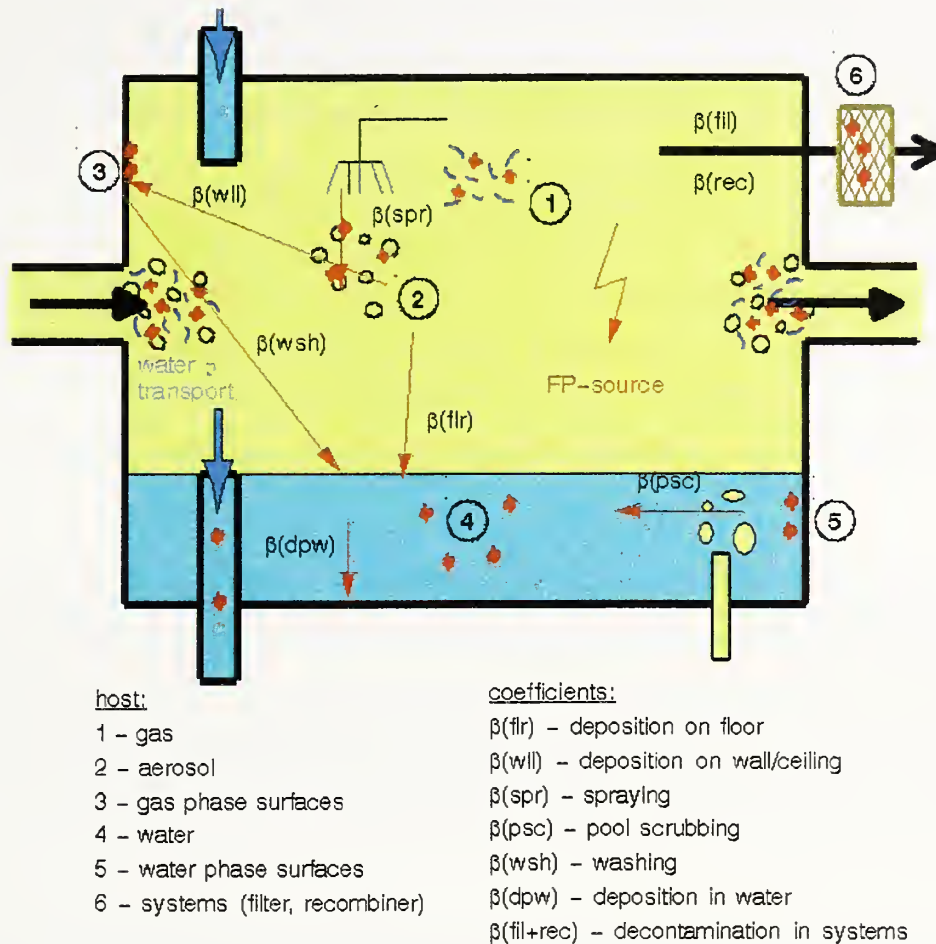
host:
1 – gas
2 – aerosol
3 – gas phase surfaces
4 – water
5 – water phase surfaces
6 – systems (filter, recombiner)

coefficients:
$\beta(flr)$ – deposition on floor
$\beta(wll)$ – deposition on wall/ceiling
$\beta(spr)$ – spraying
$\beta(psc)$ – pool scrubbing
$\beta(wsh)$ – washing
$\beta(dpw)$ – deposition in water
$\beta(fil+rec)$ – decontamination in systems

Figure 2-2   FIPHOST control volume, fission product hosts

Using the **FIPISO** module, the behaviour of all nuclides relevant for the mass transport and heat release in the containment can be simulated. FIPISO considers the core inventory of the reactor at the initial accident time and calculates the decay of the activity and the decay heat release according to established nuclide libraries and packages for up to 1296 isotopes inside each zone separately. The transport of isotopes is calculated by the FIPHOST module. The FIPISO module uses the implicit solution method ORIGEN with the exponential matrix method [6]. To reduce calculation time, FIPISO will compress the libraries to the relevant nuclides for the specific cases. Depending on the first release time, usually about 400 to 600 isotopes are considered. The core inventory has to be pre-calculated by other GRS programs. The user can mix the specific core inventory using different inventory files. The results are used for the calculation of decay heat release. The code distinguishes between alpha/beta and gamma radiation.

According to the position (host) of the nuclides, the heat is released in the corresponding zone part (atmosphere, sump) and wall structure, respectively. The heat distribution inside the wall structure is calculated according to the energy spectrum of the nuclides.

The **iodine** calculations include 70 different reactions. The iodine transport process between water and gas is taken into account. The aerosol behaviour of the particulate iodine species can be calculated by the aerosol calculation part of COCOSYS. The retention of aerosols from a carrier gas conducted through a water pool is determined by SPARC model. Thus, for example, **pool scrubbing** in the suppression pool of a boiling water reactor can be simulated.

2.3   Core-concrete-interaction main module

In case of a reactor vessel failure during a severe accident, the molten core would drop onto the concrete base structure of the reactor building. The interaction of the core melt with concrete would continue for a long period of time. The COCOSYS core-concrete-interaction (CCI) main module is based on a modified version of WECHSL, calculating the **concrete erosion** and the thermodynamics of the core melt. For a very detailed consideration of the **chemical processes** in the melt (mixed or separated option) and the gas, aerosol and fission product release, the XACCI module has been developed. This module uses the equilibrium thermochemical model ChemApp [7]. The XACCI module calculates for each phase and for the atmosphere above the melt the equilibrium conditions for the chemical components. For the future it is planned to improve the modelling of the core melt (e.g. using real geometric boundary conditions) and to introduce models for simulation of DCH and melt relocation.

2.4   Simple cable burning model

For the simulation of fires of cable tray a simplified pyrolysis model has been implemented in the THY main module. This model assumes a constant specific pyrolysis rate $R \left[\dfrac{kg}{sm^2} \right]$ and a propagation velocity $v_{\pm}$ [m/s] in the positive and negative direction. The resulting pyrolysis rate is assumed as:

$$r = Rb \, (d_0 + vt) \tag{7}$$

with the reaction rate r $\left[\dfrac{kg}{s}\right]$, the initial burning length d_0, the width b [m] of the cable tray (Fig. 2-3). The flame propagation depends on the direction of the tray. Therefore the model distinguish between horizontal and vertical cable trays. The propagation velocity may depend on the surrounding zone temperature. For the connection of different cable trays or tray segments the relative position of the connection are given by the user (Fig. 2-4). It is possible to connect the tray segments at each end point (segmentation of cable trays according the control volumes), or to define a crossing of tray segments, or to define parallel tray segments. The user defined distance Δ defines the time needed to propagate from one to the other tray segment

$$t_{prop} = \frac{\Delta}{v_{\pm}}.$$ (8)
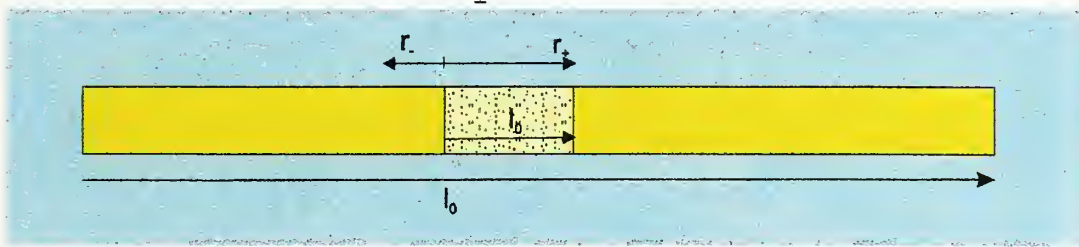
Figure 2-3   Concept of the simple cable pyrolysis model
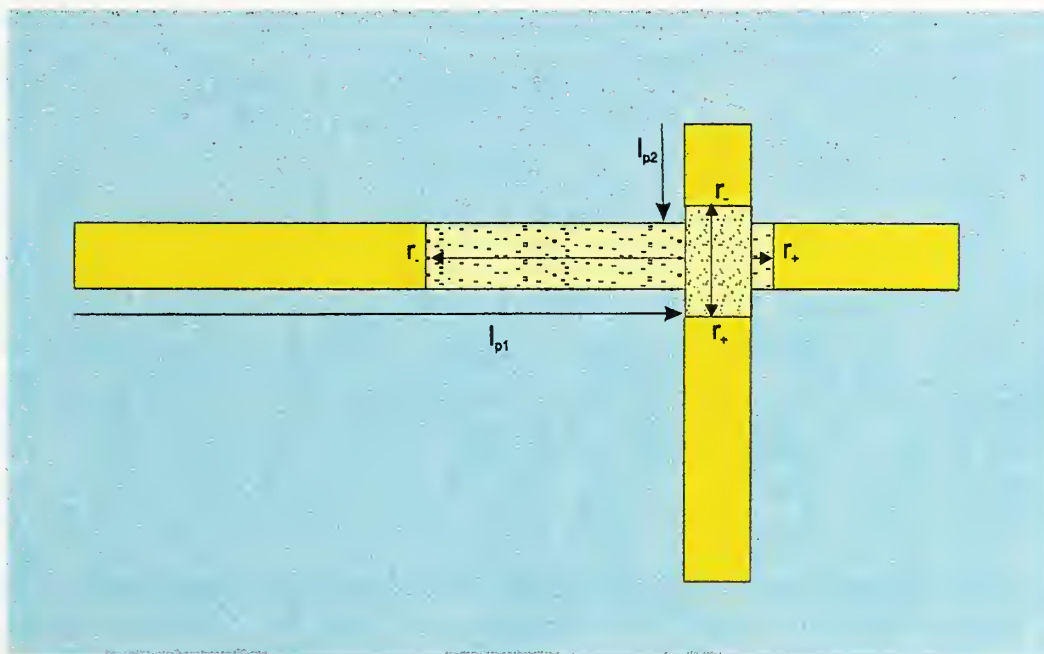
Figure 2-4   Fire propagation along connected cable trays

For a cable tray exist several conditions for ignition or stopping of pyrolysis (Tab. 2-1).

Table 2-1   Criteria for ignition of a cable tray or stop of burning

Reason	Criteria	Time delay
Ignition via signal (user input)	I_0, d_0	-
High zone temperature	T_{ign}	t_{delay}
Ignition via another cable tray	I_0, d_0 (calculated by connection data)	$\dfrac{\Delta}{v_{\pm}}$
Finish due to low zone temperature	T_{out}	t_{out}
Complete burn out	$t \geq t_{e_{\pm}}$	

The simplified cable burning model considers somewhat the thermal hydraulic boundary conditions, but the real temperatures on the cable surface needed for a deterministic calculation of the pyrolysis are not calculated. Especially under low oxygen conditions this model may lead to some deficiencies. Therefore an additional criteria has been introduced for low oxygen conditions to reduce the pyrolysis rate. The considered species in the cable burning model are H_2, HCl, CO and CH_X fractions. As already used in the oil burning model [8] these fractions may combust in the atmosphere or be transported to other regions under low oxygen conditions.

3   Description of Benchmark

The benchmark exercise is split into two parts. For both parts a representative PWR emergency switchgear room is selected. The size of the room is assumed to be 15.2 m long, 9.1 m wide and 4.6 m high. In the first part a trash bag fire is assumed as an initial event. Varying the distance to a target cable, the behaviour of the cable is evaluated. In two cases vented conditions are regarded. In the second part of the benchmark, it is assumed that one tray on the left side is already burning. Varying the evaluation and distance of the target tray, the different temperature evaluations inside the tray are evaluated. In the appendix A the complete description of the benchmark is given.

4   Nodalisation of the compartment

For the simulation of the fire in the compartment defined in the benchmark description, the compartment have to be subdivided into several zones. To be able to simulate stratified conditions several levels of zones (at least 4 levels) have to be used. It has been decided to use one nodalisation for all different cases. Therefore the special requirements, for example the plume simulation above the trash bag and the different locations of the target cables requires further subdivisions of the compartment. At least 8 levels of zones indicated by RA.., RB.. and so on have been defined (Fig. 4-1). Looking on the top view of the compartment a fine grid around the trash bag position have been used. This has been done for all possible positions of the trash bag. For a larger distance to the trash bag and the considered cable trays the grid becomes more rough. The digit number in the zone name indicate the position in x-direction. The last letter from L to Q indicates the position in y-direction. Fig. 4-2 shows the top view of the nodalisation for the different levels. For the levels A to C 27 zones are defined for each level, in the level D and E 37 zones are defined for each level and in the upper levels F to H in total 56 zones are used for each level. The number of zones per level is increased for the higher levels to consider the local effect on the cable trays in these levels. This results into 323 zones in total.

The heat release for the trash bag fire is relatively small. To calculate in detail the plume behaviour additional (cylinder) zones (RTBB to RTBE) above the trash bag have been defined. It has to be pointed out, that a specific plume model using empirical correlations is not implemented in COCOSYS. Therefore the plume behaviour have to be simulated via a more detail nodalisation around the fire position.

The zones inside the fire compartments are connected using atmospheric junctions. The cross section of these junctions results from the geometry. The resistant coefficient used are taken from validation calculations against different experiments (e.g. integral HDR experiments).

To simulate the door behaviour and leakage atmospheric junctions are defined to the environment. For the environment the same subdivision of different levels is defined. It is important to use the correct static total pressure for these zones. In the given configuration, this results in four atmospheric junctions for the open door (see side view in Fig. 4-1) and one addiional junction for the leakage. With these four junctions it is possible to calculate counter current flows through the door.
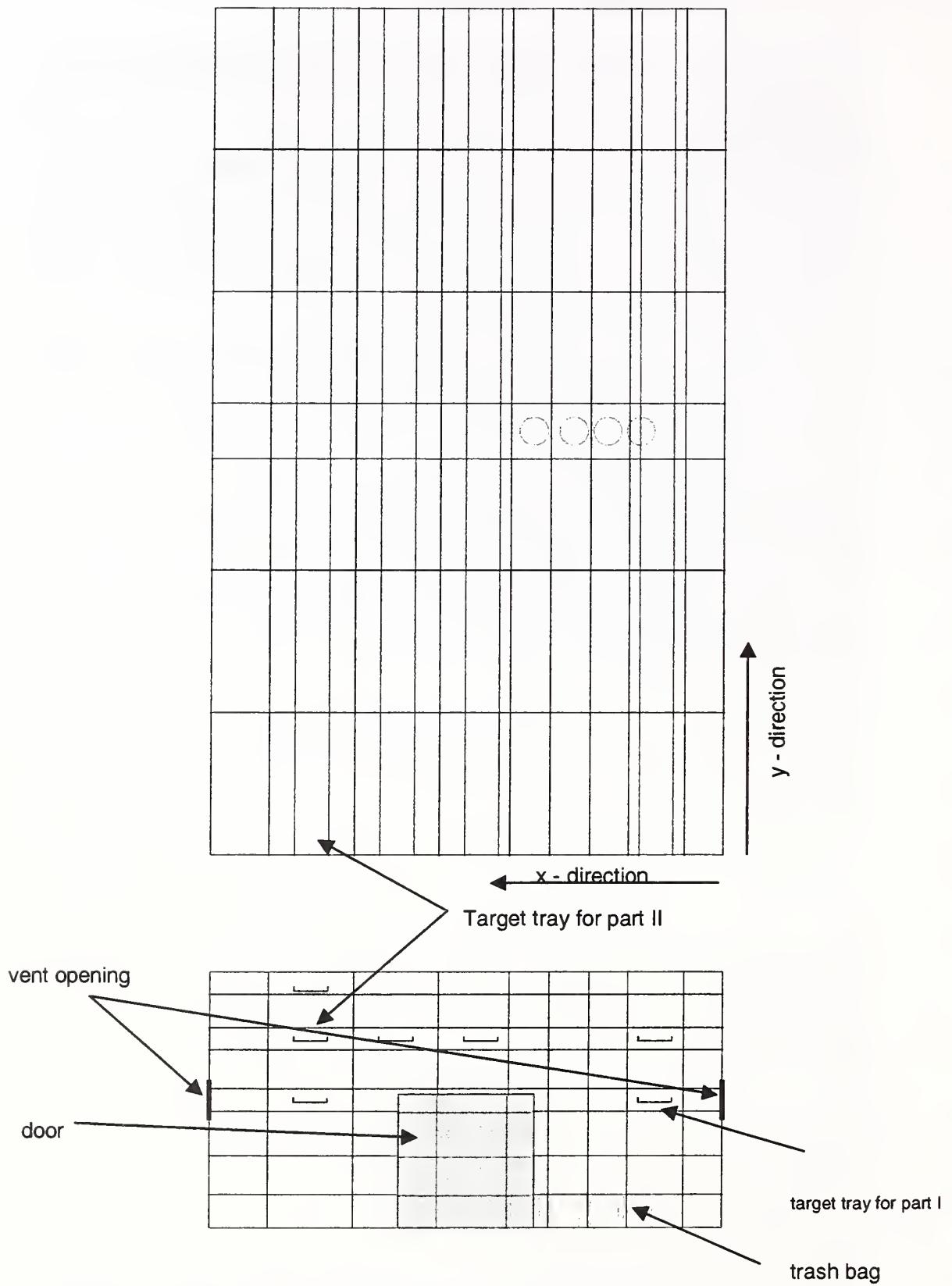
Figure 4-1 Overview of the nodalisation of the fire compartment

Figure 4-2 Nodalisation in different levels

The ventilation system is simulated by a fan system with a constant volume flow rate. It is assumed that the fan injects fresh air through the right vent opening. On the left side three atmospheric junctions are defined. The use of atmospheric junctions avoids an over or under pressure of the fire compartment.

As a boundary the concrete wall structures and the door are simulated by the structure objects as defined in the benchmark description. As defined in the benchmark description a constant heat transfer coefficient of 15 W/mK is used, although this value seems to be very high. Usually in COCOSYS calculations a combination of correlation describing free and forced convection, condensation and radiation is used.

The trash bag fire is simulated as a heat injection in the zone above the trash bag. This is possible, because the oxygen consumption is relatively small. The oxygen consumption due to the fire, is simulated by an extraction of oxygen and a corresponding CO_2 injection in the zone above the trash bag. To simulate the radiation fraction, especially the heat up of the target by radiation, a given fraction of 0.3 is released as radiative heat. For the distribution of this heat view factors are used. These view factors (especially between the flame and the target cable) are pre-calculated by a tool using a Monte-Carlo method. Therefore for different distances between trash bag and target cable different view factors are used.

For the calculations of part II, the heat release is assumed at the cable tray C2. The heat release is much larger and the oxygen consumption may influence the fire. Therefore for these cases the simple cable pyrolysis model is used. The pyrolysis rate is given by input according to the given heat release rate and distributed homogeneously over the whole cable length. This model calculates the release of pyrolysis fractions (here H, HCl, CH_x) according to the composition of the burning material. The burning process is calculated by the detail models, considering the available oxygen concentration. Because the cable tray C2 is not simulated by structure objects, view factors can not be defined and therefore the radiation fraction of heat release is not considered. Additionally the release of pure carbon fraction (as soot) is not possible.

The target cable is simulated as a cylinder type structure with a diameter of 5 cm. The heat conduction is calculated one-dimensional. Therefore the surface temperature is the same on the top and the bottom of the cable. In CFD calculations different temperatures are calculated, because only the bottom of the cable is directed to the fire. The target cable is subdivided in nine layers. So the centerline temperature can be calcu-

lated. The length of the cable is subdivided according to the subdivision of the fire compartment, leading to 7 cable segments (TCABLEL to TCABLER). The target cable in the room centre is named TCABLEO. In the case 1 of part 1 the trash bag is more or less direct below the target cable. To consider in detail the plume effect the target cable is further subdivided into two parts (TCABLEO and TCABLEO2)

5   Results for Part I

First the results of the base case (trash bag fire with a distance of 2.2 m to the target) are discussed. Then the case 1 to 3 with different distances to the target are compared with the base case. After this the cases with vented conditions (case 4 open doors and case 5 active ventilation system) are compared with the base case. To reduce somewhat the effort, only the results specified in the benchmark description are discussed. The fire compartment temperatures and concentrations shown are taken from the room centre. Because 8 level of zones are defined 8 curves are presented. The depth of the hot gas layer is not presented, because it is not a direct result of the COCOSYS calculation. The heat release rate is here the specified rate. The heat loss to the boundaries are presented only for the closed conditions.

5.1   Base case

First the results of the base case will be presented. The effect of the burning trash back is simulated as a heat injection in the zone RTBB surrounded by the zone RB5O. To simulate the oxygen consumption the corresponding mass of oxygen is removed and CO_2 is injected. The hot gas moves upward leading to a temperature stratification in the atmosphere. In Fig. 5-1 the zone temperatures of the room centre is presented. The maximum calculated temperature is about 450 K. The behaviour of the temperature corresponds to the heat injection rate, presented in Fig. 5-2. The oxygen consumption due to trash bag fire is relatively small. Therefore the oxygen concentration is only slightly reduced (Fig. 5-3). The concentration shows a stratification corresponding to the temperature stratification. In Fig 5-4 the leakage rate through the door is plotted. In the first phase with high heat release the leak flow is directed to the environment. Later the heat release is not high enough to compensate the heat loss into the concrete walls. Therefore the temperatures are decreasing leading to a leak flow into the fire compartment.
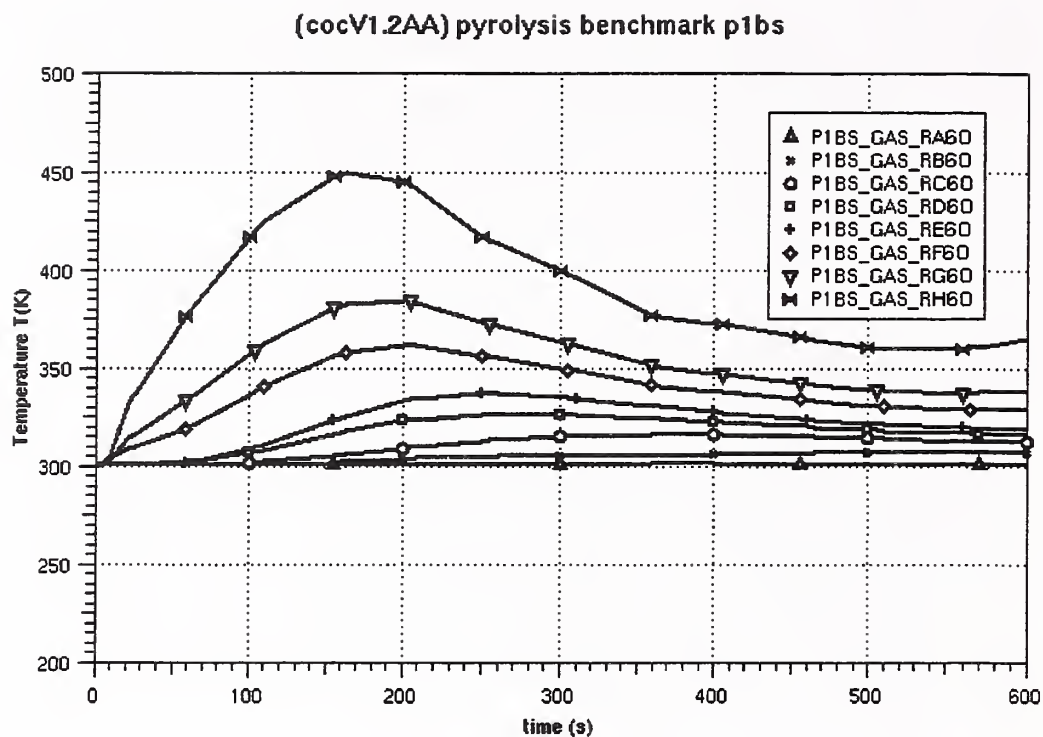
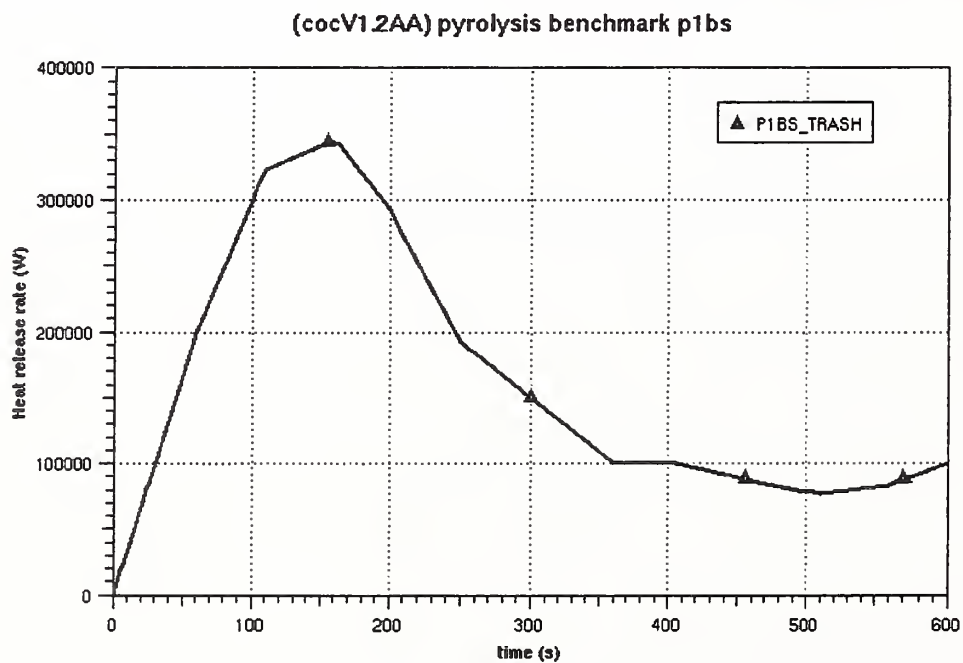**Figure 5-1** Temperature stratification in the centre of room

Figure 5-2 Heat release rate

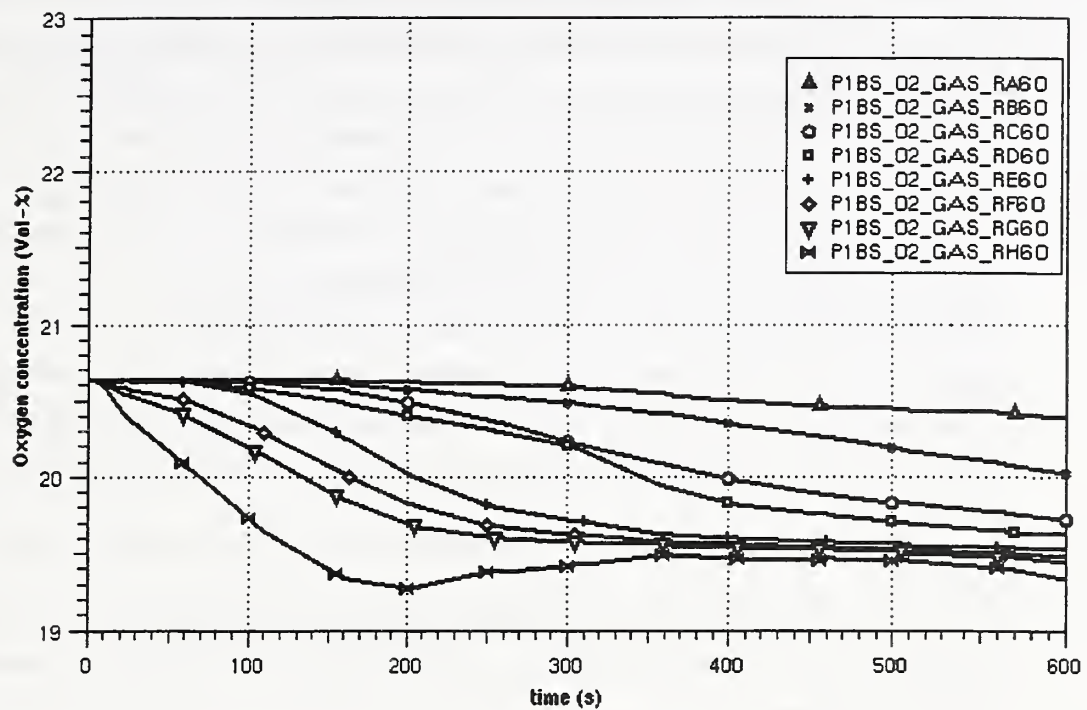## (cocV1.2AA) pyrolysis benchmark p1bs

Figure 5-3 Oxygen concentration in the room centre
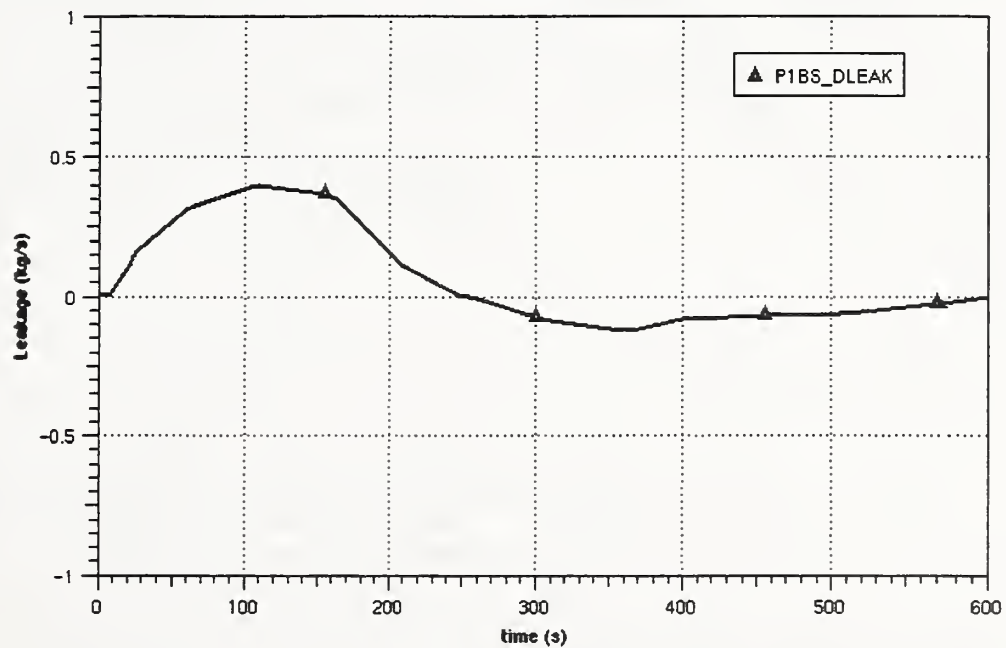
(cocV1.2AA) pyrolysis benchmark p1bs

Figure 5-4 Leak mass flow rate through the door

Fig 5-5 presents the heat flux in [W/m] into the target cable. The red curve corresponds to the total heat flux into the target and the black curve shows the fraction due to radiation. In the initial phase the main fraction is determined by the radiation, because the atmosphere around the target cable is not heated up yet. Later the heat flux is mainly caused by the convective heat transfer. In this situation the atmosphere is still hotter than the target surface but the heat release is reduced. The heat release is relatively small leading to a moderate temperature behaviour. Therefore the surface temperature rise up only about 12 K (Fig. 5-6). Due to the low heat conductivity of the (full) PVC cable and the short time period, nearly no reaction on the centerline temperature is observed. Fig. 5-7 shows the heat loss into the concrete structures. Comparing this with the total heat release, about 70% of the total heat injection is transferred into the concrete structure. To be more realistic the given constant heat transfer coefficient of

$15 \left[\dfrac{W}{m^2 K} \right]$ should be replaced by a free convection correlation resulting usually to

lower values (especially for the floor structures). The curve presented in Fig. 5-7 looks somewhat curious. This is due to the numerical derivation of the plot data with relatively large time step sizes.
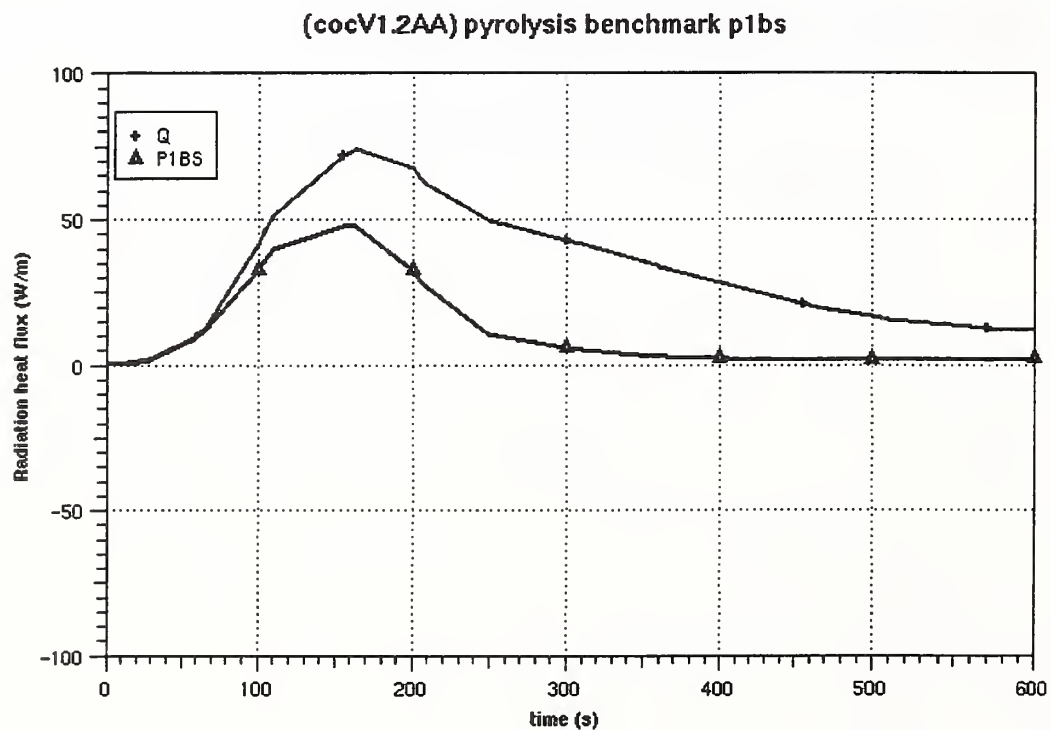
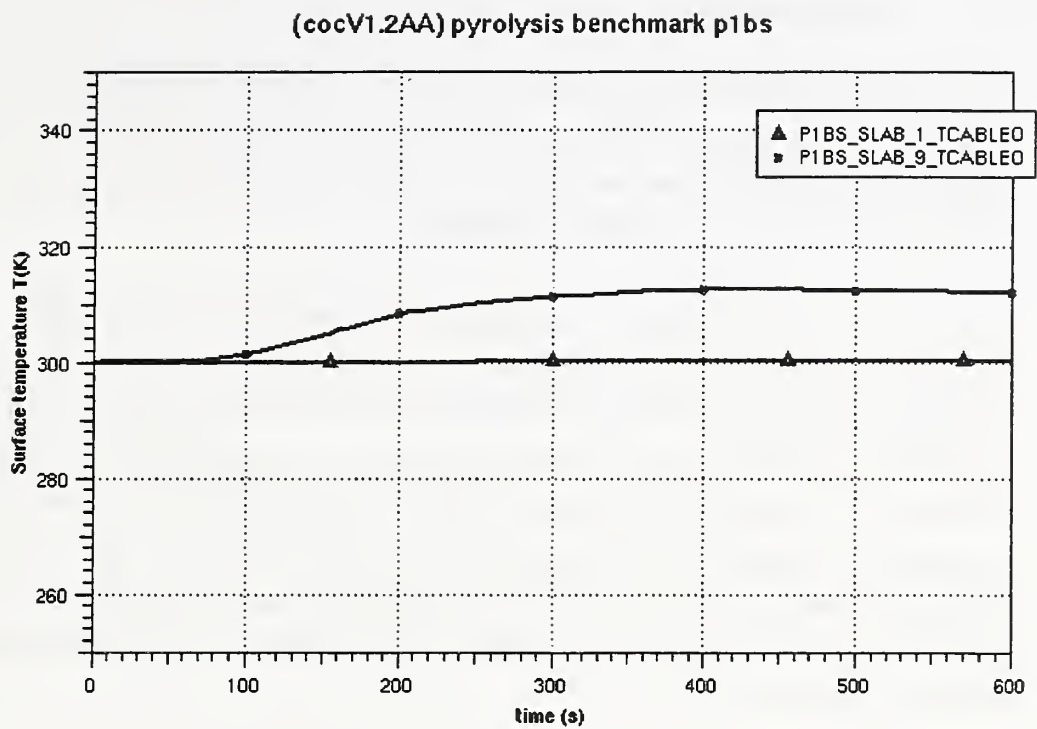
Figure 5-5 Radiation heat flux on the target

(cocV1.2AA) pyrolysis benchmark p1bs

Figure 5-6 Target surface and inner temperature

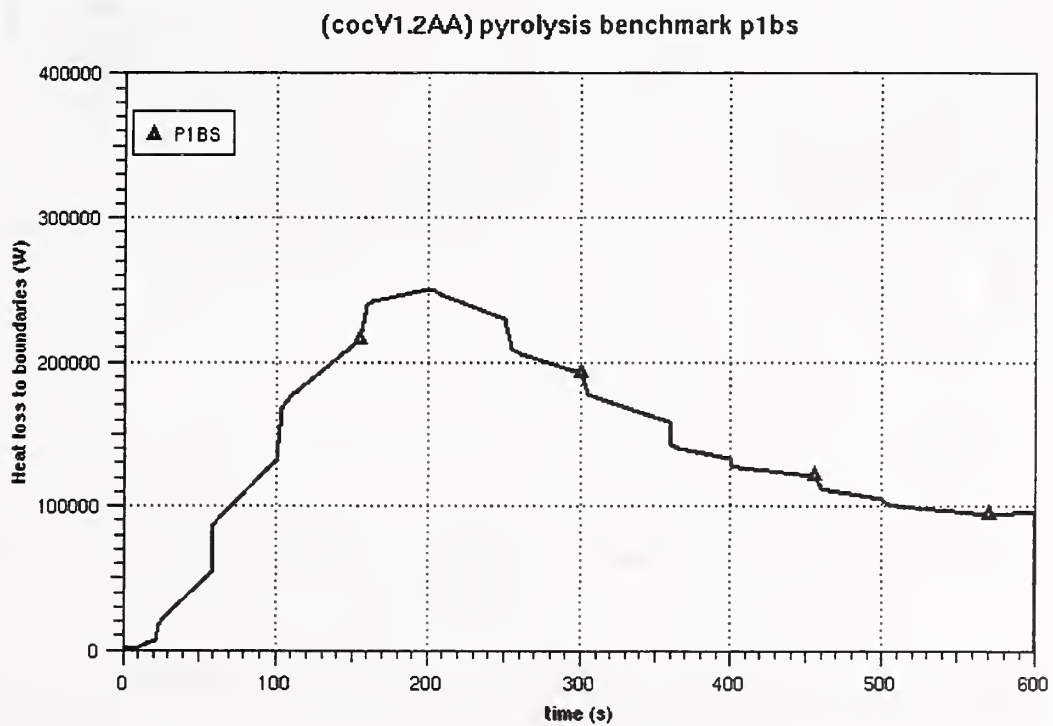**(cocV1.2AA) pyrolysis benchmark p1bs**

Figure 5-7 Total heat loss to boundaries

5.2   Case 1 to case 3

In the following the results of the cases 1 to 3 will be discussed in comparison to the base case. In these cases the position of the trash bag is shifted to the direction of the target. The nodalisation is detailed enough to consider this shift of the trash back. For each case the view factors have been recalculated.

Fig. 5-8 shows the temperatures in the highest zone RH6O in the room centre. Here the case 1 (red curve), where the trash bag is more or less below the target, but more far away from the centre leads to the lowest temperature. Also the results for the oxygen concentration (Fig. 5-9) are consistent according to the distance between the trash bag and the room centre. The leakage rate (Fig. 5-10) is practically the same for all four cases. This underlines that the overall behaviour and especially the pressure built up due to the trash bag fire is the same for all considered cases. Additionally the leak position is on the floor level, where the effect of the fire is relatively small. Therefore no differences are expected.

(cocV1.2AA) Pyrolysis Benchmark Part I
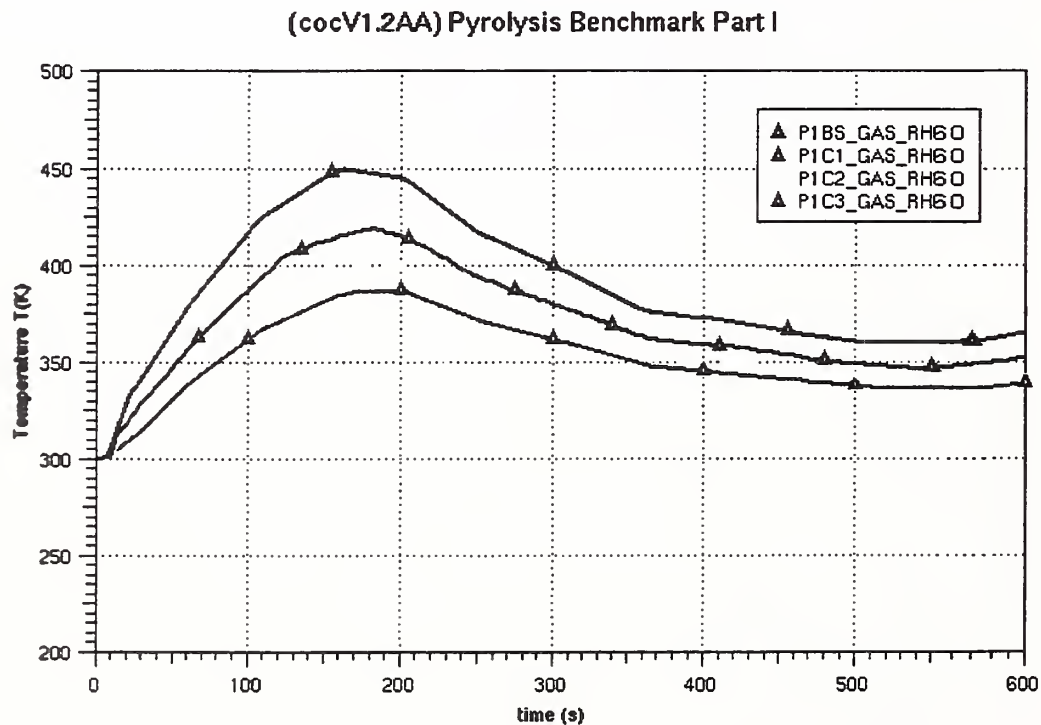
Figure 5-8 Atmospheric temperatures in the centre below the ceiling (RH6O)

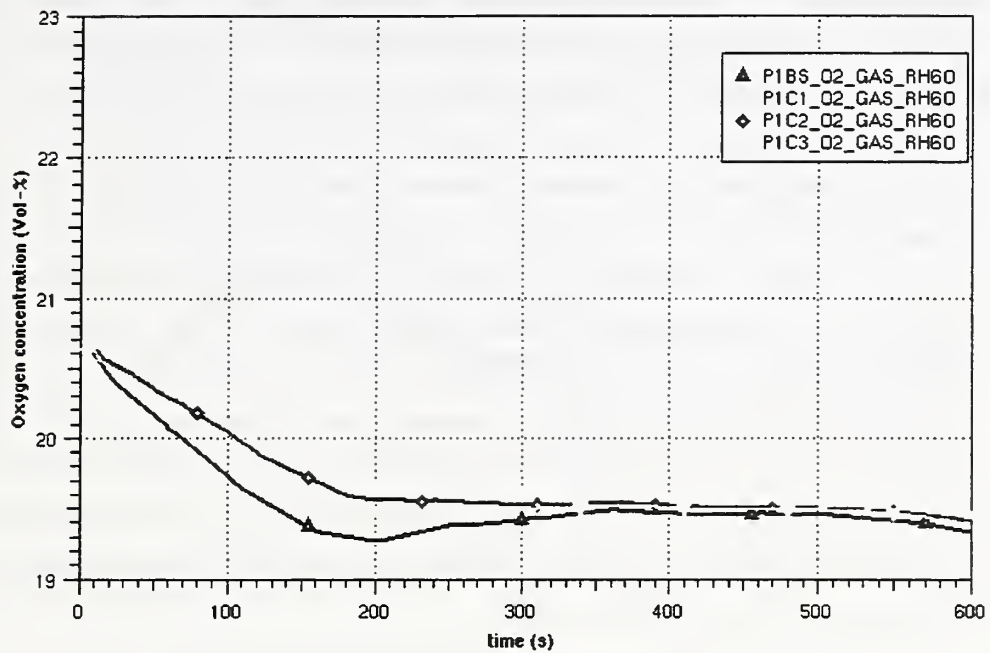**(cocV1.2AA) Pyrolysis Benchmark Part I**

Figure 5-9 Oxygen concentration in the centre of the ceiling (RH6O)

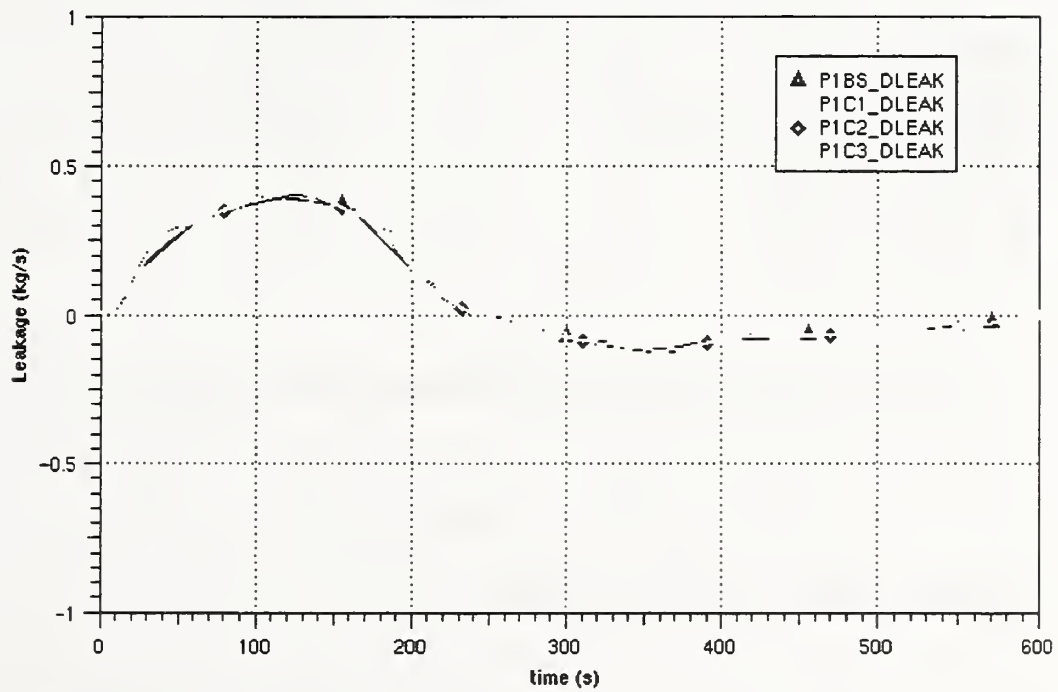**(cocV1.2AA) Pyrolysis Benchmark Part I**

Figure 5-10 Leak flow through door

For the heat flux into the target cable strong differences between the regarded cases can be observed. To simulate the fire plume the zones above the trash bag are further subdivided. An additional zone with the same diameter as the trash bag has been defined above. Therefore an increasing of the fire plume size is not calculated. This leads to similar results (Fig. 5-11 and 5-12) in case the trash bag fire is not below the target cable (blue, black and green curves). Therefore it can be concluded that the effect of the position between the trash bag and the target cable is calculated to strongly. It can be assumed, that the temperatures in case 1 (0.3 m distance) are calculated too high and on the other side the temperatures in case 2, case 3 and the base case may be somewhat to low. The consequences can be seen in Fig. 5-13. Here the calculated surface temperatures are very different between case 1 (about 900 K) and the other cases (about 330 K). Even in the case 1 the ignition temperature of 643 K in the center-line is never reached. Therefore the extrapolation mentioned in the benchmark description cannot be performed. As already mentioned the heat loss to the boundaries should be quite similar for all cases (Fig. 5-14).

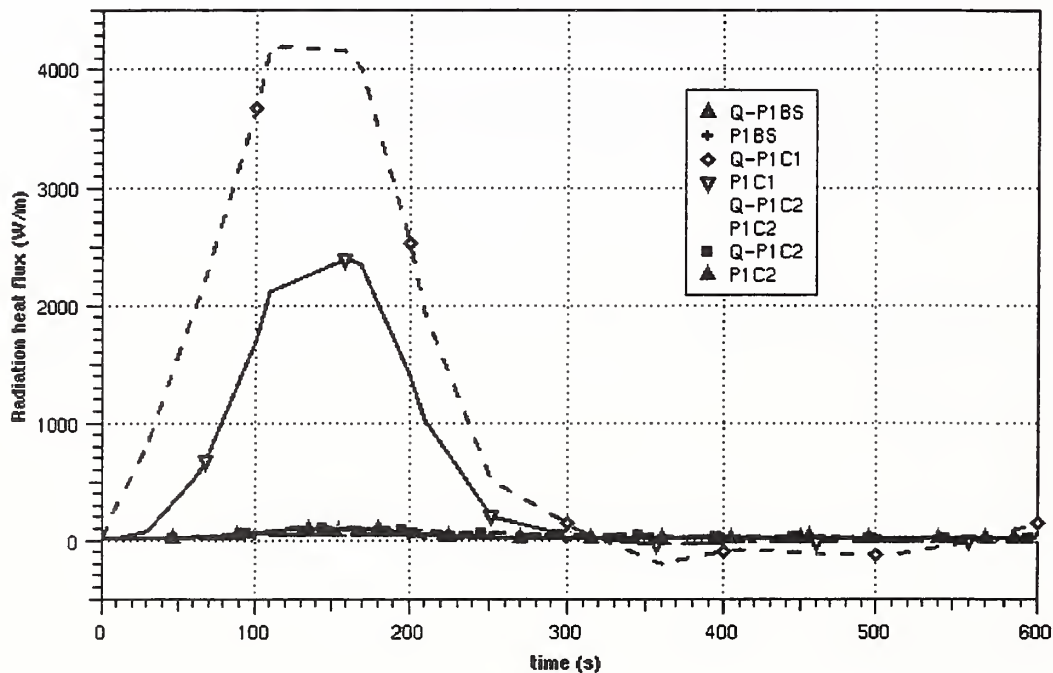**(cocV1.2AA) Pyrolysis Benchmark Part I**

Figure 5-11 Radiation heat flux on the target
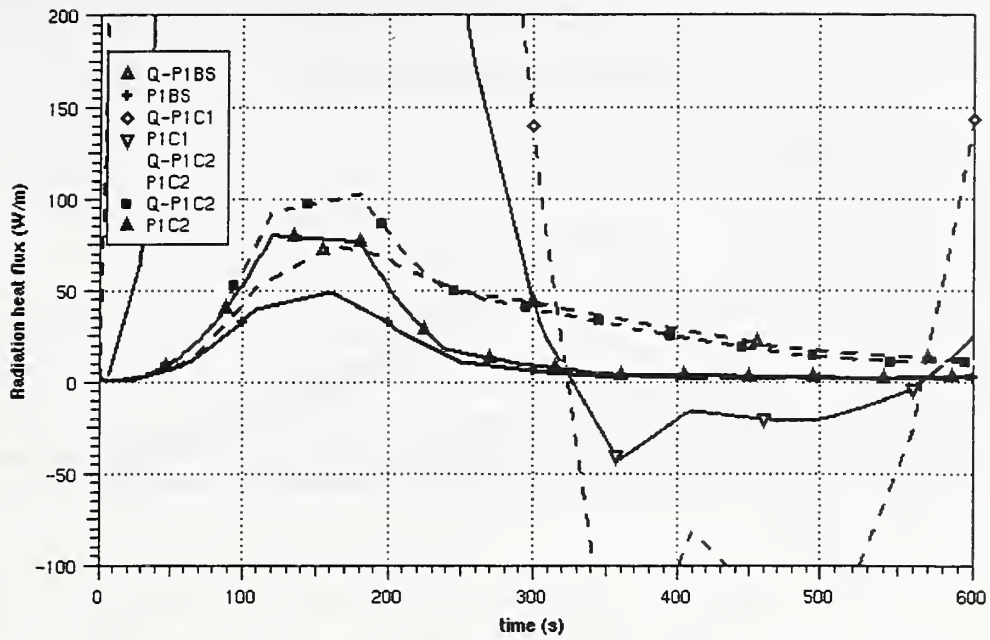
(cocV1.2AA) Pyrolysis Benchmark Part I

Figure 5-12 : Radiation flux on target (detailed view)
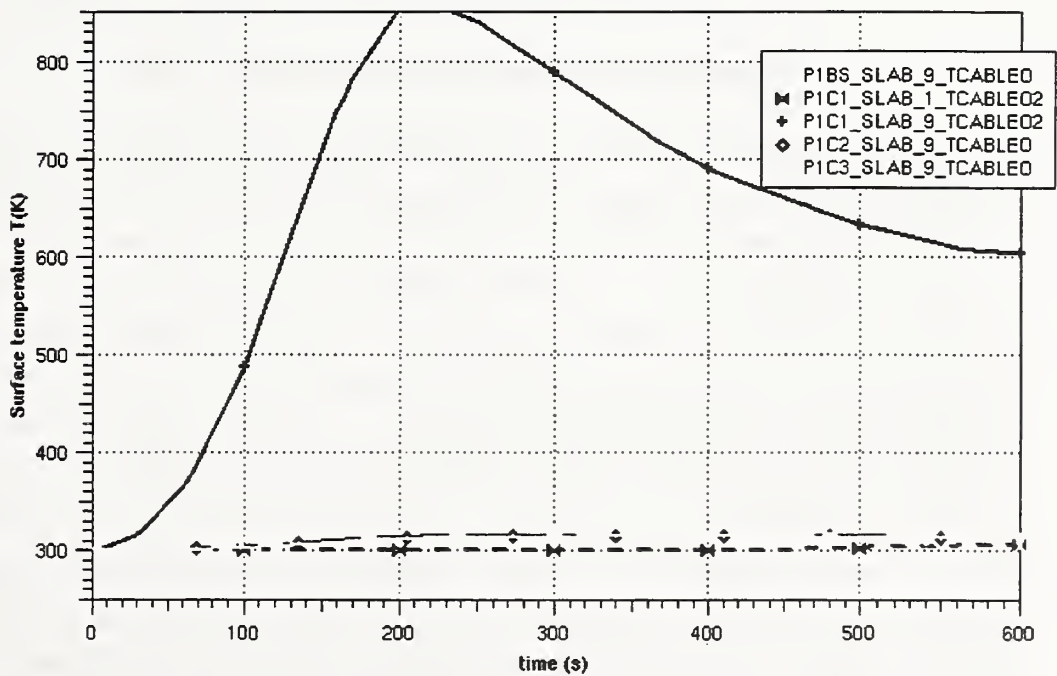
(cocV1.2AA) Pyrolysis Benchmark Part I

Figure 5-13 Target surface temperature

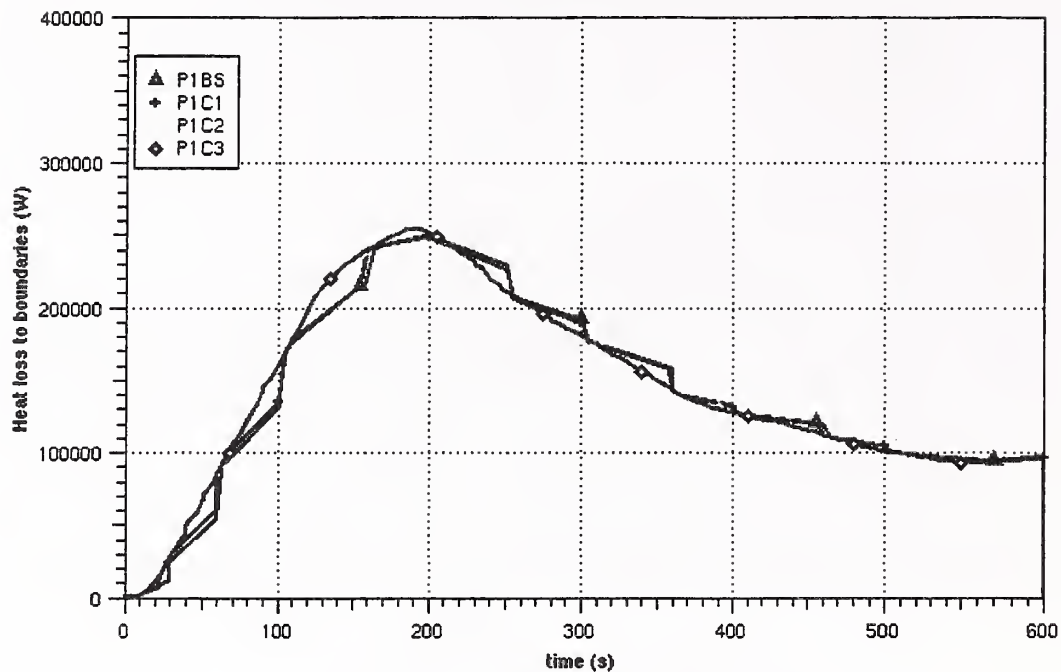**(cocV1.2AA) Pyrolysis Benchmark Part I**

Figure 5-14 Heat loss to boundaries

5.3   Case 4 and case 5: open doors or active ventilation system

In case 4 the door stays open during the whole problem time of 600s. Because the fire is relatively small leading to oxygen rich conditions, the effect on the fire is relatively small. It has to be mentioned, that the fire is simulated via a simple heat injection. There is no feed back from the oxygen concentration on the fire process. The calculated temperatures in the room centre of case 4 are very similar to the base case (Fig. 5-15). Only the temperatures in the lower levels are slightly lower. This is caused by the hot gas removal through the upper part of the door (Fig. 5-18). The behaviour in case 5 with a running ventilation system is very similar. The calculated temperatures (Fig. 5-16) are very similar to the base case. In the vented cases the oxygen concentration is somewhat higher (Fig. 5-17). Fig. 5-18 presents the mass flow rate through the open door for the case 4. The height of the door is subdivided into 4 level of zones. Therefore a counter current flow can be calculated. In the beginning the in all levels the flow rate is directed to the environment. This is due to the heat up and expansion of the atmosphere of the burning room. At about 100s the counter current flow is established.

In the upper part of the door hot gas is moved to the environment and in the lower part of the door cold gas is going into the burning room.
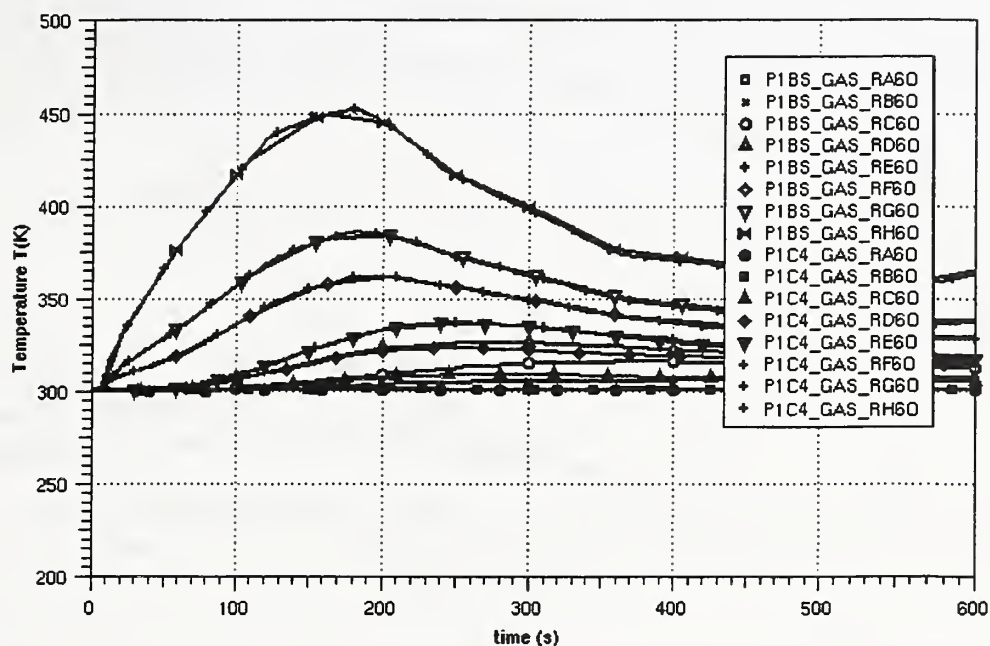
(cocV1.2AA) Pyrolysis Benchmark Part I

Figure 5-15 Comparison of temperatures (open doors)
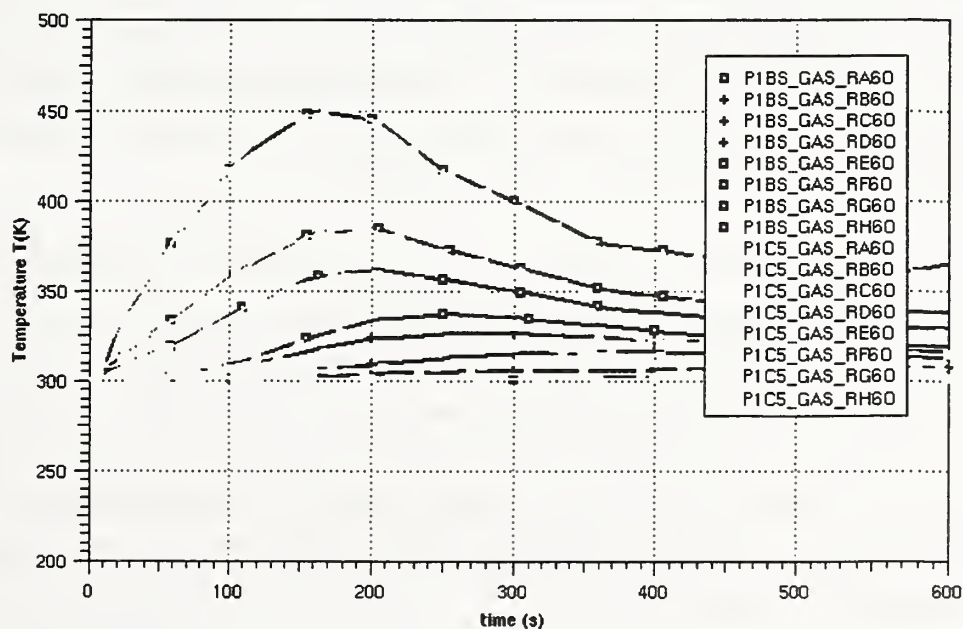
(cocV1.2AA) Pyrolysis Benchmark Part I

Figure 5-16 Comparison of temperatures (ventilation system)
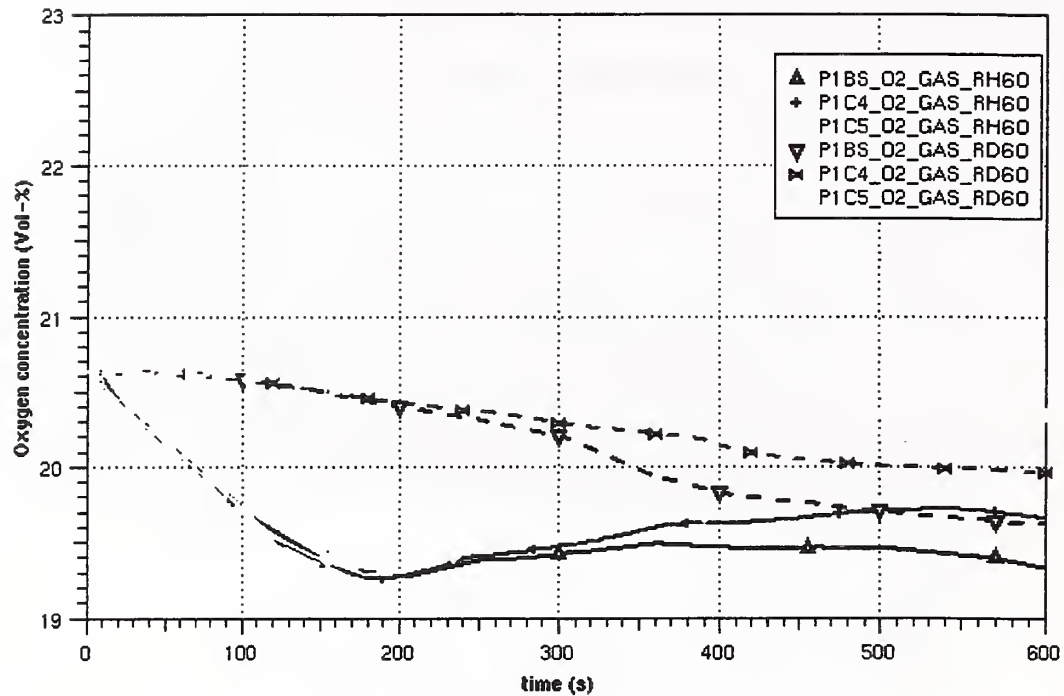
(cocV1.2AA) Pyrolysis Benchmark Part I

Figure 5-17 Comparison of oxygen concentration below the ceiling and on level D

In case 5 fresh air is injected into the burning room through the right vent opening by a fan system with a constant volume flow rate. The vent opening on the left side is opened. On this side usual atmospheric junctions are used, to avoid an over or under pressure inside the fire compartment. In Fig. 5-19 the mass flow rate through is opening is plotted. According to the defined zone levels the vent opening is subdivided into the three part. Therefore three junctions are defined.

In the considered cases 4, 5 and the base case the position of the trash bag is the same. The heat release and the radiation fraction is given by input. Therefore the radiation flux on the target cable should be the same for all cases. This is shown in Fig. 5-20. In the vented cases the atmospheric temperature near the cable are somewhat lower. Therefore the convective heat transfer is different. Especially the case 5 has a lower heat flux into the target cable, because the cold air is injected relatively close to the target cable. These effects lead to the corresponding differences for the surface temperature on the target (Fig. 5-21).
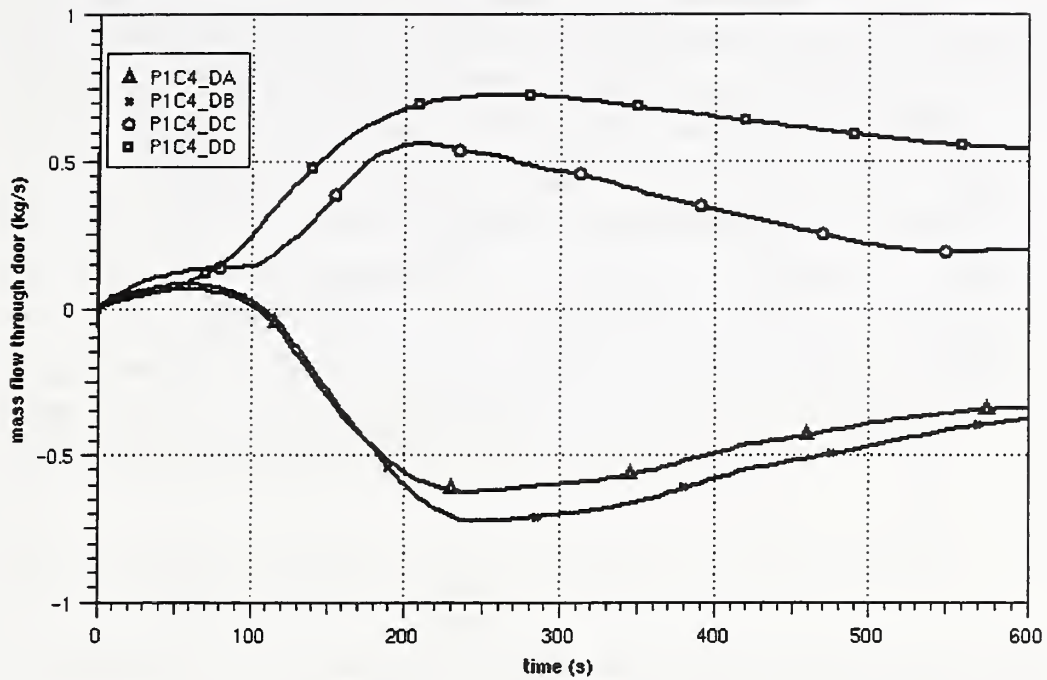
(cocV1.2AA) Pyrolysis Benchmark Part I

Figure 5-18 : Mass flow rate through door (case 4)

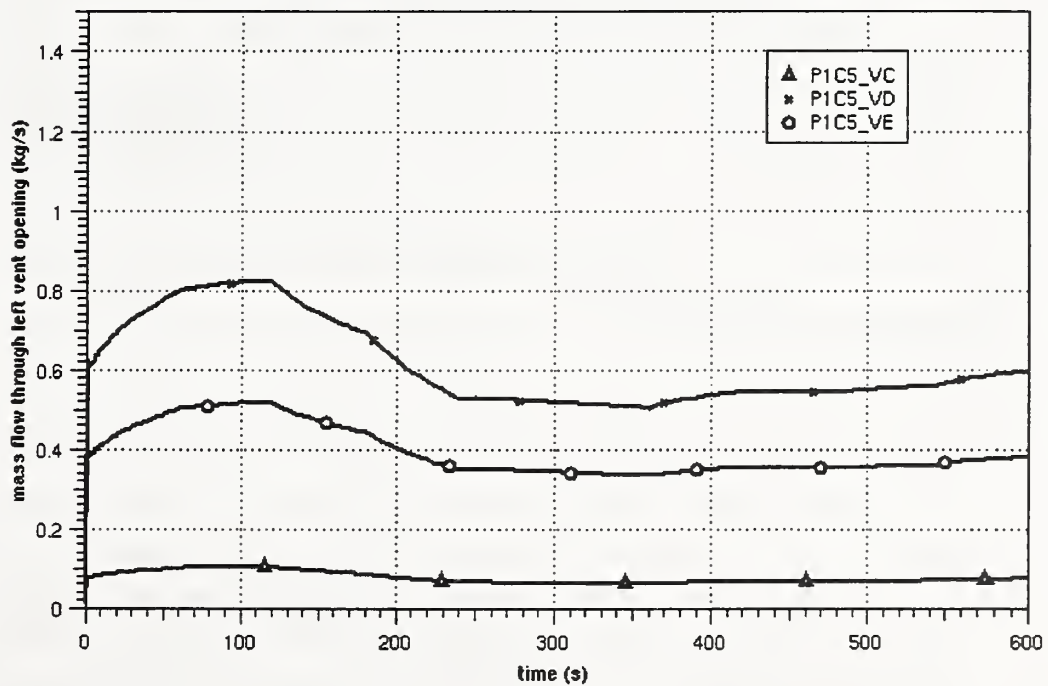**(cocV1.2AA) Pyrolysis Benchmark Part I**

Figure 5-19 Mass flow rate through the left vent opening
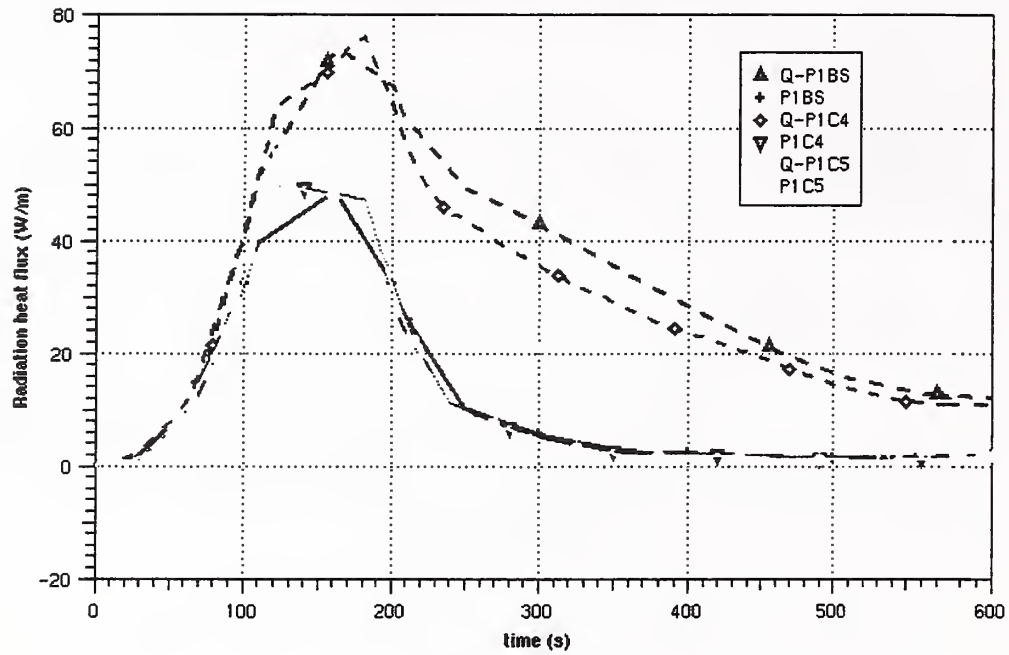
(cocV1.2AA) Pyrolysis Benchmark Part I

Figure 5-20 Total heat flow and radiation flux on the target
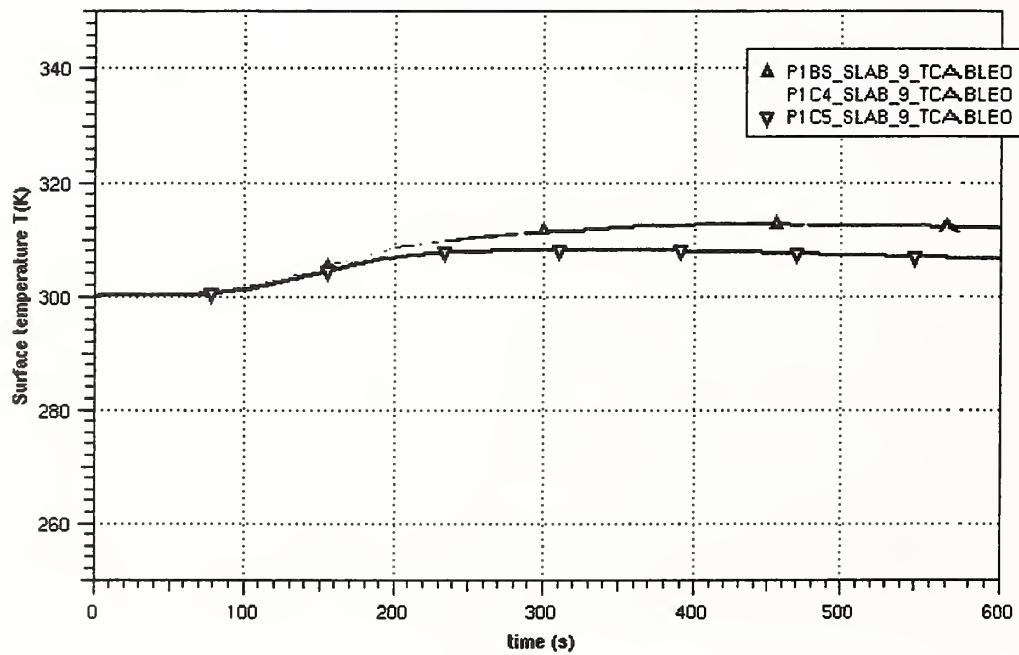
(cocV1.2AA) Pyrolysis Benchmark Part I

Figure 5-21 Surface target temperature

6 Results for Part II

First the base case of the part II of the benchmark is discussed. Here the maximum heat release is 1MW. The distance between the burning and the target tray is 6.1m. There are practically closed conditions. The results presented are corresponding to the previous part. Because the pyrolysis rate is given by input and the burning process is calculated by the models inside COCOSYS the heat release may be lower than the specified heat release. The radiation flux on the target is not considered in these calculations. Instead the total heat flux on the target are plotted. The concentrations of the chemical species CO, CO_2, HCl and unburned CH_X fractions are plotted. The optical density (smoke) is not calculated. To simplify the presentation, sometimes only the upper and lower values at the ceiling or at the floor are plotted.

6.1 Base case

In comparison to the part I the heat release and oxygen consumption are much larger for the situation considered in part II. Because the oxygen concentration should be considered for the burning process, the simple cable pyrolysis model (see 2.4) is used for this calculation. As a boundary condition the pyrolysis rate (derived from the proposed heat release rate) is given by input. This rate is not influenced by other effects. This may result to higher concentrations of unburned pyrolysis fractions. The calculated temperatures (Fig. 6-1) at the ceiling near the room centre rise up to about 700 K. At about 1000 s the temperatures are decreasing again. Here the burning rate is reduced due to the low oxygen concentration. Fig. 6-2 shows the comparison of the calculated heat release due to the cable burning and the proposed heat release underlining the situation. At this time the oxygen concentration below the ceiling falls below at about 4 Vol%. At this concentration the burning of the pyrolysis fractions is strongly restricted. In the COCOSYS calculations the value of 4 % is used instead of the proposed 12 %, due to the gained experience in the code validation. Fig 6-4 presents the leak flow through the door. In the beginning the over pressure due to the heat up is compensated. Under low oxygen conditions the leak flow is moderate indication nearly constant pressure conditions. Using the simple cable burning model up to now a radiation fraction of the heat release due to the burning process could not be considered. Therefore the heat flux into the target cable results from the convective heat transfer only. This may lead to somewhat too low values. Fig 6-5 shows the total heat flux into the target. After a strong heat up of the target, it starts to cool down after about 2250 s.

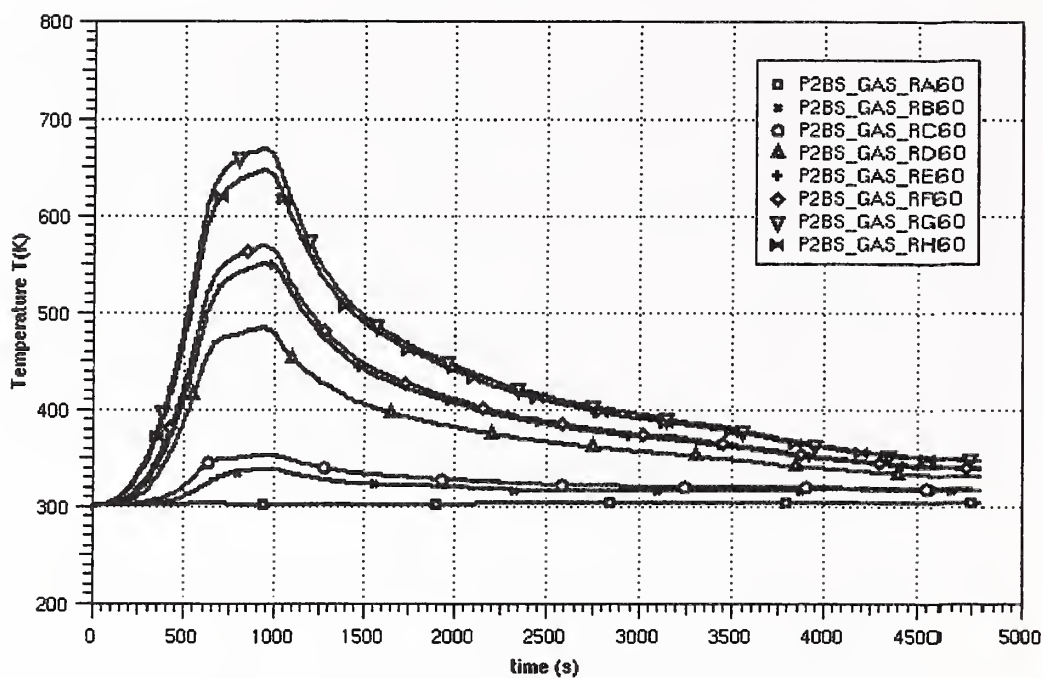## (cocV1.2AA) Pyrolysis Benchmark Part II

Figure 6-1 : Temperature profile in the room centre

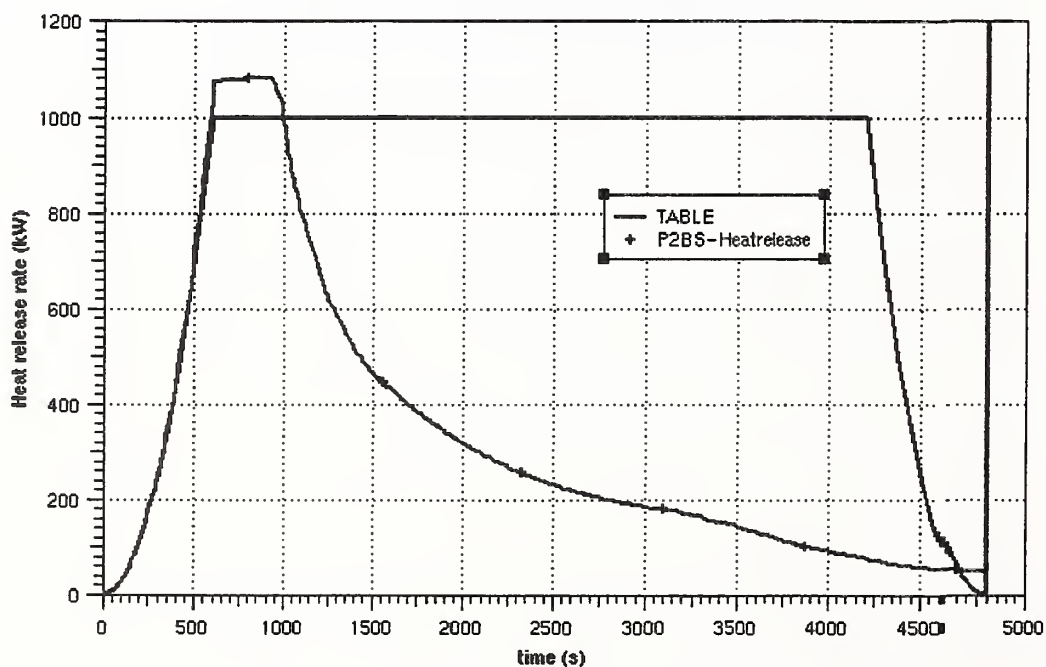## (cocV1.2AA) Pyrolysis Benchmark Part II

Figure 6-2 Heat release
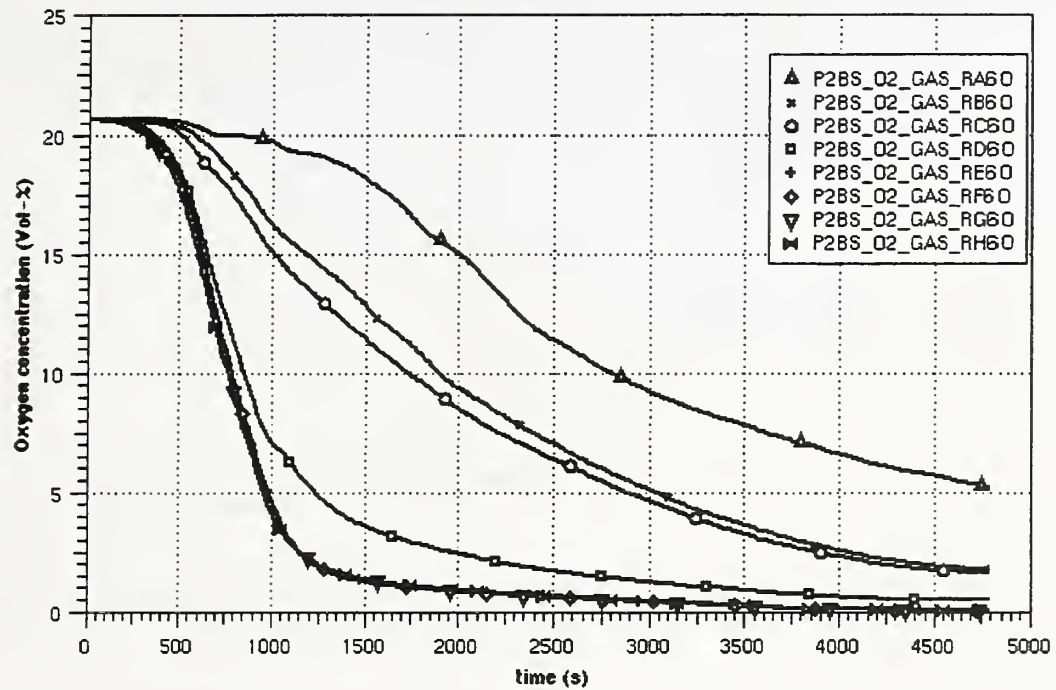
(cocV1.2AA) Pyrolysis Benchmark Part II

Figure 6-3 Oxygen concentration in the room centre

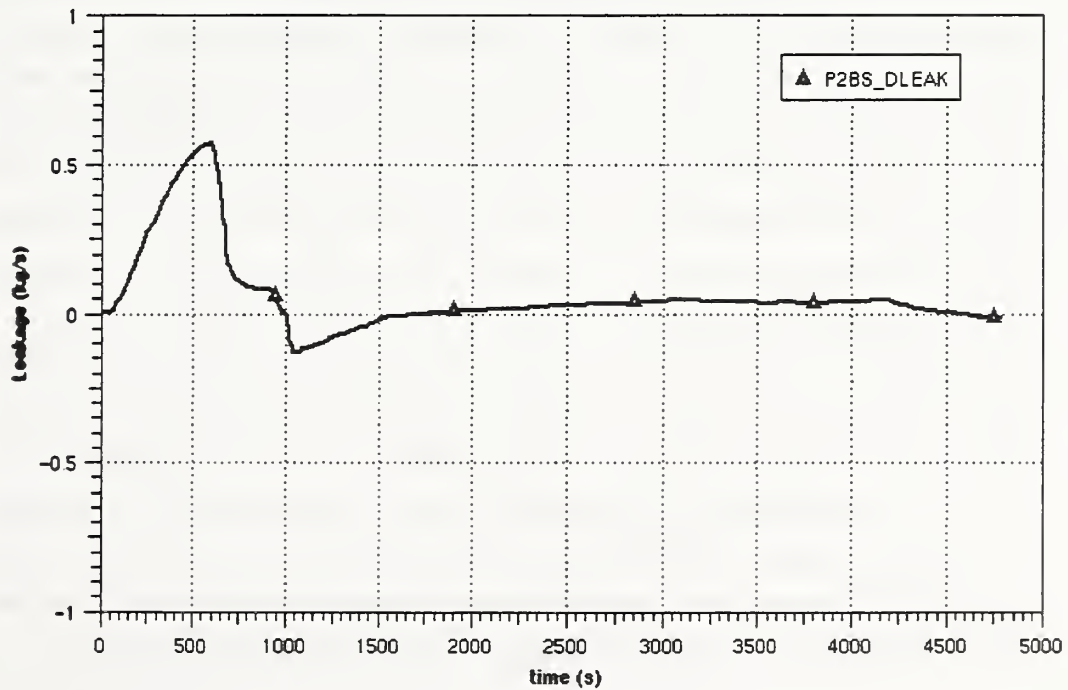**(cocV1.2AA) Pyrolysis Benchmark Part II**

Figure 6-4 Leak rate through door
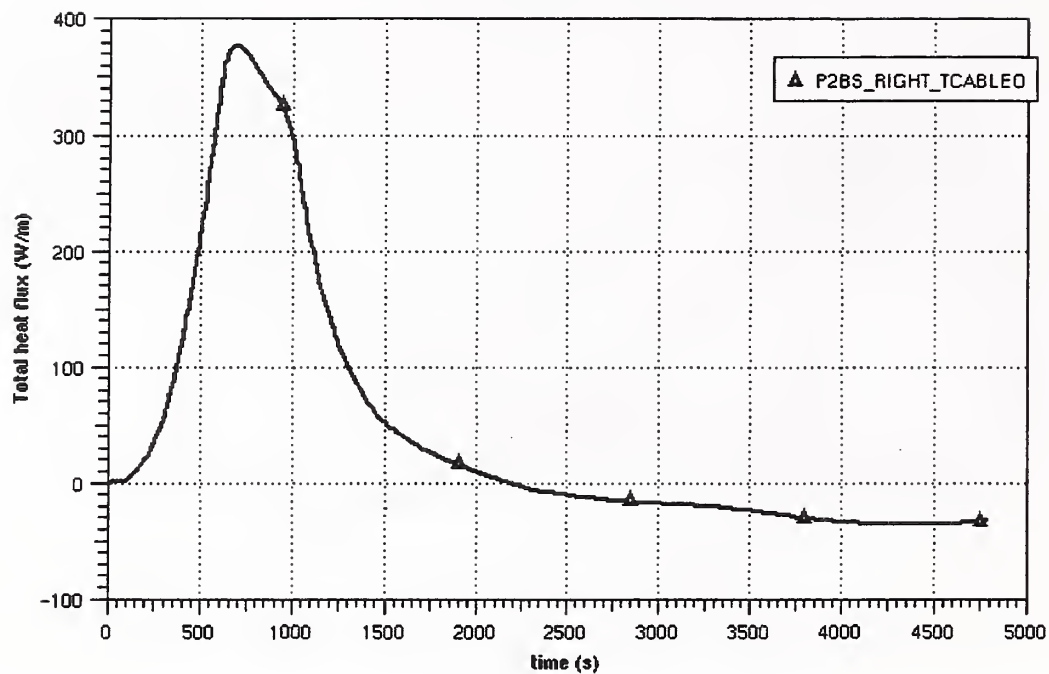
(cocV1.2AA) Pyrolysis Benchmark Part II

Figure 6-5 : Total heat flux into target

In comparison to part I the surface temperature of the target is now about 430 K and much higher (Fig. 6-6). The maximum temperature is reached at about 1000s. Although the surface temperature is decreasing the centerline temperature is still rising. At the end of 4800 s a temperature of about 375 K is reached, so the cable is not damaged, according to the definition of the benchmark exercise. In comparison to the part I the fraction of heat transferred to the boundary structures is larger (Fig. 6-7). At maximum heat release about 95% of the released heat is absorbed inside the structures. This value is higher because the atmospheric temperatures are higher in comparison to part I. Fig 6-8 to 6-11 present the concentrations of the pyrolysis fractions and products in the room centre for the different elevations. The simple pyrolysis model releases H, HCl and CH_x fractions. Against to the detailed model, a burning of the remaining carbon fraction is not possible. Considering the available oxygen the H and CH_x fractions are combust to steam and CO. The CO can be further burned to CO_2. The HCl will be released as a gas component. Chemical reactions with water and wall structures are not yet considered. This will lead to higher HCl concentrations in the atmosphere.
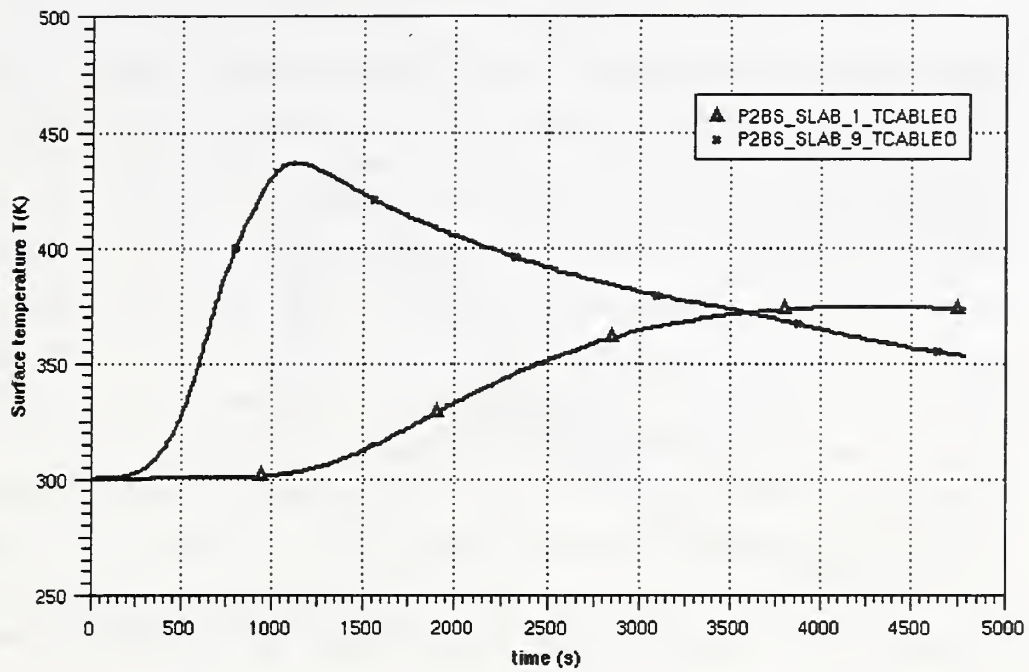
(cocV1.2AA) Pyrolysis Benchmark Part II

Figure 6-6 Surface and inner temperature of the target

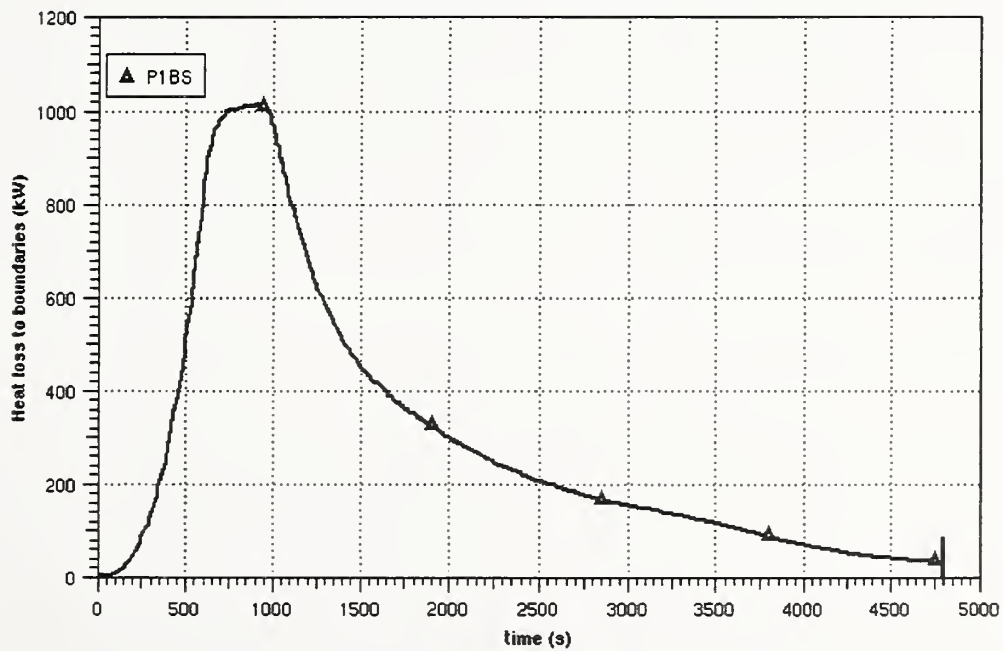## (cocV1.2AA) Pyrolysis Benchmark Part II

Figure 6-7 Heat loss to the boundaries

Fig 6-8 shows the CO concentration. If the oxygen concentration in the fire compartment is high enough the burning process is complete. Therefore the first peak of CO up to 0.8 Vol% occurs at about 1000s. Later the CO concentration decreases again. This indicates that the reductions due to the burning of CO is higher than the CO production due to the burning of the CH_x fraction. The behaviour of the CO_2 concentration is similar (Fig. 6-9). CO_2 is produced from the beginning on. Later the production rate is decreasing. As a result the stratified conditions of the CO_2 concentration is vanishing. At the end of the calculation the concentration at the ceiling is lower than the concentration at the floor level. This is caused by the increasing concentrations of CH_x and HCl. Fig. 6-10 and 6-11 presents the HCl and CHX concentration, respectively. The behaviour of both is very similar. It should be pointed out that the release of the pyrolysis fraction is given by input. In the reality there is a strong feed back of the burning process, depending on the available oxygen on the cable tray temperatures and release of pyrolysis gases.

(cocV1.2AA) Pyrolysis Benchmark Part II
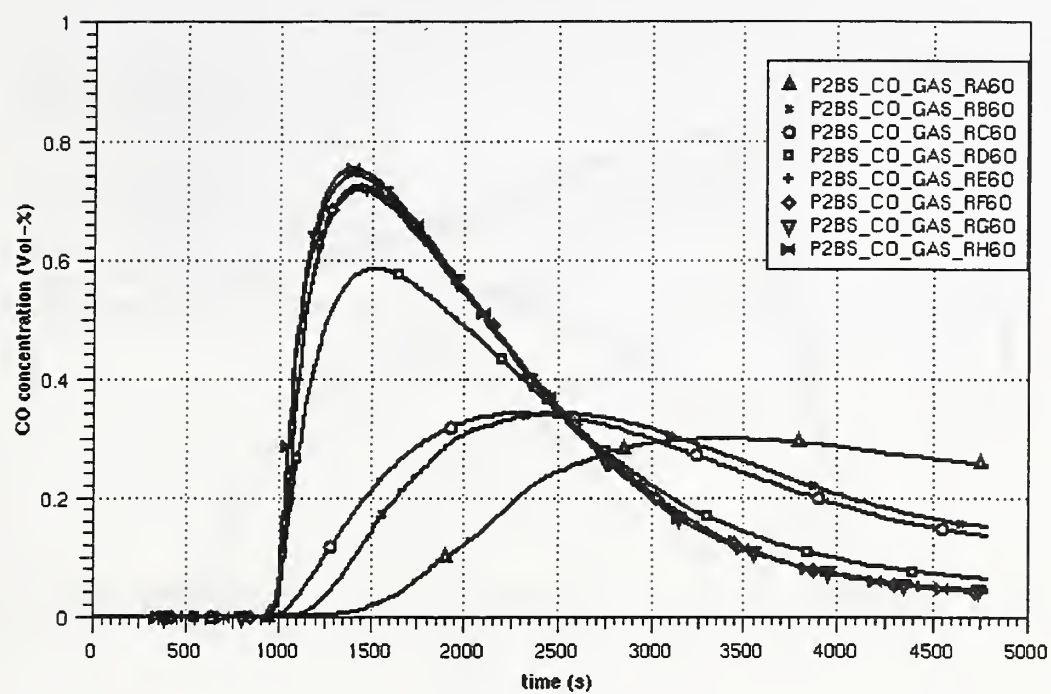
Figure 6-8 CO concentration in the room centre

(cocV1.2AA) Pyrolysis Benchmark Part II

Legend:
- P2BS_CO2_GAS_RA60
- P2BS_CO2_GAS_RB60
- P2BS_CO2_GAS_RC60
- P2BS_CO2_GAS_RD60
- P2BS_CO2_GAS_RE60
- P2BS_CO2_GAS_RF60
- P2BS_CO2_GAS_RG60
- P2BS_CO2_GAS_RH60
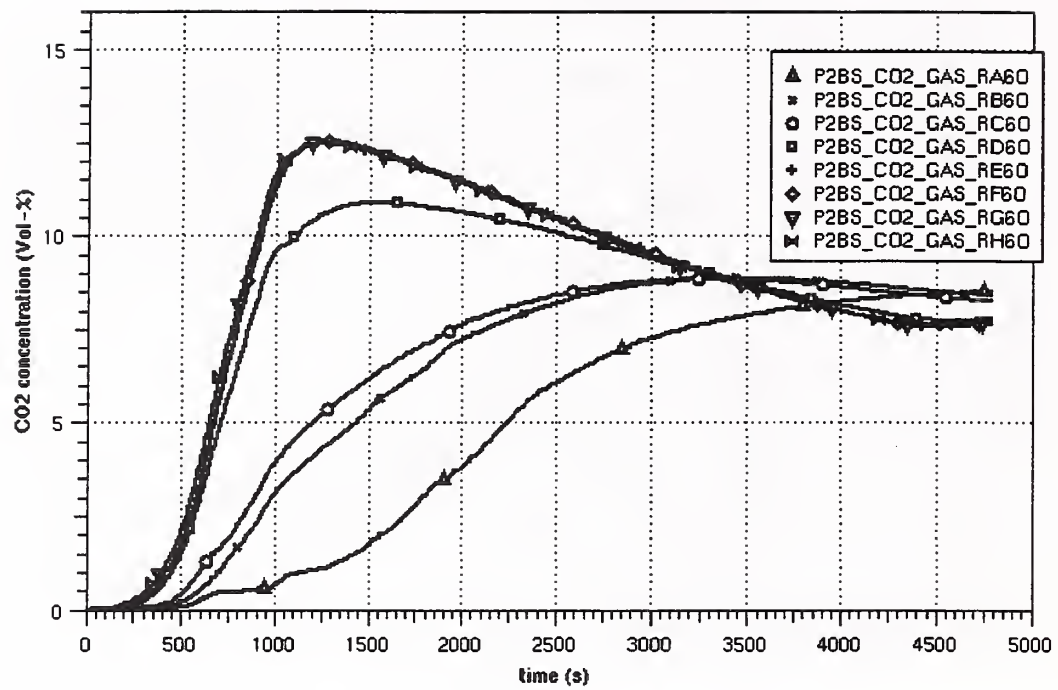
Figure 6-9 CO_2 concentration in the room centre
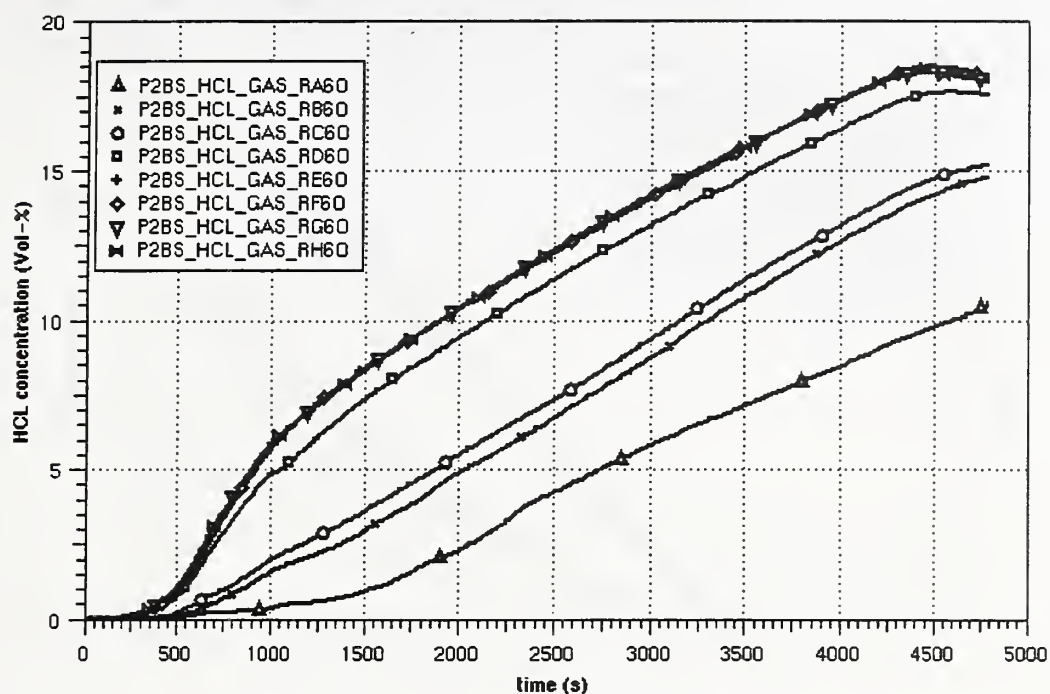
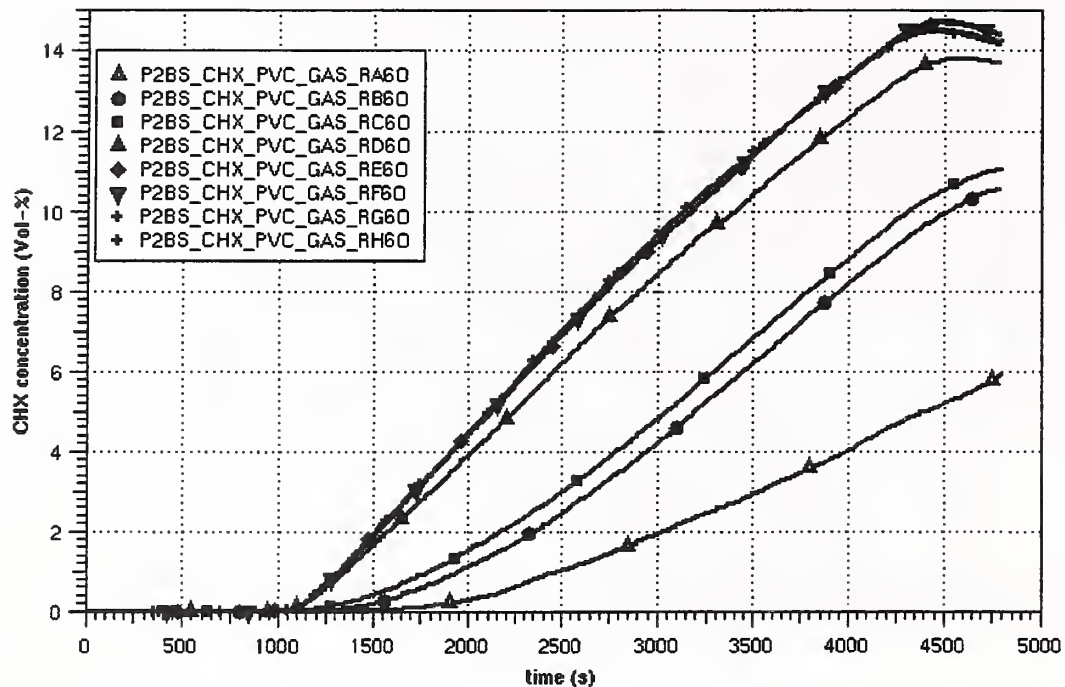**Figure 6-10** HCl concentration in the room centre

Figure 6-11 CH$_X$ concentration in the room centre

6.2 Case 1 to case 8

In these variations the position of the target cable tray is shifted sidewards and the heat release (in practice the release of pyrolysis fractions) is increased from 1MW to 3MW. In 6-12 the temperatures at the ceiling in the room centre are plotted for all cases. Shifting the target, does not influence the temperature at the ceiling. Therefore the temperatures for the base case, case 5 and case 8 are equal for example. The maximum atmospheric temperatures increases for higher heat release rates. But the effect is much higher for the increase from 1 MW to 2 MW as for the step from 2 MW to 3 MW. The time of the maximum temperature is lower also. It is interesting, that the atmospheric temperatures in the case of 1 MW release is higher than for the 2 or 3 MW release later. This corresponds to the experience gained with the code, that higher release rates can 'move' the burning process away from the release point leading to lower temperatures and may be to not conservative results. Fig. 6-13 presents the real heat release rates in comparison to the given one. The small difference in the maxi-

mum temperatures in the 2 and 3 MW case is underlined here again. Later the heat release is lower in comparison to the base case.
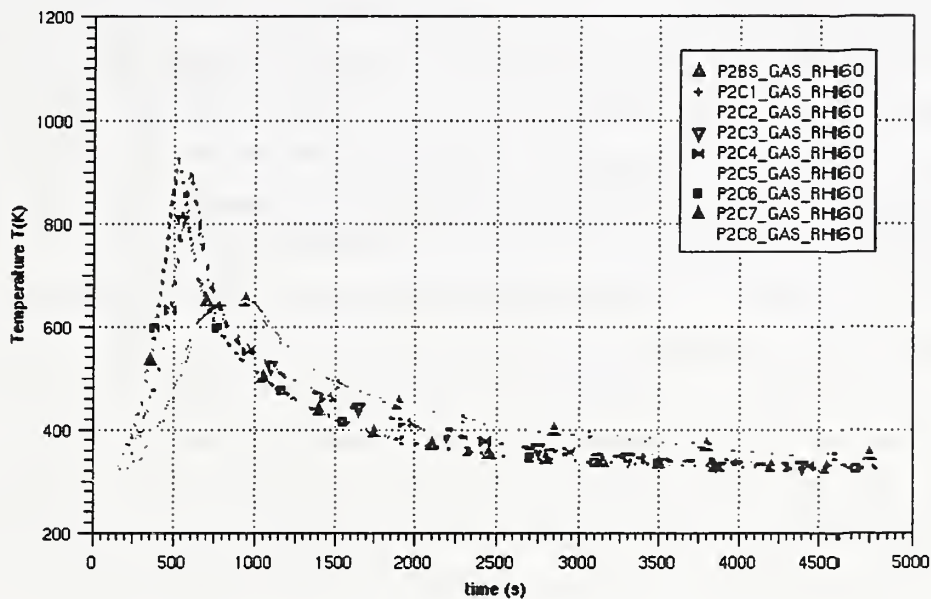
(cocV1.2AA) Pyrolysis Benchmark Part II

Figure 6-12 Temperatures below the ceiling in the room centre

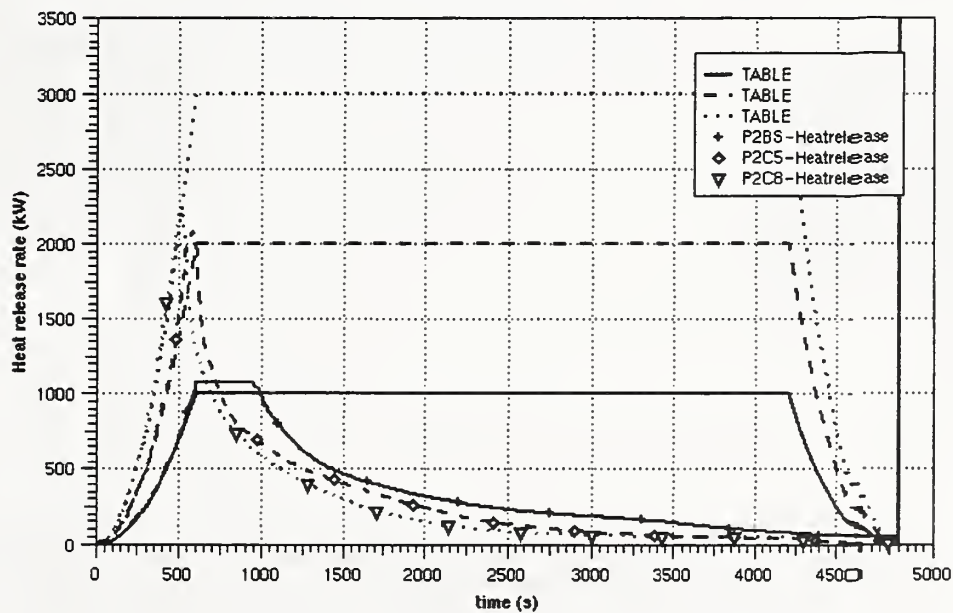**(cocV1.2AA) Pyrolysis Benchmark Part II**

Figure 6-13 Heat release (base case, case5, case8)

Fig 6-14 shows the oxygen concentrations at the ceiling for the different cases. It is evident, that the oxygen is consumed earlier in the 2 and 3 MW cases, resulting in the above described behaviour. The leak rate through the door is presented in Fig. 6-15. In the first heat up phase gas is moved in the atmosphere. After this the direction of the leak flow turns around, due to the cool down inside the fire compartment. Then between 1000s and 1500s the leak flow turns around again. Here the pressure built up due to the release of pyrolysis gases is able to compensate the cool down of the fire compartment. At this time no fresh air can enter the fire compartment. This underlines again, that the release of pyrolysis gases may inhibit the burning process. Fig 6-16 shows, that the heat flux into the target depends only on the 'heat release rate'. This is caused by the neglecting of the direct radiation. The maximum surface temperature (Fig. 6-17) is increased by about 20 K. The low difference results from the less amount of oxygen inside the fire compartment. Fig 6-18 presents the heat loss to the boundaries. Increasing the 'heat release' the consumption of oxygen is higher. Therefore the maximum CO concentration is slightly higher and earlier. The overall qualitative behaviour of the concentration for higher heat release is quite similar to the base case (Fig 6-19 to 6-22).

(cocV1.2AA) Pyrolysis Benchmark Part II
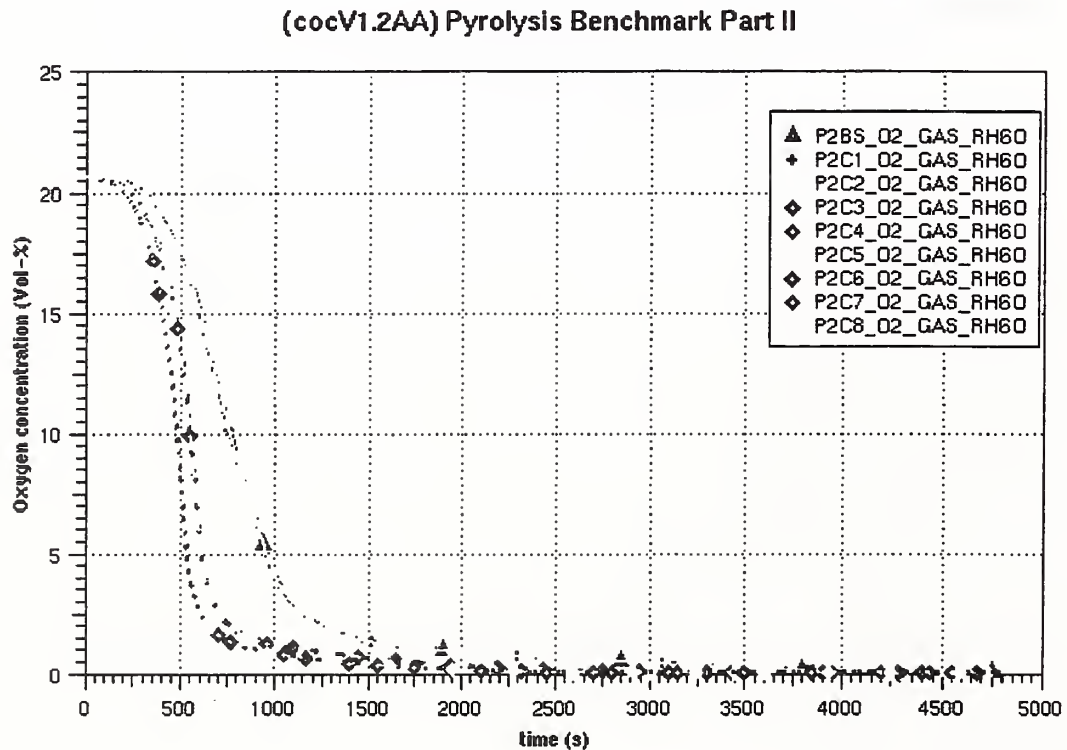
Figure 6-14 Oxygen concentration below the ceiling in the room centre

(cocV1.2AA) Pyrolysis Benchmark Part II
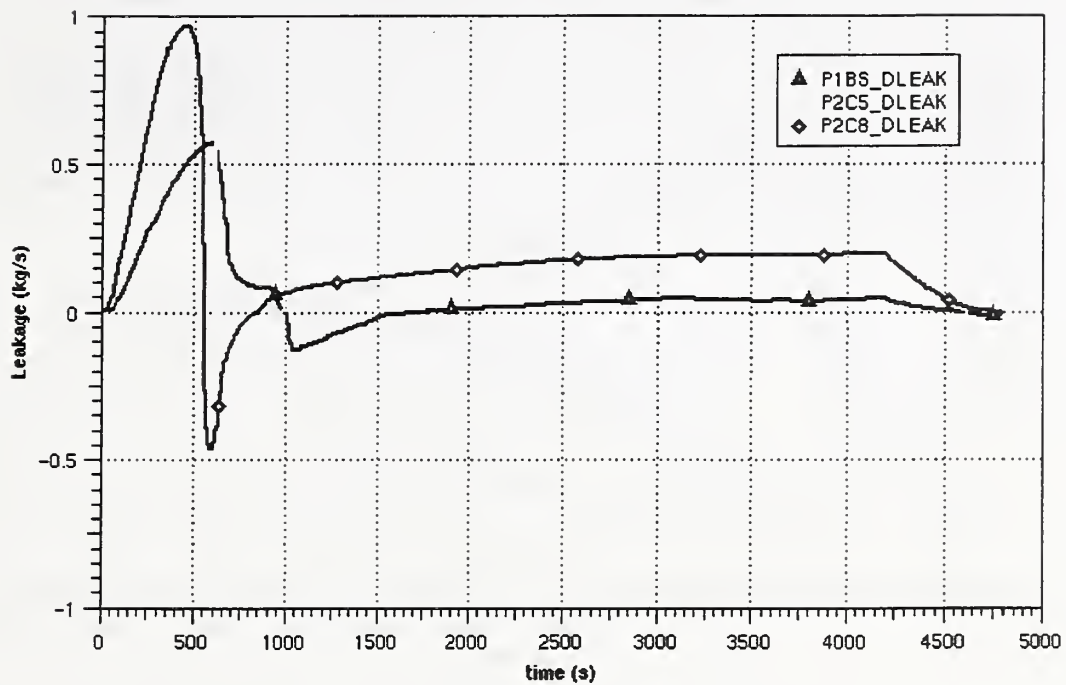
Figure 6-15 Leak rates (base case, case 5, case8)

(cocV1.2AA) Pyrolysis Benchmark Part II
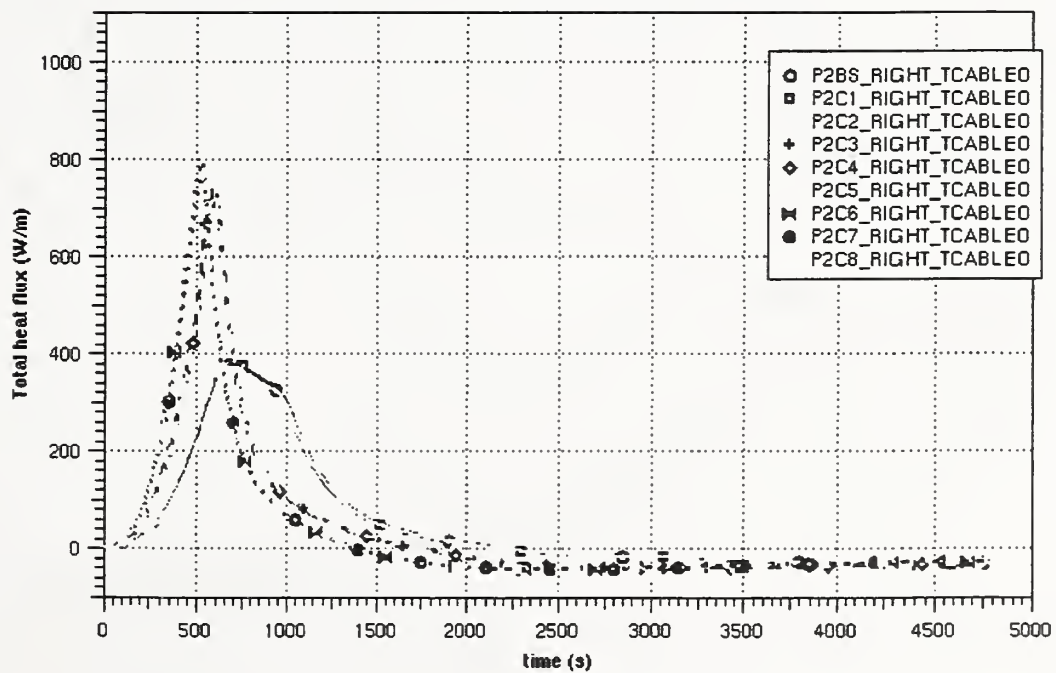
Figure 6-16 Heat flow into the target

(cocV1.2AA) Pyrolysis Benchmark Part II
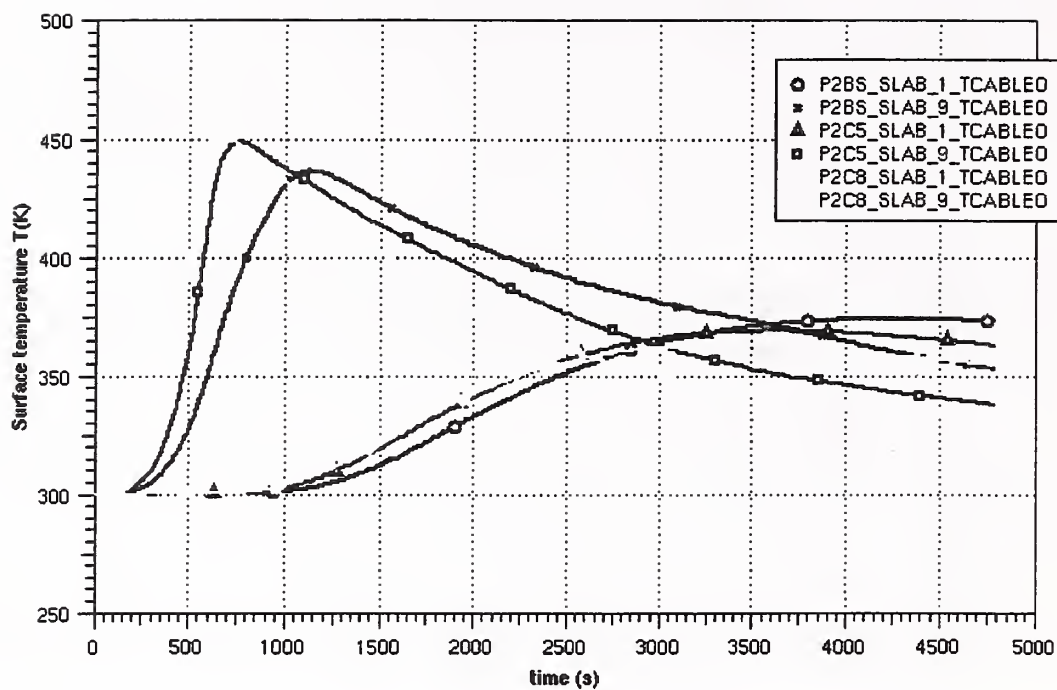
Figure 6-17 Surface and inner temperatures of the target (base case, case5, case8)

(cocV1.2AA) Pyrolysis Benchmark Part II
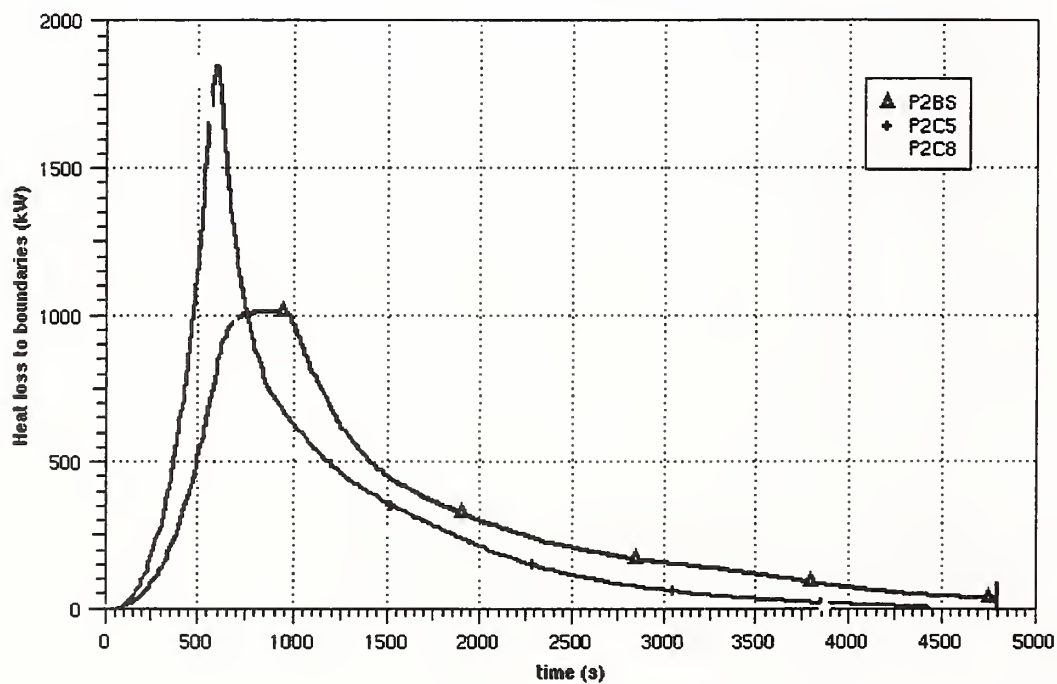
Figure 6-18 Heat loss to boundaries (base case, case5, case8)

Figure 6-19 CO concentration at ceiling and bottom in room centre

(cocV1.2AA) Pyrolysis Benchmark Part II

Figure 6-20 CO_2 concentration at ceiling and bottom in room centre
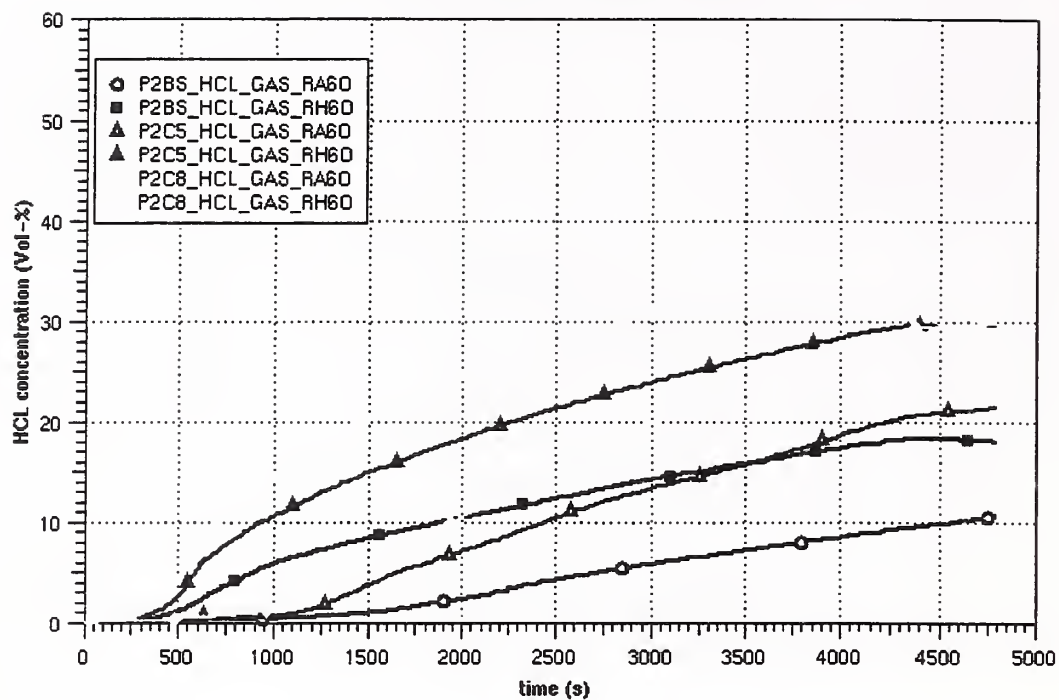
Figure 6-21 HCl concentration at ceiling and bottom of room centre

(cocV1.2AA) Pyrolysis Benchmark Part II
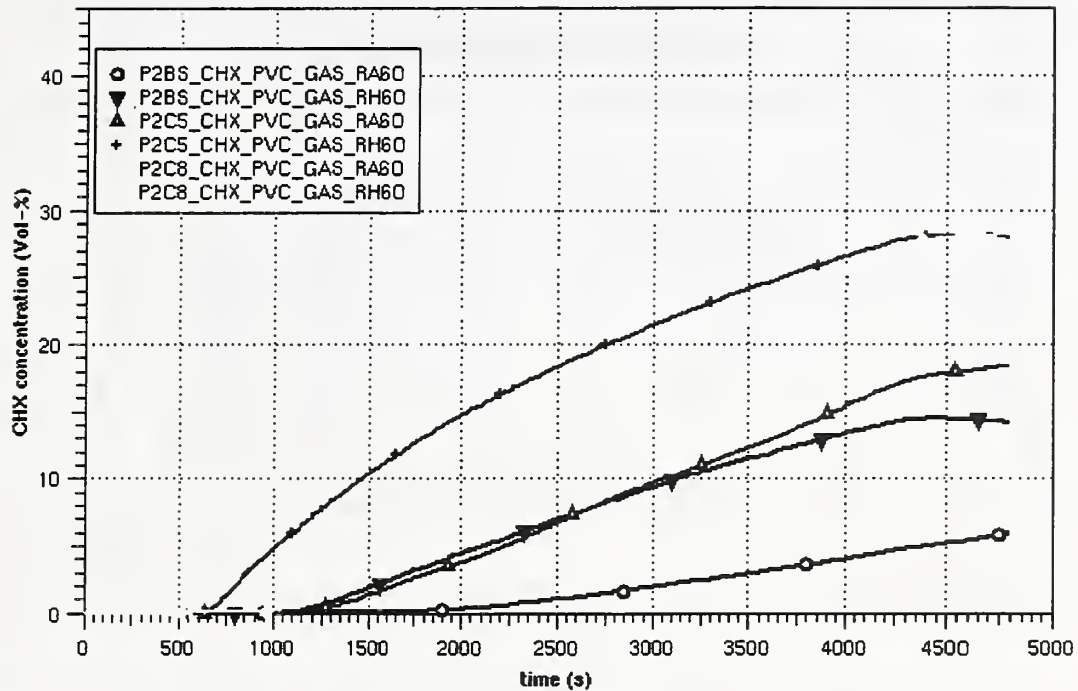
Figure 6-22 CH_X concentration at ceiling and bottom of room centre

6.3   Case 9 and Case 10 : Ventilation and door effects

In case 9 the ventilation system is running until 15 min. Then the door is opened. In case 10 the door is open and the ventilation system is running all the time. The main difference is the available oxygen concentration. Therefore the temperatures below the ceiling are much higher. The temperature at floor level is quite similar in all cases (Fig. 6-23). As it can be seen in Fig. 6-24 in case 9 and 10 the burning is nearly complete. Only in case 9 the oxygen concentration (Fig. 6-25) goes under the limit of 4 % leading to an incomplete burning of about 10%. Fig 6-26 shows the flow rate through the open door. In case 9 the counter current flow is established shortly after the opening of the door. In the cool down phase at the end of the problem time the flow through the door starts to turn around. Fig. 6-27 shows the mass flow rate through the left vent opening. In case 9 the ventilation system is stopped and additionally the vent opening is closed. The flow rate is always directed to the environment. The heat flow to the target in the vented cases is very similar according to the similar heat release (Fig. 6-28). In comparison to the base case the values are much higher, leading therefore to much higher

surface temperatures (Fig. 6-29). At about 4500s the threshold value of about 200 C for cable damage is reached.

(cocV1.2AA) Pyrolysis Benchmark Part II
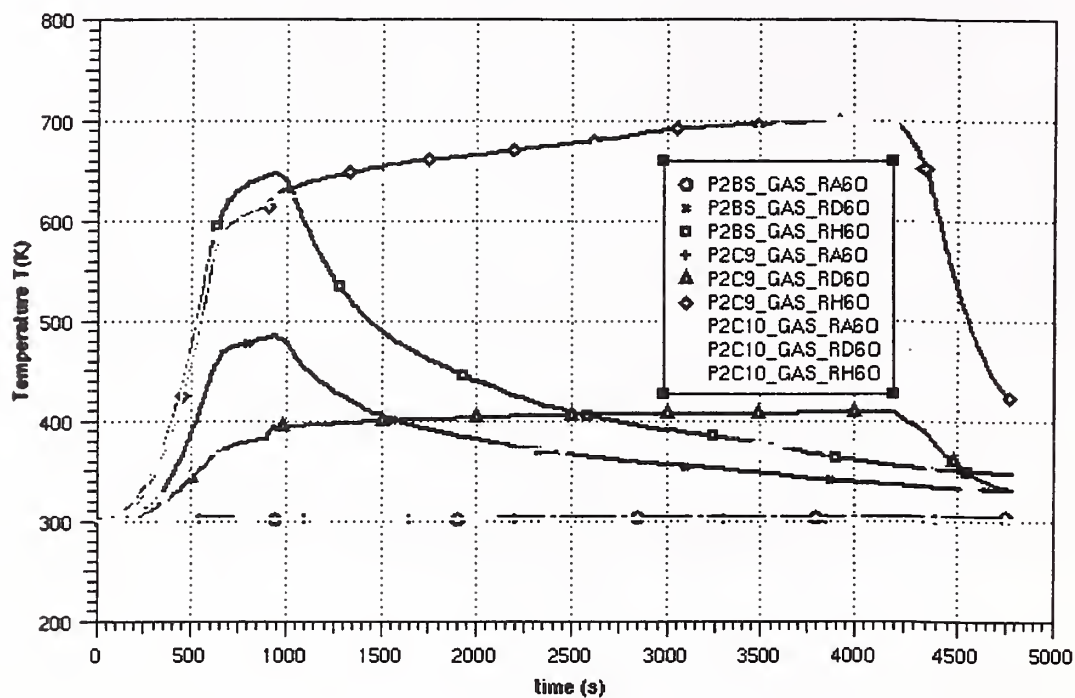
Figure 6-23 Temperatures at 0.3, 2.3 and 4.4 m in the room centre

(cocV1.2AA) Pyrolysis Benchmark Part II
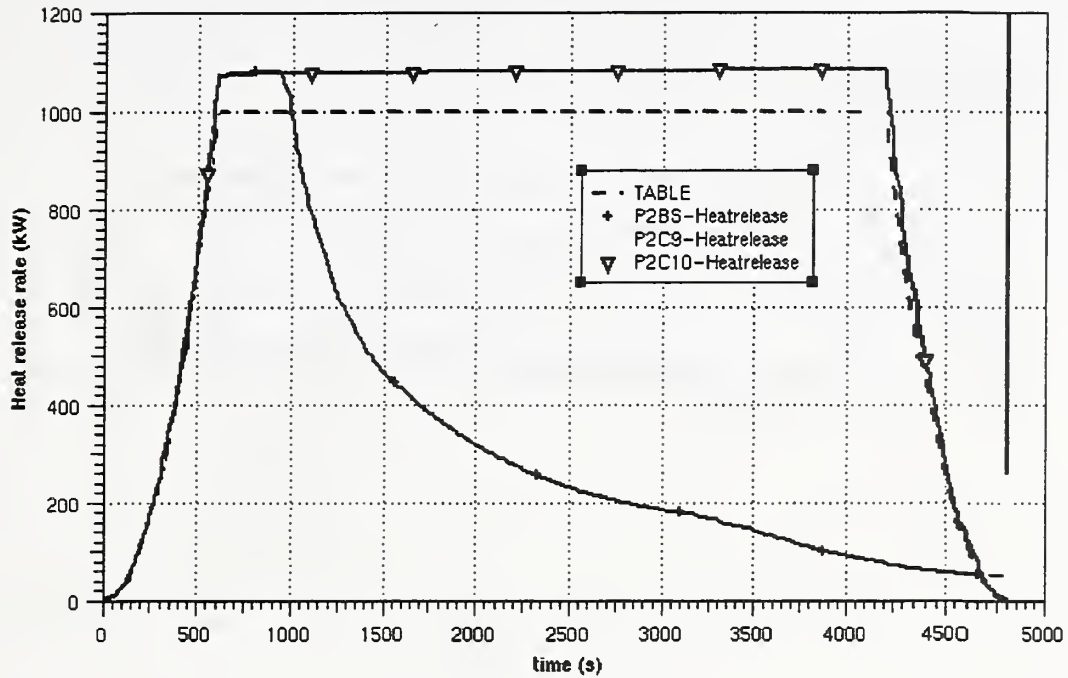
Figure 6-24 Heat release (base case, case9 and case10)
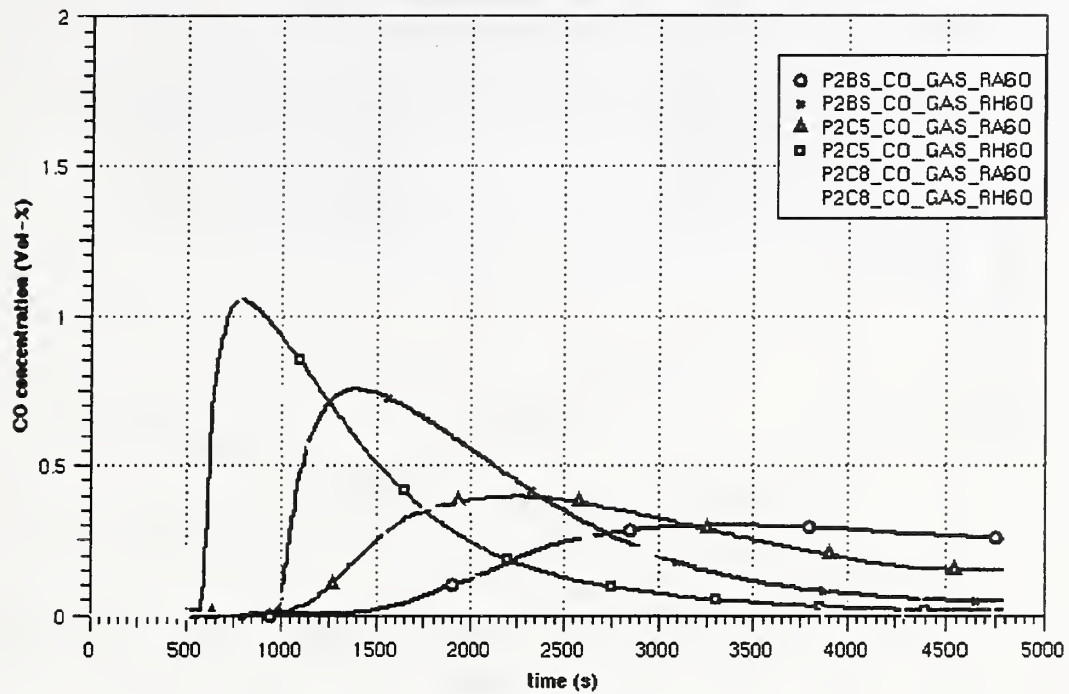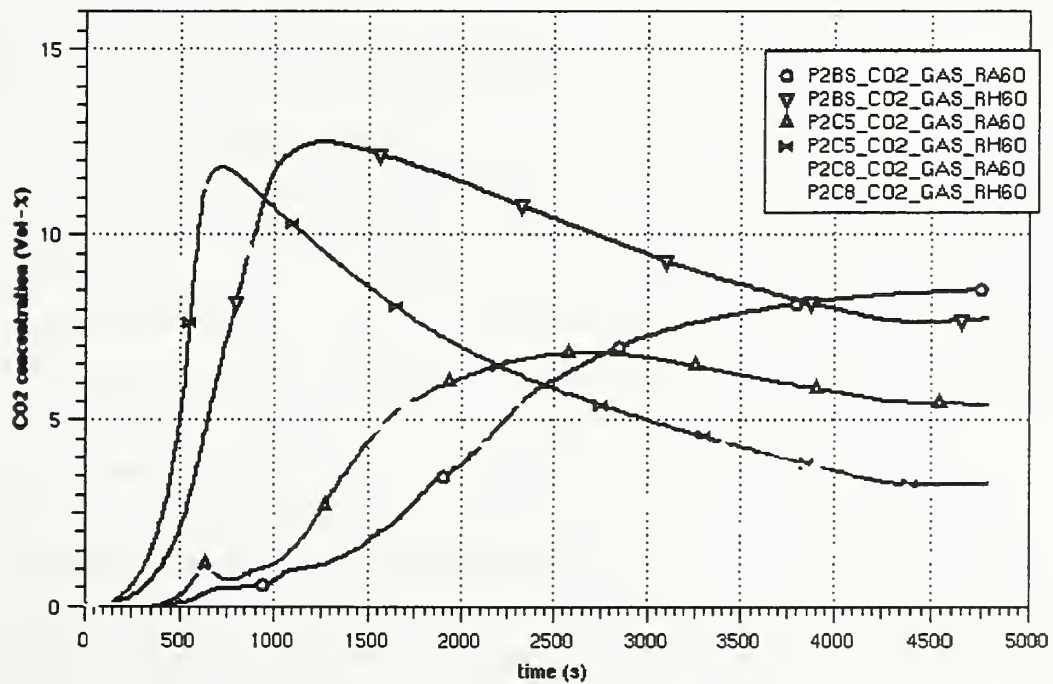
(cocV1.2AA) Pyrolysis Benchmark Part II
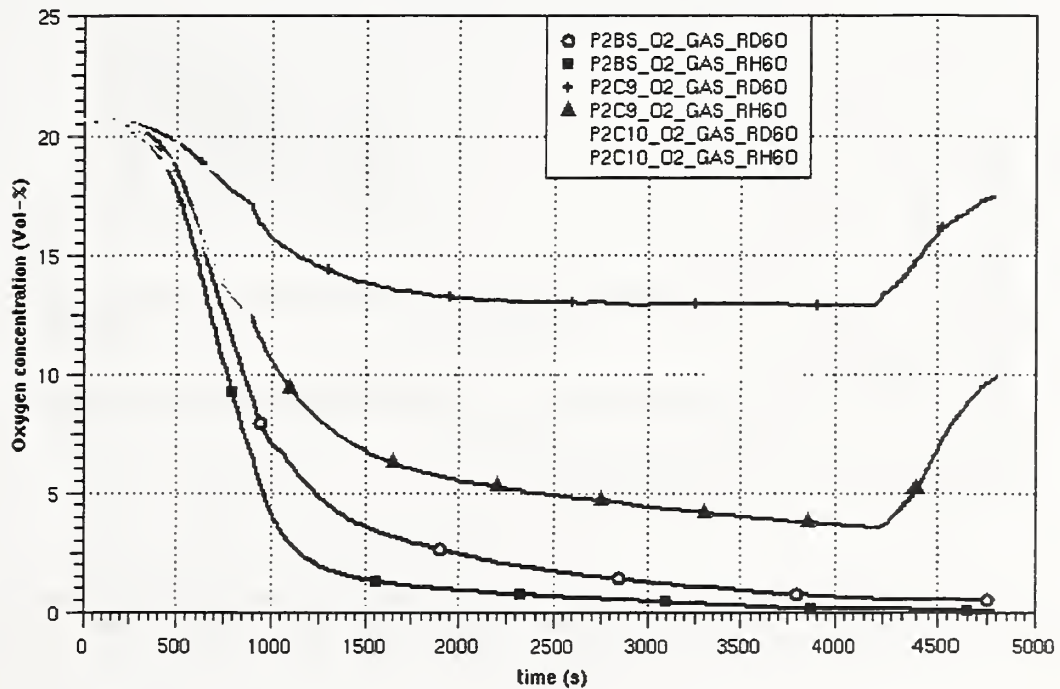
Figure 6-25 Oxygen concentration at 2.3 and 4.4m in the room centre

(cocV1.2AA) Pyrolysis Benchmark Part II
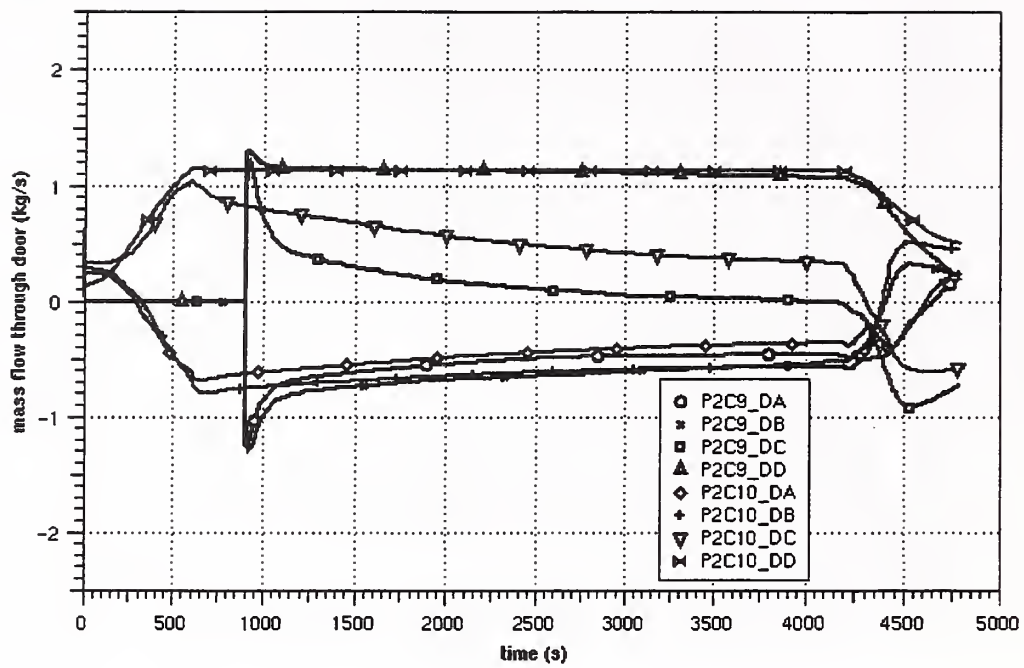
Figure 6-26 Mass flow rate through door (case 9 and 10)

(cocV1.2AA) Pyrolysis Benchmark Part II
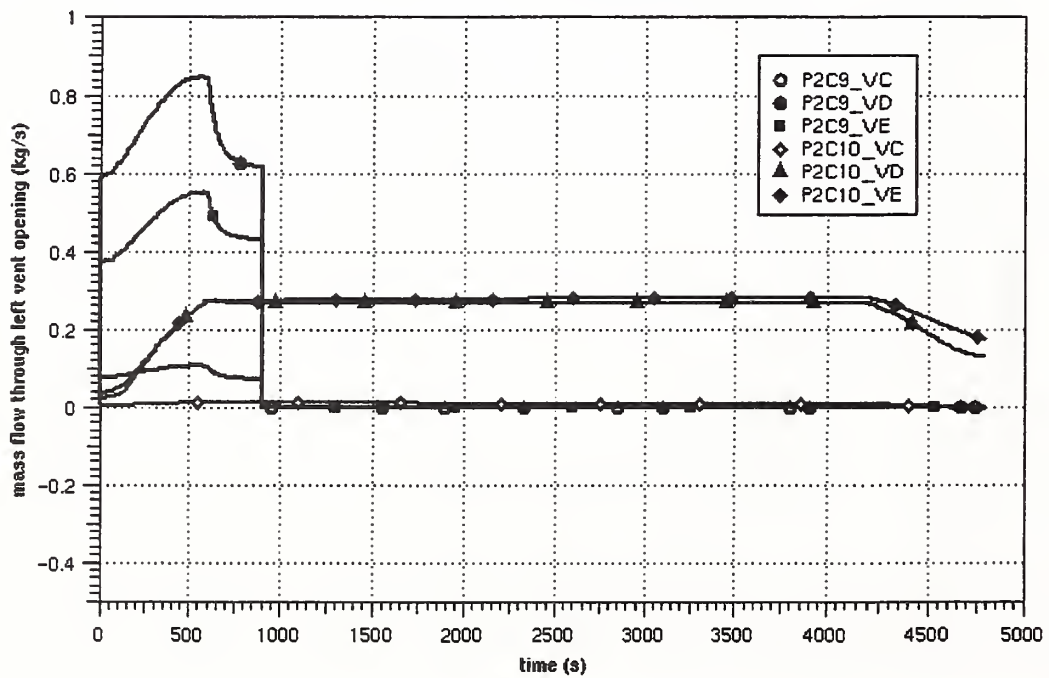
Figure 6-27 Mass flow rate through left vent opening (case 9 and 10)

(cocV1.2AA) Pyrolysis Benchmark Part II
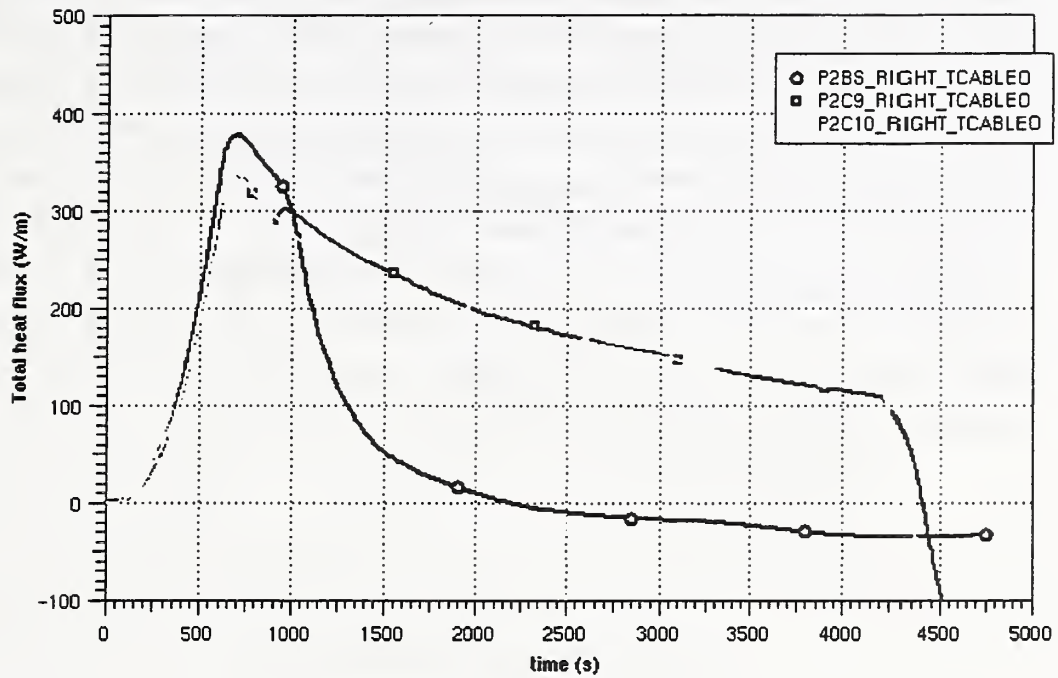
Figure 6-28 Total heat flow into target

(cocV1.2AA) Pyrolysis Benchmark Part II
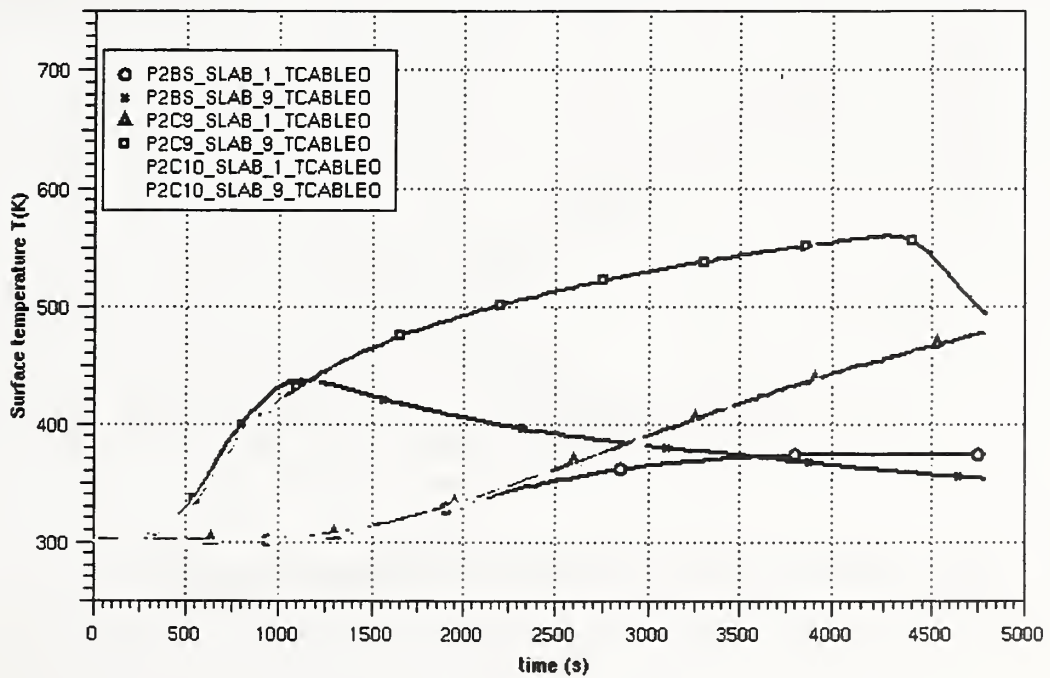
Figure 6-29 Surface and inner temperature of target

In case 10 there are always oxygen rich conditions. Therefore the CO concentration is always zero. In case 9 the oxygen concentration in the highest level is somewhat lower. At about 1500s the burning rate is incomplete, leading to some amount of CO there. The behaviour of the CO_2 concentration (Fig. 6-31) is very different in comparison to the base case. This is the result of two opposite effects: the open conditions reducing the concentrations of the gases and the higher pyrolysis and burning rate increasing the concentrations. The CO_2 concentration for case 9 is somewhat higher. The reason is the convection flow through the door needs some time to build up, leading to lower exchange rates during this time. The behaviour of HCl (Fig. 6-32) is qualitative similar to the behaviour of CO_2. The oxygen concentration in the vented cases is high enough for the complete burning of the CH_X fraction (Fig. 6-33).

(cocV1.2AA) Pyrolysis Benchmark Part II
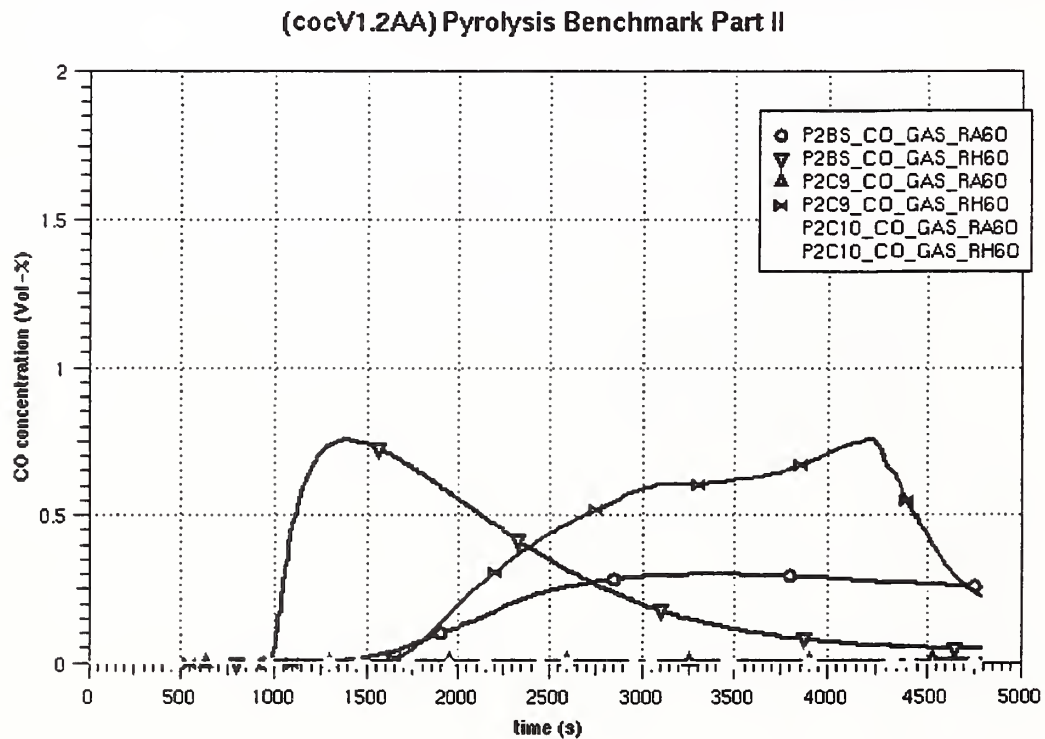
Figure 6-30 CO concentration at bottom and ceiling in the room centre

(cocV1.2AA) Pyrolysis Benchmark Part II
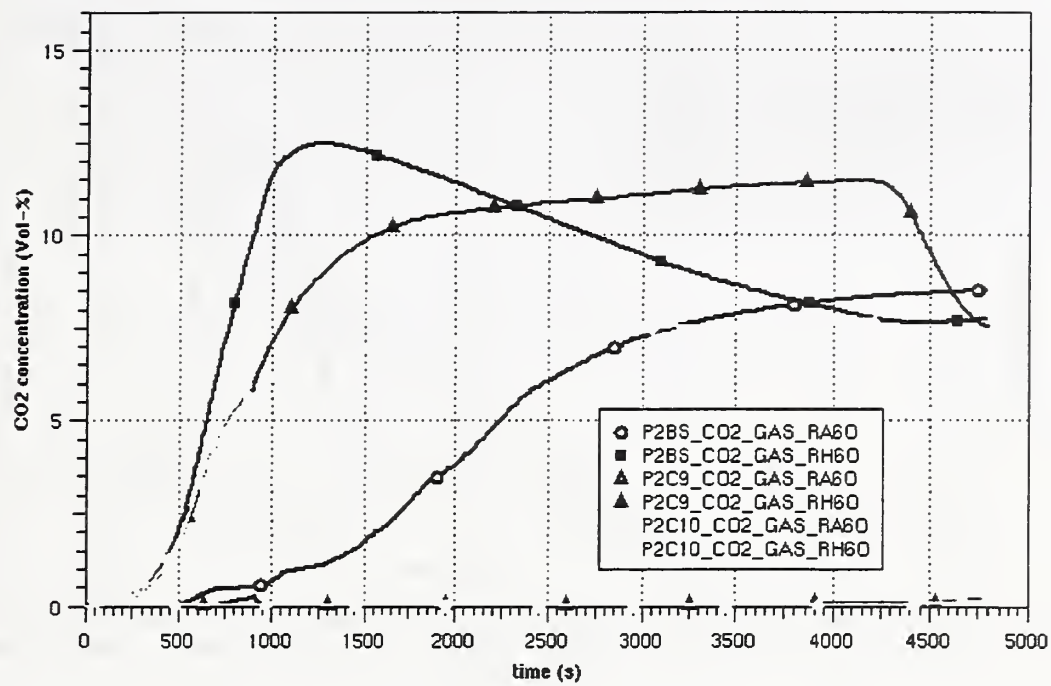
Figure 6-31 CO_2 concentration at bottom and ceiling in the room centre

(cocV1.2AA) Pyrolysis Benchmark Part II
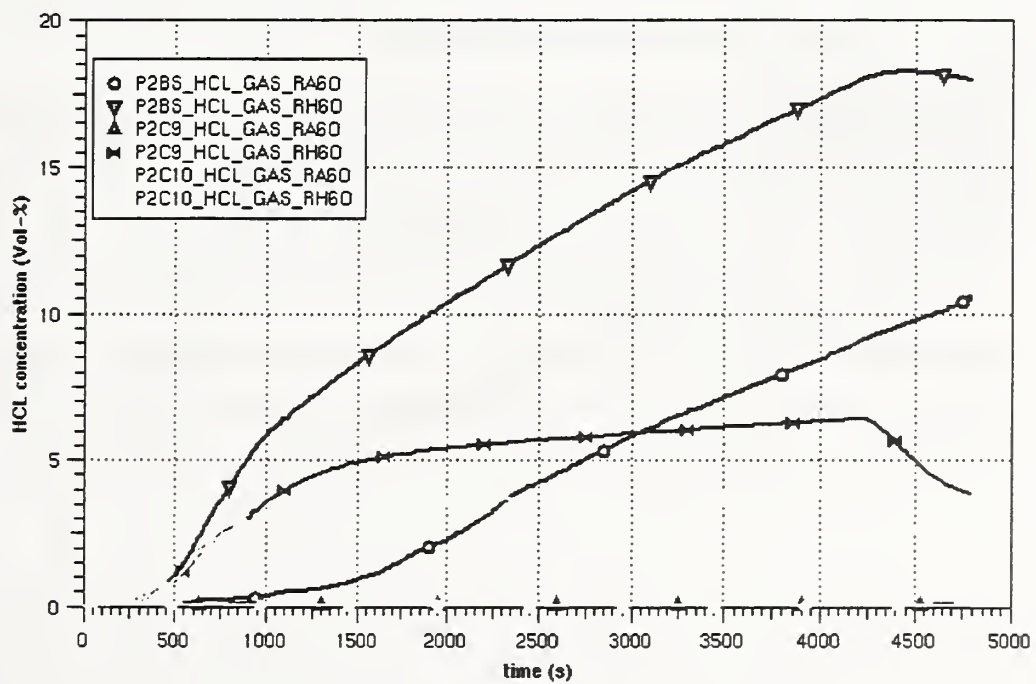
Figure 6-32 HCl concentration at bottom and ceiling in the room centre

(cocV1.2AA) Pyrolysis Benchmark Part II
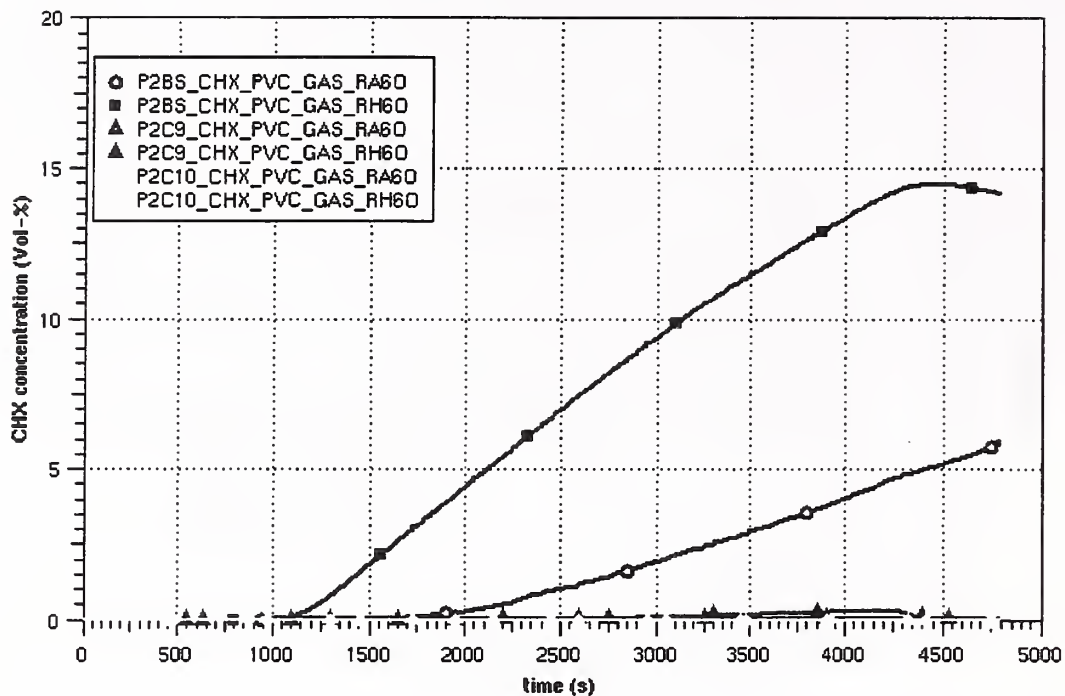
Figure 6-33 CH$_X$ concentration at bottom and ceiling in room centre

6.4 Case 11 and 12 : Elevation of the target

In this set of variations the elevation of the target is changed. In the base case the elevation of the target cable is 1.1 m above tray A and on the same level as of C2 the heat release level. In case 11 the elevation of target tray is 2.0 m above tray A and in case 12 the elevation is equal to tray A. It is clear, that the heat release and the burning process are the equal to the base case, because there is no feed back from the target cable. Due to the different elevation and the stratified conditions inside the fire compartment the heat flux into the target is different. As one would expect the heat flux and the surface temperature is higher for the higher elevations (Fig. 6-34 and Fig. 6-35).

(cocV1.2AA) Pyrolysis Benchmark Part II
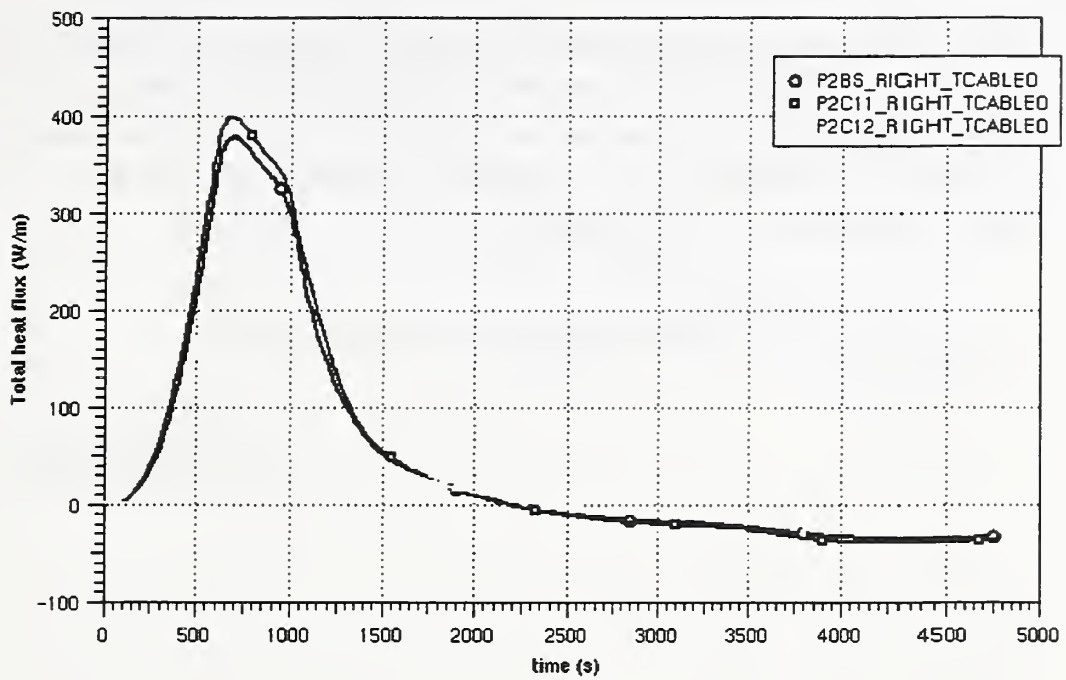
Figure 6-34 Total heat flux into target (base case, case 11, case 12)

(cocV1.2AA) Pyrolysis Benchmark Part II
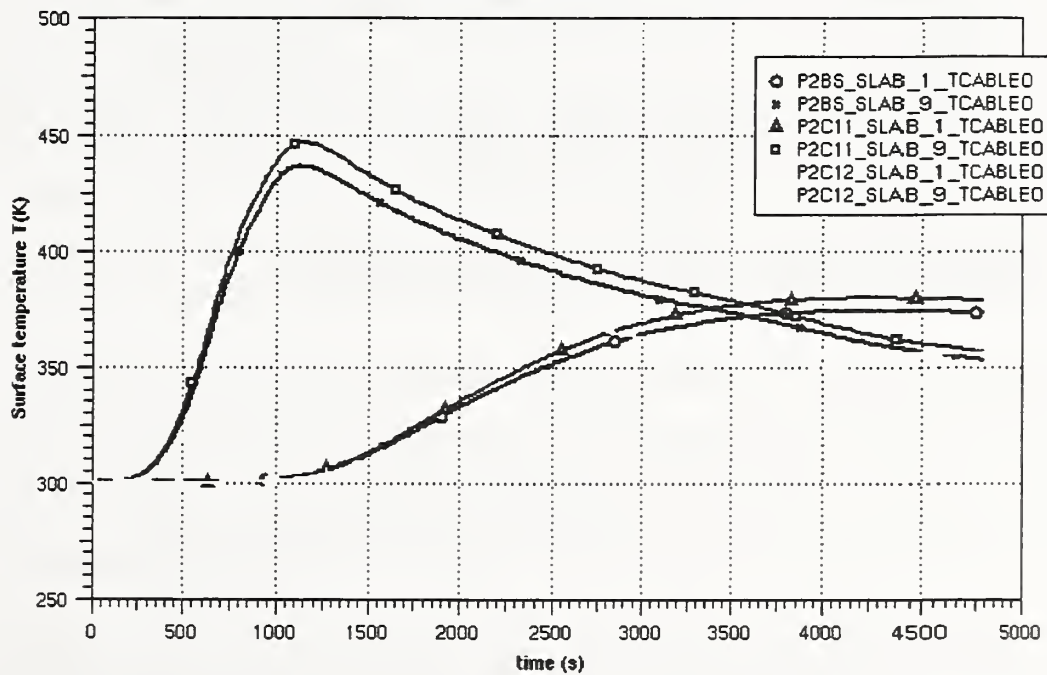
Figure 6-35 Surface temperatures (base case, case 11and 12)

6.5   Case 13 : different cable types

In this case 13 the cable type has been changed. The diameter of the target is now changed from 50 mm to 15 mm, complete filled with PVC also. The heat flux into the cable is lower, due to the reduced surface (Fig. 6-36). On the other side the surface temperature and especially the inner temperature of the target are much larger. In this case the damage criteria of 473 K is reached.
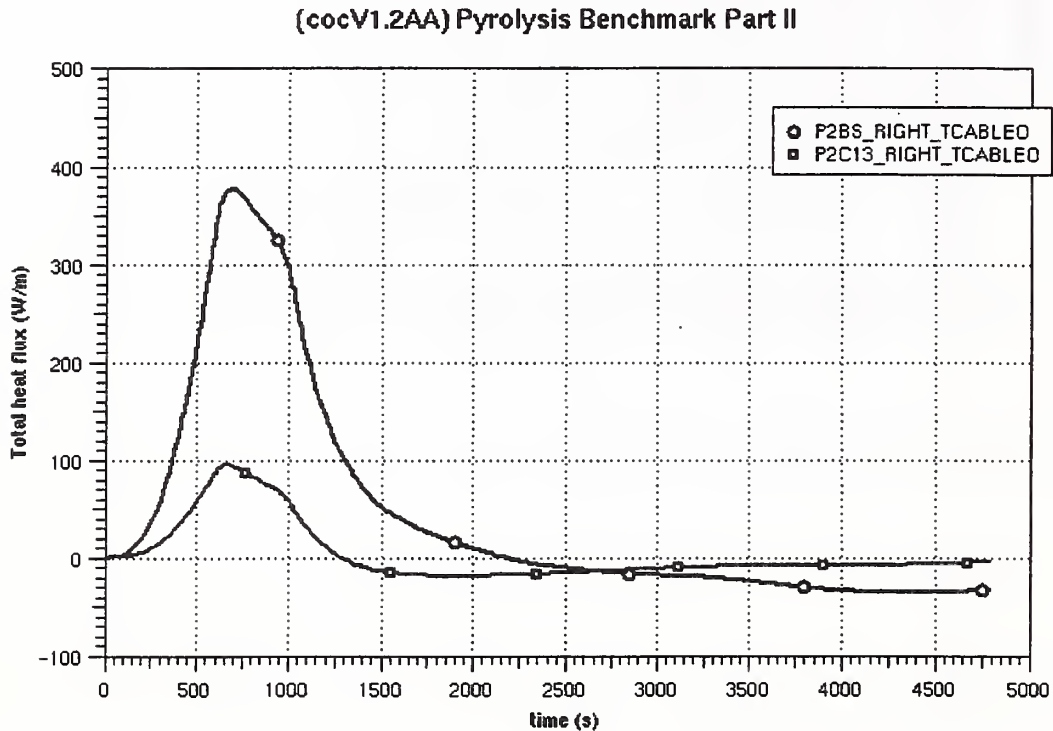
Figure 6-36 Comparison of different cable types (total heat flux)

(cocV1.2AA) Pyrolysis Benchmark Part II
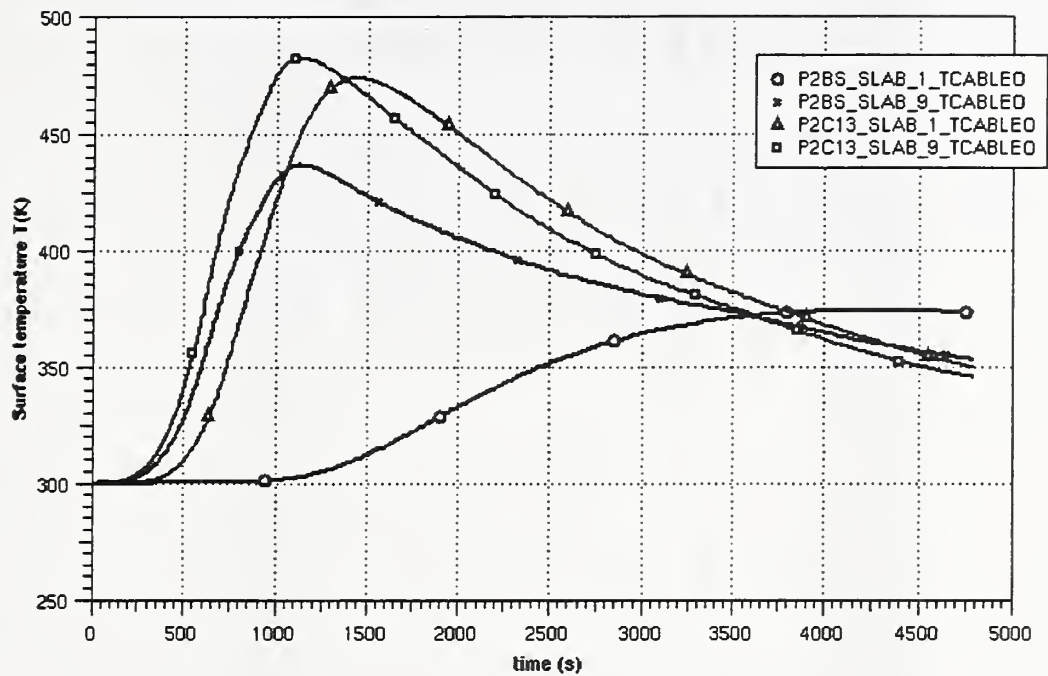
Figure 6-37 Comparison of cable types (surface and inner temperature)

7 Conclusions

To evaluate the capabilities and the applicability of different fire code a benchmark problem has been set up in the frame of the "International Collaborative Project to Evaluate Fire Models for Nuclear Power Plant Applications". In the technical note the results of the COCOSYS system code are presented.

COCOSYS is a so called lumped parameter code. Therefore a detailed nodalisation with more than 320 nodes has been set up for the simulation of all parameter variations, with different trash bag positions (part I) and different locations of the target tray (part II). Additional the detailed nodalisation is able to calculate local convection loops and stratified conditions.

Regarding the results of all variations for part I and part II could be qualitatively explained. The following tables give an overview of the analytical results:

Table 7-1 Results of part I

Part I	O$_2$ conc. @ 600s in RH6O [Vol-%]	Max. plume flow [kg/s]	Max. over-pressure [Pa]	Max. Out-flow [kg/s]	Layer height @ 240s [m]	Max. temp. at ceiling (zone RH6O) [K]	Max. flux on target [W/m^2]	Max. Target Cable Temp. [K]
Base c.	19.33	0.2910	975.	0.3978	-	449.2	total: 472.2 radiation: 302.9	surface: 312.54 centre: 300.09
Case 1					-	386.6	total: 26763 radiation: 15234	surface: 326.49 centre: 300.31
Case 2					-	400.7	total: 711.4 radiation: 624.1	surface: 314.73 centre: 300.15
Case 3					-	418.4	total: 648.0 radiation: 507.4	surface: 313.95 centre: 300.12
Case 4			open (-12.)	1.26	-	452.4	total: 485.5 radiation: 318.2	surface: 311.26 centre: 300.09
Case 5	19.74		open		-	451.1	total: 395.7 radiation: 317.5	surface: 308.09 centre: 300.07

Table 7-2 Results of part II

Part II	O$_2$ conc. in RH6O [Vol-%]	Max. over-pressure [Pa]	Layer height [m]	Max. temp. at ceiling (zone RH6O) [K]	Max. flux on target [W/m²], total	Max. Target Cable Temp. [K]
Base c.	@500s: 17.6	2104.	-	646.2	2400.	surface: 436. centre: 374.
case 1			-		814.	surface: 438. centre: 374.
case 2			-		2368.	surface: 435. centre: 373.
case 5			-		4628.	surface: 448. centre: 369.
case 10	@ 3800s: 9.85		-	702.	2158.	surface: 555. centre: 472.
case 11			-		2527.	surface: 446. centre: 379.
case 12			-		1827.	surface: 398. centre: 355.
case 13			-			surface: 482. centre: 473.

According to the benchmark description, an ignition of the target tray is assumed, if the centerline temperature exceeds 643 K. Because this temperature is never reached (even in case 1) an extrapolation was not possible. It has been found that the difference between case 1 (0.3 m distance, nearly below the target) and case 2 (0.9 m distance) is very strong. The main reason is, that the form of the plume is not really calculated. COCOSYS has no specific plume models. Therefore the form of plumes is mainly caused by the used nodalisation. Consequently the width and additionally the inner temperature inside the plume is not really calculated. In reality the form of plume will be larger and the inner temperature somewhat lower, resulting in a more smooth behaviour changing the distance.

For the nodalisation small zones are defined. Using the lumped parameter concept, one has to keep in mind, that the momentum balance is not calculated. Defining a fan system injecting fresh air into these small nodes, may lead to wrong results in the nodes around the inlet, because the momentum of the gas flow is not considered.

In part II the pyrolysis rate is much larger, so that the burning process is mainly caused by the available oxygen. In the benchmark an oxygen limit is assumed by about 12 %. In the benchmark calculations a limit of about 4 % is used. This value has been validated against the HDR 41.7 oil fire experiment. Because the fire is oxygen controlled there is a strong difference between the closed conditions and vented conditions. In case of oxygen controlled conditions, the release of pyrolyzed gases is still according to the specified formula in the benchmark description. Then these gases are transported to other nodes, where these may be burned. In reality there will be a strong feed back from the burning process (heat release, radiation) to the surface temperature and following the pyrolysis rate. To consider this effect is important. One of the reason is, that for example a reduced release of pyrolyzed gases may lead to increased temperatures in the fire compartment. This effect can be seen, comparing the cases 5 and 8 with the base case. Therefore higher pyrolysis rates will not lead automatically to conservative results for the temperatures.

Using the simple cable burning model, the radiation of the burning trays can not be calculated. Therefore the results of the cases 1 to case 8 and the base case are de-

pending only on the 'heat release' rate. The target temperatures are calculated lower, because only the convective heat transfer is used.

In all calculations a constant convective heat transfer coefficient of 15 $\left[\dfrac{W}{m^2K}\right]$ is used for the boundary structures and the cables. This value seems to be very high, especially for the low level zones near the floor. Usually composed correlations are used for free and forced convection, condensation and radiation are used. To simplify the benchmark problem, the real structure of cables is not considered. In COCOSYS it is possible, to compose a structure (plate or cylinder type) with different materials (like PVC, isolation material, copper).

8   Literature

1.   W. Klein-Heßling, B. Hüttermann, H.-J. Allelein, Application of the containment code system (COCOSYS), Proceedings ANS International Meeting on Estimate Methods in Nuclear Installations Safety Analysis, Washington DC, USA, November 2000

2.   W. Klein-Heßling, S. Arndt, H.-J. Allelein, Current status of the COCOSYS development, Eurosafe Köln 2000, Gesellschaft für Anlagen- und Reaktorsicherheit (GRS) mbH, November 2000

3.   H.-J. Allelein, Entwicklung und Verifikation eines Containment Codesytems (COCOSYS) und eines deutsch-französischen Integralcodes (ASTEC), GRS-A-2736, Gesellschaft für Anlagen- und Reaktorsicherheit (GRS) mbH, Oktober 1999

4.   Geist Al. et al., PVM: Parallel Virtual Machine, A User's Guide and Tutorial for Networked Parallel Computing, MIT Press, Cambridge, Massachusetts, London, 1994

5.   Gelbard F., Modelling Multicompartment Aerosol Particle Growth by Vapour Condensation, Aerosol Science and Technology 12, pp. 399 – 412, 1990

6.   Bell J., ORIGEN – the ORNL Isotope Generation and Depletion Code, ORNL-4628, UC-32-Mathematics and Computers, 1973

7.   GTT-Technologies, ChemApp Ver. 2.04, A programmable thermodynamic calculation interface, Gesellschaft für Technische Thermochemie und -Physik mbH, 1998

8.   Klein-Heßling W., Implementation of a Pyrolysis Model into the Containment Code System COCOSYS, Structural Mechanics in Reactor Technology, Post Conference Seminar No. 6, Fire Safety in Nuclear Power Plants and Installations, Sep. 1999

9   Acknowledgement

10   Appendix A

In the following the benchmark description is given:

Room Size and Geometry

A representative PWR emergency switchgear room is selected for this benchmark exercise. The room is 15.2 m (50 ft) deep x 9.1 m (30 ft) wide and 4.6 m (15 ft) high. The room contains the power and instrumentation cables for the pumps and valves associated with redundant safe-shutdown equipment. The power and instrument cable trays associated with the redundant safe-shutdown equipment run the entire depth of the room, and are arranged in separate divisions and separated horizontally by a distance, D. The value of D, the safe separation distance, is varied and examined in this problem. The cable trays are 0.6 m (~24 in.) wide and 0.08 m (~3 in.) deep.

A simplified schematic of the room, illustrating critical cable tray locations, is shown in the attached figure. The postulated fire scenario is the initial ignition of the cable tray labelled as "A", located at 0.9 m (~3 ft) from the right wall of the room at an elevation of

2.3 m (7.5 ft) above the floor, by a trash bag fire on the floor. Cables for the redundant train are contained in another tray, labelled "B," the target. A horizontal distance, $\underline{D}$, as shown in the attached figure separates tray B from tray A. The room has a door, 2.4 m x 2.4 m (8 ft x 8 ft), located at the midpoint of the front wall, assumed to lead to the outside. The room has a mechanical ventilation system with a flow rate of 5 volume changes per hour in and out of the room. Assume a constant flow rate in the mechanical ventilation system. The midpoint of the vertical vents for the supply and exhaust air are located at an elevation of 2.4 m and have area of 0.5 m^2 each. Assume vents are square and located at the centre of the side walls (parallel to the cable trays). Assume air is supplied from the outside through the right wall, and exhausted to the outside from the left wall.

The effects of the fire door being open or closed, and the mechanical ventilation on and off will be examined.

It is assumed that:

- Other cable trays (C1 and C2) containing critical and non-critical cables are located directly above tray A.

- No combustible material intervenes between trays A and B.

Analyses

There are two parts to the analyses. The objective of Part I is to determine the maximum horizontal distance between a specified transient fire and tray A that results in the ignition of tray A. This information is of use in a fire PRA to calculate the area reduction factor for the transient source fire frequency, which are derived to be applicable to the total area of the rooms. Analyses of this part of the problem will also provide insights regarding the capabilities of the models to predict simpler fire scenarios for risk analyses than those associated with fires of redundant cable trays.

Part II will determine the damage time of the target cable tray B for several heat release rates of the cable tray stack (A, C2, and C1), and horizontal distance, D. The effects of target elevation and ventilation will also be examined.

Thermophysical Data for Walls, Floor, and Ceiling (Concrete)

Specific Heat	1000 J/KgK
Conductivity	1.75 W/mK
Density	2200 Kg/m3
Emissivity	0.94

Assume the walls, floor and ceiling are 152 mm thick.

Thermophysical Data for Cables

Heat of combustion of insulation	16 MJ/kg
Fraction of flame heat released as radiation	0.48
Density	1710 kg/m3
Specific Heat	1040 J/kgK
Thermal Conductivity	0.092 W/mK
Emissivity	0.8

Chemical Properties of Cables

Assume cable insulation is PVC – polyvinyl chloride. Chemical formula is C_2H_3Cl. The oxygen-fuel mass ratio = 1.408. The yields (mass of species/mass of fuel) are listed in the following Table.

Yields for PVC

Species	Yield
CO_2	0.46
CO	0.063
HCl	0.5
Soot	0.172

Assume the Smoke Potential of PVC = 1.7 ob.m3/g, where the smoke potential is defined as the optical density (dB/m or ob) x Volume of the compartment (m3)/mass of the fuel pyrolyzed (g).

Ambient Conditions (Internal and External)

Temperature	300 K
Relative Humidity	50
Pressure	101300 Pa
Elevation	0
Wind Speed	0

Other Constants and Indices

Constriction coefficient for flow through door	0.68
Convective heat transfer coefficient (assume same for all surfaces)	$15 \ Wm^{-2}K^{-1}$
Lower Oxygen Limit	12 %

Construction and Properties of Fire Door

The following are properties of the fire door for use in models that allow the incorporation of such features. Assume fire door is a metal-clad door with a wood core, and insulating panels between the wood core and the metal clad (on both sides of the wood core). Assume metal clad = 0.6 mm, wood core = 40 mm, and insulating panel = 3 mm.

Properties of Fire Door

	Conductivity (W/mC)	Density (Kg/m^{3})	Specific Heat (kJ/KgC)
Metal Clad - Carbon Steel	43	7801	0.473
Wood Core - Yellow Pine	0.147	640	2.8

Fiber, insulating panel	0.048	240	

Input Data for Part I

Heat Release Rates

Assume heat release rate for a trash fire as characterized in the following Table (assume linear growth between points).

<div align="center">32 Gallon Trash Bag Fire</div>

Time (minutes)	Heat Release Rate (kW)
1	200
2	350
3	340
4	200
5	150
6	100
7	100
8	80
9	75
10	100

The trash bag consists of: (1) straw and grass cuttings = 1.55 kg; (2) eucalyptus duff = 2.47 kg; and (3) polyethylene bag = 0.04 kg. Contents were thoroughly mixed, and then placed in the bag in a loose manner. Approximate the trash bag as a cylinder with a diameter = 0.49 m and height = 0.62 m. Assume the fraction of heat released as radiation is 0.3, and the heat of combustion of the trash bag material = 24.1 MJ/Kg.

Assume the trash bag and the target (representing tray A) are at the center of the cable tray lengths. In order to conduct a simplified and conservative analysis, assume the

target is a single power cable with a diameter = 50 mm at the bottom left corner of the cable tray A. For models in which targets are represented as a rectangular slab, assume the slab is oriented horizontally with a thickness of 50 mm. Assume the cable ignites when the centerline of the cable reaches 643 K.

Base case

Distance between the midpoints of the trash bag and tray A = 2.2 m (~7 ft), the door is closed, and mechanical ventilation system is off.

Variation of Parameters

A. To facilitate comparisons of code results, simulations for horizontal distances between the trash bag and tray A of 0.3, 0.9, and 1.5 (~1, ~ 3, and ~ 5 ft) should be conducted (Cases 1–3)

B. Simulations should also be conducted with (a) the door open and mechanical system off; and (b) mechanical ventilation system on and door closed (Cases 4-5).

Summary of Cases for Part I

	Distance from Fire	Door	Ventilation System
Base Case	2.2 m	Closed*	Off
Case 1	0.3+		
Case 2	0.9		
Case 3	1.5		
Case 4		Open	
Case 5			On

* For simulations with the door closed, assume a crack (2.4 m x 0.005 m) at the bottom of the doorway.

+A value in a cell indicates the parameter is varied from the base case.

The maximum horizontal distance between the trash bag and tray A, that results in the ignition of tray A, should be determined by extrapolation of results for the simulations with the door closed and mechanical ventilation system off (Base case to Case 3).

The resulting centerline temperature of the cable should be presented for these simulations. In addition, the following parameters should be reported:

- Upper layer temperature
- Lower layer temperature
- Depth of the hot gas layer
- Heat release rate
- Oxygen content (upper and lower layer)
- Flow rates through door and vents
- Radiation flux on the target
- Target surface temperature
- Total heat loss to boundaries

For CFD and lumped-parameter models, the profile at the midpoint of the room should be presented. All results should be presented in SI units.

Input Data for Part II

Heat Release Rates

The modeling of and predicting the heat release rate of a burning cable tray stack is extremely complex, and current models are not capable of realistically predicting such phenomena. Therefore, the heat release rates of the burning cable tray stack is defined as input in the problem. The consecutive ignition and burning of all 3 cable trays (trays A, C2, and C1) will be modeled as one fire. Conduct analyses assuming peak heat release rate for the whole cable tray stack between 1 – 3 MW. Assume t-squared growth with $t_0 = 10$ min., and $Q_0 = 1$ MW.

$$Q = Q_0 \, (t/t_0)^2$$

Assume a fire duration of 60 minutes at peak heat release rate, and then a t-squared decay with similar constants as for growth.

Geometry

For point source calculations, assume the heat source (trays A, C2, and C1) is at the center of the cable tray length and width and at the elevation of the bottom of tray C2. For 3-D calculations, assume the fire source is the entire length of tray C2 (15.2 m), width (0.6 m), and height of 0.24 m (0.08 x 3). Assume the target (representing tray B) is at the center of the cable tray length. In order to conduct a simplified and conservative analysis, assume the target is a single power or instrumentation cable with no electrical conductor inside the cable, and with a diameter of 50 mm or 15 mm respectively at the bottom right corner of cable tray B. For models in which targets are represented as a rectangular slab, assume the slab is oriented horizontally with a thickness of 50 mm or 15 mm. Assume the cable is damaged when the centerline of the cable reaches 200 C.

Base Case

Heat Release Rate for cable tray stack = 1 MW (reaching peak heat-release rate and decaying as specified above) at a horizontal distance, D = 6.1 m (20 ft). Door is closed and ventilation system is off. Target is a power cable 1.1 m (3.5 ft) above tray A.

Variation of Parameters

A. Vary D = 3.1, 4.6 m (~10, ~15 ft.) – Cases 1-2

B. Vary peak heat release rate for cable tray stack = 2 MW, and 3 MW (reaching peak heat-release rate and decaying as specified above) at a horizontal distance, D = 3.1, 4.6, 6.1 m (Cases 3-8).

C. Door closed and ventilation system operational initially; and door opened, and ventilation system shut after 15 minutes (Case 9).

D. Door and ventilation system open throughout the simulation (Case 10).

E. Two elevations for tray B should be analyzed to examine the possible effects of the ceiling jet sub-layer and the elevation of the target:

   •2.0 m (6.5 ft) above tray A, (i.e., 0.3 m (1 ft) below the ceiling) – Case 11

   •Same elevation as tray A – Case 12

F. Instrumentation cable with diameter = 15 mm (Case 13)

The resulting centerline temperature of the target, and time to damage of target, should be presented for these analyses. In addition, the following parameters should be reported:

- Upper layer temperature
- Lower layer temperature
- Depth of the hot gas layer
- Heat release rate
- Oxygen content (upper and lower layer)
- Flow rates through door and vents
- Radiation flux on the target
- Target surface temperature
- Total heat loss to boundaries
- Chemical species (CO, HCl, soot) in upper layer
- Optical density of smoke (optional)

For CFD and lumped-parameter models, the profile at the midpoint of the room should be presented. All results should be presented in SI units.

Summary of Cases for Part II

	HRR (MW)	**D (m)**	**Door**	**Vent. Sys.**	**Target**	**Elev. (m)**
Base Case	1 MW	6.1	Closed*	Off	Power	1.1
Case 1		3.1+				
Case 2		4.6				
Case 3	2	3.1				
Case 4	2	4.6				
Case 5	2	6.1				
Case 6	3	3.1				
Case 7	3	4.6				
Case 8	3	6.1				
Case 9			Open>15 min	Off>15 min		
Case 10			Open	On		
Case 11						2.0
Case 12						Same
Case 13					Instrument	

* For simulations with the door closed, assume a crack (2.4 m x 0.005 m) at the bottom of the doorway.

+A value in a cell indicates the parameter is varied from the base case.

All dimensions are in meters.

Fig. 9-1 Representative PWR Emergency Switchgear Room

Appendix G: Benchmark Analysis with JASMINE and CFAST, Stewart MILES, BRE, UK

International Collaborative Project to Evaluate Fire Models for Nuclear Power Plant Applications

Benchmark Exercise # 1 - Cable Tray Fires of Redundant Safety Trains

Simulations using JASMINE and CFAST

S.D. Miles
Building Research Establishment, UK

SUMMARY

As part of its participation in the International Collaborative Project to Evaluate Fire Models for Nuclear Power Plant Applications, BRE has made numerical predictions for Benchmark Exercise # 1 – cable tray fires of redundant safety trains. Trash bag and cable tray fires inside a switchgear room were modelled, with the main objective to ascertain the likelihood of thermal damage to a 'target' cable at various distances form the fire source.

BRE has performed simulations using a CFD model (JASMINE) and a zone model (CFAST). Results and analysis were presented at a meeting of the collaborative project in January 2001. This paper summarises the findings from the BRE simulations.

Due to the nature of the benchmark scenarios, both CFAST and JASMINE indicated that damage to the target cables was unlikely in all scenarios. However, some important observations were made, including the difficulty in modelling nearly-sealed rooms where the difference in pressure predicted by CFAST and JASMINE providing the most noticeable difference in the output from the two models. Other issues that were found to be important included the modelling/assessment of the heating of the target cables, and the influence of using different oxygen starvation criteria and fire source locations.

INTRODUCTION

In October 1999 the U.S. Nuclear Regulatory Commission and the Society of Fire Protection Engineers organised a planning meeting with international experts and practitioners of fire models to discuss the evaluation of numerical fire models for nuclear power plant applications. Following this meeting an international collaborative project was set up with a view to sharing knowledge and resources from various organisations and to evaluate and improve the state of the fire modelling methods and tools for use in nuclear power plant fire safety.

The UK Building Research Establishment (BRE) was represented at the next meeting of the collaborative project (ISPN, Paris, June 2000). The main outcome from this meeting was a finalised problem definition for a nuclear power plant fire scenario, to be used as a benchmark exercise for which the participating organisations would undertake numerical predictions and then compare results.

BRE's Fire and Risk Sciences (FRS) Division performed zone model (CFAST) and CFD (JASMINE) simulations of selected scenario cases from the benchmark exercise. Results and analysis were presented during the third meeting of the international collaborative project at the Electric Power Research Institute (EPRI), California in January 2001.

This paper summarises the CFAST and JASMINE simulations and findings. Following sections describing briefly the fire models used, there is a section highlighting the main results and analyses.

CFAST DESCRIPTION

CFAST is one of the most widely used zone models, available from the National Institute of Standards and Technology (NIST), USA. It is the main component of the program suite FAST, which is controlled through a graphical user interface. CFAST/FAST version 3.1.6 was used in the current study, which is the most recent complete version to be released.

CFAST is a multi-room zone model, with the capability to model multiple fires and targets. Fuel pyrolysis rate is a pre-defined input, and the burning in the compartment is then modelled to generate heat release and allow species concentrations to be calculated. For most applications CFAST is used as a conventional two-zone model, whereby each compartment is divided into a hot gas upper layer and a cold lower layer. In the presence of fire, a plume zone/model transports heat and mass from the lower to upper layer making use of the McCaffrey correlation [1]. Flows through vents and doorways are determined from correlations derived from the Bernoulli equation. Radiation heat transfer may be included using an algorithm derived from that of Siegel and Howell [2]. Other features of CFAST of relevance to the benchmark exercise include a one-dimensional solid phase heat conduction algorithm employed at compartment walls and targets and network flow model for mechanical ventilation.

Publications available on the NIST website (www.nist.gov) [3,4] provide a comprehensive description of CFAST and the models employed. A summary of comparison with experimental measurements is provided also.

JASMINE DESCRIPTION

JASMINE is a CFD fire code that has undergone continual development at the BRE over nearly 20 years. It simulates fire and smoke movement in three-dimensions, for steady state and time-dependent applications. Version JASMINE 3.1 was used in this benchmark exercise.

JASMINE is a finite-volume CFD code, employing a variant of the SIMPLE pressure-correction scheme on a structured, Cartesian mesh. The program can model single and multiple compartment enclosures with arbitrary openings (doors, windows and vents), obstructions, fire/heat sources and mechanical ventilation systems. External wind profiles, static pressure boundaries and symmetry planes may be specified.

A modified, enhanced version of an early PHOENICS code provides the core pressure-correction solver. Turbulent closure is by a k-ε model using the standard constants and additional buoyancy source terms. Standard wall functions for enthalpy and momentum describe the turbulent boundary layer adjacent to solid surfaces. A suite of sub-models for combustion, radiation, data analysis etc has been added as part of the code development.

A scenario may be set-up using the graphical user interface (JOSEFINE), which allows the user to define the geometry and boundary conditions and view the results with a graphical post-processor. The results may be viewed also with the commercial CFD post processor FIELDVIEW. A detailed summary text file is generated, containing convergence information, analysis data etc.

JASMINE has been validated against data from pre-flashover fire experiments inside domestic size rooms, atria, tunnels, hospital wards and other enclosures. More recently it has been validated against data from post-flashover fire tests also. Further details are provided in the validation section.

Modelling Details

Mathematical details of the differential-integral equations describing the fluid flow processes may be found elsewhere, see for example [5]. In summary, the equations describing the fluid dynamics of Newtonian fluids (which includes most common fluids such as air and water) are the Navier-Stokes equations for momentum and mass conservation and the related advection-diffusion transport equation describing conservation of other properties such as energy and species concentration. These equations, together with equations of state for density and temperature, describe very accurately the physics of Newtonian fluids.

CFD models approximate the underlying equations with a coupled system of algebraic equations that are solved numerically on a discrete mesh or grid. This yields predictions for velocity, pressure, temperature etc at each mesh point in space and time. JASMINE, in common with most other CFD fire models, employs the finite volume method [6,7], in which the differential equations are first transformed into an integral form and then discretised on the control volumes defined by the mesh.

JASMINE solves a time/ensemble-averaged form of the Navier-Stokes and transport equations, where the turbulent fluctuations are not modelled explicitly, but instead are 'incorporated' into the solution by a 'turbulence model'. The particular model used in JASMINE is the industry standard, k-ε model [8], which employs the eddy viscosity assumption in which the effect of turbulence is included as an additional 'turbulent viscosity'. Additional source terms are included in the k-ε model to account for the effects of buoyancy [9].

The ensemble-averaged Navier-Stokes and transport equations, coupled with an equation of state (ideal gas law) and the various sub-models for the fire physics, defines the equation set in JASMINE. This is discretised and solved numerically on a structured three-dimensional grid using the SIMPLEST scheme, a variant of the SIMPLE pressure-correction scheme [7,10]. Convection terms are discretised with the first-order 'upwind' scheme and time advancement is by the first-order, fully implicit, backward Euler scheme. Standard wall functions for enthalpy and momentum [8] describe the turbulent boundary layer adjacent to solid surfaces.

Combustion is generally modelled using an eddy breakup assumption [11] in which the fuel pyrolysis rate is specified as a boundary condition, and combustion is then calculated at all control volumes as a function of fuel concentration, oxygen concentration and the local turbulent time-scale (provided by the k-ε model). Simple one-step, infinitely fast chemical reaction is assumed. The eddy breakup model is appropriate for turbulent diffusion flames characteristic of fire, where the rate of reaction is controlled by the comparatively slow mixing of fuel with oxygen. Complete oxidation of the fuel is assumed when sufficient oxygen is available, and therefore predictions of carbon monoxide are not provided by this approach.

Radiant heat transfer is modelled with either the six-flux model [12], which assumes that radiant transfer is normal to the co-ordinate directions or the slower, but potentially more accurate, discrete transfer method [13]. Local absorption-emission properties are computed using Truelove's mixed grey-gas model [14], which calculates the local absorption coefficient as a function of temperature and gas species concentrations and, if available, soot concentration also.

Density is defined from the equation of state, and gas temperature is calculated from the definition of enthalpy, in which specific heat is itself a function of temperature and species concentrations. Thermal conduction into solid boundaries is approximated by a quasi-steady, semi-infinite one-dimensional assumption.

Code Validation

JASMINE has been validated against experimental measurement for a range of scenarios, ranging from small enclosure fire experiments to large, fully developed fires in tunnels and offshore structures. Some of the more important validation cases are referenced below.

The Steckler experiments [15]. In these experiments steady state mass flow rates, velocity profiles and temperatures associated with a burner at various locations inside a 2.8 m x 2.8 m x 2.18 m compartment with a single doorway opening were measured. Good agreement was found for the doorway flow rates, with the CFD model capturing the influence of plume lean on the entrainment process.

The Lawrence Livermore experiments [16]. A series of steady state experiments were performed with a spray pool fire inside a 6 m x 4 m x 4.5 m nuclear test cell with mechanical ventilation. Good agreement was obtained for temperatures inside the test cell, and the prediction of fire-induced pressure rise was reasonably close to the measured value.

Hospital ward experiments [17]. An experiment was performed involving a burning PU-foam mattress in a ward of dimensions 7.3 m x 7.9 m x 2.7 m. Pre-fire steady condition, driven by the heat released from a set of wall radiators, and the subsequent transient fire phase were simulated. Good temperature agreement was achieved, and good species (CO_2) agreement at head height also. However, there was some discrepancy in CO_2 at bedside height.

Sports stadium [18]. Simulations were made of fire tests performed in a 1/6th-scale physical model of a proposed sports stadium. Comparisons were made for temperatures at thermocouple tree locations, which showed good agreement. Some discrepancy at ceiling level was attributed to the approximate 'staircase' representation of the dome shape.

Zwenberg railway tunnel experiments [19,20]. Predictions made by TUNFIRE, the tunnel specific version of JASMINE, were compared to measurements from a series of fire tests in the disused Zwenberg railway tunnel in Austria. The tunnel is 390 m long wit a 2.18% gradient. Steady state scenarios involving natural and forced longitudinal ventilation with fires of approximately 20 MW were modelled. Predictions of the temperature and species downstream of the fire source were in good agreement with measurement. However, the need for further model development in the treatment of radiation and heat transfer in the vicinity of the fire was highlighted.

Memorial Tunnel experiments [21]. The decommissioned Memorial Tunnel in the USA was used for an extensive set of fire tests involving natural, longitudinal and transverse ventilation. A selection of the longitudinal ventilation tests, involving pool fires from 20 to 100 MW, was modelled with TUNFIRE. The transient simulations captured the main features of the tests, predicating the performance of various jet fan configurations reasonably well. Some discrepancy was found in the pre-ventilation stage where the smoke layer dropped to ground level more quickly in the simulations compared to the tests.

Channel Tunnel shuttle wagon tests [22]. As part of the safety study for the Channel Tunnel, JASMINE was validated against fire experiments inside a car shuttle wagon. It was shown that by considering properly the mechanical ventilation system and the boundary heat losses reasonably good agreement could be achieved for temperature and gas species.

LBTF tests [23]. An eight-storey, steel framed building, constructed at BRE's Cardington Hanger, provided an ideal opportunity to perform full-scale fire tests. The 8.4 m high atrium and part of the first floor were used in the study of fully-ventilated fires up to 5 MW in size. Predictions of smoke layer depth and temperature matched experimental measurement reasonably closely, as did the entrainment rates.

Post-flashover compartment fire tests [24]. A series of fully developed, ventilation-controlled fire tests was sponsored by the European offshore industry to validate zone and CFD models. Tests involving pool fires up to 80 MW inside single opening enclosures were modelled with JASMINE. Good agreement was found in the vent flow rates and temperatures. Furthermore, the simulations captured the oxygen depletion process correctly. The main discrepancy was in the temperatures and fluxes at the back of the compartment, attributed in part to the

complexity of the wall lining behaviour, which involved the steel sheeting becoming partly detached during the tests.

CIB round robin activity [25]. The Commission of the International Council for Research and Innovation in Building and Construction (CIB) co-ordinated a series of round robin fire model validation exercises in which participants made 'blind' predictions for fire tests in the knowledge of only a limited amount of information (geometry, thermal properties, fire pyrolysis rate). JASMINE simulations were made for a compartment (7.2 m x 7.2 m x 3.6 m) with a 'letter-box' opening and two crib fire sources. Good agreement was found for species predictions, and reasonable agreement for temperatures. Predicted incident wall fluxes were noticeably lower than those 'estimated' from the measurement data, attributed in part to the quasi-steady heat conduction treatment used in the simulations.

Balcony spill plume tests [26]. As part of a wider study into the entrainment processes associated with spill plumes, JASMINE simulations of various 1/10th-scale experiments were performed. Predicted and measured entrainment rates were in reasonable agreement. An important conclusion was that grid refinement did have an important influence on the predicted entrainment rate.

Sprinkler model validation [27]. As part of the development of a sprinkler model for JASMINE, simulations were undertaken of a full-scale fire test where the influence of the water spray on gas temperatures and velocities at ceiling level was investigated. Reasonable agreement was found, and areas of further improvement identified.

BENCHMARK EXERCISE

Problem Definition

Following publication of the specification for the benchmark exercise # 1, BRE has undertaken CFD (JASMINE) and zone model (CFAST) predictions for selected scenario cases. The benchmark exercise is described in Appendix A.

Table 1 shows the scenario cases modelled by BRE. Due to the long duration of the Part II scenarios (80 minutes), the CFD (JASMINE) simulations were undertaken for between 20 and 45 minutes only (depending on the case). This was sufficiently long to investigate the main features of each scenario, and allowed more cases to be undertaken with the available computing resource. Whereas individual JASMINE simulations were undertaken for each Part I case, some of the Part II cases were 'doubled up' in that a CFD solution was used to investigate more than one case. This was due to some cases differing only in the location of the target cable, which itself did not influence the CFD solution, i.e. one CFD solution was used to predict the thermal damage to multiple target locations.

Table 1.   Benchmark scenarios modelled

Numerical Model	Scenarios Modelled
JASMINE	Part I: base case, case 1 and case 4 Part II: base case and cases 1,2, 9,10,11,12 & 13
CFAST	Part I: all cases Part II: all cases

While the problem specification was followed as closely as possible, some user interpretation was required, in particular in respect to the target description and the treatment of radiation. Most simulations were completed prior to the third project meeting, and the findings were presented at that meeting. Some further simulations have been performed since, looking at the effect of mechanical ventilation with CFAST and the prediction of pressure in the door-crack scenarios with JASMINE.

In CFAST, heat transfer to a rectangular target object, orientated in a particular direction, can be modelled using a one-dimensional equation. The simulations showed that the choice of target orientation could have a significant influence on the size of the incident heat flux. JASMINE also allows heat transfer to solid objects to be modelled using a semi-infinite, quasi-steady approximation. For the current work, however, an assessment of the likelihood of target cable damage was based on the local gas temperature and mean radiation flux. This will in general provide a conservative approach, over-predicting the thermal hazard.

For the CFAST simulations radiation from the fire plume was incorporated, as specified, by reducing the fire size by 30%. For the JASMINE simulations a six-flux radiation model was employed, and rather than defining the radiation loss explicitly it was predicted by the solution of the CFD and radiation models. Some later simulations investigated the effect of using a fixed radiation loss of 30% and no radiation model.

The two-zone assumption was used for all the CFAST simulations. A constrained fire was assumed, which allowed for oxygen availability to control the rate of heat release from the pre-defined pyrolysed fuel. As stipulated in the benchmark specification, a 30% radiative loss was included. Although the wall and ceiling thermal properties were specified exactly, the separate door properties were not included. To investigate the effect of orientation on the predictions of target surface temperature, two normal directions were considered, namely facing towards the ceiling and towards the floor. The ceiling jet sub-model was used.

The JASMINE simulations employed between 124,000 and 175,000 control volumes, resolving the vertical extent of the door crack with two control volumes. An eddy break-up combustion model was used, which allowed the oxidation of the pre-defined pyrolysed fuel to be calculated as a function of oxygen concentration and local turbulent mixing. The six-flux radiation model, combined with Truelove's emissive power model, was used in the majority of simulations, allowing the radiation losses from the plume and hot gas layer to be calculated with reasonable accuracy. However, to compute fluxes to target cables with greater accuracy would have required the computationally more expensive discrete transfer model. Soot formation and oxidation was not modelled. Although not generally employed in the JASMINE combustion model, a oxygen cut-off was applied in the majority of simulations, using a figure of 12% as requested.

Both JASMINE and CFAST showed that for Part I sufficient oxygen was available for continual combustion in all cases, i.e. the open doorway and door crack cases. The 12% LOL was not reached in either set of simulations. Both models indicated that target cable damage would be very unlikely due to only a modest rise in gas temperature. Figures 1 and 2 show CFAST and JASMINE temperature predictions for the base case and cases 4 and 5 of Part I. Whereas the CFAST values are for the upper layer in the two-zone approximation, the JASMINE temperatures are for a location just below the centre of the ceiling. This will account in part for the difference in predicted values for CFAST and JASMINE, since the CFD model does not consider an average layer/zone temperature. A further point to note is that JASMINE predicted a slight increase in temperature in the presence of mechanical ventilation, which was not shown in the CFAST simulations. Additional, forced airflow will effect the flow pattern in the plume and upper layer, and this is not captured by a zone model. Figure 3 illustrates the effect that mechanical ventilation has on the plume shape in the JASMINE simulations.

A significant finding from the CFAST simulations was that the target orientation could have an important bearing on the incident flux, and resultant target temperature. By facing the target downwards the incident flux was in some instances more than double that obtained when the target faced upwards, as illustrated in Figures 4 and 5. If the target had been directed directly towards the fire, i.e. at an oblique angle, then the incident flux and heating of the cable would most probably been higher still.

Figure 6 shows target radiation fluxes estimated from the JASMINE simulations, where because the target was not modelled explicitly, an average directional flux has been taken. Whereas for case 1 the flux levels are comparable between CFAST and JASMINE, for the other cases examined with JASMINE the similarity is much less. A significant factor here is

that JASMINE models radiation emission and absorption from the gas layer (CO_2 and H_2O), which may be an important transfer mechanism.

As shown in Figures 7-9, both models produced similar flow rates across the doorway for the open doorway scenario (case 4). This scenario represents the classic enclosure fire for which both zone and CFD models would be expected to give similar results.

The most significant difference between the JASMINE and CFAST predictions for Part I was in the pressure predictions for the door crack cases, with CFAST predicting significantly higher pressure build up inside the room. Furthermore, whereas JASMINE predicted outflow form the door crack throughout the duration of the scenario (10 minutes), CFAST predicted a period of moderate inflow after the initial pressure build-up had been dissipated due to venting of gases through the door crack. Figures 10 and 11 show the pressure predictions for CFAST and JASMINE, without (base case) and with (case 5) additional mechanical ventilation. The outflow and subsequent inflow predicted in the CFAST simulation can be seen in Figures 9 and 10.

On initial examination, the pressures predicted by CFAST for the door crack cases (peak value approximately 2000 Pa) seem perhaps too high, whereas the JASMINE values (of the order 50 Pa) seem more reasonable for a compartment fire scenario. While the 'background' pressure level within a sealed compartment is generally not important from the point of modelling fire development (although structural/mechanical considerations may be important), it may be more significant when venting through small orifices is included. Here, the difference in pressure between the inside and outside will have a strong bearing on the flow rate through the opening.

JASMINE adopts the usual assumption adopted in 'low speed' CFD models and treats the air as weakly compressible, i.e. density is defined as a function of temperature and species concentration. The coupling between pressure and density, included in 'high speed' fully compressible models, is ignored. Whether this is important for 'nearly sealed' compartment fire simulations is not clear. CFAST does not solve for conservation of momentum, and the bearing this may have on the door crack scenarios is also not clear.

Further JASMINE analysis of the door crack scenario for Part I has been undertaken since the third meeting of the collaborative project. By defining a 30% radiation loss explicitly, and switching off the radiation model, the period of over-pressure inside the room was followed by a period of under-pressure and associated inflow of outside air. This behaviour was predicted by CFAST, albeit with significantly higher over-pressure. Interestingly, using a volume heat source instead of a combustion model resulted in a higher over-pressure (approximately 120 Pa peak), and again a subsequent period of under-pressure and air inflow. The effect of replacing the door crack with a square opening of equivalent area was investigated, producing a similar result but, as expected, a reduced level of over-pressure. Figure 12 shows the JASMINE pressures for the original base case and also the above modified scenarios. Figure 13 shows that a period of inflow follows, as expected, if the pressure inside the room decreases below ambient.

Clearly the thermodynamics of fire within a 'nearly sealed' compartment is a complex issue that has received much less attention by the fire safety community than fire inside enclosures with at least a moderate level of venting to the outside. Further work in this area is recommended.

For Part II, both JASMINE and CFAST indicated again that target cable damage was unlikely. Oxygen depletion was a significant feature in the door crack cases for Part II, with both models predicting oxygen consumption after about ten minutes. Figure 14 shows the upper layer temperatures predicted by CFAST for the base case and cases 3 and 6 with the larger fires. Figure 15 shows the JASMINE gas temperatures at the target locations for the door-crack scenarios with the smaller fire. The peak temperature at the target location for the base case is similar to the peak upper layer temperature predicted by CFAST. The actual LOL value was not very significant, with the effect of reducing the LOL to zero being to allow combustion to continue for a while longer before stopping due to a lack of available oxygen.

The effect of placing the burning cable tray at floor level was investigated with CFAST, and this did have an influence on the level thermal hazard predicted. In particular, with the larger (3 MW) fire the effect of more combustion occurring before the layer height reached the level of the fire source was an increased upper layer temperature. Figure 16 shows that, combined with a 0% LOL value, this resulted in predicted target surface temperatures that might signify damage. Note that the difference in peak temperature for the three cases is most likely a numerical effect of the model.

However, for both CFAST and JASMINE, a more sophisticated treatment of heat transfer to the target cable, and the subsequent conduction of heat into the cable, would be required in order to obtain more precise estimates of cable temperature and thermal damage. It is likely that the main contributing factor to cable damage for the scenarios like those of Part II would be due to radiative heat transfer from the flaming region, which in cases where the fire source is close to the target cable could be sufficient to cause thermal damage. However, as posed, the Part II scenarios did not allow for this process to be addressed realistically. This was due to the burning area of the fire source being approximated as the entire length of the source (burning) cable, which obviously reduces drastically the intensity of the fire source during the fire growth phase.

In respect to the target orientation issue in CFAST, it was found for Part II that upward facing targets were exposed to greater thermal fluxes than downward facing ones. This was in contrast to Part I, and indicated the importance of this aspect of user interpretation in setting up a scenario.

For Part II, the main discrepancy between CFD and zone model predictions was again in the level of over-pressure in the door crack cases. However, the discrepancy was less than in Part I. Figures 17 and 18 show that the peak over-pressure in the base case was approximately 300 Pa with JASMINE and 750 Pa with CFAST. Furthermore, the CFAST pressure predictions for the door crack cases in Part II were not entirely convincing. As illustrated in Figure 19, placing the cable tray fire source in the base case at floor level resulted in the peak over-pressure increasing from 750 Pa to nearly 5000 Pa, which seems out of proportion compared to the much more modest increase in temperature. Moreover, the peak pressure in excess of 12000 Pa obtained when locating the 3 MW cable tray fire at floor level is certainly surprisingly high.

Cases 9 and 10 of Part II, involving combinations of mechanical ventilation and open doorway conditions, were undertaken with JASMINE. However, in Part II it was not possible to obtain sensible CFAST results with mechanical ventilation.
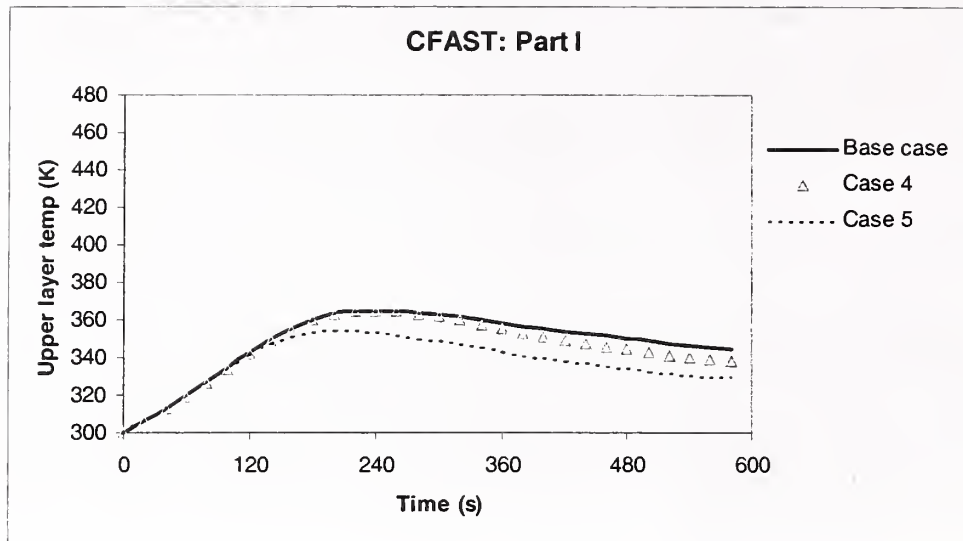
Figure 1   CFAST predictions of upper layer temperatures in Part I
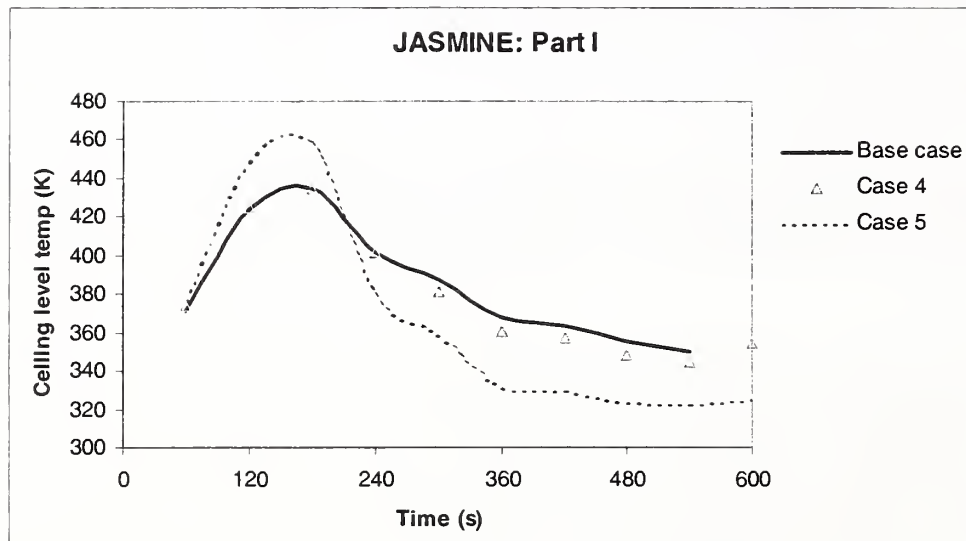

Figure 2   JASMINE predictions of ceiling level temperatures in Part I

Part I base case – no mechanical ventilation

Part I case 5 - with mechanical ventilation

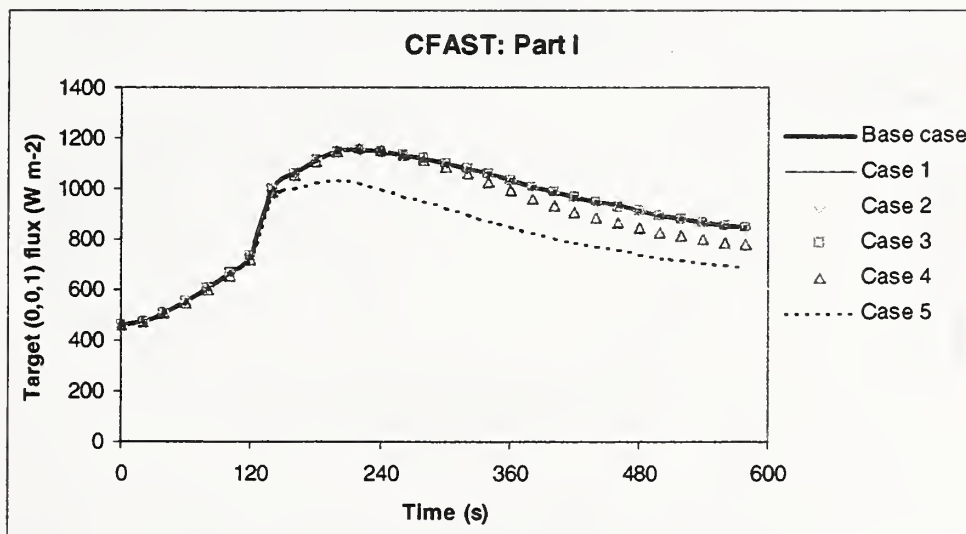Figure 3   JASMINE plume shape at 180 s with and without mechanical ventilation

Figure 4   CFAST predictions of fluxes to upward facing targets in Part I
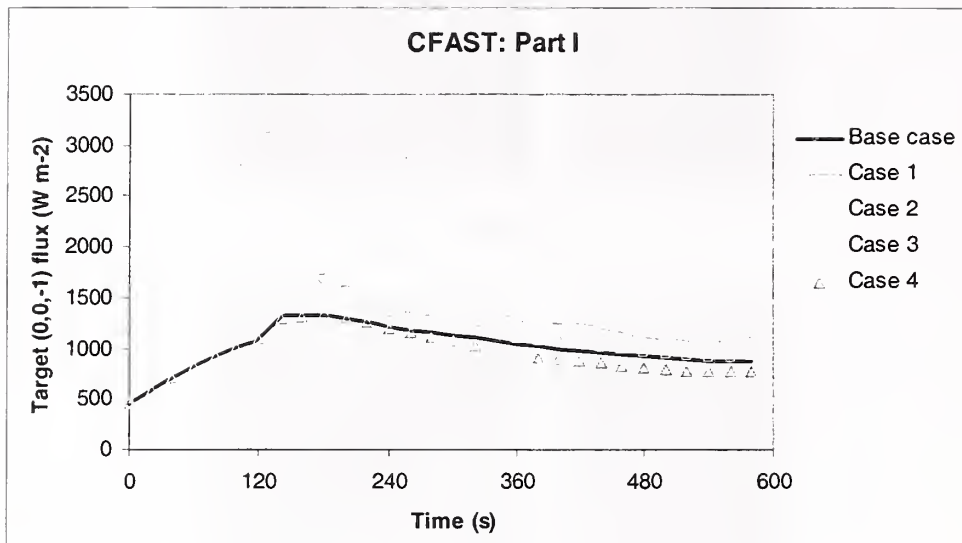
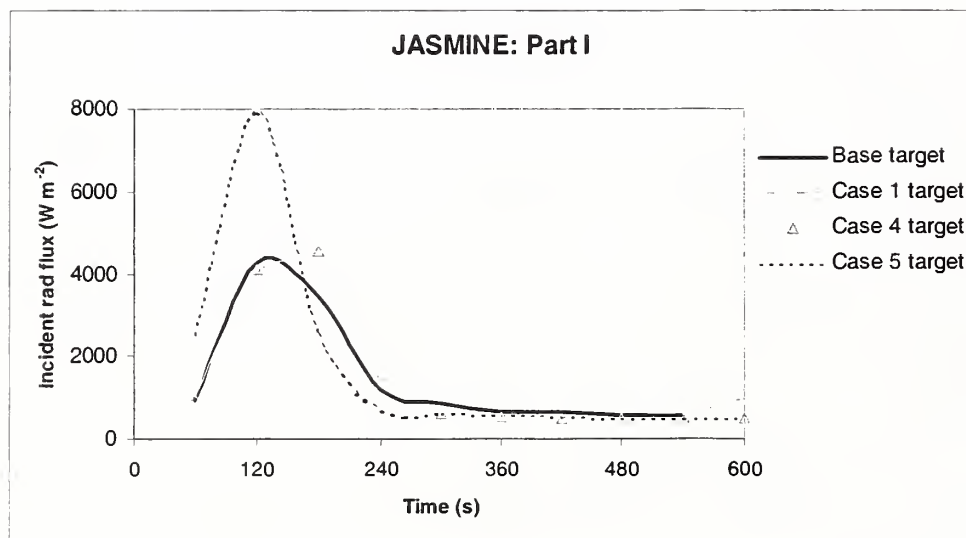Figure 5   CFAST predictions of fluxes to downward facing targets in Part I

Figure 6   JASMINE predictions of incident fluxes in Part I
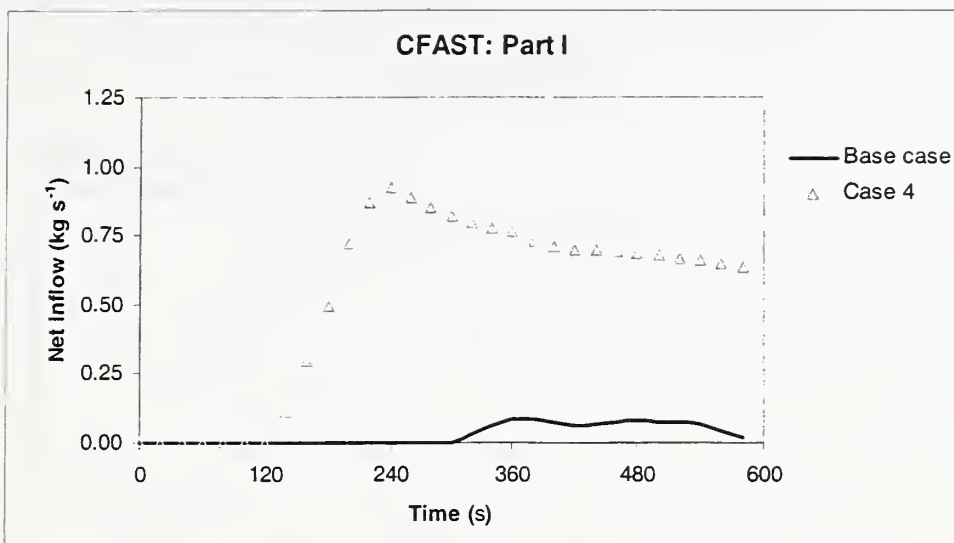
Figure 7   CFAST predictions of inflow rates in Part I
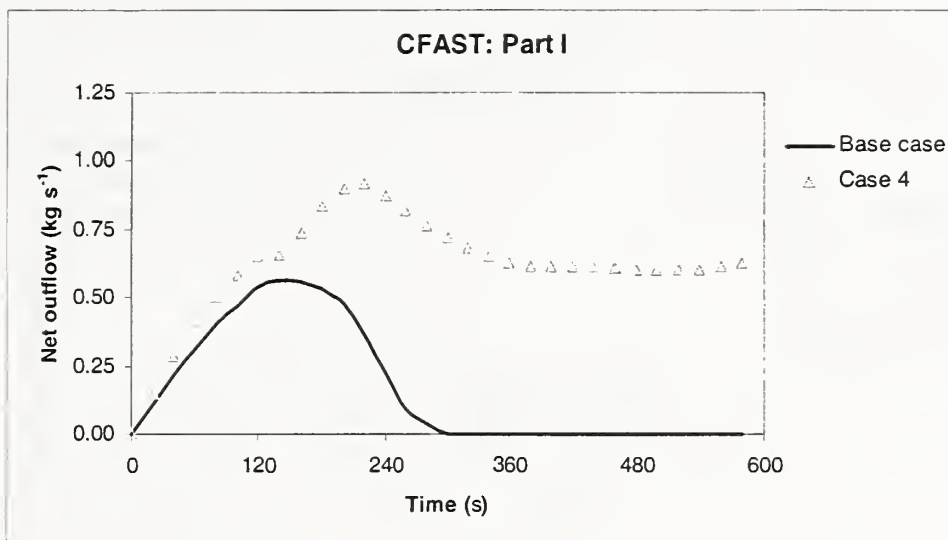
Figure 8   CFAST predictions of outflow rates in Part I
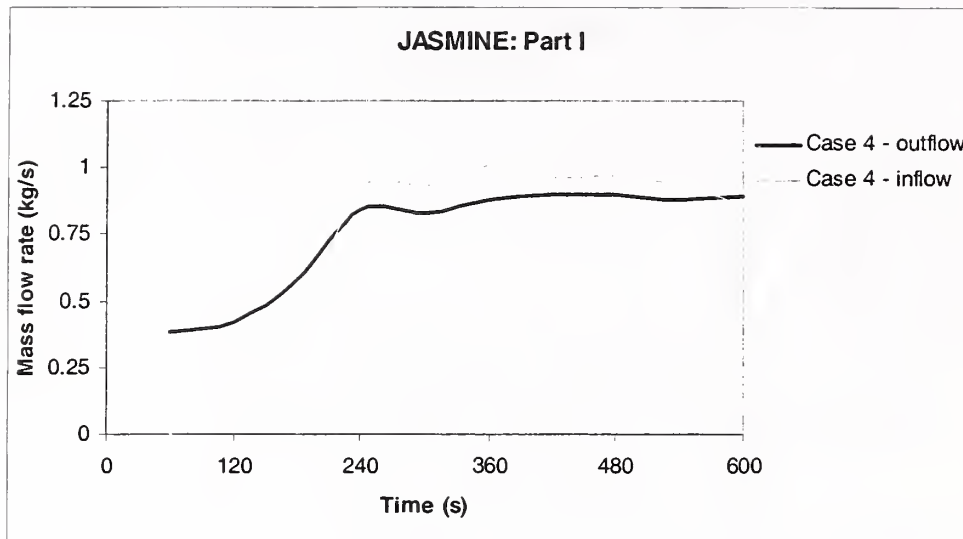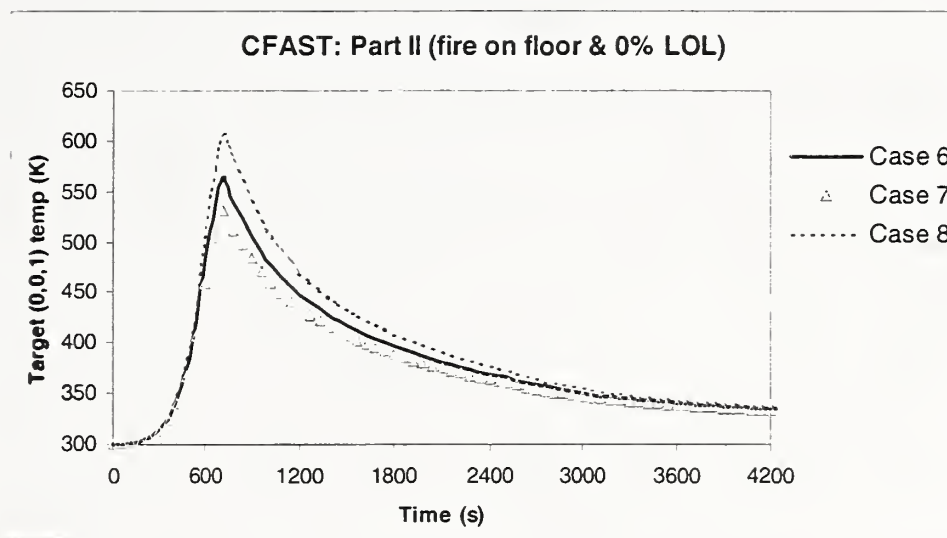
Figure 9   JASMINE predictions of inflow/outlow rates in Part I
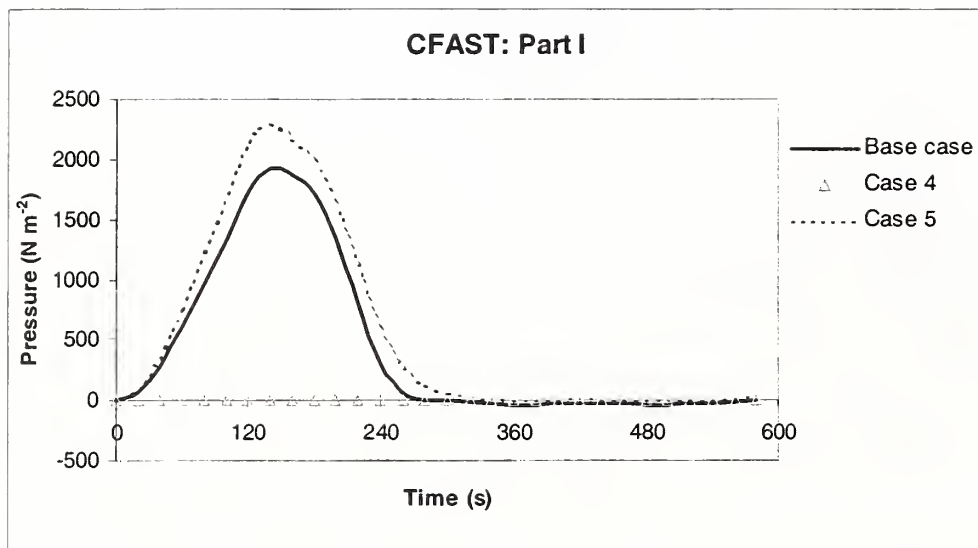
Figure 10   CFAST predictions of pressure in Part I
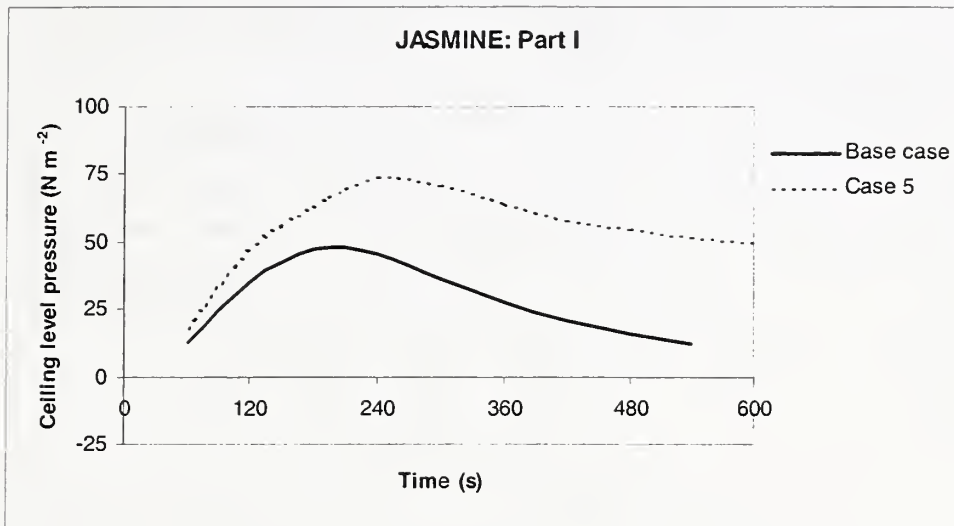
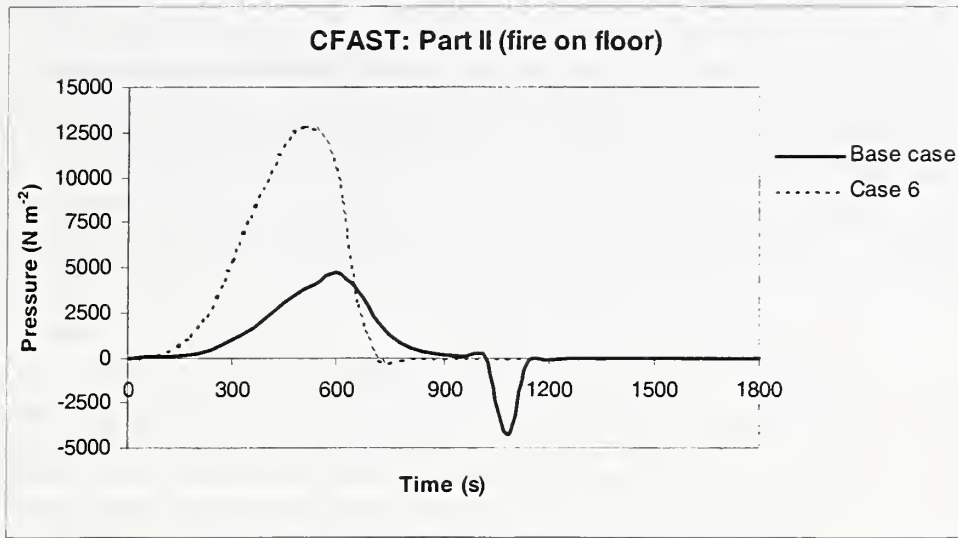Figure 11   JASMINE predictions of pressure in Part I
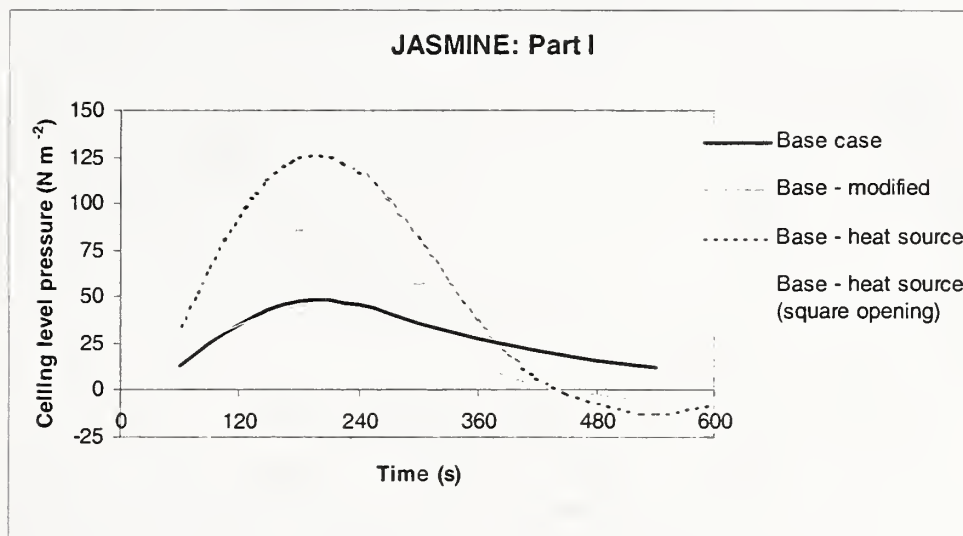
Figure 12   JASMINE predictions of pressure in Part I
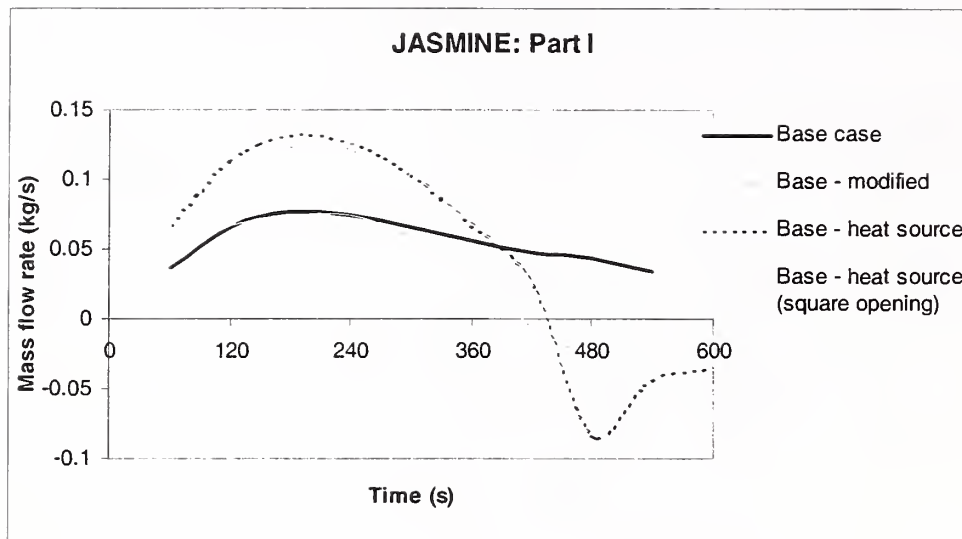
Figure 13   JASMINE predictions of inflow/outflow in Part I
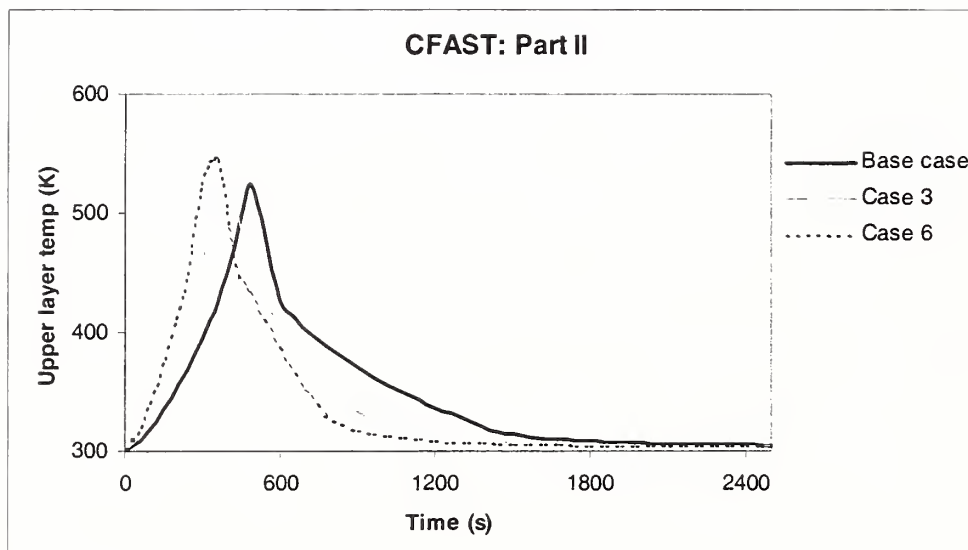
Figure 14   CFAST predictions of upper layer temperature in Part II
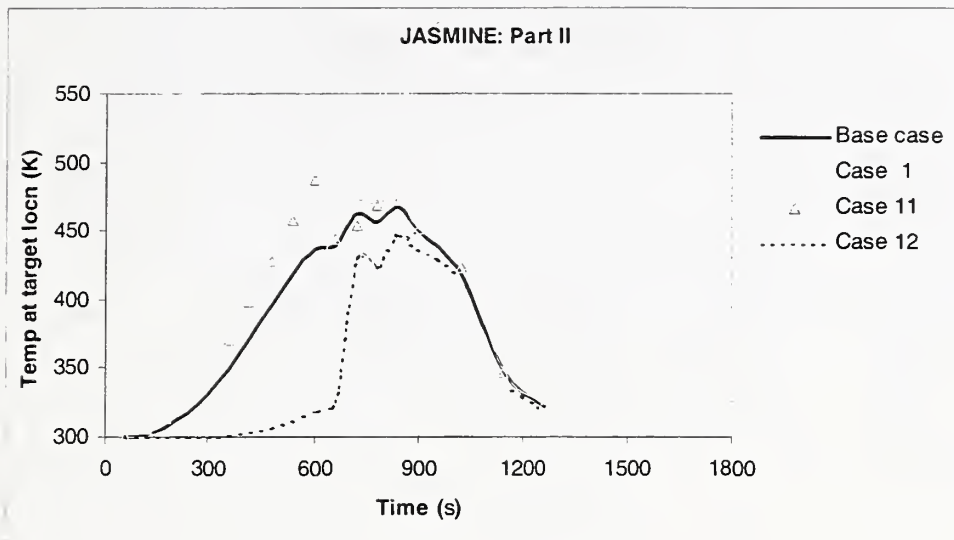
Figure 15   JASMINE predictions of gas temperatures in Part II

Figure 16   CFAST predictions of target temperatures in Part II
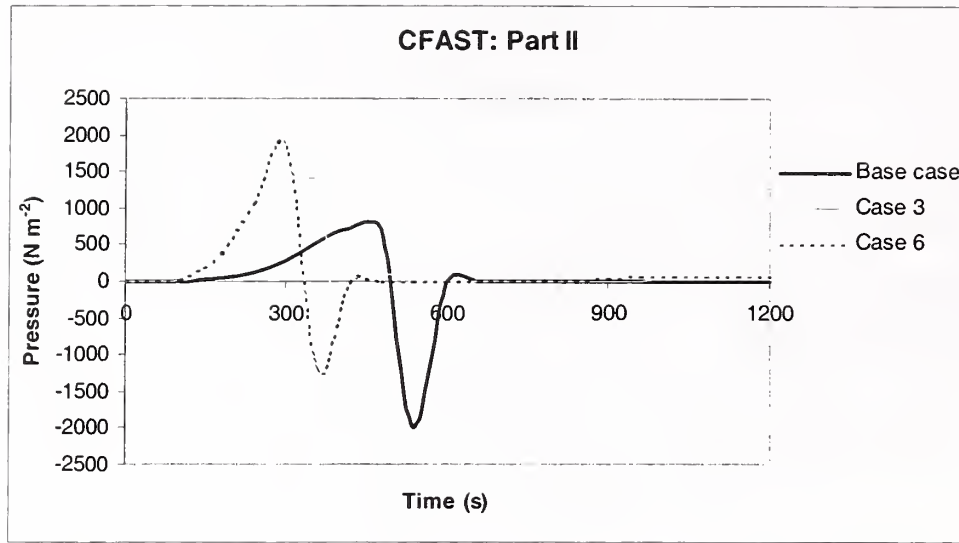
Figure 17   CFAST predictions of pressure in Part II
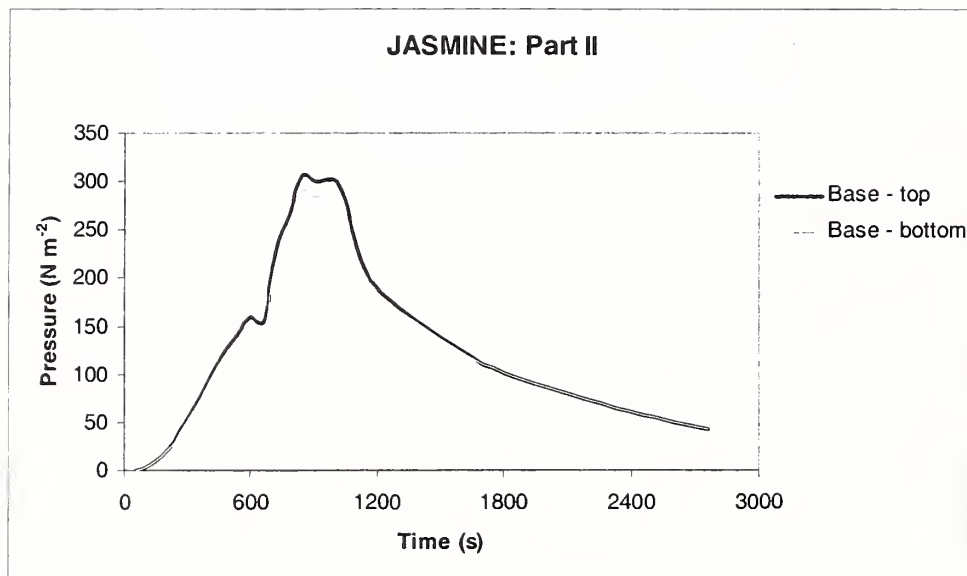
Figure 18   JASMINE predictions of pressure in Part II

CFAST: Part II (fire on floor)

Figure 19   CFAST predictions of pressure in Part II

CONCLUDING REMARKS

BRE simulations of the benchmark exercise with JASMINE and CFAST indicate that target cable damage is unlikely for either Part I or Part II. In Part I this is a consequence of the small fire size, while for Part II with the bigger fires the effect of oxygen depletion was important. Although the temperatures predicted by JASMINE and CFAST were broadly similar, the pressure predictions for the door crack cases were not. For Part II the over-pressure differed by a factor of two, while in Part I the CFAST predicted over-pressures were a factor of ten or more greater than for JASMINE. There are assumptions made in both models that may have a bearing. However the issue has not been resolved yet, and requires further consideration.

Some other important issues remain, in particular in respect to modelling the fluxes to the cable targets and the heat conduction within the target. Further work is required in developing conduction models for cable type targets, and the task of modelling radiation from the flaming region and hot gas layer to the target needs to be considered more carefully. Here the use of CFD models, in combination with appropriate radiation models, may offer significant benefit. Furthermore, to address properly the hazard associated with cable tray fires, some form of fire growth/spread model may be required. The assumption that the entire length of cable tray burns from the start of the fire under-estimates the potential the potential thermal damage to the target cable during the growing stage of the fire.

Although the results of the benchmark exercise would seem to provide confidence in using either zone or CFD models to that type of scenario, it is felt that the problem of 'nearly-sealed' compartments needs further thought. The particular cases studied may have masked the potential problems associated with such scenarios since other effects such as oxygen depletion were here more important. However, in another situation the degree of pressure build-up, and the associated venting and reverse-venting of air, may be more crucial.

The next stage of the collaborative project will need to consider more carefully the limits of fire models for other types of scenario. Here, issues such as the limitation of zone models for very large or complex geometries, or the presence of complex mechanical ventilation systems, need addressing.

REFERENCES

1. MaCaffrey B.J. "Momentum implications for buoyant diffusion flames", *Combustion and Flame*, Vol 52, 1983, p 149.

2. Siegel R. & Howell J.R. *Thermal Radiation Heat Transfer*, Hemisphere Publishing Corporation, New York, 2nd ed., 1981.

3. Peacock R.D. et al. "A User's Guide for FAST: Engineering Tools for Estimating Fire Growth and Smoke Transport", Special Publication 921, NIST, U.S. Dept of Commerce, 2000.

4. Peacock R.D. et al. "CFAST, the Consolidated Model of Fire Growth and Smoke Transport", NIST Technical Note 1299, NIST, U.S. Dept of Commerce, 2000.

5. Ferziger J.H. & Perić M. "Computational methods for fluid dynamics – 2nd ed.", Springer, 1999.

6. Versteeg H.K & Malalasekera W. "An introduction to computational fluid dynamics – the finite volume method", Addison Wesley Longmann, 1995.

7. Patankar S.V. "Numerical heat transfer and fluid flow", Hemisphere Publishing Co., 1980.

8. Launder B.E. & Spalding D.B. "The numerical computation of turbulent flows", Computer Methods in Applied Mechanics and Engineering, vol. 3, 1974, pp 269-289.

9. Markatos N.C., Malin M.R. & Cox G. "Mathematical modelling of buoyancy induced smoke flow in enclosures", Int. J. Heat Mass transfer, vol. 25, 1982, pp 63-75 (and letter on above: vol. 25, 1982, pp 1777-1778).

10. Patankar S.V. & Spalding D.B. "A calculation procedure for heat, mass and momentum transfer in three-dimensional parabolic flows", Int. J. Heat Mass Transfer, vol. 15, 1972, p 1787.

11. Magnussen B.F. & Hjertager B.H. "On mathematical modelling of turbulent combustion with special emphasis on soot formation and combustion", Proceedings of the 16th Symposium (International) on Combustion, The Combustion Institute, 1976, pp 719-729.

12. Gosman A.D. & Lockwood F.C. "Incorporation of a flux model for radiation into a finite-difference procedure for furnace calculations", Proceedings of the 14th Symposium (International) on Combustion, The Combustion Institute, 1973, pp 661-671.

13. Lockwood F.C. & Shah N.G. "A new radiation solution method for incorporation in general combustion prediction procedures", Proceedings of the 18th Symposium (International) on Combustion, The Combustion Institute, 1981, pp 1405-1414.

14. Truelove J.S. "Mixed grey gas model for flame radiation", UK Atomic Energy Authority Report AERE HL 76/3448, 1976.

15. Kumar S., Gupta A.K. & Cox G. "Effects of thermal radiation on the fluid dynamics of compartment fires", Fire Safety Science – Proceedings of the Third International Symposium, Elsevier Science Publishing, 1991, pp 345-354.

16. Cox G. & Kumar S. "Field modelling of fire in forced ventilated enclosures", Combustion. Science and Technology, vol. 52, 1987, pp 7-23.

17. Cox G., Kumar S. & Markatos N.C. "Some field model validation studies", Fire Safety Science – Proceedings of the First International Symposium, Hemisphere Publishing, 1986, pp159-171.

18. Pericleous K.A., Worthington D.R.E. & Cox G. "The field modelling of fire in an air-supported structure", Fire Safety Science – Proceedings of the Second International Symposium, Hemisphere Publishing 1989, pp 871-880.

19. Kumar S. & Cox G. "The mathematical modelling of fires in road tunnels", Proc. 5th International Symposium on the Aerodynamics & Ventilation of Vehicle Tunnels, Lilie, France, BHRA, 1985, pp 61-76.

20. Kumar S. & Cox G. "Radiant heat and surface roughness effects in the numerical modelling of tunnel fires", Proc. 6th International Symposium on the Aerodynamics & Ventilation of Vehicle Tunnels, Durham, England, BHRA, 1988, pp 515-526.

21. Miles S., Kumar S. & Andrews R. "Validation of a CFD model for fires in the Memorial Tunnel", Proc. 1st International Conference on Tunnel Fires, Lyon, France, Independent Technical Conference, 1999, pp 159-168.

22. Kumar S. "Field model simulations of vehicle fires in a Channel Tunnel shuttle wagon", Fire Safety Science – Proceedings of the Fourth International Symposium, IAFSS, 1994, pp 995-1006.

23. Kumar S., Welch S. & Chitty R. "Evaluation of fire models for fire hazard assessment in buildings. Part 2 – evaluation of fire models", BRE Client Report 75982, 1999.

24. Miles S. "The predictive capability of CFD for fully developed fires", Proc. 3rd International Symposium on Fire and Explosion Hazards, Windermere, UK, 2000.

25. Miles S.D., Kumar S. & Cox G. "Comparisons of 'blind predictions' of a CFD model with experimental data", Fire Safety Science – Proceedings of the Sixth International Symposium, IAFSS, 2000, pp 543-554.

26. Miles S., Kumar S. & Cox G. "The balcony spill plume – some CFD simulations", Fire Safety Science – Proceedings of the Fifth International Symposium, IAFSS, 1997, pp 237-247.

27. Kumar S., Heywood G.M. & Liew S.K. "Superdrop modelling of a sprinkler spray in a two-phase CFD-particle tracking model", ", Fire Safety Science – Proceedings of the Fifth International Symposium, IAFSS, 1997, pp 889-900.

Appendix H: Benchmark Analysis with CFAST, Juergen WILL, GRS, Germany

Report

Benchmark Exercise #1
Cable Tray Fires of Redundant Safety Trains

Blind Simulations using
CFAST 4.0.1

**International Collaborative Project to
Evaluate Fire Models for
Nuclear Power Plants**

May 23, 2001

Contens

1   COMPUTER CODE

All calculations were performed applying the multi-room zone model CFAST [1], most actual version 4.0.1. The older Version 3.1.6 could not be used because all available personal computers (PCs) were running under Microsoft WINDOWS NT operation system. Testing CFAST version 3.1.6 on a WINDOWS 98 platform also failed. PCs (without hardware handicaps) with WINDOWS 95 operational system were not available.

All the information referring to the model or the computer code was taken from

- NIST TN 1431: A technical reference for CFAST: An engineering tool for estimating fire and smoke transport. January 2000, [1],
- NIST Special Publication 921 2000 Edition: A user's guide for FAST: Engineering tools for estimating fire growth and smoke transport. January 2000, [2],
- NIST Technical Note 1299: CFAST, the consolidated model of fire and smoke transport. September 1995, [3]
- personal information given by Mr. G. Blume (iBMB of TU Braunschweig), who performed a lot of calculations with CFAST 3.1.6 in the past.

In our opinion it does not make a strong difference whether CFAST version 3.1.6 or version 4.0.1 is used. Comparing the manuals of these two program versions, no changes in the physical basis were found. Applying the more actual version does not seem to be as comfortable as the older one because the grafic user interface (GUI) FAST is no longer available and creating an input data file is a little more difficult.

2   BENCHMARK EXERCISE PART I

2.1   INPUT DATA FOR PART I

All the information was taken from "Benchmark Exercise #1: Cable Tray Fires of Redundant Safety Trains", revised September 11, 2000, [4].

The thermophysical data for walls, floor and ceiling as well as for the PVC insulation material of the cables were put in a new file THER_ST.DF as well as THER_ST.NDX. The cable of tray A was described on the one hand as a target, on the other hand as an object. Using the object model, a set of new files (OBJE_ST.DF, OBJE_ST.NDX) for the object properties was set up.

In each case of part I tray A was treated as an object or as a target. Preliminary calculations had shown that there is a considerable difference in the results using the unconstrained or the constrained fire algorithm. Therefore, these two algorithms were used in the calculations of the base case and of the cases 1 to 5. These two additional parameters lead to four different calculations for each case.

2.2   RESULTS OF PART I

2.2.1   Distance between tray A and trash bag (base case and cases 1 - 3)

From the base case up to case 3 the fire as well as the ventilation conditions were not changed. Therefore, it is obvious that the temperature of the upper and the lower layer, the depth of hot gas layer, the heat release rate and the oxygen content did not change either. The time curves of these parameters are shown in Figure 2.1 - Figure 2.5.

The course of the parameter describing the fire itself or the upper and lower layer is not affected by using different models (object or target) for tray A.

Starting the calculations, it was expected that in case of using constrained fire algorithm (fire type 2) the heat release rate is limited by oxygen consumption. But this did not happen, the heat release rate of the main fire (trash bag) is not affected by lack of oxygen (Figure 2.4). The oxygen content in the lower layer is not reduced by the trash bag fire (Figure 2.5). In the upper layer, there is a high amount of oxygen until the end of the simulation time, too.

Although it is not mentioned in the CFAST manuals, the two types of fire lead to totally different results with respect to the layer temperatures. Using the constrained fire algorithm, much higher upper and lower layer temperatures were calculated. This is surprising, because the interface height did not seem not to be affected (Figure 2.3) by the fire algorithm. But most surprising is the fact that in all runs of the program the surface temperature of tray A (as well as ceiling, walls and floor) is higher if the unconstrained fire algorithm is used, resulting in a lower gas temperature (Figure 2.6). For the analyst, it seems that something went wrong in calculating the convective and radiative heat flux on the target surface. Maybe in case of the unconstrained fire absorption by carbon dioxide and water vapour in the gas layers is ignored: Without absorption the layers do not heat up as much and the radiative heat flux on the ceiling, walls, floor and targets is higher, so that the surface temperature increases.
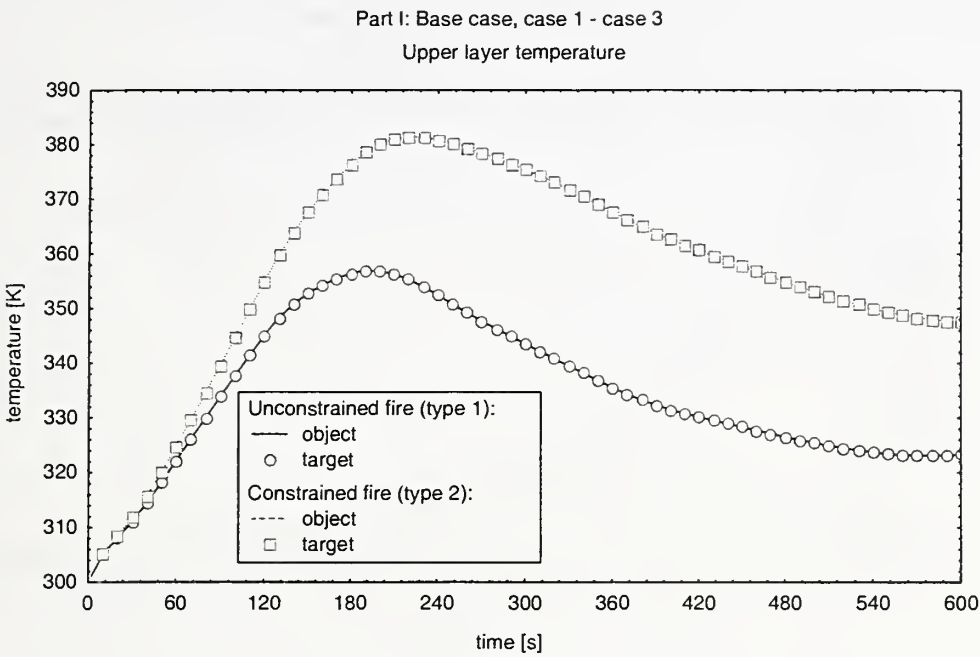
Part I: Base case, case 1 - case 3

Upper layer temperature
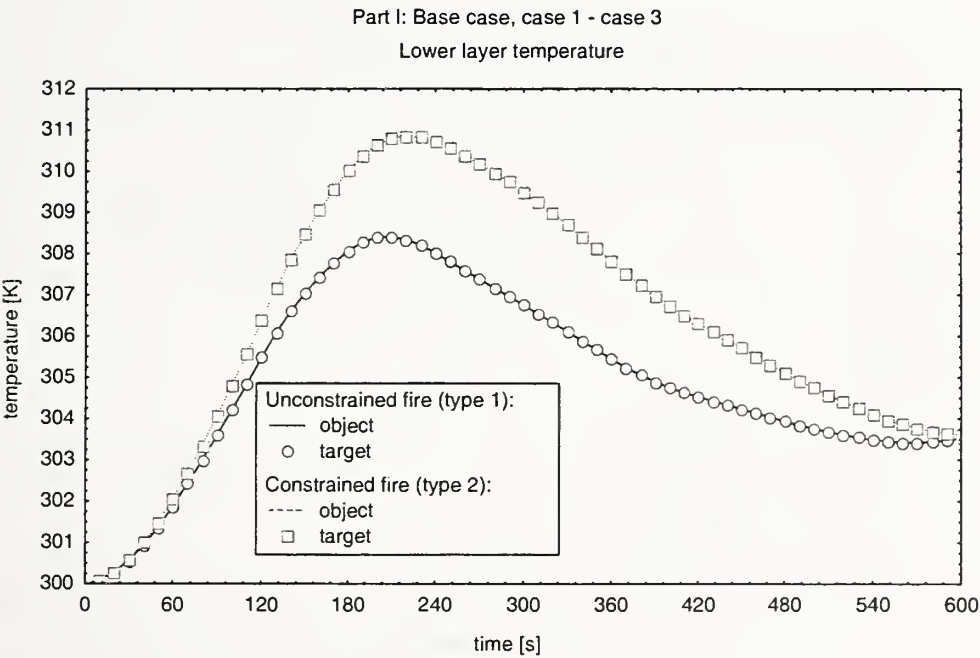

Figure 2.1   Upper layer temperature (base case, cases 1 - 3)

Part I: Base case, case 1 - case 3

Lower layer temperature

Figure 2.2   Lower layer temperature (base case, cases 1 - 3)

Part I: Base case, case 1 - case 3
Interface height
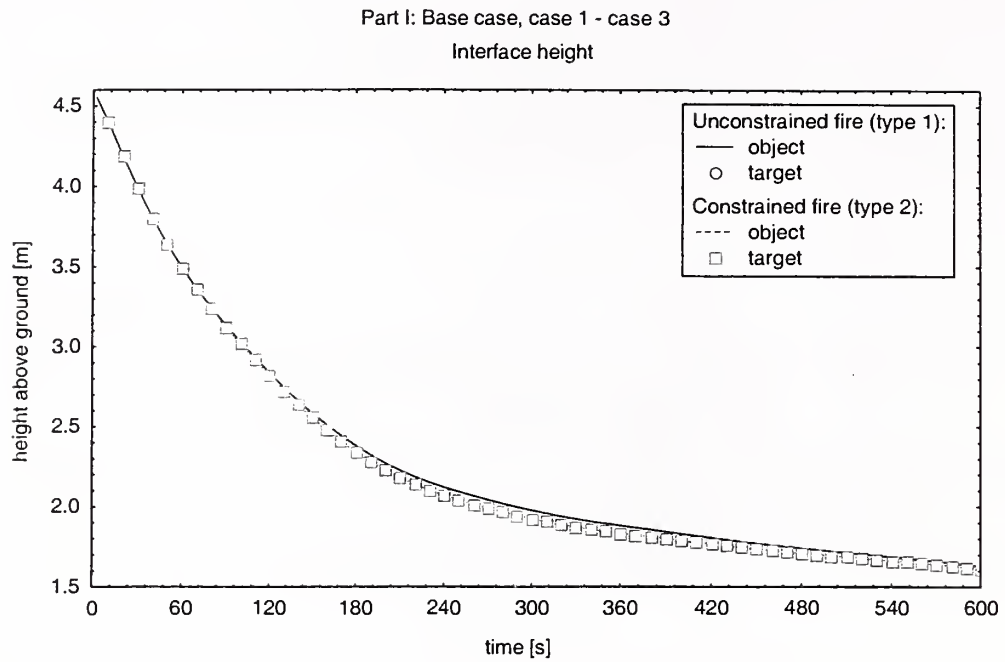
Figure 2.3   **Interface height (base case, cases 1 - 3)**

Part I: Base case, case 1 - case 3
Heat release rate
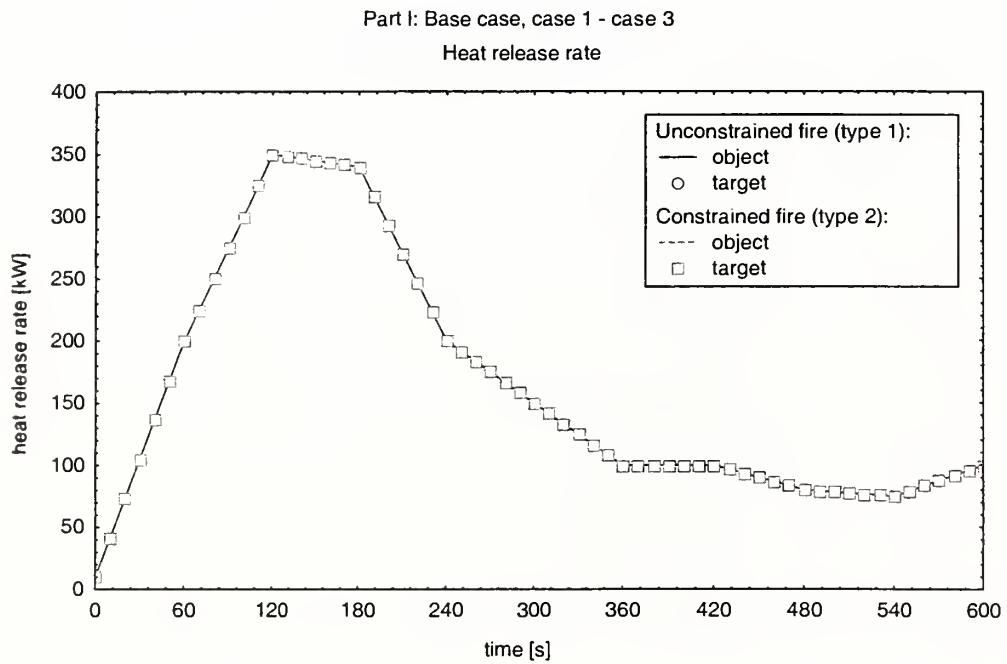
Figure 2.4   **Heat release rate (base case, cases 1 - 3)**

Part I: Base case, case 1 - case 3
Constrained fire (type 2): Oxygen content
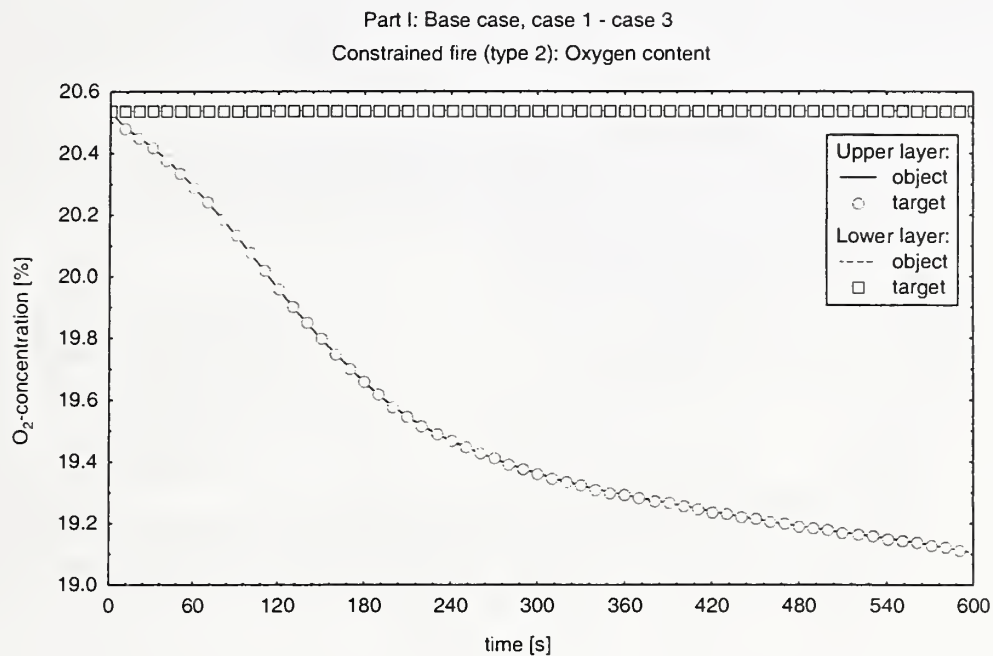
Figure 2.5   Oxygen content (base case, cases 1 - 3)

Part 1: Base case
Object/target (tray A) surface temperature
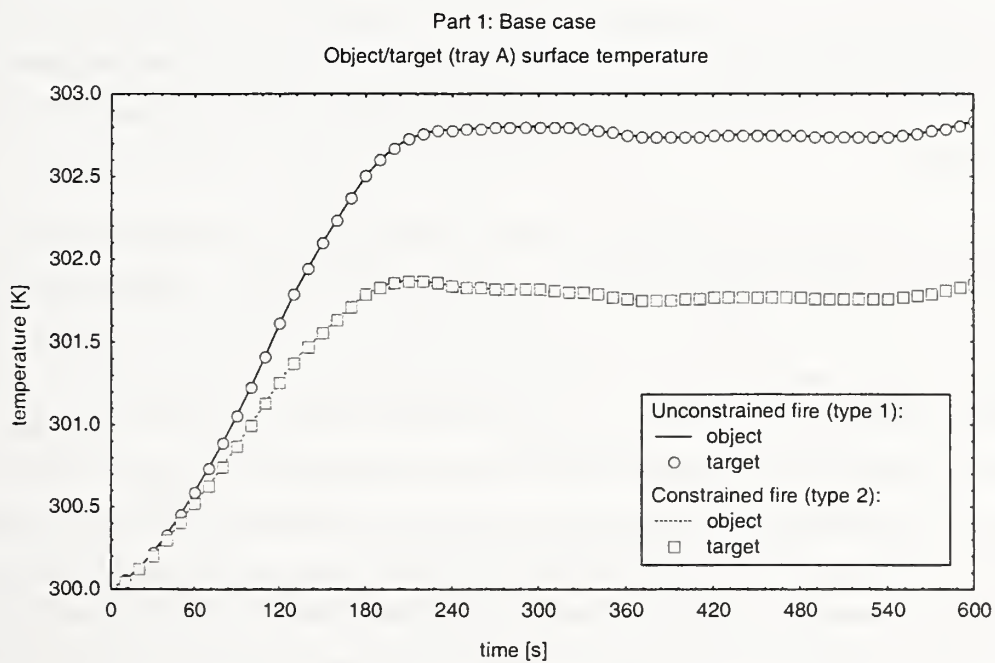
Figure 2.6   Surface temperature of tray A (base case)

Part I: Base case, case 1 - case 3
Target (tray A) surface temperature
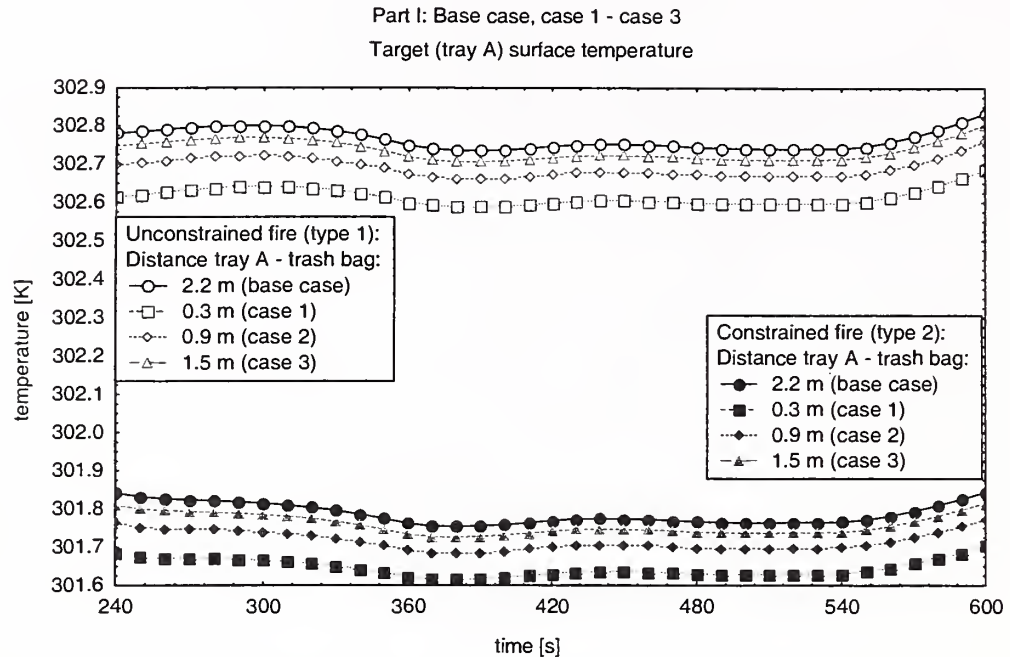
Figure 2.7   Surface temperature of tray A, unconstrained fire (base case, cases 1 - 3)

Comparing the surface temperature of tray A for different distances between the main fire (trash bag) and the target (base case, cases 1 - 3) is more amazing: Increasing the distance between target and heat source leads to an increase of the surface temperature (Figure 2.7), the opposite was expected.

As originally the x-position of the target (tray A) was fixed and the position of the main fire (trash bag) was moved in x-direction, further calculations were performed to find out what has gone wrong: Using the unconstrained fire algorithm (type 1), defining the door closed and the ventilation system switched off, the main fire (trash bag) was fixed in the center of the room (x-position 4.55 m), and the target (tray A) was moved in x-direction to get the distance of 2.2 m, 0.3 m, 0.9 m and 1.5 m between tray A and the trash bag. Looking at the results of these additional calculations (Figure 2.8), the amazing result is reasonable: The x- or y-position of a target does not affect the result of surface temperature, it was always treated as if it is positioned in the centre of the compartment. Only the position of the main fire (trash bag) will affect changes in the surface temperature of targets or objects. This weakness in the heat transfer model of CFAST is not mentioned in any manual. Due to this, in the former calculations the distance between tray A and trash bag was treated by the program as 1.15 m (base case), 3.05 m (case

1), 2.45 m (case 2) and 1.85 m (case 3), giving reasonable results for surface temperature (Figure 2.7) calculations.
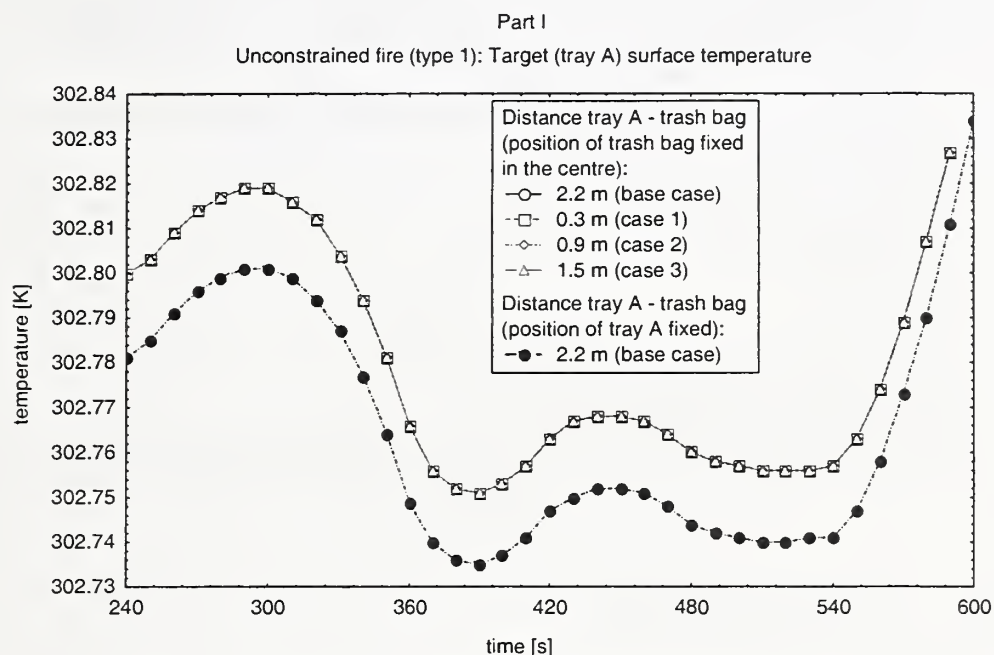
Part I
Unconstrained fire (type 1): Target (tray A) surface temperature

Figure 2.8   **Surface temperature of tray A, constrained fire, position of trash bag fixed**

2.2.2   Ventilation conditions (base case, cases 4 and 5)

The effects of different ventilation conditions should be shown by comparing the results of base case calculations and calculations with open door (case 4) or active ventilation system (case 5, case 5b).

It has been mentioned before that there have been some problems running CFAST with forced inflow (case 5). In this case, the oxygen content decreases until there is no more oxygen in the upper layer (Figure 2.9). It seems obvious that pure nitrogen was pumped into the compartment. There was no possibility in the input data file of CFAST to define the composition of the gas, which will be sucked in from the ambient into the compartment by a duct system. This problem did not appear in case of natural ventilation if the door is open (case 4). Thus the mechanical ventilation system was redefined: Concerning the following calculations, the outflow is managed by a fan and instead of the forced inflow a natural vent for horizontal flow is created to allow air to flow into the compartment (case 5b).
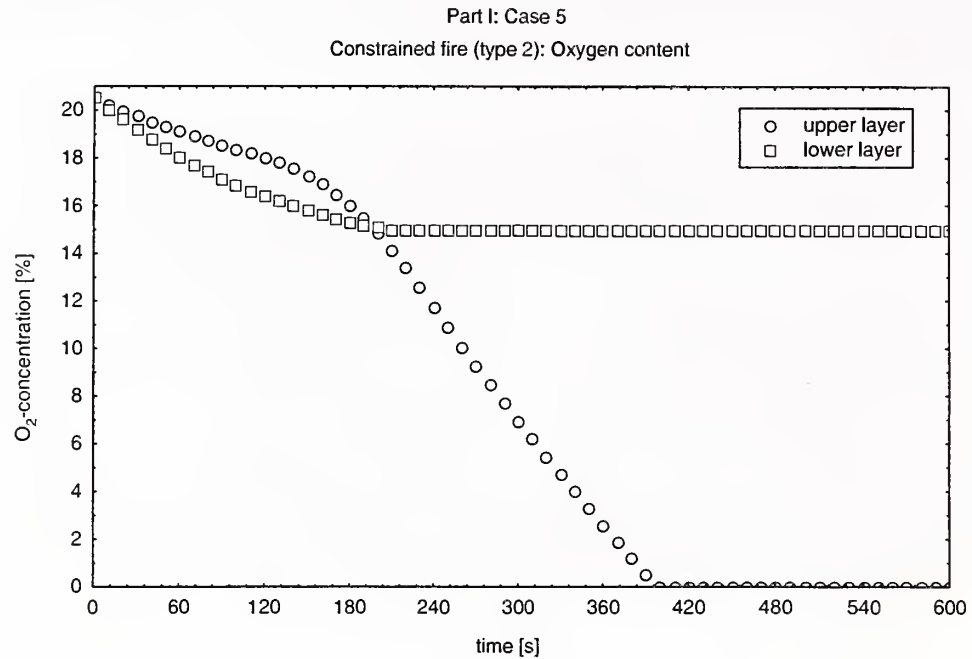
Part I: Case 5

Constrained fire (type 2): Oxygen content

Figure 2.9   Oxygen content (case 5)

If an exchange of gases between the compartment and the ambient air is possible using openings as the door or a mechanical ventilation system, the temperature of the upper layer decreases nearly in the same magnitude (Figure 2.10, Figure 2.11). The increase in the lower layer temperature (Figure 2.12, Figure 2.13) and the decrease of the oxygen content in this layer are no longer important. Looking at the depth of the upper layer, which is not influenced by the fire type (Figure 2.14), and the oxygen content of this layer (Figure 2.15) it is discernible that the mechanical ventilation system (case 5b) is more effective than the natural ventilation by the open door (case 4). In case of the door opened or the mechanical ventilation system being active the surface temperature does not increase as much as without ventilation (Figure 2.16, Figure 2.17).

It has to be admitted that the increase of the oxygen concentration in the lower layer in case of an active ventilation (case 4, case 5b) is not reasonable. It has to be checked if the composition of ambient air and the air in the compartment at the beginning of the simulation are identical. It does not seem to be possible to define the gas composition in CFAST.
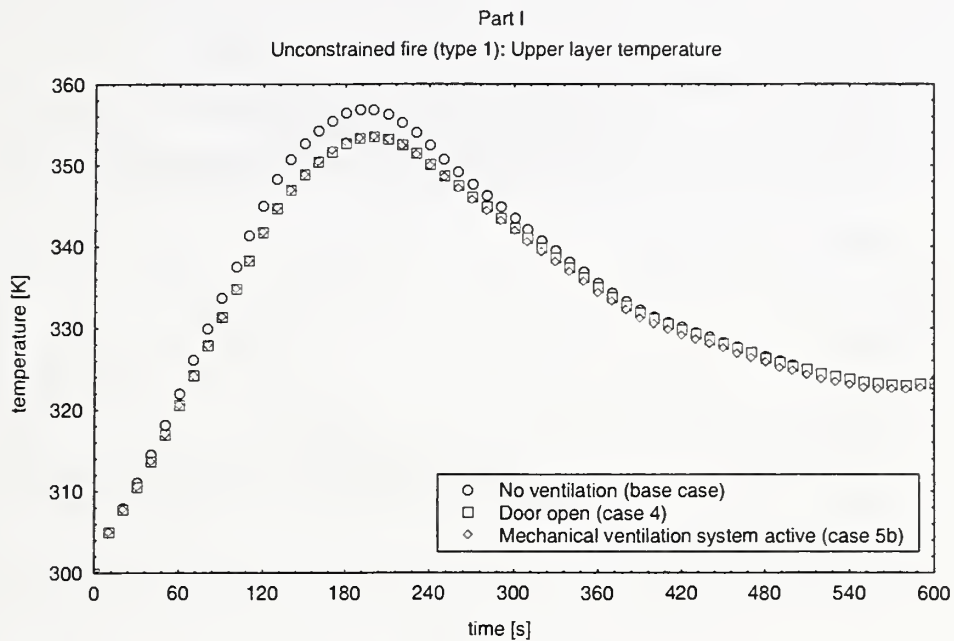
Part I

Unconstrained fire (type 1): Upper layer temperature

Figure 2.10   Upper layer temperature, unconstrained fire (base case, case 4, case 5)

Part I

Constrained fire (type 2): Upper layer temperature
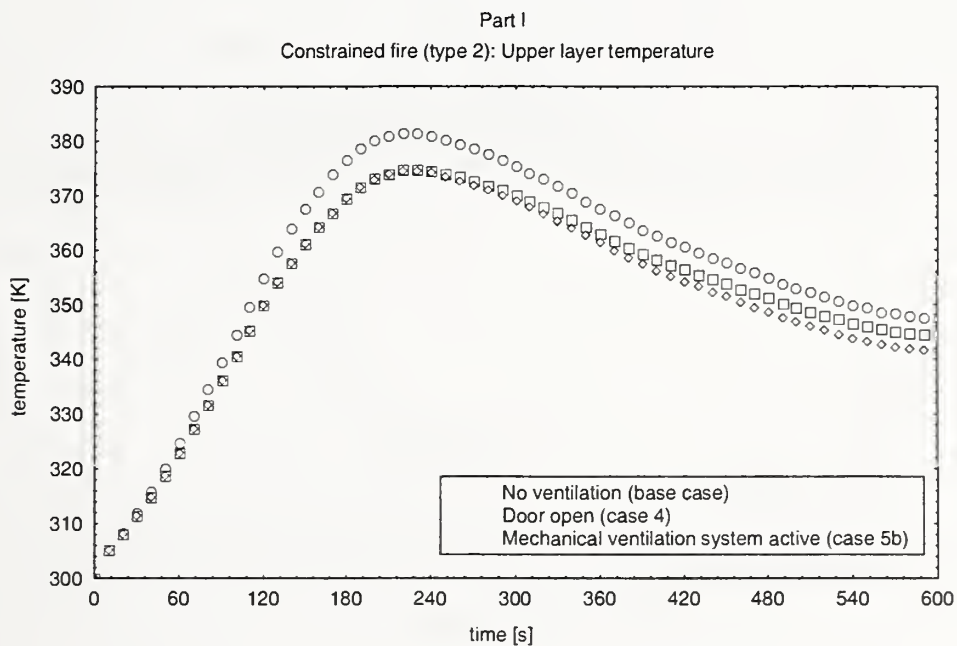
Figure 2.11   Upper layer temperature, constrained fire (base case, case 4, case 5)

Part I
Unconstrained fire (type 1): Lower layer temperature
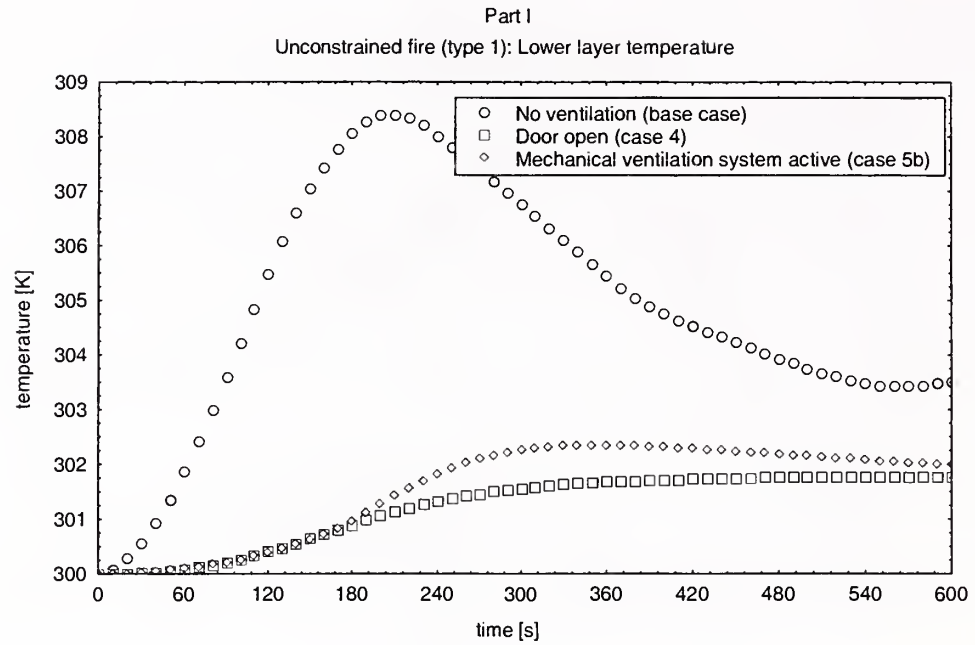
Figure 2.12   Lower layer temperature, unconstrained fire (base case, case 4, case 5)

Part I
Constrained fire (type 2): Lower layer temperature
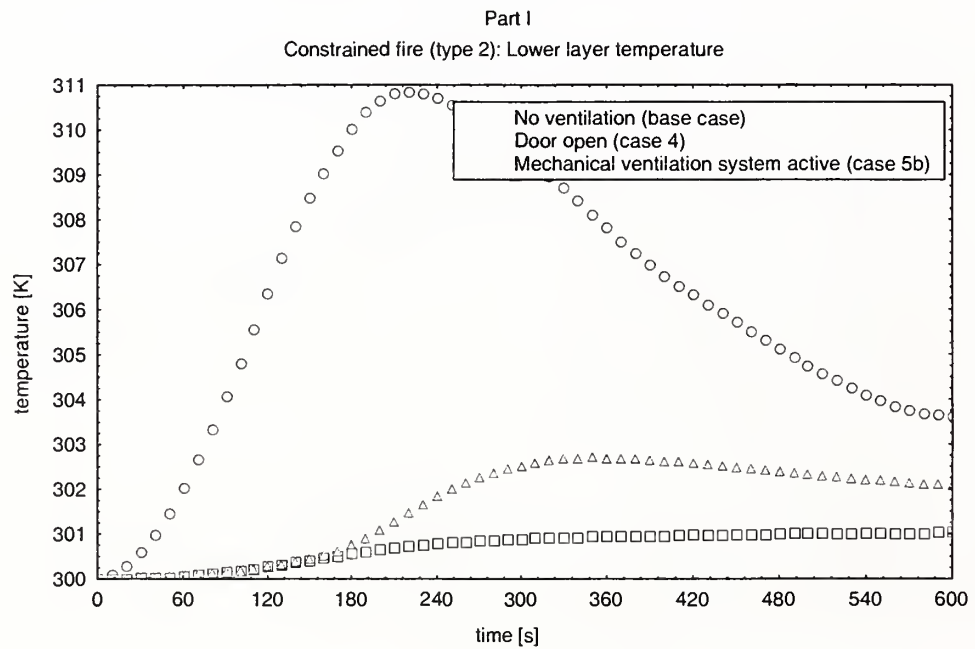
Figure 2.13   Lower layer temperature, constrained fire (base case, case 4, case 5)

Part I
Unconstrained fire (type 1): Interface height
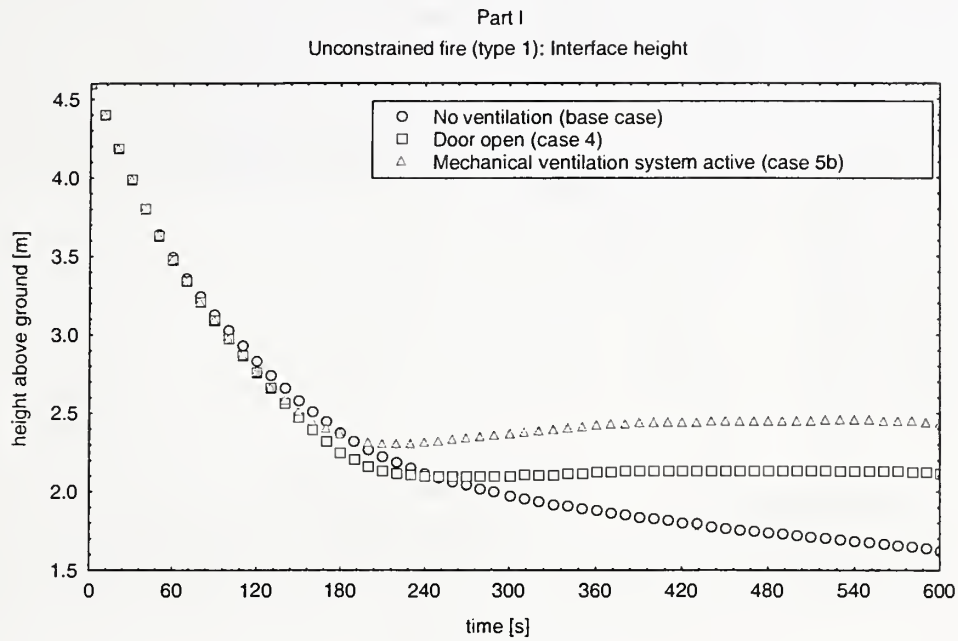
Figure 2.14   Interface height, unconstrained fire (base case, case 4, case 5)

Part I
Constrained fire (type 2): Oxygen content, upper layer
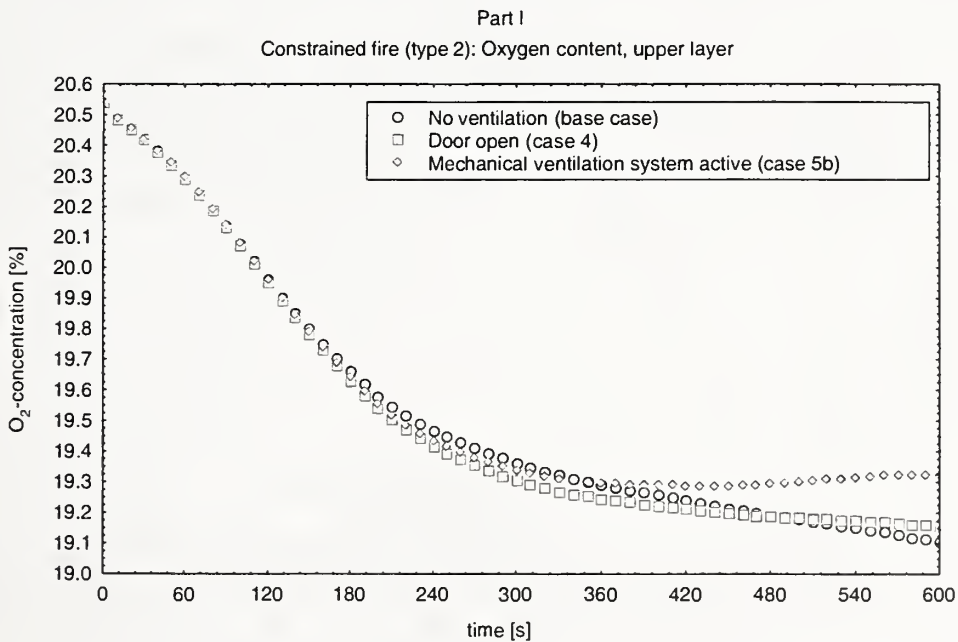
Figure 2.15   Oxygen content of upper layer (base case, case 4, case 5)

Part I
Unconstrained fire (type 1): Object/target (tray A) surface temperature
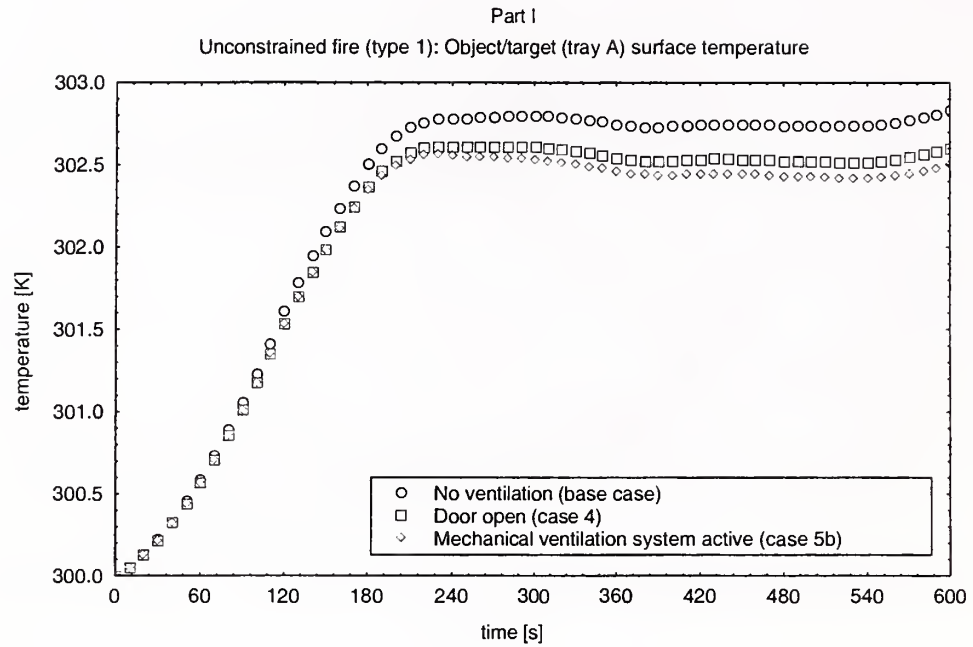
Figure 2.16   Surface temperature of tray A, unconstrained fire (base case, case 4, case 5)

Part I
Constrained fire (type 2): Object/target (tray A) surface temperature
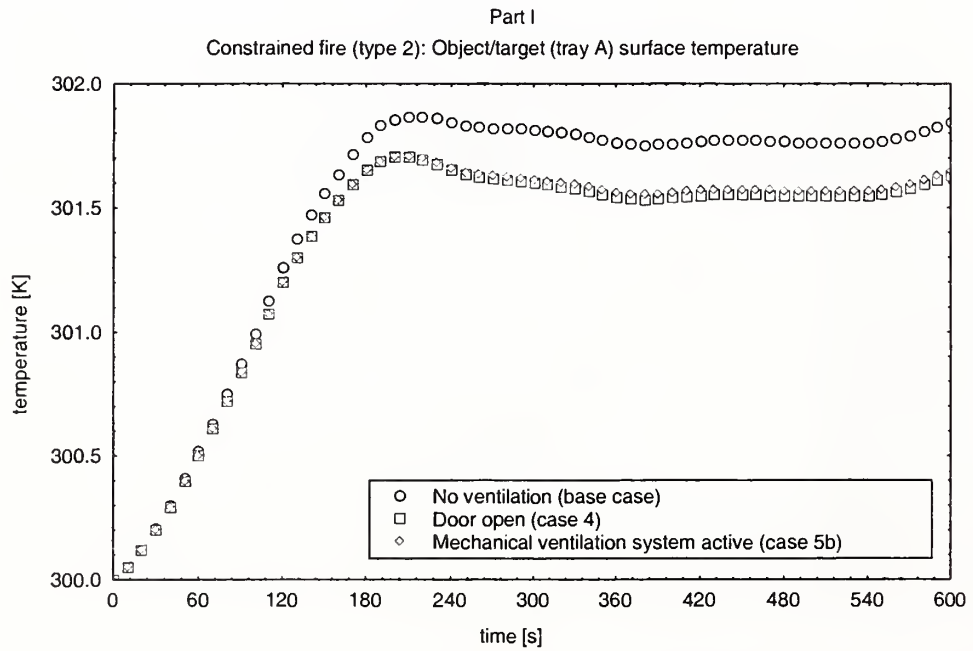
Figure 2.17   Surface temperature of tray A, constrained fire (base case, case 4, case 5)

Part 1: Case 4

Door: Flow from outside into lower layer
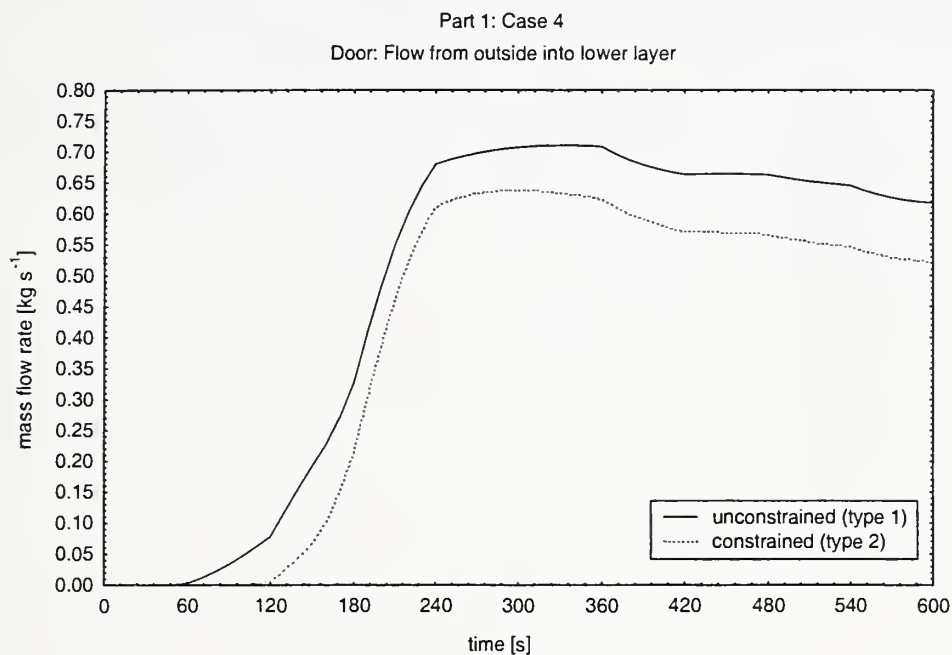
Figure 2.18   Mass flow rate through the opened door (outside - lower layer)

Part I: Case 4

Door: Flow from lower layer to outside
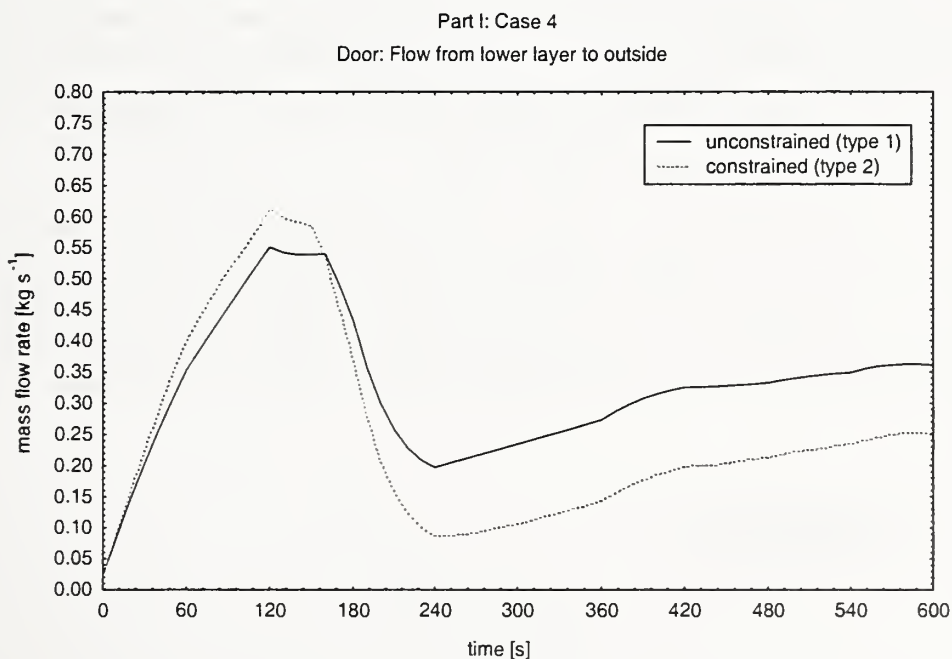
Figure 2.19   Mass flow rate through the opened door (lower layer - outside)
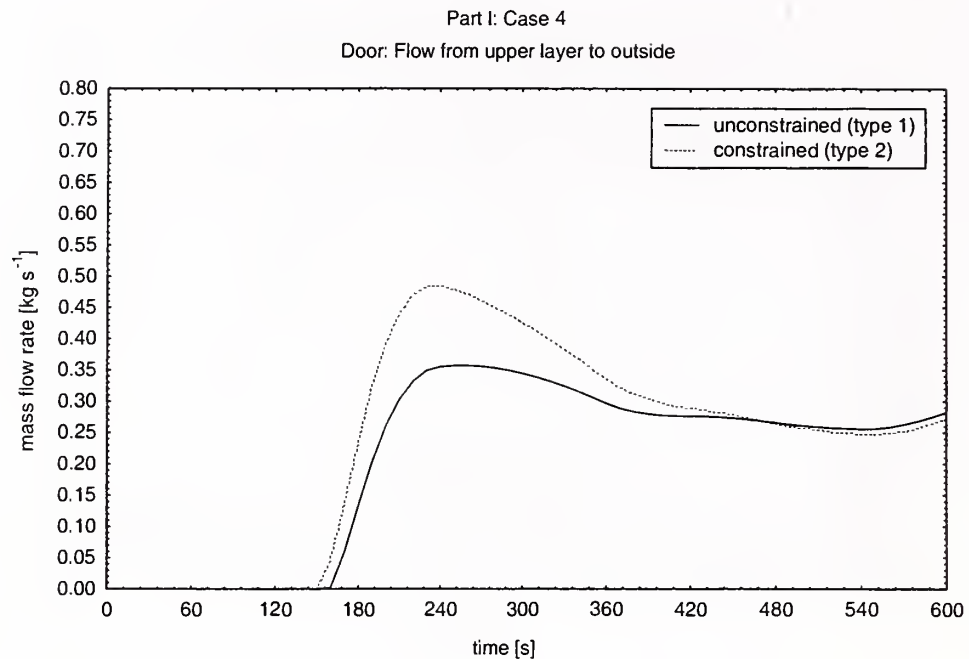
Part I: Case 4
Door: Flow from upper layer to outside

Figure 2.20   Mass flow rate through the opened door (upper layer - outside)

If the door of the compartment is opened (case 4), only lower layer gas flows out of the compartment. After approximately 2 minutes the interface reaches the top of the door, the gas flow from the upper layer to the outside starts, and the gas flow from the lower layer to the outside decreases (Figure 2.18, Figure 2.19, Figure 2.20).

In case 5b (mechanical ventilation system on but only for outflow, inflow by natural ventilation), the gas flows only in one direction through the opening (vent 1) from the outside into the lower layer (Figure 2.21). On the other hand, the fan sucks gas out of the lower layer until the interface reaches the bottom of the duct system opening. After that the fan sucks gas out of the upper layer.
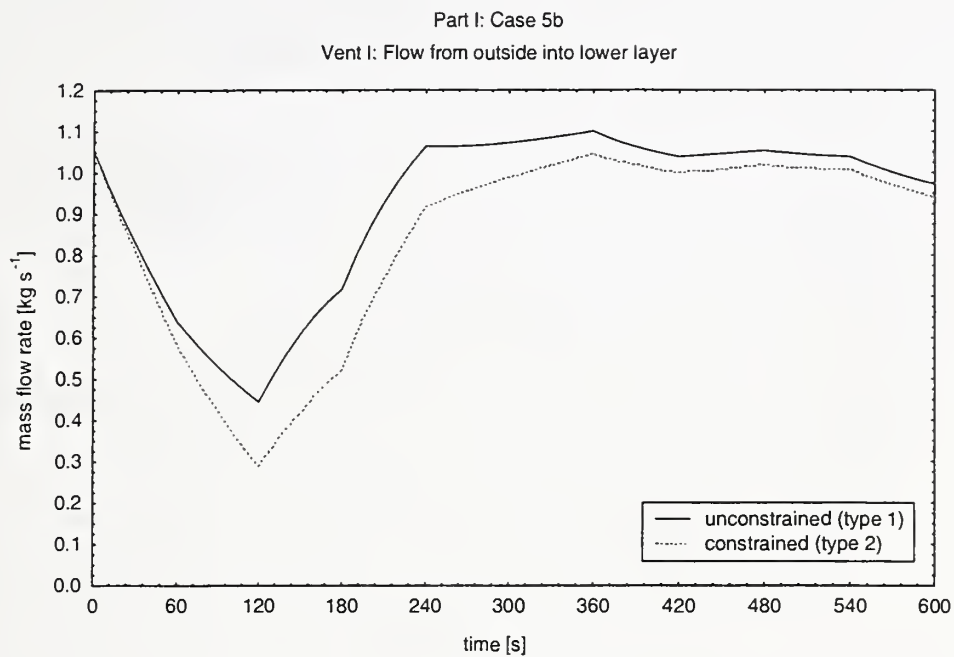
Part I: Case 5b

Vent I: Flow from outside into lower layer

Figure 2.21   Mass flow rate through air inlet (outside - lower layer)

Part I: Case 5

Forced outflow: Flow from lower layer to outside

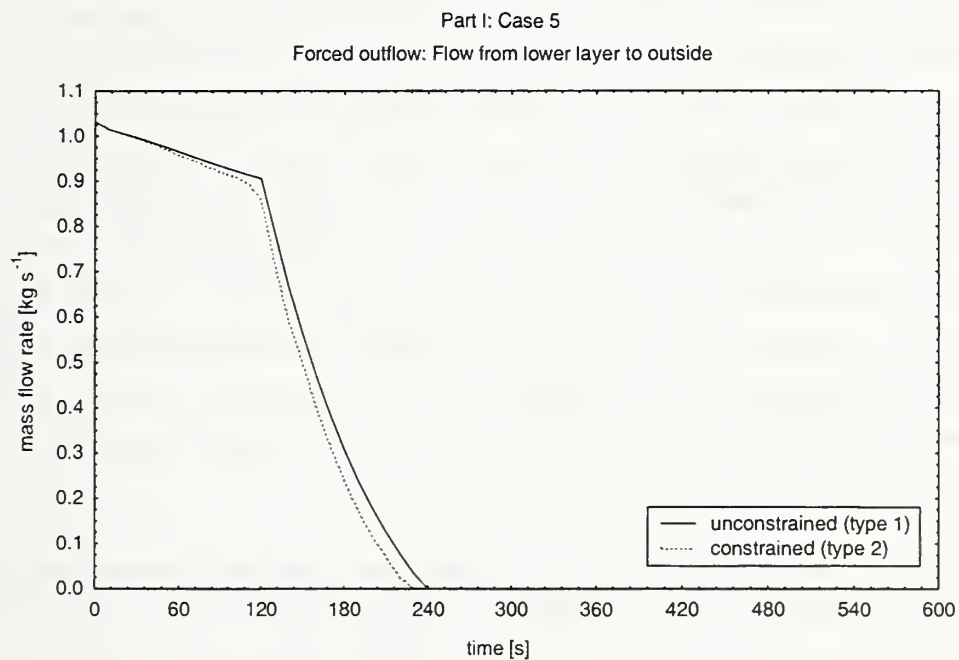Figure 2.22   Mass flow rate of fan (lower layer - outside)
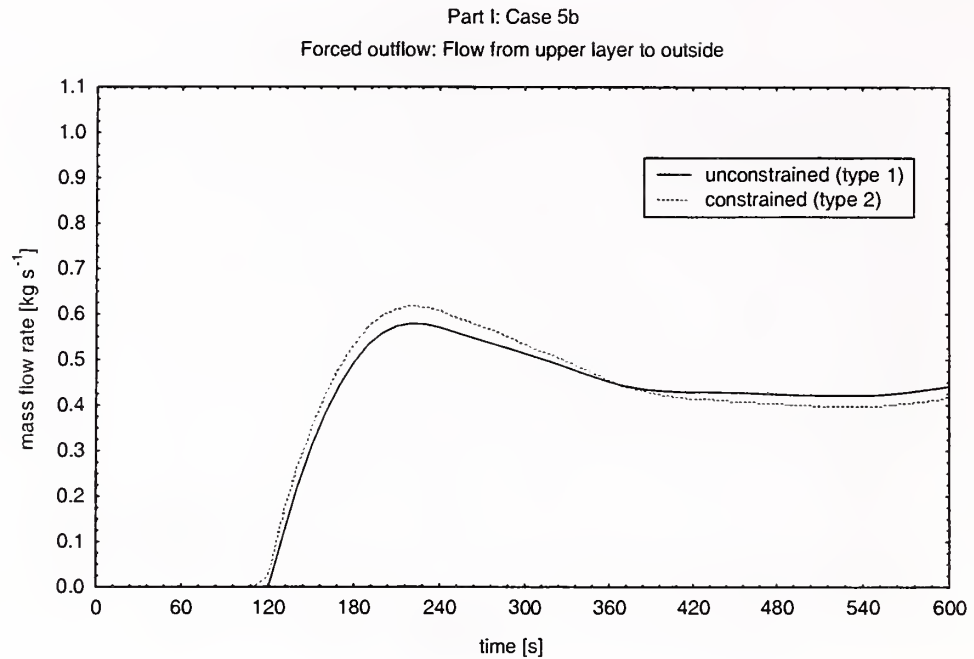
Part I: Case 5b

Forced outflow: Flow from upper layer to outside

Figure 2.23   Mass flow rate of the fan (upper layer - outside)

Having a closer look at the pressure in the compartment it becomes visible that the base case is not realistic because the walls of the compartment (as well as the dampers of the ventilation system) have to resist a pressure of more than 10000 Pa (Figure 2.24). Even if a gap of 5 mm width under the door is assumed the pressure will reach a level of more than 1.000 Pa. If there is a sufficient ventilation area in the compartment like the open door (case 4), the pressure difference is very small (Figure 2.25). The pressure in the compartment hardly reaches the limitation of the fan in case of air being pumped into the room by a mechanical ventilation system (case 5), although another fan with the same sucks gas out of the compartment. (Figure 2.26). At least, if the mechanical ventilation system consists only of a fan sucking out gas and air flows into the compartment by natural ventilation (case 5b), the pressure inside the compartment is below atmospheric pressure (Figure 2.27).

In this context, it has to be pointed out that all results and statements are only valid in this special case of a very small fire of at least 350 kW heat release rate.
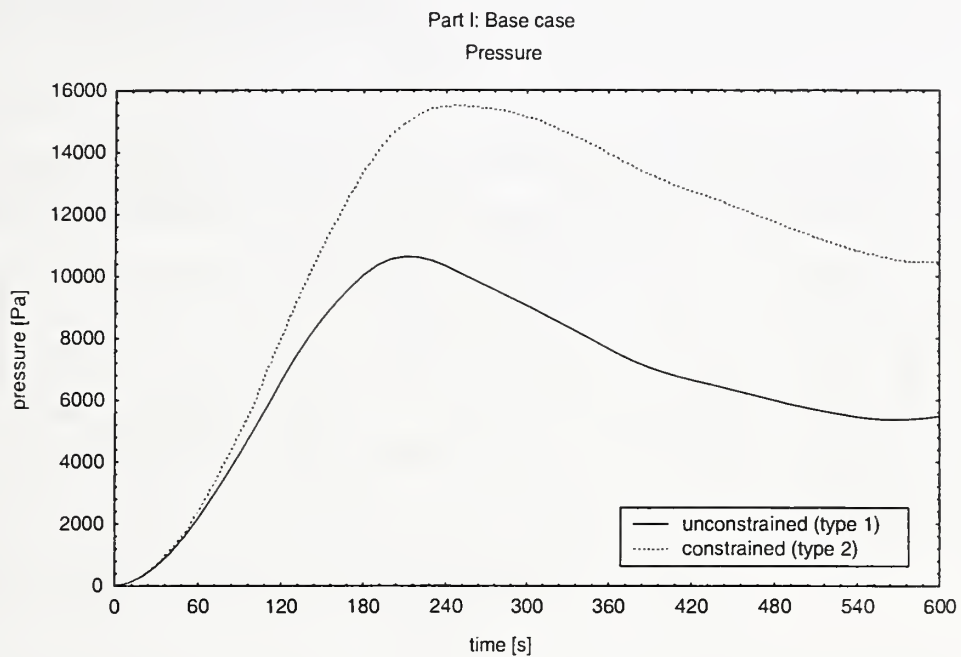
Part I: Base case

Pressure

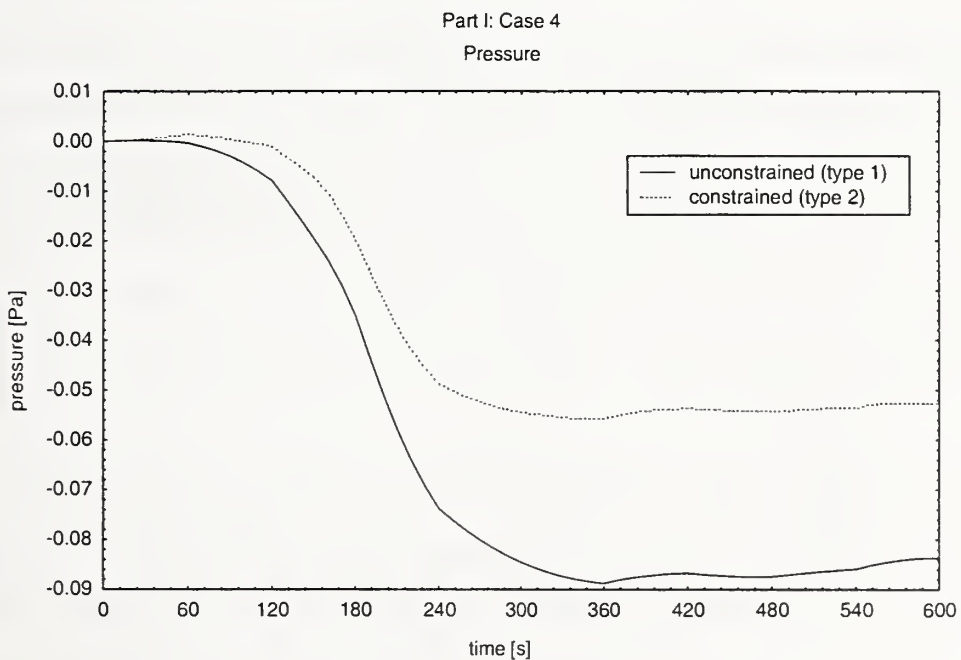**Figure 2.24   Pressure (base case)**

Part I: Case 4

Pressure

Figure 2.25   Pressure (case 4)

Part I: Case 5

Pressure

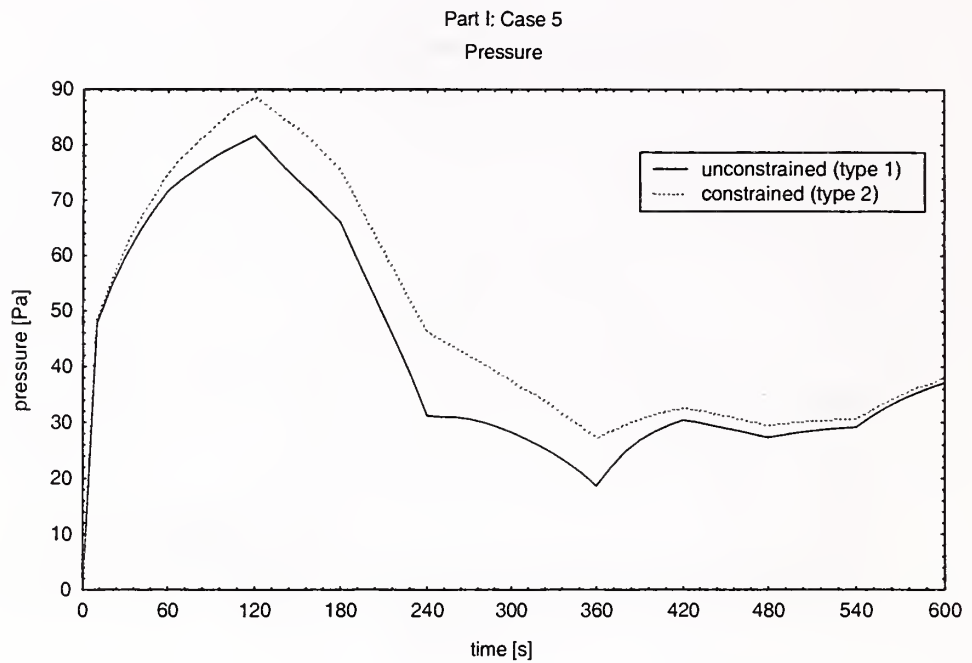**Figure 2.26   Pressure (case 5)**
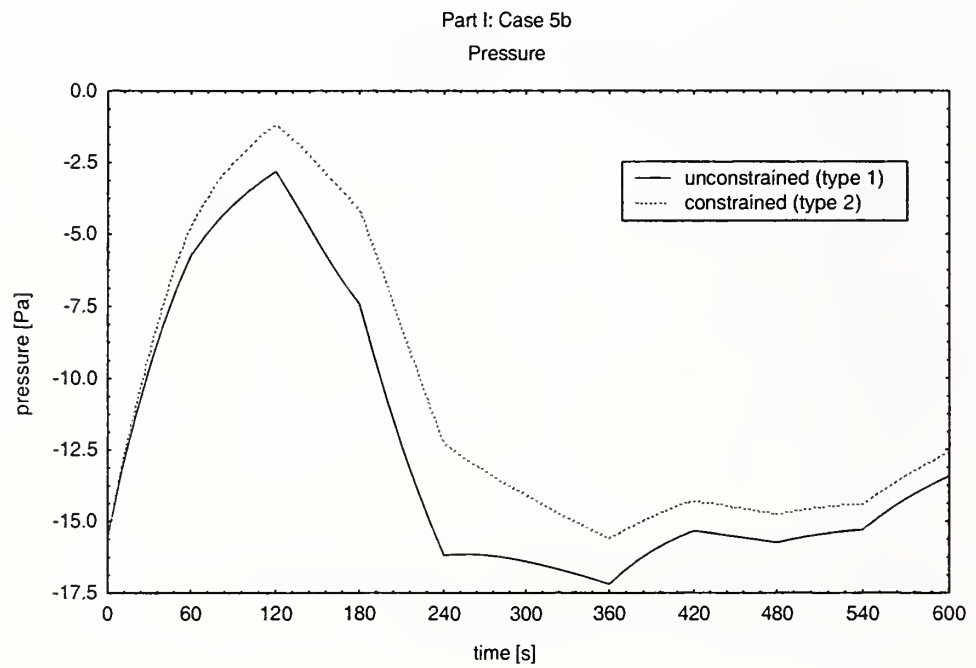
Part I: Case 5b

Pressure

Figure 2.27   Pressure (case 5b)

3   BENCHMARK EXERCISE PART II

3.1   INPUT DATA FOR PART II

The thermophysical data for the walls, floor and ceiling as well as for the PVC cable insulation material were put in the former mentioned file THER_ST.DF as well as in the file THER_ST.NDX. As the heating of an object is treated like the heating of a target, only the object model of the files (OBJE_ST.DF, OBJE_ST.NDX) was used for cable tray B in part II. In all examined cases of part II both fire algorithms (unconstrained, constrained) were used. Using fire type 2 (constrained fire, the time curves of variables HCl, HCr, OD and CO were additionally specified. CFAST cannot treat a variable position of an object or target in the horizontal plane, therefore it was assumed that the object / target (tray B) was positioned in the center of the compartment and the main fire (tray A, C1, C2) was moved in y-direction to get the distances of 6.1 m, 4.6 m or 3.1 m (not in x-direction, because the compartment is not wide enough).

The mechanical ventilation system in case 9a and case 10 was defined in the same way as in case 5b of part I. To run the simulations for case 9, the variable CVENT was used, and two points were added to the time curve of the 1 MW cable fire.

The user of CFAST is not able to specify the volume flow rate of a forced ventilation (an option, which is included in the older zone model HARVARD 6) or to specify the capacity of a mechanical ventilation system as a function of time. Trying to run a simulation for a problem time of up to 15 min (with mechanical ventilation system being active and door closed) creates a restart file for this point of time. A restart of the simulation with a modified input data file (switch off mechanical ventilation system and door open) also failed. Therefore, case 9 was calculated on the one hand with mechanical ventilation (called case 9a) and without a mechanical ventilation system (called case 9b) on the other hand, while the door is opened after 15 min simulation time.

To run case 13, the file OBJE_ST.DF was modified: Instead of a panel thickness of 50 mm (third value in line 3) a thickness of 15 mm was applied to simulate a typical NPP specific instrumentation cable. Since the variations of the object elevation or thickness did not effect the surface temperature, case 11 to case 13 will not be mentioned anymore.

3.2   RESULTS OF PART II

3.2.1   Heat release rate

Using the unconstrained fire algorithm (type 1) the heat release rate reached the predicted level of 1 MW, 2 MW or 3 MW (Figure 3.1). On the other hand, if the constrained fire algorithm was used, the development of the heat release rate was limited by the position of the upper layer and the oxygen content of this layer.

Without natural or forced ventilation the heat release rate reached 1 MW (base case), stayed on this level for a short time period until there was no more oxygen in the upper layer. After that, the heat release rate decreased rapidly. A maximum value of about 1.3 MW was reached, although a peak heat release rate of 2 MW or 3 MW had been defined. After reaching this value the heat release rate decreased rapidly.

The heat release rate of the 1 MW fire was affected by opening the door after 15 min simulation time (Figure 3.2): The heat release rate did not increase as expected, but it decreased rapidly (base case - case 9b). More astonishing was the fact that the decrease of the heat release rate started earlier, if the mechanical ventilation system was active all the time (cases 9a, 10). This behaviour could be explained when looking at the position of the interface (Figure 3.15), which was a little bit deeper in case that the mechanical ventilation system was running and the main fire was placed in the pure oxygen layer at an earlier point of time.

In part I, the trash bag fire was very small (peak heat release rate of 350 kW) and did not last very long. In addition, the trash bag was positioned near the floor, so that the fire was in the lower layer and there was no lack of oxygen any time. In part II, the distance between floor and bottom of the main fire (cable fire of tray A, C1, C2) could influence the course of the heat release rate if the constrained fire algorithm (type 2) was used. To demonstrate this effect, base case (1 MW), case 5 (2 MW) and case 8 (3 MW) were modified so that the main fire was positioned on the floor ($z = 0.0$ m). Locating the fire on the floor even the peak heat release of 3 MW could be reached and kept for some minutes. If the fire was placed near the ceiling, it would be located inside the upper layer (with very low oxygen content) very soon and the fire development would slow down or stop. Therefore, a peak heat release rate of more than 1.3 MW could not be reached if the fire was placed 3.4 m above the floor. The course of heat release rate of main fire for the different cases is shown in Figure 3.3.
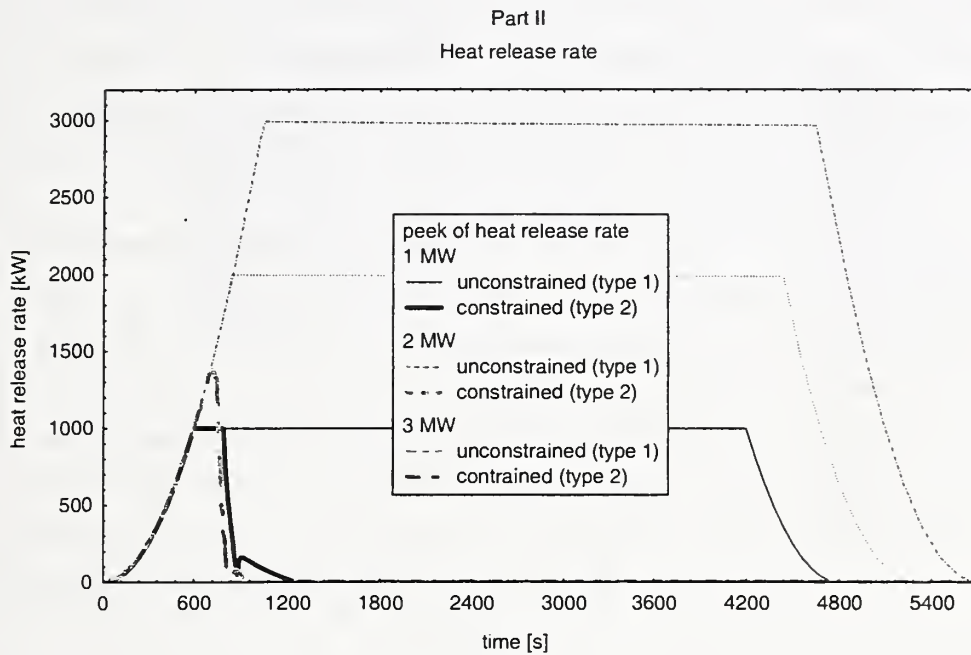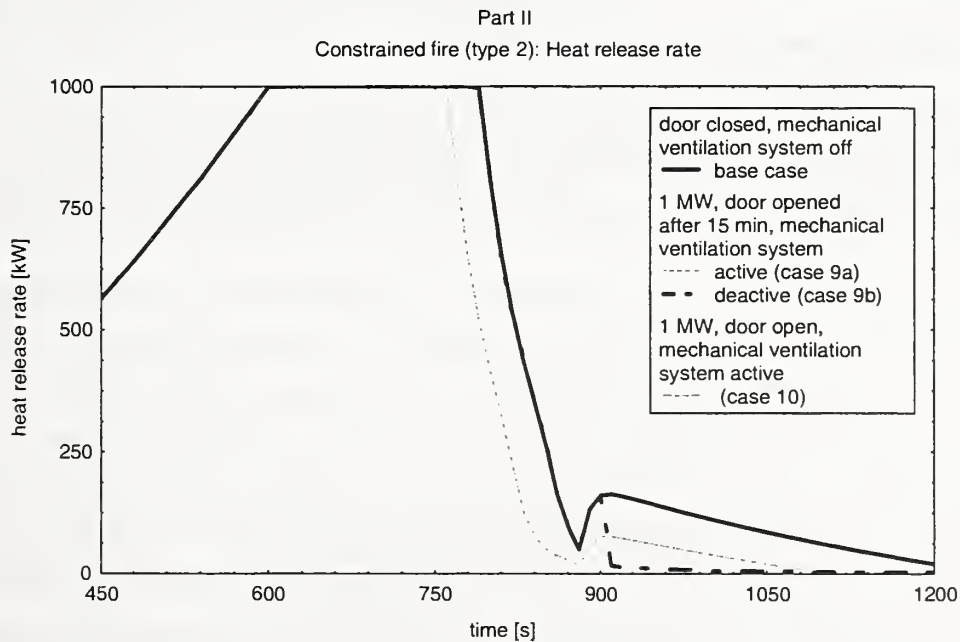
Part II

Heat release rate

Figure 3.1   Effect of fire algorithm: Heat release rate

Part II

Constrained fire (type 2): Heat release rate

Figure 3.2   Effect of ventilation condition: Heat release rate
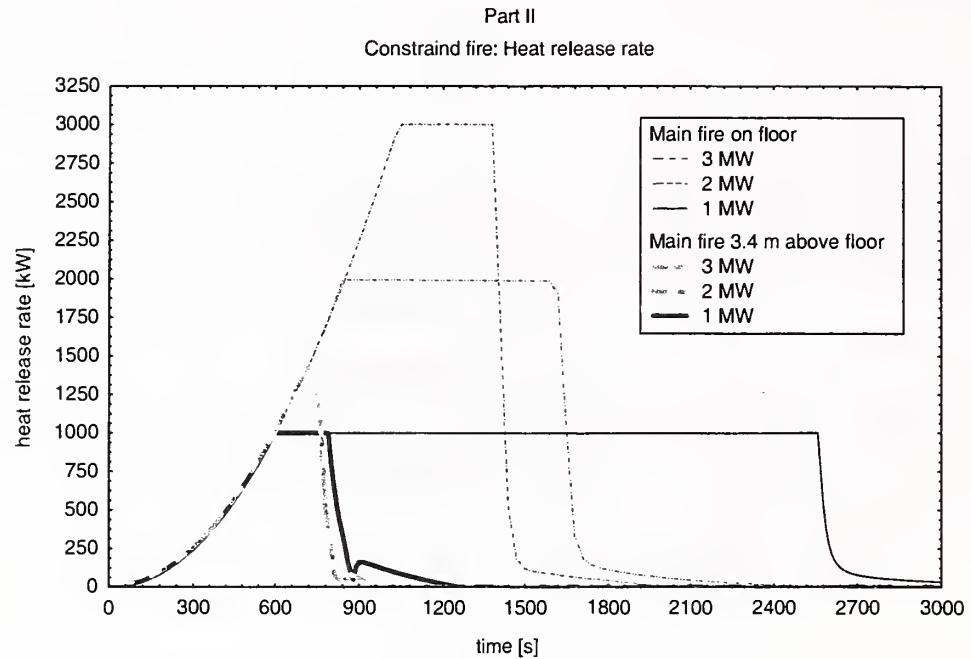
Part II
Constraind fire: Heat release rate

Figure 3.3   Effect of vertical fire position: Heat release rate

3.2.2   Layer temperatures and interface height

The distance between tray A, C1, C2 and tray B or the elevation of tray B do not affect the characteristics of the upper or lower layer. The temperatures of the layers and their thickness are mainly affected by the fire type, the heat release rate of the fire and the ventilation conditions.

Due to the fact that the fire growth is identical for the different cases of peak heat release rates (1 MW, 2 MW or 3 MW), the courses of the upper layer temperature (Figure 3.4, Figure 3.5), the lower layer temperature (Figure 3.6, Figure 3.7) and the interface height (Figure 3.8, Figure 3.9) are identical up to 600 s simulation time in all cases without any ventilation opening (base case - case 8, cases 11 - 13). Using the unconstrained fire algorithm (type 1), the course of these parameters runs simultaneously in case of a 2 MW fire and a 3 MW fire until a value of 2 MW is reached (840 s simulation time). The break in the course of the temperature and the interface height occurs earlier (750 s simulation time) if the constrained fire algorithm (type 2) is used. After reaching the break point (1 MW: 600 s, 2 MW: 840 s respectively 750 s), the temperature of the upper and the lower layer and the interface height develop in their own way in each different case of peak heat release rate.

To explain the influence of the ventilation conditions, the results of the 1 MW fire calculations (base case, cases 9a, 9b, 10) have to be compared. Looking at the course of the upper layer temperature (Figure 3.10, Figure 3.11), the ventilation conditions seem to have only a limited influence on the results. Obviously, the temperature of the lower layer is smaller if the door is open from the beginning and/or the mechanical ventilation system is active (Figure 3.12, Figure 3.13). The lower and upper layer cool down after 15 min simulation time if the door has been opened (base case - case 9b). In this case, there is also a discontinuity in the interface height (Figure 3.14, Figure 3.15). The lower layer temperature and the interface height do not differ if the door stays open all the time (case 10) or if it is opened after 15 min while the mechanical ventilation system has been active from the beginning (case 9a). Only the lower layer temperature grows a little bit higher if the door is closed at the beginning of the simulation and opened after 15 min (case 9b). The upper layer increases faster if the mechanical ventilation system is active all the time (case 9a, case 10).

The course of the upper layer temperature (Figure 3.16) is not affected by the fire algorithm used in the calculations until 600 s simulation time. But from 600 s until the point of time when a lack of oxygen occurs a faster increase of temperature is calculated using the constrained fire algorithm. This effect has also been observed in the simulations of part I.
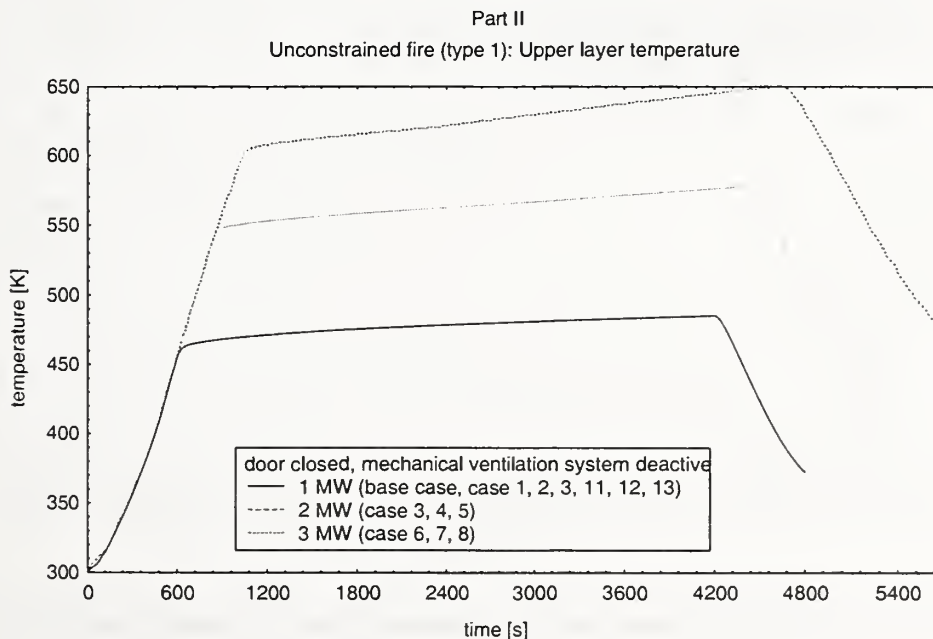

Part II
Unconstrained fire (type 1): Upper layer temperature

Figure 3.4   **Effect of heat release rate: Upper layer temperature, unconstrained fire**

Part II

Constrained fire (type 2): Upper layer temperature
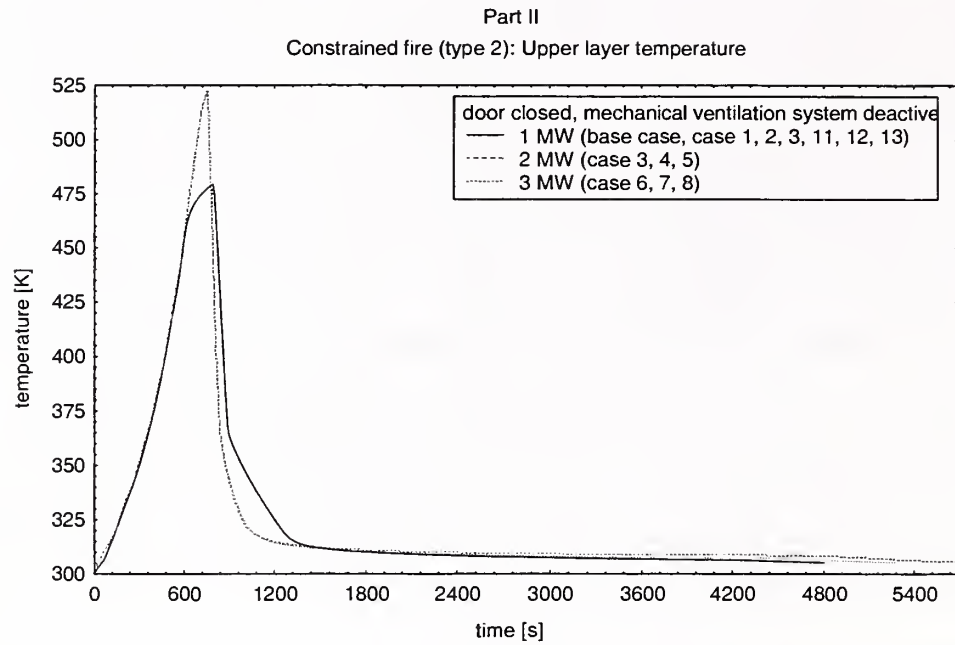
Figure 3.5 **Effect of heat release rate: Upper layer temperature, constrained fire**

Part II

Unconstrained fire (type 1): Lower layer temperature
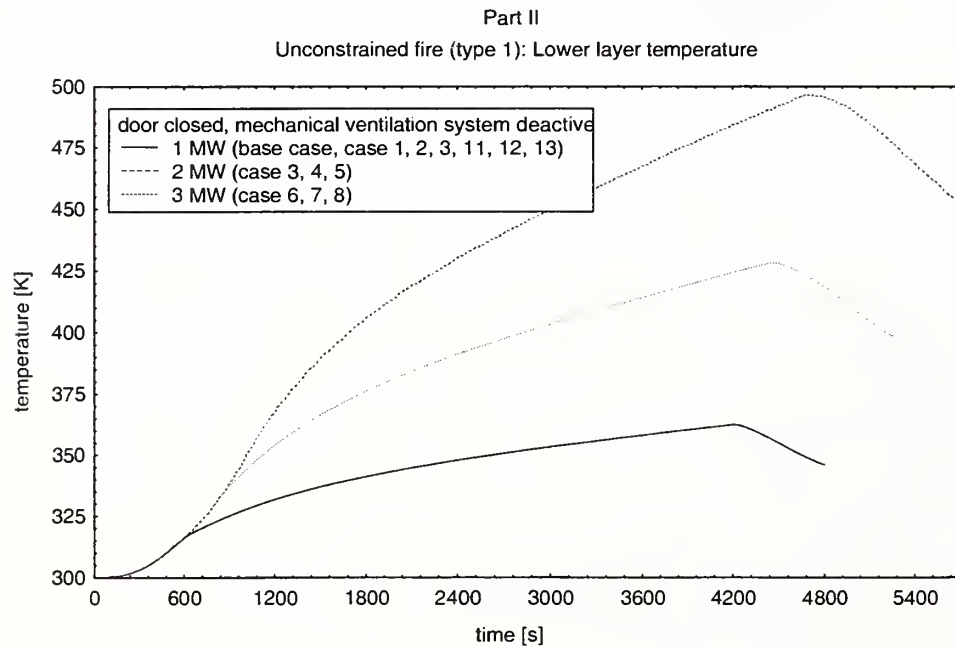
Figure 3.6 **Effect of heat release rate: Lower layer temperature, unconstrained fire**

Part II
Constrained fire (type 2): Lower layer temperature
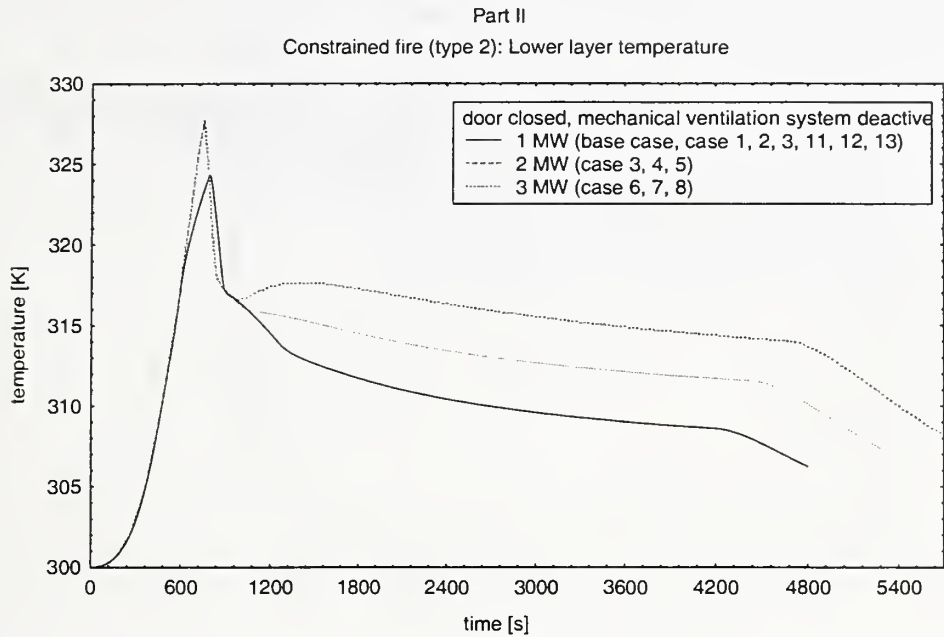
Figure 3.7   Effect of heat release rate: Lower layer temperature, constrained fire

Part II
Unconstrained fire (type 1): Interface height
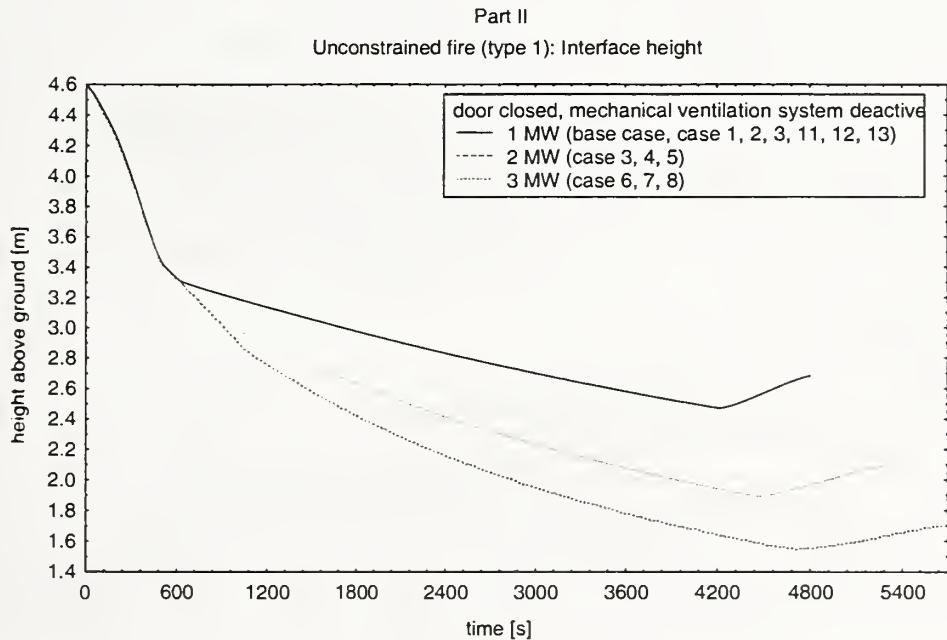
Figure 3.8   Effect of heat release rate: Interface height, unconstrained fire

Part II
Constrained fire (type 2): Interface height
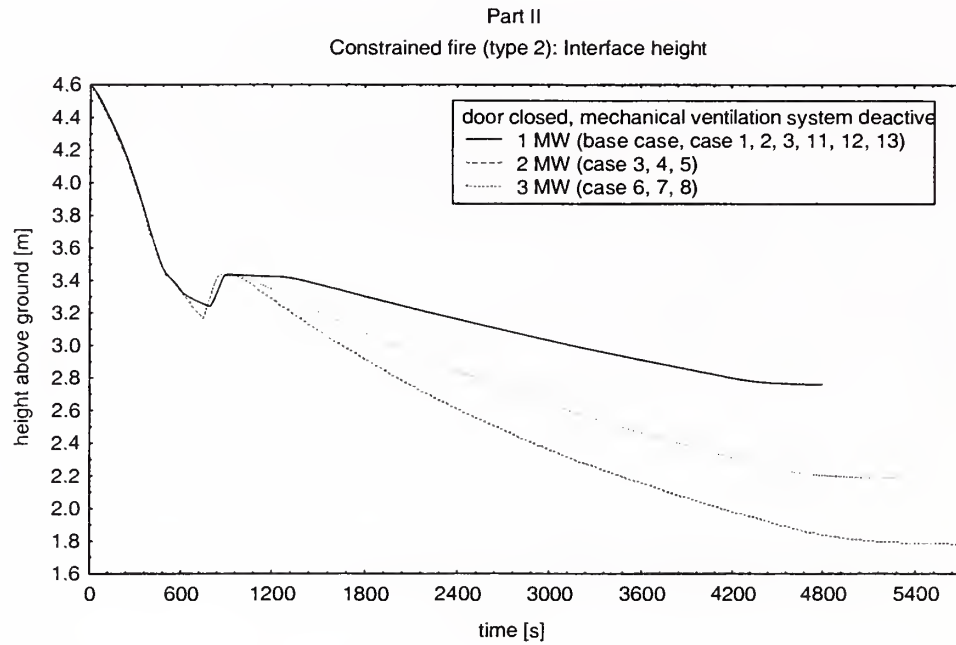
Figure 3.9   Effect of heat release rate: Interface height, constrained fire

Part II
Unconstrained fire (type 1): Upper layer temperature
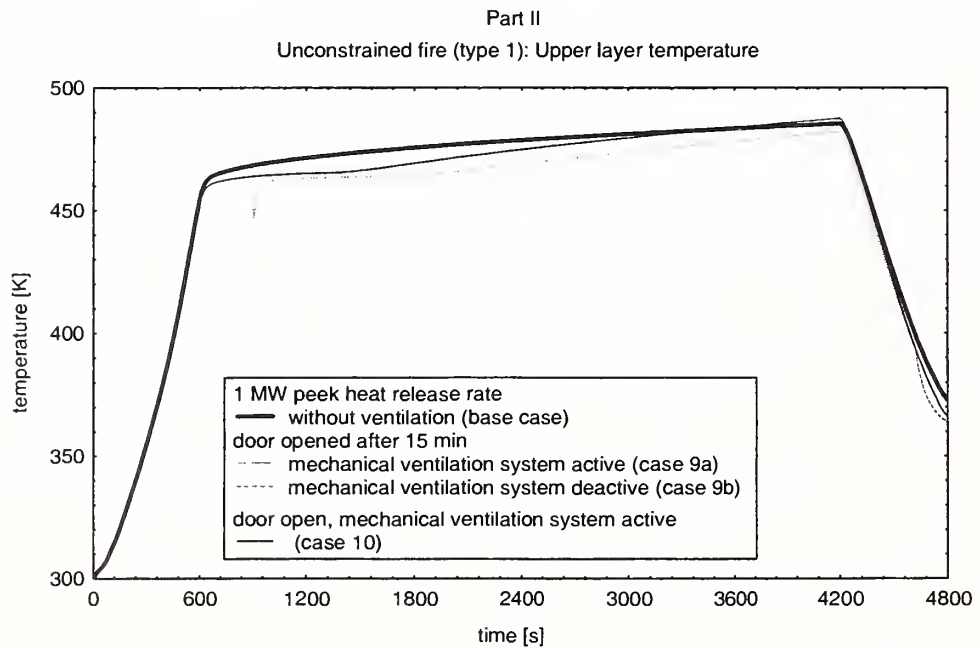
Figure 3.10   Effect of ventilation condition: Upper layer temperature, unconstrained fire

Part II
Constrained fire (type 2): Upper layer temperature
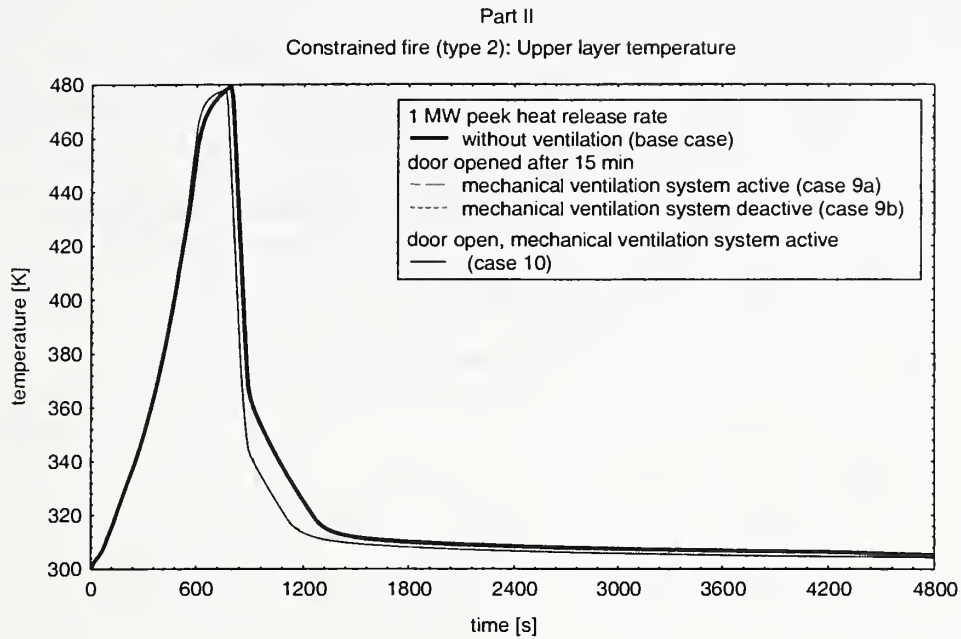
Figure 3.11   Effect of ventilation condition: Upper layer temperature, constrained fire

Part II
Unconstrained fire (type 1): Lower layer temperature
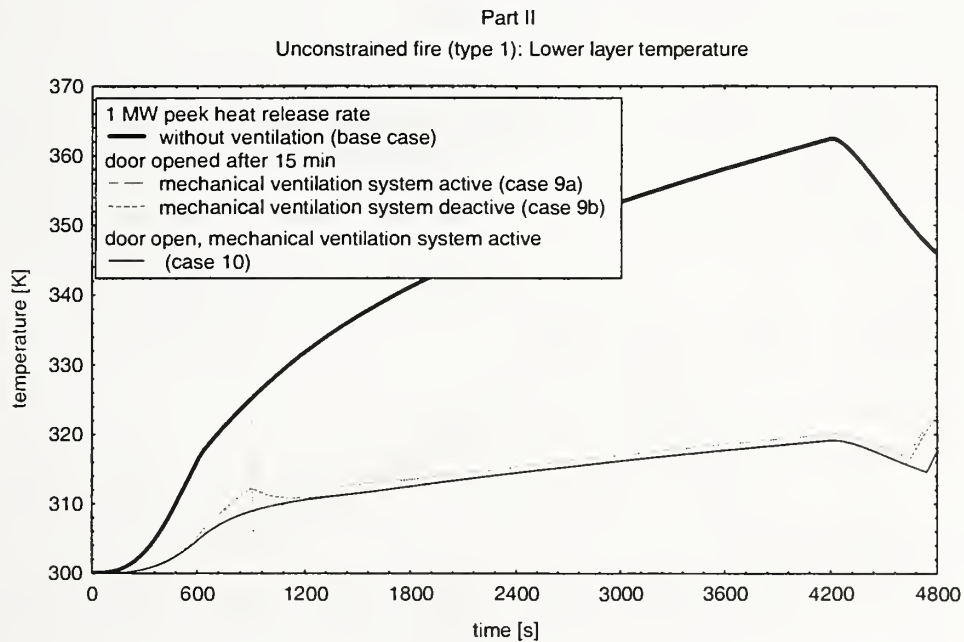
Figure 3.12   Effect of ventilation condition: Lower layer temperature, unconstrained fire

Part II

Constrained fire (type 2): Lower layer temperature
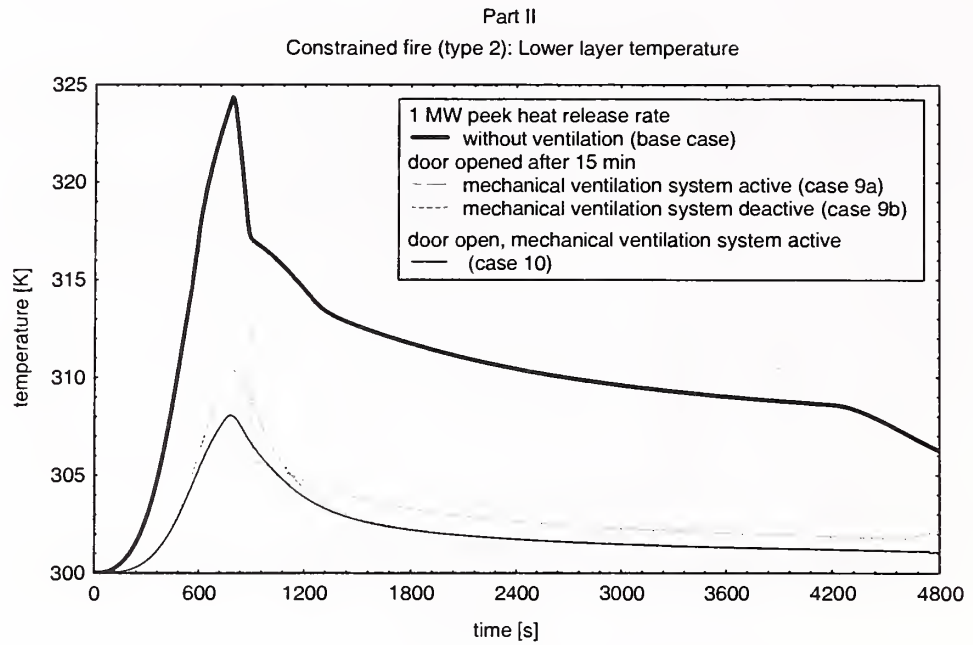
Figure 3.13   **Effect of ventilation condition: Lower layer temperature, constrained fire**

Part II

Unconstrained fire (type 1): Interface height
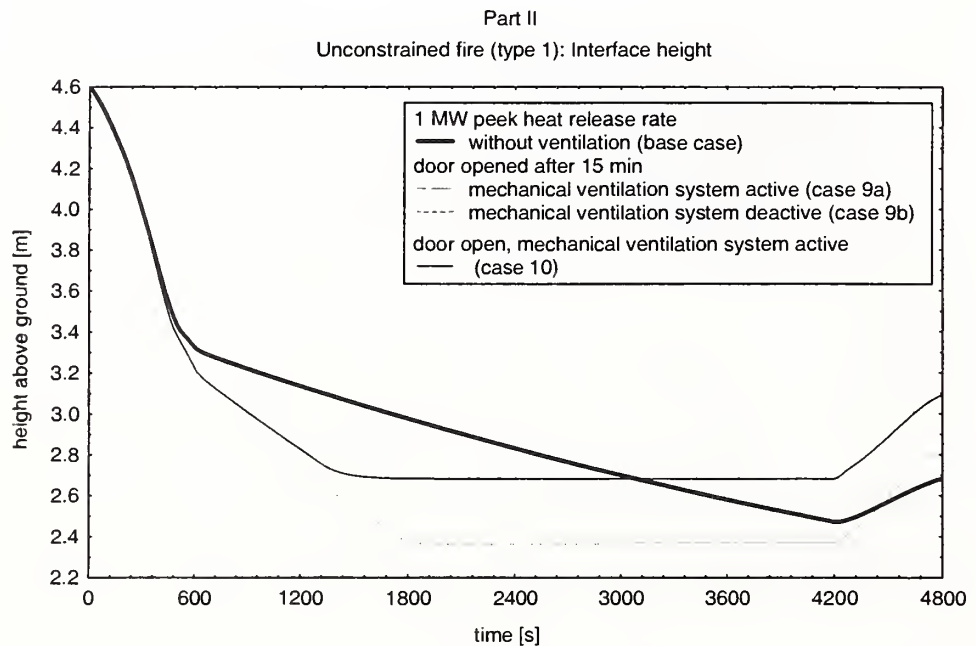
Figure 3.14   **Effect of ventilation condition: Interface height, unconstrained fire**

Part II
Constrained fire (type 2): Interface height
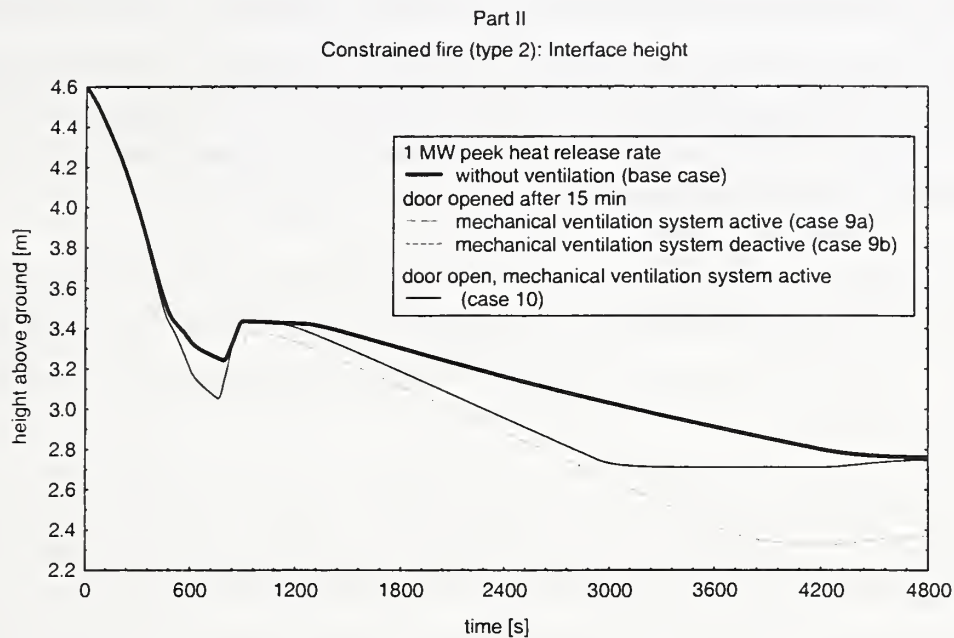
Figure 3.15   Effect of ventilation condition: Interface height, constrained fire

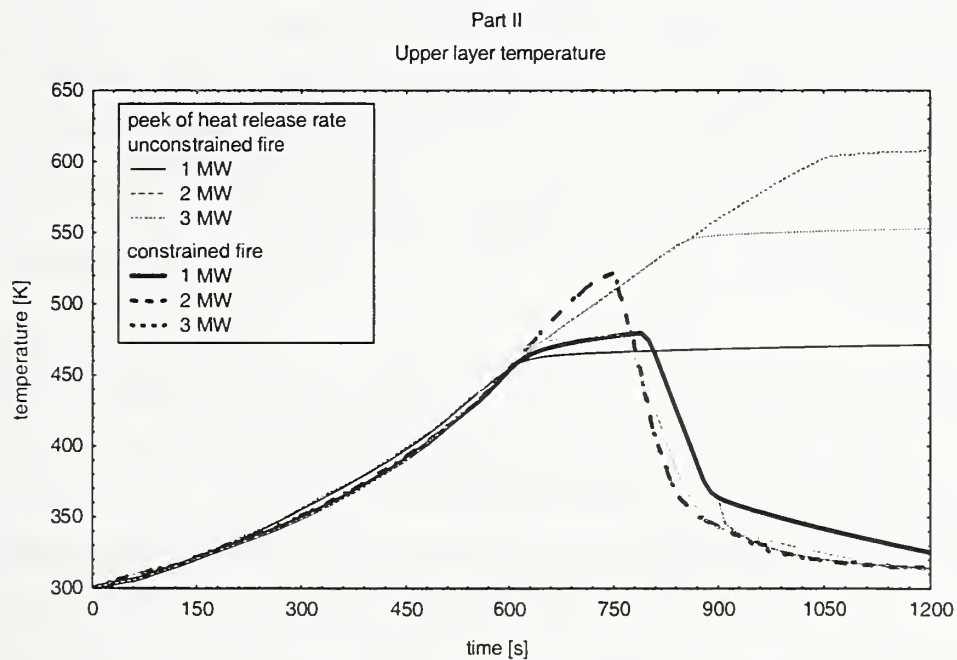Part II
Upper layer temperature

Figure 3.16   Effect of fire type: Upper layer temperature

Using the unconstrained fire algorithm (type 1), there is no restriction in the heat release rate. On the other hand, a maximum heat release rate of less than 1.5 MW is reached in case of using a constrained fire (type 2). In this case, a higher temperature of the upper layer is calculated until a lack of oxygen occurs. An increase of the heat release rate of course leads to an increase of the upper and lower layer temperatures and a decrease of the interface height.

Using the constrained fire algorithm (type 2), the oxygen contents of the upper and the lower layer are calculated. Neither the definition of the peak heat release rate nor the ventilation conditions seemed to have any remarkable influence on the oxygen content of the lower as well as of the upper layer (Figure 3.17).

It has been demonstrated that the vertical fire position has a strong effect on the course of the heat release rate. Using the same configurations and placing the fire on the floor level, the changes in the course of the upper layer oxygen content are calculated (Figure 3.18). The heat release rate decreases rapidly at that point of time at which the value of the oxygen content in the upper layer decreases to less than 1 %.
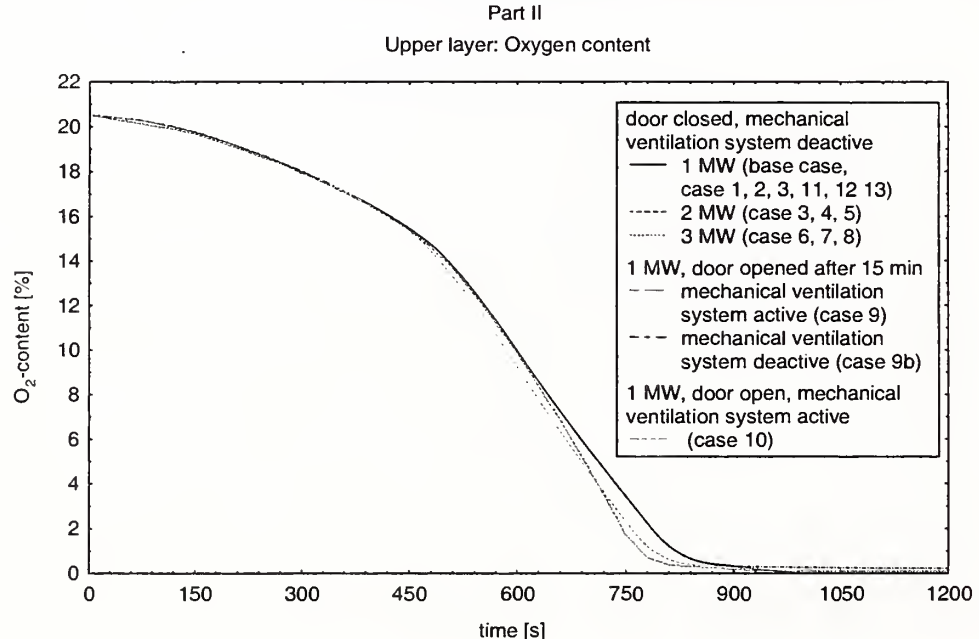

Figure 3.17   Effect of heat release rate and ventilation condition: Oxygen in the upper layer

Part II
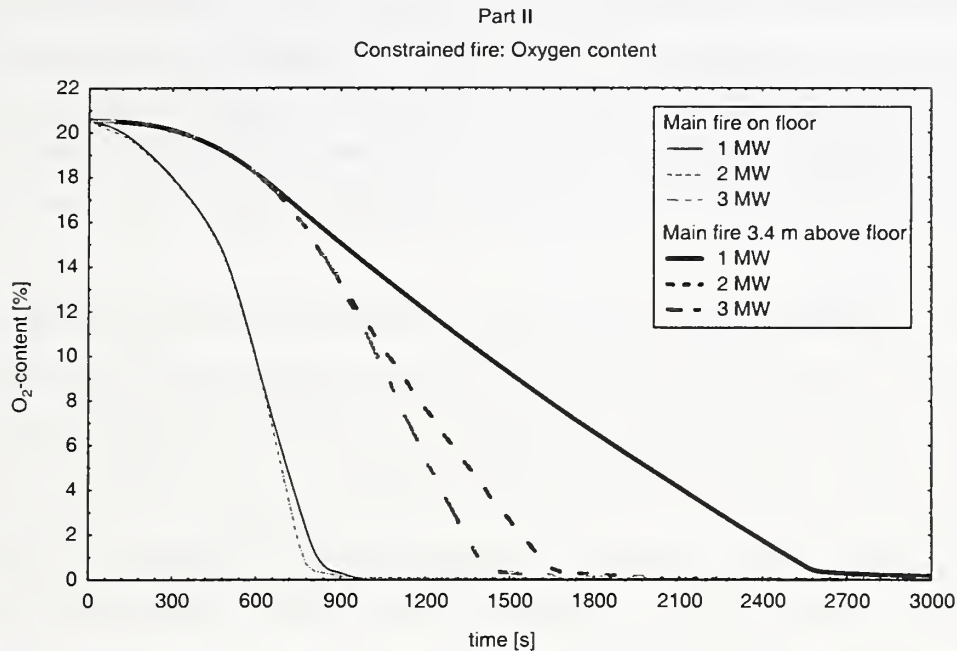Constrained fire: Oxygen content

Figure 3.18   Effect of vertical fire position: Oxygen in the upper layer

If the mechanical ventilation system is active or the door is opened, only the upper layer temperature is affected. In case of using the unconstrained fire algorithm (type 1) it is slightly lower. The lower layer temperature is significantly lower in case of an additional ventilation and the interface height increases. In case of the door being opened and the mechanical ventilation system switched off (case 9b) the lower layer temperature reaches the lowest and the interface height reaches the highest level.

3.2.3   Mass flow rate of the mechanical ventilation system and through the opened door

Only in the cases 9 and 10 the door was assumed to be opened and the mechanical ventilation system was assumed to be used. As mentioned above, it was not possible to simulate deactivating the mechanical ventilation system while the calculation is still running, although it is possible to open or close a natural vent such as the door (using parameter CVENT).

The flow rates through the door and the vent (natural inflow) or the ducts of the mechanical ventilation system (forced outflow) are nearly independent of the fire algorithm until the fire is constrained by lack of oxygen. With very few exceptions, from this point of time the mass flow rates into the compartment and out of the compartment are higher if the constrained fire algorithm is used.

If there is no additional mechanical ventilation system (case 9b), nearly the same amount of gas flows through the door (after it has been opened) from outside into the lower layer as from the lower layer out of the compartment (Figure 3.19). As soon as the door has been opened while the mechanical ventilation system is running from the beginning (case 9a) the flow rates through the door become very soon equal to the flow rates calculated in case of the door being open all the time (case 10).

If there is no additional vent such as the door, a considerable amount of air flows into the lower layer through the vent (inflow) of the ventilation system (Figure 3.20). This mass flow stops and changes its direction (lower layer to outside) after the door has been opened (case 9a). Most of the gas, which is pumped through the ventilation system out of the compartment, is taken out of the lower layer (Figure 3.21). After 50 min simulation time a small amount of gas is also taken out of the upper layer (case 9a, case 10). The flow rates through the open door are not affected very much by the mechanical ventilation system. As soon as the door is opened the flow through the vent from outside into the lower layer stops.
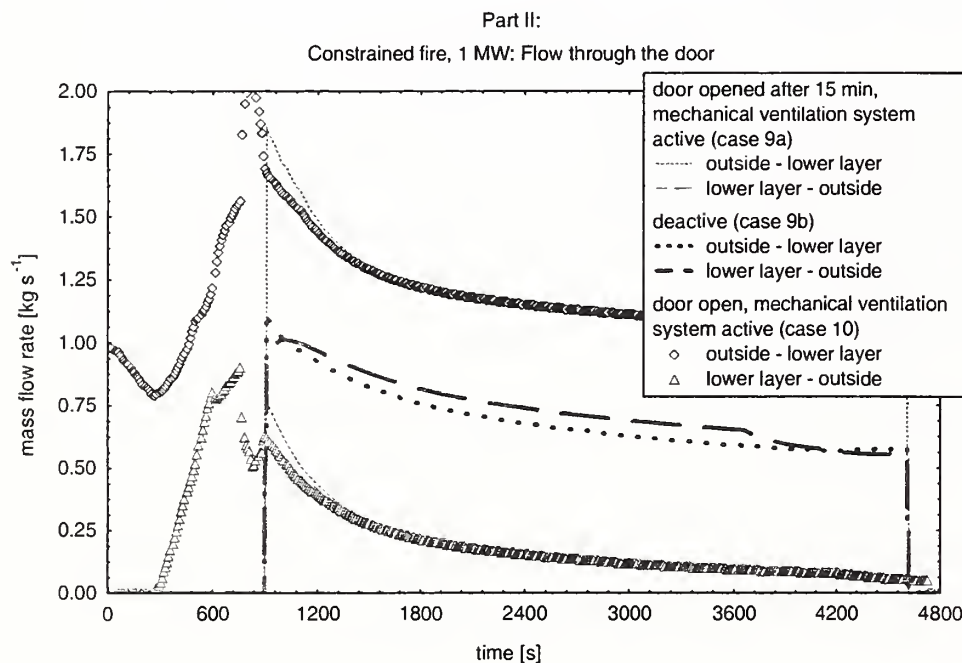

Part II:
Constrained fire, 1 MW: Flow through the door

Figure 3.19   Effect of mechanical ventilation system: Mass flow rate through the door

Part II

Constrained fire, 1 MW: Mechanical ventilation system, inflow
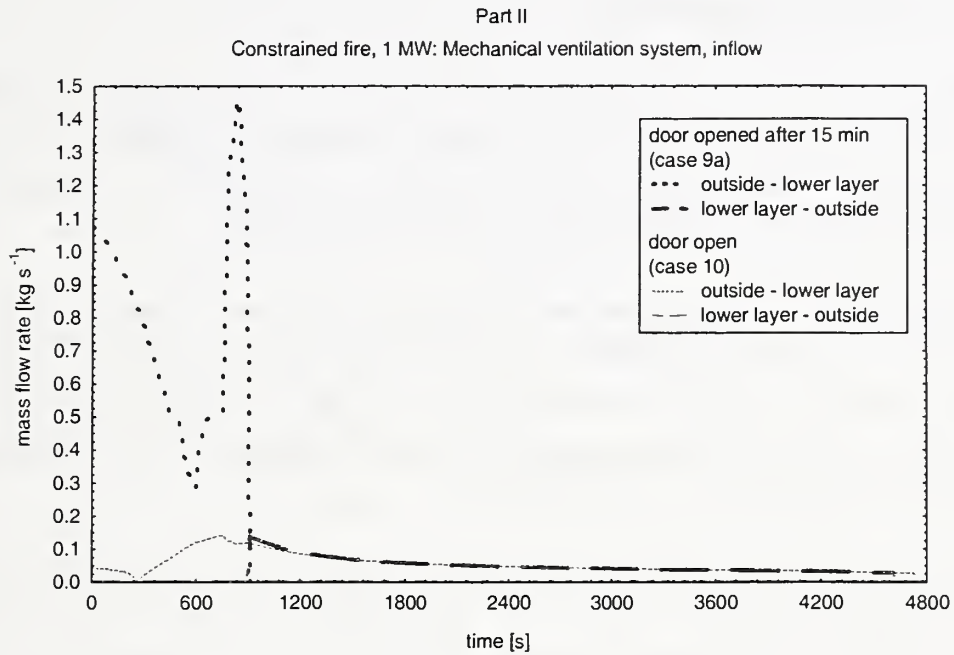
Figure 3.20   Effect of door opening: Mass flow rate through vent I (inflow)

Part II

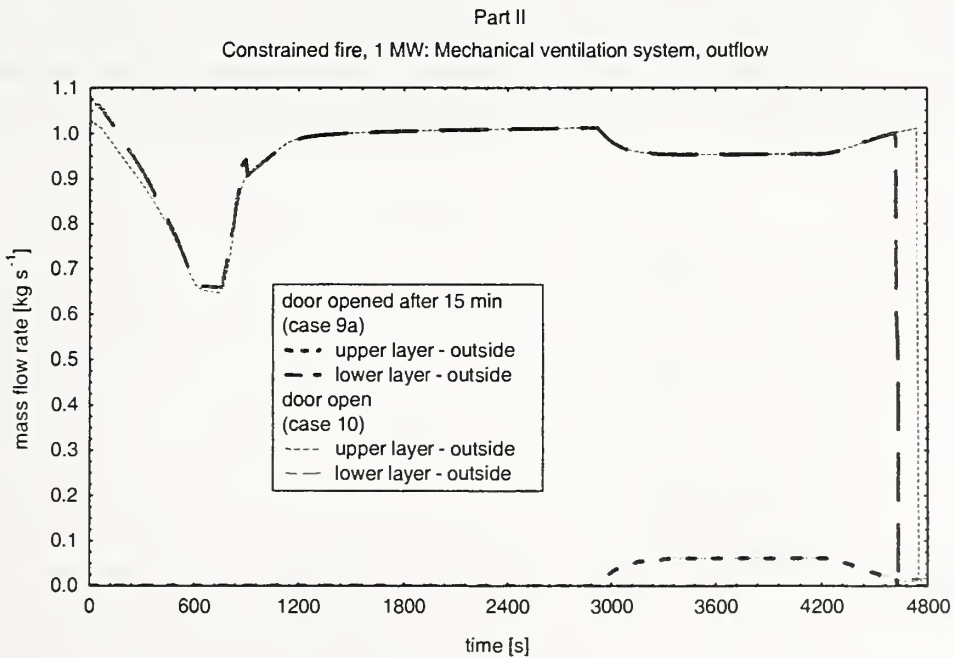Constrained fire, 1 MW: Mechanical ventilation system, outflow

Figure 3.21   Effect of door opening: Mass flow rate through duct system (outflow)

3.2.4 Target surface temperature

Starting the calculations of Part II it was checked, whether the physical model of heating an object or target acts as in Part I, indicating that an object will always be assumed as being positioned in the center of a horizontal plane in the compartment. Obviously this happened, although the surface temperature is independent of the horizontal object position.

All other calculations of Part II were performed assuming that tray B (object / target) is placed in the center of the compartment (4.55 m, 7.6 m) and the main fire of tray A, C1, C2 (main fire) is moved in y-direction to get the distance D of 6.1 m (4.55 m, 1.5 m), 3.1 m (4.55 m, 4.5 m) or 4.6 m (4.55 m, 3.0 m). Prior to this calculations it had been demonstrated that it does not matter if the main fire is moved in x- or in y-direction.

The distance between the main fire of tray A, C1, C2 and the target tray B has only a minor effect on the surface temperature in case of an unconstrained fire (Figure 3.22). The differences between the maximum surface temperatures are small as well (Table 3.1). In case of a constrained fire the temperature does not increase very much (Figure 3.24). It does not make a difference whether the maximum heat release rate is 2 MW or 3 MW. This result is reasonable, because the calculations show that this level of the heat release rate is not reached. The distance between main fire and target has only small effects on the maximum surface temperature (Figure 3.26). The differences of the maximum surface temperatures are only 0.2 - 0.4 K.
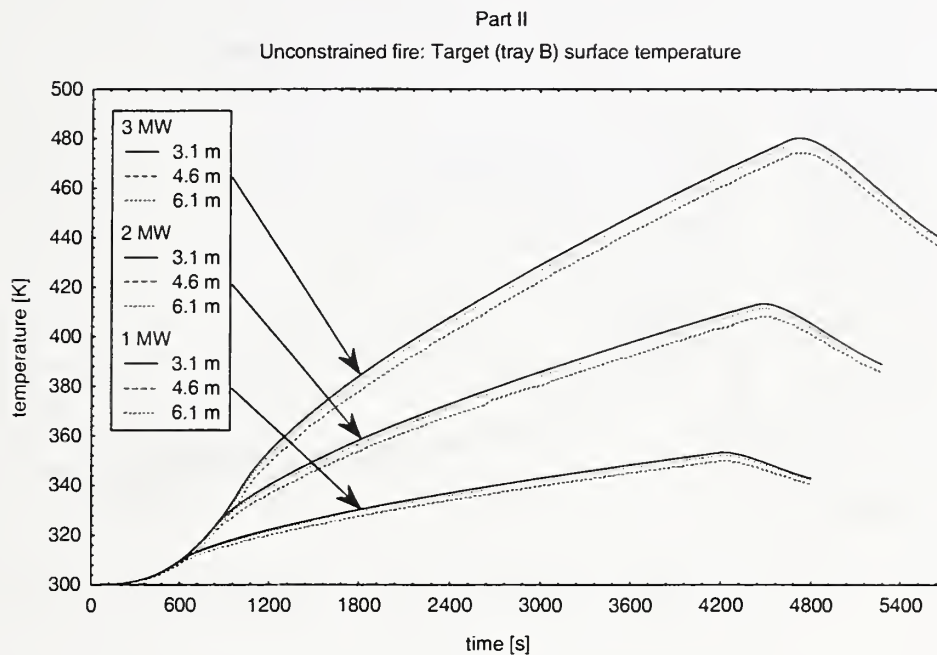
Part II
Unconstrained fire: Target (tray B) surface temperature

Figure 3.22   Effect of heat release rate and distance: Target (tray B) surface temperature

Part II
Unconstrained fire. Target (tray B) surface temperature

Figure 3.23   Effect of ventilation condition: Target (tray B) surface temperature

Part II
Constrained fire: Target (tray B) surface temperature

Figure 3.24   Effect of heat release rate and distance: Target (tray B) surface temperature

Part II
Constrained fire: Target (tray B) surface temperature

Figure 3.25   Effect of ventilation condition: Target (tray B) surface temperature

Part II
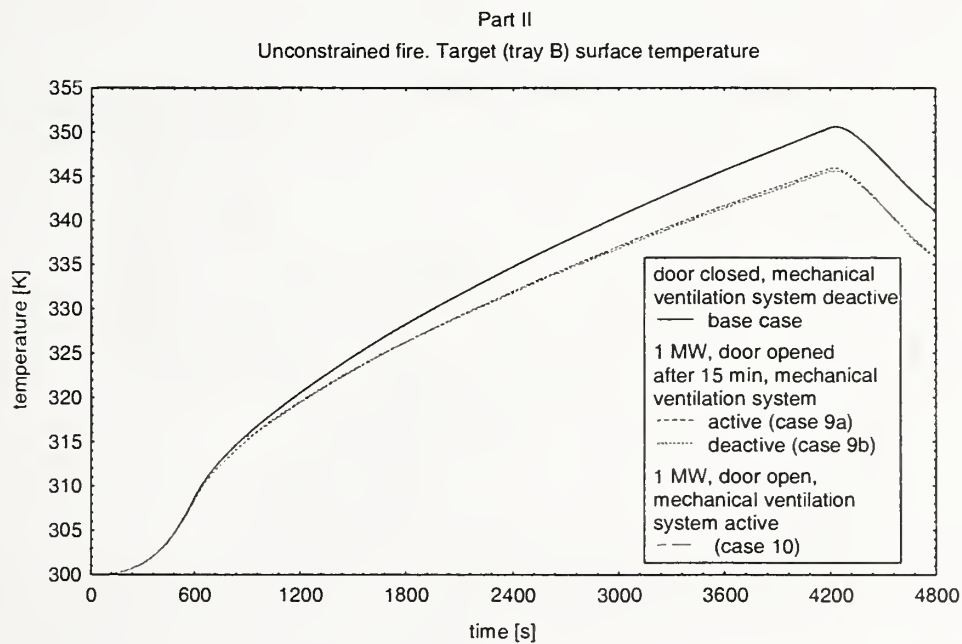
Constrained fire: Target (tray B) surface temperature

Figure 3.26   Effect of heat release rate and distance: Target (tray B) surface temperature

Part II

Constrained fireTarget (tray B) surface temperature

Figure 3.27   Effect of ventilation condition: Target (tray B) surface temperature

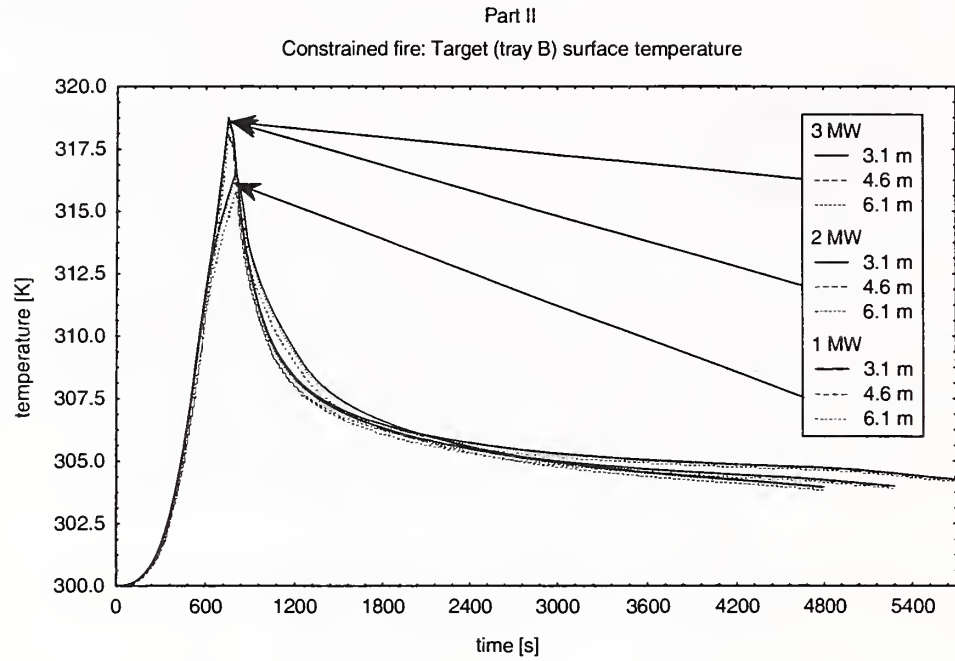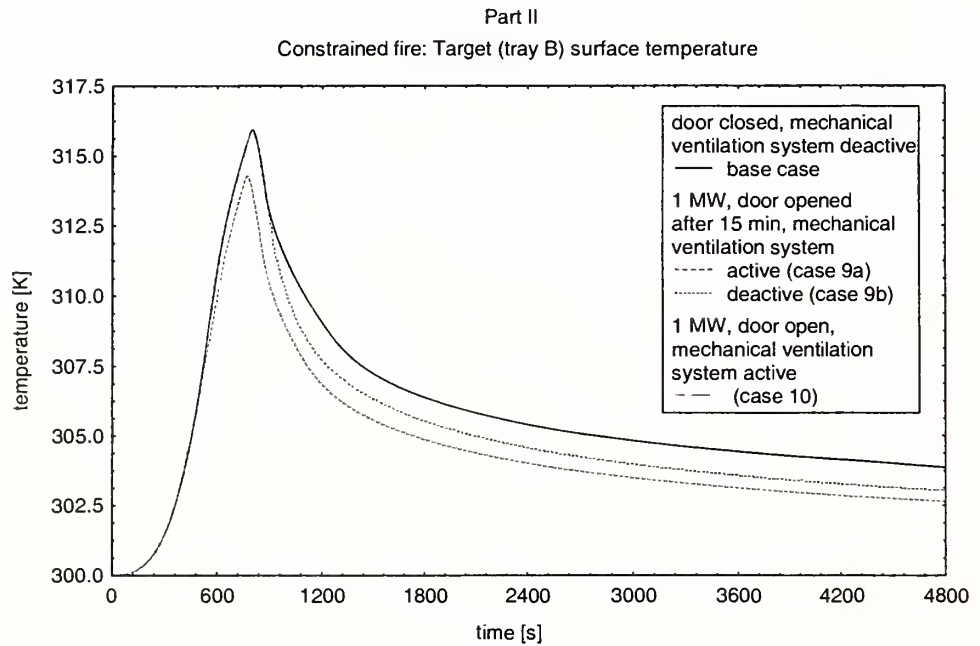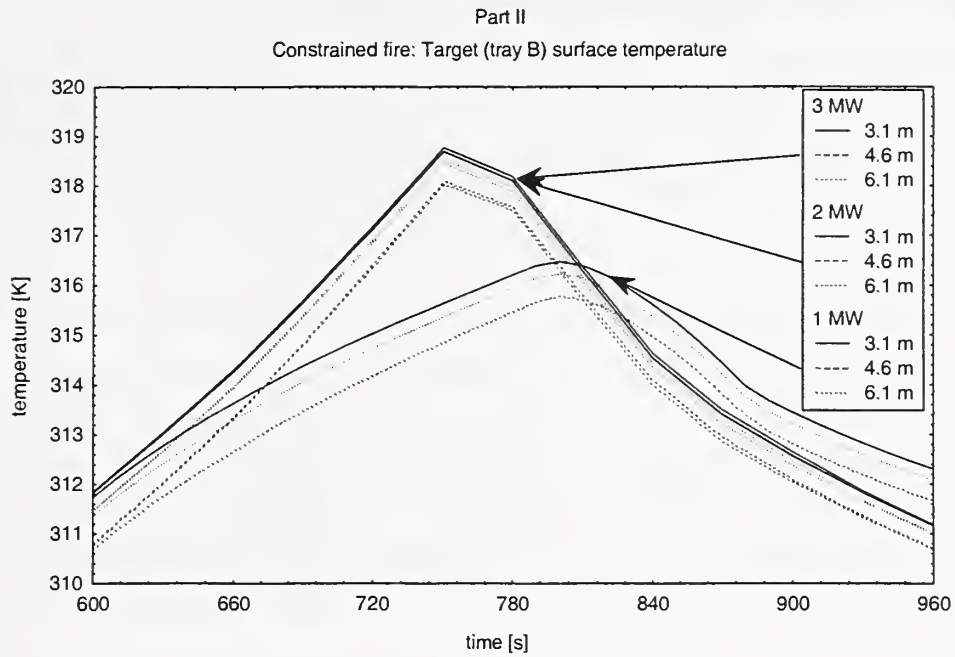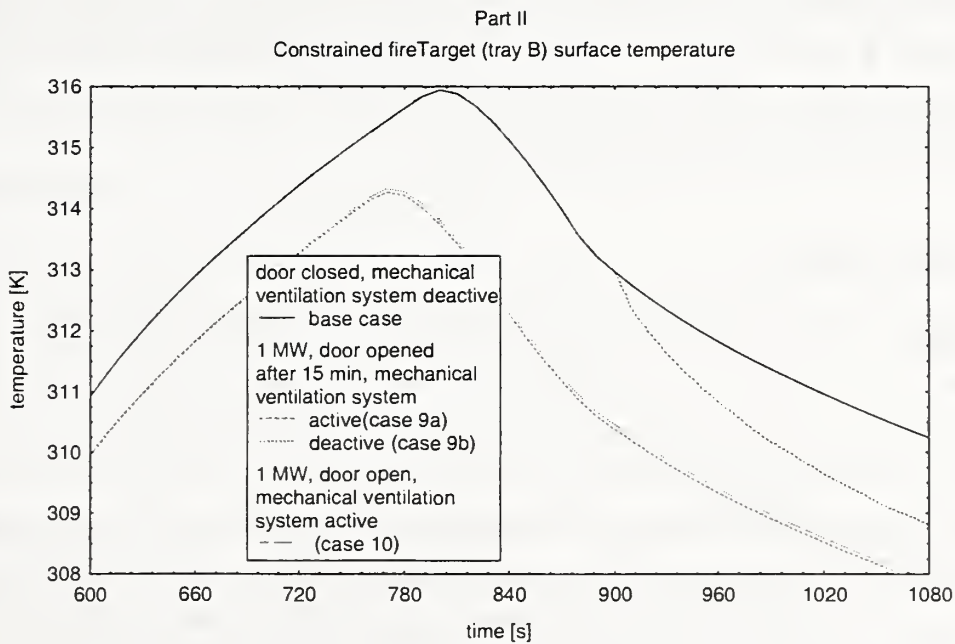**Table 3.1   Maximum target (tray B) surface temperature**

Case	heat release rate	distance	maximum surface temperature	
			unconstrained fire	constrained fire
1	1 MW	3.1 m	353.33 K	316.22 K
2		4.6 m	352.17 K	316.47 K
base case		6.1 m	349.94 K	315.77 K
3	2 MW	3.1 m	413.33 K	318.70 K
4		4.6 m	411.56 K	318.45 K
5		6.1 m	408.08 K	318.02 K
6	3 MW	3.1 m	480.25 K	318.77 K
7		4.6 m	478.25 K	318.53 K
8		6.1 m	474.22 K	318.09 K

In case of an unconstrained fire the maximum target (tray B) surface temperature is approximately 6 K lower if the is door opened or the mechanical ventilation system running (Figure 3.23). In case of a constrained fire, the maximum surface temperature is approximately 1.8 K lower if the mechanical ventilation system is running (Figure 3.27). In case that the mechanical ventilation system is not running and the door is opened after 15 min fire duration the temperature decreases a little faster (Figure 3.27).

4   CONCLUSIONS

The multi-room multi-zone model CFAST, version 4.0.1 has been applied has been applied to perform the calculations for the Benchmark Exercise # A "cable tray fires of redundant safety trains". In Part I of this exercise the base case and five additional cases with varying distance between the trash bag as an ignition source and the tray A on the one hand and the ventilation conditions on the other are calculated. In addition, two fire algorithms are used. Defining a cable fire of tray A, C1, C2 the effects on cable tray B are studied in Part II of the Benchmark exercise. In this case, three different levels of heat release rate, different operation modes of the ventilation system, and door status as well as different cable diameters and tray elevations should be investigated.

The results calculated using the constrained fire algorithm seem to be more realistic. Neverthe-less, there are some uncertainties. Particularly the upper layer temperature differs slightly in case

of a sufficient oxygen amount available comparing the two fire algorithms. The gas temperature and the layer thickness are calculated convincingly by CFAST. The mass flow rates through natural vents seem to be plausible. It is necessary to describe the main fire in more detail by defining the pyrolysis rate, the effective heat of combustion and the yields of combustion products, such as carbon dioxide, carbon monoxide and hydrochloride. It is obvious that the vertical position of the main fire has a strong influence on all results.

The computer code CFAST is not optimal for the Benchmark Exercise # 1 because the heat transfer to a target, as a main task of this exercise, is calculated by a very rough model. Due to this, no quantitative results can be produced. In addition, the forced ventilation model does not work in case of inflow. The composition of the incoming air seems to be wrong. Since it is not possible to define a time dependent fan power, switching the forced ventilation on or off cannot be simulated, but a mechanical ventilation system is a main tool to remove hot gases out of a fire compartment in a nuclear power plant.

Although CFAST does not seem to be appropriate for all of the questions of the given Benchmark Exercise, it is a very useful engineering tool for estimating fire and smoke transport in several other cases. The results of the CFAST calculations can be used to answer special questions such as heating of targets with more detailed models.

5   LITERATURE

[1]   Jones, W. W.; Forney, G. P.; Peacock, R. D.; Reneke, P. A.: A technical reference for CFAST: An engineering tool for estimating fire and smoke transport. NIST TN 1431, January 2000

[2]   Peacock, R. D.; Reneke, P. A.; Jones, W. W.; Bukowski, R. W.; Forney, G. P.A   : User's guide for FAST: Engineering tools for estimating fire growth and smoke transport. NIST Special Publication 921 2000 Edition, January 2000

[3]   Peacock, R. D.; Forney, G. P.; Reneke, P. A.; Portier, R. M.; Jones, W. W.: CFAST, the consolidated model of fire and smoke transport. NIST Technical Note 1299, September 1995

[4] Dey, M. K.: International Collaborative Project to Evaluate Fire Models for Nuclear Power Plant Applications: Benchmark Exercises #1, Cable tray fires of redundant safety trains, revised September 11, 2000